MASTER OF SCIENCE

Investigating the clinical value of hyperactivation and intracellular calcium signalling of human spermatozoa and their value in drug screening

Ruso, Halil

Award date:
2013

Awarding institution:
University of Dundee

MASTER OF SCIENCE

Investigating the clinical value of hyperactivation and intracellular calcium signalling of human spermatozoa and their value in drug screening

Halil Ruso

2014

University of Dundee

Investigating the Clinical Value of Hyperactivation and Intracellular Calcium Signaling of Human Spermatozoa and Their Value in Drug Screening

Halil Ruso

MSc by Research

University of Dundee

December 2013

Table of Contents

List of Figures

List of Tables

Declaration

The data used in Chapter 4 was gathered jointly by Dr. Sarah Martins Da Silva, Dr. Anthony Hope, and myself. I collected all the remaining data alone and I am the author of this thesis. The report is written in my own words and conforms to the University of Dundee's Policy on plagiarism and academic dishonesty. Unless otherwise indicated, I have consulted all of the references cited in this thesis.

Halil Ruso

Acknowledgements

I would like to give my special thanks to my supervisors Prof. Christopher Barratt and Dr. Sarah Martins Da Silva for sharing their highly valuable knowledge with me. I also would like to thank all the staff in the Assisted Conception Unit for their time and understanding and of course all the anonymous patients who consented to contribute science. I would like to thank my father Ahmet Ruso, my mother Gülsün Ruso, my brother Mustafa Ruso, my sister-in-law Ayşen Ruso and my friends, in particular Yeliz Fahriye Köroğlu, Kayra Aldağ, and Mustafa Yenigüç for their endless support. I would like to offer my gratitude to the Ministry of Education of Turkish Republic of North Cyprus for the bursary I received. Further thanks to Prof. Steve Hubbard for his statistical help.

Summary

Hyperactivation is described as a type of motility with asymmetrical bending of the flagella, increased amplitude of lateral head displacement, and decreased linearity. The resulting increase in thrust by hyperactivated motility is required for successful fertilization. Semen samples panels of patients were induced to hyperactivate with 4-AP (putative Ca^{2+} store mobilizer), progesterone (CatSper activator), NH_4Cl (increased intracellular pH), or IBMX (AC/cAMP/PKA pathway) and hyperactivation levels were quantified using CASA. Induced hyperactivation levels with 4-AP (r_p=0.5242, p=0.0123, n=22), IBMX (r_p=0.8361, p=0.0026, n=11), and spontaneous hyperactivation levels (r_p=0.4420, p=0.0347, n=23) were correlated with fertilization rates in IVF. Furthermore, ICSI patients showed significantly lower responses to all inducers than that of IVF patients and research donors. Based on these findings and the knowledge that Ca^{2+} is pivotal to sperm function, it was hypothesized that screening compounds on their ability to induce intracellular Ca^{2+} signalling, as a surrogate of physiological response would identify novel compounds to stimulate human sperm motility. This hypothesis was tested with known motility inducers. PDE inhibitors Ibudilast, Etazolate HCl, Tofisopam, MMPX, and Papaverine were found to be poor inducers of Ca^{2+} signalling and their actions on sperm motility are thus hypothesized to be via mechanisms other than Ca^{2+} signalling. A chemogenomics library consisting of 223 compounds was screened using Ca^{2+} as a surrogate for physiological response and identified 25 compounds, which significantly increased intracellular Ca^{2+} levels. Trequinsin HCl and BRL 50481, two of the hit compounds were tested on human sperm motility. Trequinsin HCl was found to be a novel and effective motility inducer. Conversely, BRL 50481 had no significant effect on human sperm motility. In conclusion, spontaneous-, induced-hyperactivation levels, and CASA parameters ALH, VCL and LIN were found to be significant prognostic indicators for fertilization at IVF.

Furthermore, Ca^{2+} responses can be utilised in compound HTS as part of a drug discovery programme for male factor subfertility, and Trequinsin HCl is a novel human sperm motility stimulator.

List of Abbreviations

ART: Assisted reproductive technologies

BSA: Bovine serum albumin

cAMP: Cyclic adenosine monophosphate

sAC: Soluble adenylyl cyclase

AC: Adenylyl cyclase

tmAC: Trans-membrane adenylyl cyclase

ICSI: Intracytoplasmic sperm injection

IVF: *In vitro* fertilization

2PN: 2-pronucleus

4-AP: 4 aminopyridine

NH_4Cl: Ammonium chloride

IBMX: 3-isobutyl-1-methylxanthine

MMPX: 8-Methoxymethyl-3-isobutyl-1-methylxanthine

NE: Nuclear envelope

ALH: Amplitude of lateral head display

VAP: Average path velocity

VCL: Curvilinear velocity

VSL: Velocity on a straight line

BCF: Beat-cross frequency

LIN: Linearity

CASA: Computer assisted sperm analyser

Fura-2/AM: Acetoxymethyl ester Fura-2

WHO: World Health Organization

E_m: Membrane potential

PE: Phosphatidiylethanolamine

PS: Phosphatidylserine

Trequinsin: Trequinsin hydrochloride

Chapter 1: General Introduction

1.1 Sperm Structure

Sperm cells have highly compartmentalized and compact structure that is specifically evolved to achieve its one and only task — fertilization (Barratt *et. al.*, 2009). Additionally, sperm cells can be considered as very selective cells as they are highly streamlined and devoid of any excess cellular luggage that is not required for fertilization such as protein production machinery (endoplasmic reticulum). Therefore, it is important to briefly describe its cellular and subcellular structures. A spermatozoon consists of a head and a tail (or flagellum, consists of mid-piece, principal piece, and end-piece) that are covered with a continuous plasmalemma (Figure 1.1).

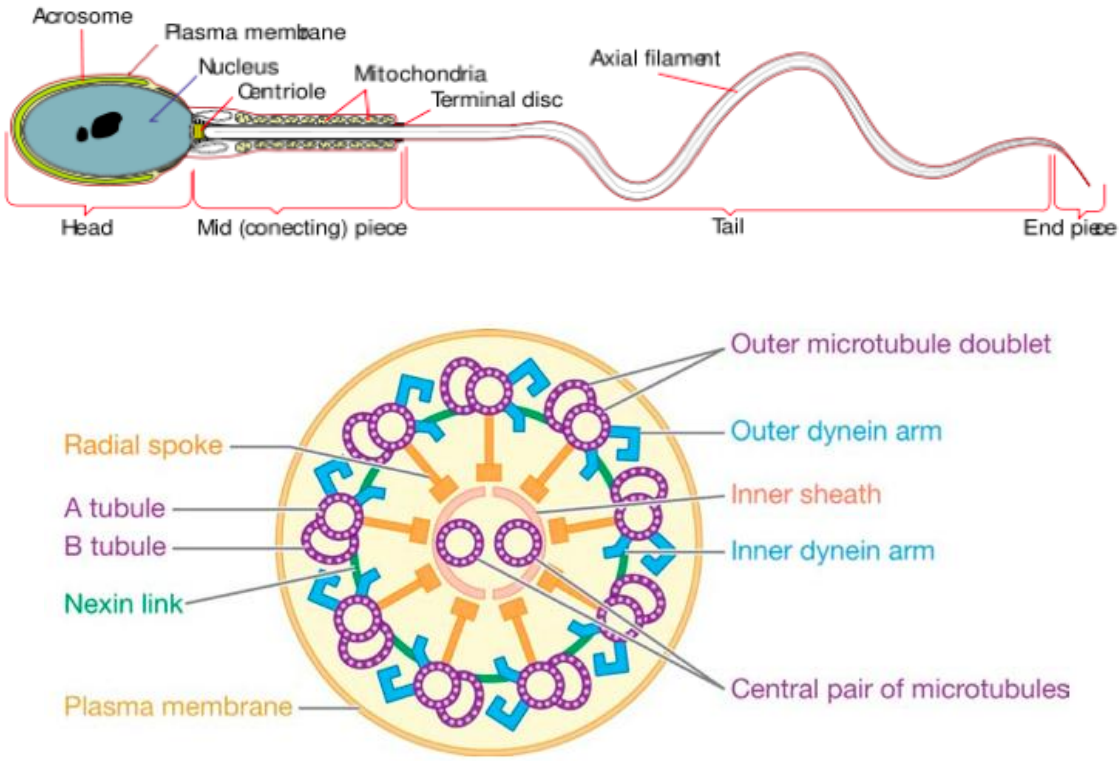

Figure 1.1: Structure of a human spermatozoon and selected ultrastructure of the flagella. Illustrates the cross section of the mid-piece that consists of the plasma membrane, nine outer dynein arms, and nine outer microtubule doublets (both tubule A and B indicated) and their associated, radial spokes, and central pair of microtubule doublets. Figure is taken from Fauci and Dillon, (2006).

1.1.1 Sperm Head

Sperm head consists of a nucleus that contains hypercondensed DNA (in an almost crystalline state) with histones and protamines, a reduced NE that covers the nucleus, and acrosome that contains the enzymes required for penetration through zona pellucida. Hypercondensation enables the sperm head to take a hydrodynamic shape to permit efficient swimming (especially in viscoelastic media) and therefore aids motility (Brewer *et. al.,* 2002; Dadoune, 2003; Fauci and Dillon, 2006). The sperm nucleus is protected by the perinuclear theca, which consists of 3 segments and is composed of structural proteins tightened by disulphide bonds and other proteins (Oko, 1995). Some of these proteins have other signalling features upon fertilization.

1.1.2 Sperm Flagellum

Sperm flagellum is the driving motor of sperm motility; therefore, understanding its structure and ultrastructure is important. The flagellum of a human spermatozoon consists of a mid-piece, a principal piece, and an end-piece (Figure 1.1). The motile force is generated through the 9+2 arrangement of microtubules of axoneme (discussed in detail in section 1.2). The 9+2 arrangement refers to the nine peripheral, symmetrical doublets of microtubules that are connected by dynein arms and to the sheath of central pair of microtubules by radial spokes (Murase, 1992; Witman, 1990; Figure 1.1).

1.2 Control of Sperm Motility

Human spermatozoa are held immotile within the epididymis by the low pH (Carr *et. al.,* 1985). They acquire motility upon deposition into the vagina. However, sperm motility must be regulated in order to achieve fertilization in the viscoelastic and variable environments of the female reproductive tract.

1.2.1 Flagellum

Flagellar waves create the necessary forward movement required for successful fertilization *in vivo* or *in vitro.* The flagellar ultrastructures are subject to post-translational modifications at different levels. These can be divided into 4 categories; (i) the axoneme, (ii) outer dense fibres (iii) fibrous sheath and (iv) mitochondrial sheath.

1.2.1.1 The Axoneme

Axoneme is the most common structure for motility in different organisms and cells (ciliary or flagellar) and its structure remains similar from prokaryotic to eukaryotic organisms (Witman, 1990; Murase, 1992). It is the core structure that propels flagella and consequently enables the sperm motility in mammals. The axoneme is made of nine microtubule doublets around the central pair of microtubules, making the 9+2 formation (Figure 1.1). Each of the nine outer doublets is connected to each other with nexin (protein links) and radial spokes. Dynein arms are the pivotal structures that enable the active sliding of the microtubules that result in a flagellar wave (Bozkurt and Wooley, 1993; Fauci and Dillon, 2006). The force that is required for sliding dynein arms is generated by the axonemal motor protein dynein ATPases that propagates towards the end of the flagellum. Dynein arms at one side of the flagellum bend the flagella at one side where the dynein arms of the other side bend the sperm in the opposite direction. Consequently, the result of opposite bending propagates towards the end of the flagellum by an undulatory switch of dynein arms, thus creating a wave of the flagella (Brokaw, 2009). This cascade of dynein arm activation and inactivation is controlled within the axoneme itself.

The inner and outer dynein arms have different functions within a microtubule doublet. The outer dynein arms are insensitive to ATP and they are bound to tubulin through a dynein-docking complex (Di Bella and King, 2001; Porter and Sale, 2000; Takada *et. al.,* 2002). They determine the maximal velocity of outer doublet

microtubule sliding (Brokaw, 2009). The inner dynein arms regulate the beating symmetry and affect the flagellar wave formation (Brokaw and Kamiya, 1987). Dynein arms are protein motor complexes that consist of heavy chains (α and β), intermediate chains, and light chains, where each chain has different functions. Heavy chains have ATPase activity and are responsible for the active sliding of the microtubules. Intermediate chains serve as a binding location for the microtubules. Light chains are the regulatory centres of the dynein arms, where they have multiple binding sites for different molecules, such as calcium binding site, which is required for fine adjustments of the beating pattern (Inaba, 2002). The presence of multiple binding sites on the light chain of the dynein complex indicates the possible contribution of multiple regulatory molecules resulting in a complex regulatory system for the dynein arms.

The dynein regulatory complex is tightly bound to the microtubule lattice that has regulatory functions on the axoneme. There are seven polypeptides on the dynein regulatory complex, which are subject to post-translational modifications that result in control of sperm motility such as; acetylation, palmitylation, phosphorylation, polyglutamylation and polyglycation, all of which are important for axonemal motility (Gagnon *et. al.,* 1996; Huitorel *et. al.,* 2002; MacRae, 1997; Lindemann and Lesich, 2010).

Demembranation studies on sea urchin spermatozoa showed that Ca^{2+} ion modulates flagellar curvature. Brokaw *et. al.,* (1975) performed experiments on sea urchin using increasing Ca^{2+} concentrations in reactivation media. It was observed that as Ca^{2+} concentration increased, the sperm trajectories also increased. This observation suggested that Ca^{2+} controls flagellar beat asymmetry by directly acting on the axoneme. The main action of Ca^{2+} on the axoneme is to convert linear symmetrical beating pattern into non-linear and asymmetrical beating pattern, called hyperactivation

(see section 1.4 for more detail). Additionally, a recent study by O'Rand and Widgren (2012) showed that intracellular Ca^{2+} loss through EPPIN consequently results in loss of progressive motility of human spermatozoa. EPPIN coats human spermatozoa and during ejaculation it binds to SEMG1 that inhibits progressive motility by decreasing intracellular Ca^{2+} concentration (O'Rand and Widgren, 2012). Therefore, it is believed that Ca^{2+} has important regulatory function on human sperm motility other than controlling hyperactivation. However, it is possible that the actions of Ca^{2+} on controlling progressive motility can be closely associated with the capacitation.

1.2.1.2 Mitochondrial sheath

Mitochondria that are found in the mid-piece can have multiple functions in sperm, which is entirely different from mitochondria in somatic cells. These organelles are appropriately positioned to control Ca^{2+} buffering in mouse sperm and Ca^{2+}-ATPases are associated with the giant mitochondrion in sea urchin sperm (Wennemuth *et. al.*, 2003; Gunaratne and Vacquier, 2006). Therefore, it is believed that mitochondria might have a role in Ca^{2+} homeostasis. However, mitochondrial uncouplers were found to have no effect on Ca^{2+} signals of human sperm stimulated with progesterone (Harper *et. al.,* 2004). Consequently, it is unclear if mitochondria have a role in controlling human sperm motility through Ca^{2+} signalling.

1.2.2 cAMP control of motility

Pharmacological evidence suggests that phosphorylation of several residues on axonemal proteins is associated with flagellar motility regulation. Central to these phosphorylation cascades is the PKA, as well as secondary messengers cAMP and Ca^{2+}. Soluble adenylyl cyclase is the enzyme responsible for producing cAMP from ATP. This enzyme has unique features including insensitivity to forskolin and G-protein modulation (Buck *et. al.,* 2001). However, a recent study by Wertheimer *et. al.,* (2013)

showed that mice sperm have tmAC activity only on the sperm head. This finding suggests compartmentalization of cAMP signalling, which may be important in controlling acrosome reaction (Wertheimer *et. al.,* 2013). Therefore, understanding the control of cAMP concentration and its downstream actrions are crucial.

1.2.2.1 Bicarbonate stimulation

Seminal plasma (70-80% of the ejaculate) is bicarbonate rich. Effects of bicarbonate are best illustrated on mice sperm. Experiments show that demembranated epididymal sperm (poorly motile) diluted in media lacking bicarbonate remain poorly motile. However, when cAMP (together with ATP) is added to the test medium mice sperm motility increases (Si and Okuno, 1999). Additionally, it was shown that adding intact epididymal mice sperm to bicarbonate rich media results in the induction of motility (Si and Okuno, 1999). This result is the same for porcine, human, bovine, rat, dog, and bull sperm (Okamura *et. al.,* 1985; Garty *et. al.,* 1987; Rojas *et. al.,* 1992). Following bicarbonate stimulation, cAMP is no longer required for the maintenance of motility. These results suggest that cAMP is the central regulatory secondary messenger required for sperm motility induction and cAMP production is initiated by bicarbonate stimulation. The main effects of bicarbonate on sperm cells are; increased pH, stimulation of respiratory activity, opening of voltage-gated Ca^{2+} channels, and direct activation of sAC (Jaishwal and Conti, 2001; Wennemuth *et. al.,* 2003). Increase in cAMP and Ca^{2+} consequently induces and maintains sperm motility.

1.2.2.2 Phosphodiesterases

Phosphodiesterases (PDE) are the enzymes responsible for hydrolysing cAMP into 5'-AMP or cGMP into 5'-GMP. Therefore, they have very important functions on sperm. Pharmacological experiments on human sperm show that PDE inhibitors are effective in stimulating sperm motility (Wennemuth *et. al.,* 2002). Human sperm motility was observed to increase by treating sperm with caffeine or pentoxifylline (first

generation PDE inhibitors) at high concentrations (1-10mM, Rees *et. al.,* 1990; Yovich *et. al.,* 1990; Pang *et. al.,* 1993). There are different subtypes of PDEs located within the sperm controlling different functions of sperm cells. PDE type 4 is located mainly on the mid-piece and it is proposed to control motility, whereas type 1 PDE is distributed along the sperm head and it is proposed control acrosome reaction (Fisch *et. al.,* 1998). PDE type 1 family is a calcium-calmodulin dependent enzyme that has higher affinity for hydrolysing cGMP although it can also hydrolyse cAMP (Beavo, 1995). PDE type 4 family, on the other hand, is a cAMP-specific enzyme and it is controlled by phosphorylation of residues on the enzyme (Conti *et. al.,* 1995). Second generation PDE inhibitors IBMX and Rolipram, identified by Fisch *et. al.,* (1998), were both shown to modulate human sperm motility or acrosome reaction discretely. However, there is a lack of research in identifying third generation PDE inhibitors, which could ignite dramatic changes in clinical embryology. Developing/finding new PDE inhibitors that specifically affect selected sperm function would be highly valuable in clinical embryology in shifting the current situation into *in vivo* treatment options.

Lefievre *et. al.,* (2000) showed that sildenafil (IC_{50}= 4nM, PDE type 5 specific inhibitor) treatment at 30μM, 100μM, and 200μM increases intracellular cAMP concentration and stimulates both capacitation and motility of human spermatozoa without stimulating acrosome reaction. However, Lefievre *et. al.,* (2000) suggested that, the increase in motility and stimulation of capacitation in response to sildenafil is via its inhibitory action on PDE activity other than PDE type 5 specific inhibition. Richter *et. al.,* (1999) identified mRNA transcripts of 6 different PDEs from ejaculated human spermatozoa. These PDEs are PDE type 1-A/B/C, PDE type 2, PDE type 3-A/B, PDE type 4-A/B/C, PDE type 5, and PDE type 7. It is possible that these mRNA transcripts remained intact through spermiogenesis. However, as spermatozoa are believed to be transcriptionally and translationally silent, the presence of some of these 6 PDE

enzymes is questionable in the mature sperm. As different subtypes of PDEs are located at different location and each have different modulators, it can be said that spatio-temporal regulations of different types of PDEs can result in spatio-temporal cAMP concentration fluctuations in order to respond to extracellular stimulation. It was shown that using PKA selective antagonist H89 completely inhibits sperm motility stimulated with bicarbonate (Holt and Harrison, 2002). Therefore, the main action of cAMP is to activate PKA.

	Km (μM)					
Family	**cAMP**	**cGMP**	**Number of Genes**	**Property**	**Specific Inhibitors**	**IBMX sensitivity**
PDE1	1-30	3	3	Calcium-Calmodulin activated	8-methoxy IBMX, phenothiazines, Nimodipine	+
PDE2	30-100	10-30	1	cGMP activated	EHNA	+
PDE3	0.1-0.5	0.1-0.5	2	cGMP inhibited	Cilostamine, Milrinone	+
PDE4	0.5-4	>50	4	cAMP specific	Rolipram, Ro 20-1724, Roflumilast, Ariflo	+
PDE5	>40	1.5	1	PKA/PKG phosphorylated	Zaprinast, DMPPO, E4021, Sildenafil	+
PDE6	2000	60	4	Transducin activated	Zaprinast, DMPPO, E4021, Sildenafil	+
PDE7	0.2	>1000	2	cAMP high affinity, Rolipram insensitive	BRL 50481, ICI242	+
PDE8	0.7	>100	2	cAMP high affinity, Rolipram insensitive	-	-
PDE9	>100	0.07	1	cGMP high affinity	-	-
PDE10	0.5	3	1	Dual substrate	-	+
PDE11	1	0.5	1	Dual substrate	-	+

Table 1.1: PDE families. 11 PDE families; their names, their affinities for substrates, their number of genes, their selective inhibitors, and their sensitivity for IBMX are shown. Table is adapted from Mehats *et. al.*, 2002 and Lugnier, 2006.

1.3 Capacitation

Spermatozoa from mammals are not able to fertilize oocytes immediately after ejaculation. Two independent experiments showed that rabbit sperm are not able to fertilize oocytes in the fallopian tubes without a period of time spent in the female reproductive tract (Chang, 1951; Austin, 1951). In other words, sperm cells acquire the capacity to fertilize oocytes only after a period of time in the female reproductive tract (which varies from species to species). The acquisition of capacity to fertilize an oocyte is accompanied by various physiological, biochemical, and molecular changes through highly complex signal transduction is termed “capacitation” (Figure1.2; Chang, 1952; Austin, 1951). Markers of the capacitation process are lipid rearrangements in the plasma membrane, ion fluxes resulting in alteration of E_m, and increased tyr phosphorylation of proteins involved in induction of hyperactivation and acrosome reaction. It is very important to understand the physiological mechanics of this central process, as this is a key process for fertilization.

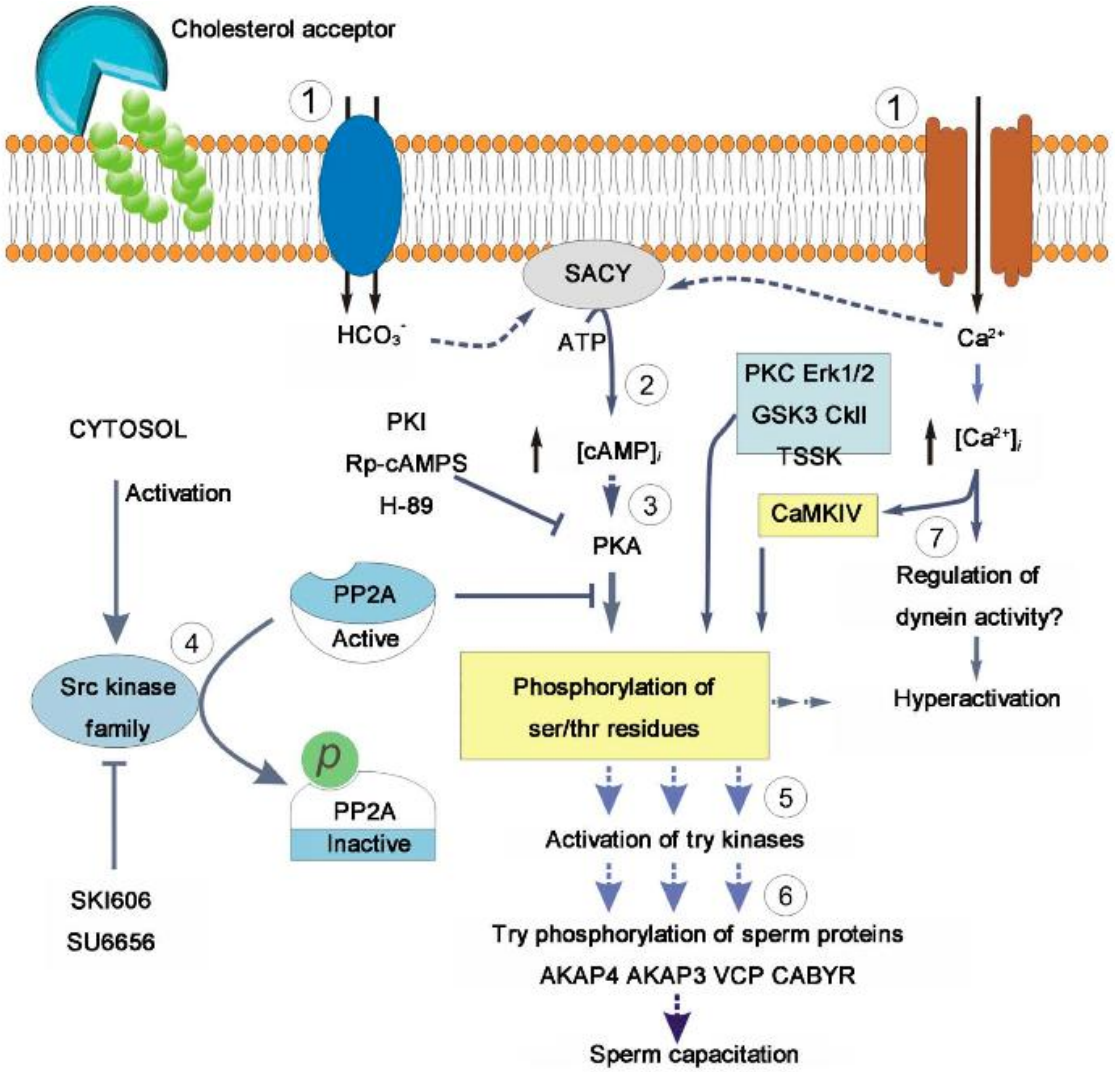

Figure 1.2: Biochemical pathways involved in capacitation. 1) Transport of bicarbonate and Ca^{2+} ions stimulate sAC (SACY). 2) Intracellular cAMP levels increase. 3) Secondary Messenger cAMP activates PKA (could be inhibited by PKA selective inhibitors H89/Rp-cAMPs/PKI). 4) Enzymes phosphorylated by PKA are subject to regulation by phosphatases, likely PP2A, that in turn regulated by Src kinases (could be inhibited by SKI606/SU6656). 5) PKA activates unidentified protein kinases that (6) phosphorylates try residues on target proteins/enzymes such as AKAPs and CABYR. 7) Ca^{2+} influx possibly regulates dynein activity that leads to hyperactivation. Figure is taken from Visconti *et. al.*, 2011.

1.3.1 Molecular basis of capacitation

Although it has been 62 years since the capacitation was discovered, the molecular mechanisms underlying capacitation remains largely unknown. Most if not all of the studies about capacitation were done under *in vitro* conditions, therefore, it

should be noted that further experiments will be required to confirm *in vitro* findings are reproducible under *in vivo* conditions. The capacitation process can be divided into two events, fast events and slow events, that require the presence of bicarbonate, cholesterol acceptor (albumin, high-density lipoproteins (HDL), and apolipoproteins), and Ca^{2+} ion (Aitken and Nixon, 2013). However, it was shown that none of these factors are probably essential for tyr phosphorylation (Aitken *et. al.,* 1998; Baker *et. al.,* 2004; Ecroyd *et. al.,* 2004). Increased tyr phosphorylation has been reported to correlate with capacitation in mouse, hamster, bovine, pig, and human sperm (Visconti *et. al.,* 1995; Devi *et. al.,* 1999; Galantino-Homer *et. al.,* 1997; Kalab *et. al.,* 1998; Luconi *et. al.,* 1996).

1.3.1.1 Fast events

Fast events can be summarized by; transfer of bicarbonate through Na^+/bicarbonate co-transporter (Demarco *et. al.,* 2003), activation of sAC resulting in increased cAMP levels (Chen *et. al.,* 2000), activation of PKA resulting in modulation of CatSper therefore changes in E_m (Wennemuth *et. al.*, 2003), activation of scramblases (Harrison *et. al.,* 1996; Gadella and Harrison, 2002), and increased availability of cholesterol for external acceptors (Flesch *et. al.*, 2001). Sperm cells are exposed to a significant increase in bicarbonate ion concentration after deposition into the vagina (Setchell *et. al.*, 1994). There are various studies, which confirm that bicarbonate is the key agent required for capacitation (Boatman and Robbins, 1991; Gadella and Harrison, 2000; Lee and Storey, 1986; Neil and Olds-Clarke, 1987; Shi and Roldan, 1995; Visconti *et. al.*, 1995). Bicarbonate is also the key agent mediating the fast events of capacitation through the bicarbonate/sAC/cAMP/PKA pathway. Bicarbonate transport into the cell results in an increase in pH, however, the role of pH is not well understood (Parrish *et. al.*, 1989; Zeng *et. al.*, 1996; Demarco *et. al.*, 2003). The main role of

bicarbonate is to stimulate sAC to increase intracellular cAMP concentration (Garbers *et. al.,* 1982). In turn, cAMP activates PKA. cAMP levels rise to its maximal levels by 60 seconds in boar sperm (Harrison and Miller, 2000) and PKA-dependent phosphorylation levels begins in 90 seconds (Harrison, 2004). Following these series of events, cAMP concentration and PKA-catalysed protein phosphorylation starts to fluctuate (7 minutes intervals) due to the activation of phosphodiesterases by PKA (Hanoune and Defer, 2001; Mehats *et. al.,* 2002).

Mammalian sperm cells appear to have asymmetrical phospholipid architecture (Pomorski *et. al.,* 1995; Nolan *et. al.,* 1995; Gadella *et. al.,* 1999). Experiments on boar sperm revealed that physiological levels of bicarbonate under *in vitro* conditions induce a collapse in phospholipid asymmetry (Harrison *et. al.,* 1996). Harrison *et. al.* (1996) showed that the direct staining of PE and PS is subsequently detectable. Normally, PE and PS are found only in the inner leaflet of the plasma membrane. This finding suggests that the enzymes responsible for this collapse appear to be activated by the bicarbonate/sAC/cAMP/PKA pathway. This stainability starts to be detectable quite rapidly (2 min). Therefore, it is certain that there are fast events during the capacitation that involves changing the architecture of phospholipid structure among the sperm plasma membrane bilayer.

1.3.1.2 Slow events

Surprisingly, slow events are also regulated by the bicarbonate/sAC/cAMP/PKA pathway with the only exception of the requirement of a cholesterol acceptor, albumin. In the absence of albumin, slow events of the capacitation are not initiated (Salicioni *et. al.,* 2007). It was found that cholesterol depletion does not initiate without bicarbonate induced phospholipid scrambling (Flesch *et. al.,* 2001). Therefore, albumin is only required for cholesterol depletion. After the initial increase in cAMP levels with

fluctuations in temporal concentrations, cAMP levels follow a more sustained increase in concentration. This more sustained level of cAMP concentration enables the slow events of capacitation to take place. However, the mechanism(s) that allow such complex events in a minute amount of cytoplasm is not understood (Salicioni *et. al.,* 2007). Most of the slow events of capacitation involve phosphorylation of tyr residues on proteins, which start to be detected by 45 min in mouse sperm (Visconti *et. al.,* 1995). PKA is a ser/thr kinase; therefore, tyr residues cannot be phosphorylated by PKA directly. This explains why try phosphorylation is a slow event and it can be related to the sustained concentration phase of cAMP. This is supported by experiments on mice that lack sAC (knockout), show no tyr phosphorylation (Esposito *et. al.*, 2004). The primary kinase responsible for tyr phosphorylation is the SRC family kinases both in mice and human sperm (Aitken and Nixon, 2013). There are several crucial differences in the function and localization of Src between mice and human sperm (Varano *et. al.,* 2008). Inhibition of mouse Src results in inhibition of hyperactivation (Baker *et. al.,* 2006). Conversely, inhibition of the human Src has no effect on hyperactivation but inhibits the progesterone-induced acrosome reaction (Varano *et. al.*, 2008). Recent experiments showed that cAMP/PKA activation should be supported by ser/thr phosphatase suppression that requires the Src family kinases in human sperm (Battistone *et. al.*, 2013). This finding suggests that phosphorylation events associated with PKA should be prolonged for capacitation by downregulating phosphatases.

1.3.2 Calcium and capacitation

Capacitation of mammalian sperm is a Ca^{2+} dependent process in both the fast and slow events. Ca^{2+} has both negative and positive effects throughout the capacitation process. Ca^{2+} calmodulin can activate AC to promote the synthesis of cAMP, and therefore promote capacitation (Gross *et. al.*, 1987). Oppositely, Ca^{2+} binds to the

regulatory subunit of PDEs to promote the hydrolysis of cAMP, therefore down regulating the capacitation (Wasco and Orr, 1984). Nevertheless, it is believed that the Ca^{2+} concentration is crucial for the capacitation dependent functions of sperm such as acrosome reaction or hyperactivation. There are some studies on human (Leclerc *et. al.,* 1998) and mouse (Visconti *et. al.,* 1995) sperm suggesting that increasing the extracellular Ca^{2+} concentration correlates with increased try phosphorylation. Conversely, there are other studies, which suggests the opposite where increasing the extracellular Ca^{2+} concentration negatively correlates with try phosphorylation (Luconi *et. al.,* 1996; Carrera *et. al.,* 1996; Baker *et. al.,* 2006). Additionally, a recent study by Tateno *et. al.,* (2013) showed that Ca^{2+} ionophore A23187 could make mouse sperm capable of fertilizing cumulus intact oocytes even before activating the cAMP-dependent phosphorylation pathways (i.e. try phosphorylation). Mouse sperm incubated with A23187 were immobilized (due to excessive intracellular Ca^{2+} levels) however, upon removal of A23187, sperm gained motility and were able to fertilize cumulus intact oocytes within 30 minutes. This finding is important, as tyr phosphorylation events in mouse sperm do not start before 45 minutes (Visconti *et. al.,* 1995). Therefore, increase in intracellular Ca^{2+} levels were shown to bypass cAMP-dependent capacitation events in mouse sperm and enabled "non-capacitated" spermatozoa to fertilize oocytes *in vitro*. This finding is confirmed with ionophore treated mouse sperm were able to fertilize oocytes even in the presence of H89 (i.e. there is no PKA-dependent phosphorylation events). Therefore, it is clear that Ca^{2+} is a critical secondary messenger controlling capacitation.

1.4 Hyperactivation

As hyperactivation is required for fertilization, it is also considered to be a part of capacitation. However, this definition is controversial as non-capacitated bovine and human sperm are able to hyperactivate (Ho and Suarez, 2001; Marquez and Suarez, 2004; Bedu-Addo *et. al.,* 2008). Therefore, hyperactivation may be regulated by different mechanisms than that of capacitation, although it is possible that they are closely related.

1.4.1 Definition and importance of hyperactivation

Hyperactivated motility is described as asymmetrical bending of flagella, increased amplitude of head displacement, and decreased linearity (Yanagimachi, 1970). The result of this movement is reduced linearity of the sperm trajectory but an increase in thrust that is necessary for cumulus and zona pellucida penetration (Stauss *et. al.,* 1995; Suarez *et. al,* 1991; Ren *et. al.,* 2001). Not surprisingly, increased propulsion generated by hyperactivated motility is associated with fertility both *in vitro* and *in vivo* (Johnston *et. al.,* 1994). It has been suggested that sub-fertile males have lower hyperactivation levels (Munire *et. al.,* 2004). Another study by Liu *et. al.* (2007) showed that hyperactivation of capacitated sperm showed high correlation with the zona pellucida-induced acrosome reaction. This finding is important, as the human zona-binding assay has been proven to be a good diagnostic tool (Barratt *et. al.,* 2010). Furthermore, the basal human sperm hyperactivation levels have been found to correlate with fertilization rates in IVF (Wang *et. al.,* 1993; Alasmari *et. al.,* 2013; see chapter 2) and artificial insemination (Johnston *et. al.,* 1994). Hyperactivated motility is also listed as one of the influential factors for sperm quality that can be measured reasonably well (Amann and Hammerstedt, 1993).

1.4.2 Function of hyperactivation

As defined above, hyperactivation has potential clinical value and shown to be an indicator of fertilization both *in vitro* and *in vivo*. The reason why hyperactivation has a value in reproductive biology/medicine is as it has 4 critical functions that are prerequisites of successful fertilization. These functions are; (i) hyperactivation enables effective passage through viscous oviductal mucous, (ii) hyperactivated motility enables spermatozoa to be released from epithelial cells of the lumen of the oviduct, hyperactivation enables sperm to penetrate (iii) cumulus cells and (iv) zona pellucida.

Hyperactivated mouse and hamster sperm show a non-progressive and vigorous beating of flagella in non-viscous media whereas in viscous media it shows a progressive swimming (Suarez *et. al.,* 1991; Suarez and Dai, 1992). Therefore, it is believed that only the hyperactive sperm are able to swim through viscous media. However, recent experiments by Alasmari *et. al.,* (2013) demonstrated that human sperm induced with progesterone or ammonium chloride that did not induce hyperactivation showed increased penetration into methylcellulose (viscous media mimicking cervical mucus or cumulus matrix). Penetration into methylcellulose was sensitive to NNC55-0396 treatment, indicating a role for CatSper. Ca^{2+} store mobilizing agents thimerosal and 4-AP caused high hyperactivation levels, however, only 4-AP showed penetration into methylcellulose in a NNC55-0396 sensitive manner. This study suggests that the hyperactivated motility may not be involved in penetration into the viscous media and Ca^{2+} originating from different sources can determine the sperm motility pattern in human sperm.

In vitro experiments demonstrate that human sperm binds to the epithelial cells of the fallopian tubes (Pacey *et al.,* 1995; Baillie *et. al.,* 1997). This binding has been proposed to hold the sperm cells in a quiescent state to preserve their motility (i.e. their

survival) until the time of ovulation (Suarez *et. al.*, 1992; Suarez, 2008; Holt and Fazeli, 2010; Bjorndahl *et. al.*, 2010). Spermatozoa were originally observed to attach-to and detach-from epithelial cells (Pacey *et. al.*, 1995). Furthermore, it was observed that the sperm detaching from epithelial cells were observed to show higher ALH and VCL, and lower LIN, which is the definition of hyperactivated motility. This implies that the hyperactivated motility is required in order to free the bound spermatozoa into the lumen of the oviduct (Suarez, 2008; Demott and Suarez, 1992; Ho *et. al.*, 2009).

In vivo oocytes are surrounded by cumulus cells that support its development. These cells are linked together with proteins, as well as hyaluronic acid, that form an elastic matrix. There are hyaluronidase enzymes on the sperm head that degrade hyaluronic acid (Kim *et. al.*, 2008) however; enzymatic degradation is insufficient for penetrating through this matrix. Therefore, increased thrust by hyperactivation is also required for efficient penetration (Suarez and Dai, 1992). However, there are some species differences. For example, frog and hamster sperm were observed to penetrate the extracellular matrix of hamster oocyte cumulus complexes without hyperactivating (Talbot *et. al.*, 1985; Drobnis *et. al.*, 1988), indicating that hyperactivated motility may not be fundamental to penetrating cumulus cells.

Zona pellucida is a glycoprotein complex that surrounds the egg. This glycoprotein complex is the last obstacle that sperm must penetrate with the aid of acrosomal enzymes and hyperactivated motility to achieve fertilization. CatSper knockout mice sperm studies show that spermatozoa unable to hyperactivate (but showing normal acrosome reaction and motility) cannot fertilize zona-intact oocytes. However, when the zona pellucida of the oocytes was removed, the sperm were able fertilize the eggs, despite the inability to hyperactivate (Quill *et. al.*, 2003; Ren *et. al.*, 2001). This clearly

demonstrates that hyperactivation is required for penetrating the zona pellucida in mice sperm.

1.4.3 Control of hyperactivation

As sperm cells have no endoplasmic reticulum, minimal amount of cytoplasm, and highly compact genetic material they are believed to be transcriptionally and translationally inactive (Costello *et. al*., 2009). Control of hyperactivation therefore has to rely on modifying and changing the activity of proteins or enzymes that are already present. Hyperactivation is a directionless movement pattern in non-viscous media and have several critical physiological functions (see above). Therefore, its activation and inactivation should be tightly regulated. Post-translational modifications that control hyperactivation by secondary messengers (cAMP and Ca^{2+}) are tightly bound to extracellular stimuli. Among these secondary messengers, the Ca^{2+} ion appears to be the crucial one (Publicover *et. al.,* 2007). Indeed, hyperactivation appears to be only controlled by Ca^{2+} by acting directly on the cytoskeletal components of the axoneme and by binding to calmodulin/calmodulin binding proteins to alter their function (Ho *et. al.,* 2002; Ignotz and Suarez, 2005). However, the exact functional mechanism of Ca^{2+} signalling and how it controls hyperactivation is not entirely known. Demembranation studies performed by Ho *et. al.* (2002) on bull spermatozoa showed that Triton X-100 treatment disrupts the plasma membrane, acrosomal vesicles, and mitochondrial membranes leaving the nucleus, cytoskeletal elements and proteins that are associated to these structures intact. This treatment abolishes sperm motility but under the presence of ~50 nM Ca^{2+} and ATP, motility can be rescued. Increasing the Ca^{2+} concentration to ~100 nM resulted in the development of hyperactivation expressed by 40% of the cells, and further increase in Ca^{2+} concentration to ~400 nM resulted in 80% of the cells hyperactivated.

Some studies support a crucial role for tyr phosphorylation in hyperactivation (Segare-Patil *et. al.,* 2012). As a result, cAMP might be hypothesized to carry important regulatory functions on hyperactivation. However, non-specific PDE inhibitors such as procaine and caffeine induce hyperactivation before tyr phosphorylation (Marquez and Suarez, 2004). Furthermore, H89 and Rp-cAMPS, both relatively selective PKA inhibitors, blocks bicarbonate/sAC/cAMP/PKA resulting in lack of tyr phosphorylation but do not inhibit hyperactivation. Therefore, the role of cAMP on controlling hyperactivation remains unclear, whereas Ca^{2+} is clearly the main secondary messenger that controls hyperactivation in mammalian spermatozoa. As Ca^{2+} is the secondary messenger that controls hyperactivation, the source of Ca^{2+} merits further investigation.

1.4.3.1 CatSper

CatSper channels are encoded by 4 CATSPER genes that are specifically expressed in testis (Quill *et. al.,* 2001; Ren *et. al.,* 2001; Carlson *et. al.,* 2003). CatSper 1-2-3-4 form a pore together with the CatSperβ, CatSperγ, and CatSperδ auxiliary subunits, where the pore forming CatSper 1-4 resembles the Ca_v channels (Arias *et. al.,* 2003; Chung *et. al.,* 2011; Jin *et. al.,* 2005; Liu *et. al.,* 2007; Quill *et. al.,* 2001; Lobley *et. al.,* 2003; Ren *et. al.,* 2001; Wang *et. al.,* 2009). Each of the CatSper 1-2-3-4 has 6 transmembrane segments. CatSper 3 and 4 has the typical positively charges residues on the 4^{th} transmembrane segment. This explains why the channel is mildly voltage-sensitive. CatSper1 on the other hand has a histidine rich N-terminal (cytoplasmic site) which enables post-translational changes in response to the pH (Ren *et. al.,* 2001). CatSperβ and CatSperγ auxiliary units are absent in the CatSper1 knockout sperm (Liu *et. al.,* 2007; Wang *et. al.,* 2009). This strongly suggests that these auxiliary units form a complex with the CatSper1 protein. CatSperβ and CatSperγ are believed to serve as a regulatory unit of the CatSper complex as they have large extracellular binding domains. CatSperδ knockout sperm show a remarkable decrease in the amount of

CatSper1, indicating a role for the expression of CatSper proteins on the transcription level (Ren *et. al.,* 2001).

CatSper knockout studies in mouse show that all of the CatSper subunits are required for fertility (Ren *et. al.,* 2001; Jin *et. al.,* 2005; Jin *et. al.,* 2007; Qi *et. al.,* 2007). These CatSper knockout mouse sperm show normal capacitation and motility except for hyperactivation. Fertilization capacity of the knockout sperm is restored upon zona removal (i.e. removal of the final barrier that requires hyperactivation to penetrate, Ren *et. al.,* 2001). These experiments showed very clearly that the CatSper channels are essential for hyperactivation in mouse spermatozoa and crucial for fertility. A study reported by Avidan *et. al.* (2003) showed that a human male with CATSPER2 gene mutation is infertile. The semen from this male shows normal (within WHO reference values) volume and sperm concentration but the motility was severely hampered and there were morphological defects on the tails. Another study on humans show that mutations on CATSPER1 gene results in infertility (Avenarius *et. al.,* 2009). Same phenotypical observations were found in these patients as CATSPER2 mutations. Therefore, these two studies suggest that maybe there are species differences between mice and humans on the function of CatSper as mouse knockout sperm were relatively normal. A very recent study by Smith *et. al.,* (2013) showed by patch-clamping that a human CatSper2-deficient patient had disrupted patch-clamp recording in response to progesterone. This confirms that the CatSper is indeed the principal Ca^{2+} channel in human sperm. This finding fills the gap partially between mouse models and humans. Due to technical challenges, researchers have, as yet, failed to clone and express a functional CatSper channel to examine and unlock all the mysteries of this polymodal channel. Therefore, our knowledge on CatSper is limited to the wild-type mice, CatSper knockout, and CatSper2-deficient human at the moment. It should be noted that mouse CatSper and human CatSper show some critical variation in the functionality, such as:

mice CatSper is not responsive to progesterone while human CatSper is highly responsive (Lishko *et. al.,* 2011*;* Strunker *et. al,* 2011). Therefore, findings on the mice model should be evaluated carefully.

CatSper channels are the main source of Ca^{2+} and they appear to be a polymodal sensor as they can be controlled by various compounds, pH, and E_m (Brenker *et. al.,* 2012). Progesterone also activates the CatSper channels by directly binding to the CatSper channels on an extracellular site on human sperm (Lishko *et. al.,* 2011*;* Strunker *et. al,* 2011). A study by Torres-Flores *et. al.* (2008) showed that incubating human sperm cells with papaverine (a non-selective PDE inhibitor) under non-capacitating conditions resulted in progesterone-induced Ca^{2+} influx similar to that of capacitated cells, whereas non-capacitated spermatozoa fail to respond as much. Additionally, the same group showed that progesterone-induced Ca^{2+} influx was inhibited by H89 and genistein (PKA inhibitors). This strongly suggests that progesterone-induced Ca^{2+} influx is regulated through bicarbonate/sAC/cAMP/PKA pathway. Hypothetically, there might be phosphorylation (or other post-translational) events that take place during the capacitation resulting in post-translational modifications required for the CatSper channels in order to bind progesterone.

1.4.3.2 Intracellular calcium stores

There are some studies, indicating that it is possible to induce Ca^{2+} signalling and hyperactivation in Ca^{2+} free media (Ho and Suarez, 2001; Ho and Suarez, 2003; Marquez *et. al.,* 2007). These findings challenged the original assumption of a lack of calcium store(s) in sperm. Sperm cells lack endoplasmic reticulum, which is the organelle responsible of storing Ca^{2+} in somatic cells. However, the acrosome and a store found in the neck/mid-piece region of the sperm are now acknowledged to serve as Ca^{2+} stores (Florman *et. al.,* 1998; Herrick *et. al.,* 2005; Bedu-Addo *et. al.,* 2007).

Pharmacological stimulation of sperm by Ca^{2+} releasing agents strongly suggests the existence of intracellular Ca^{2+} stores in the neck region (Ho and Suarez, 2001). Treatment of spermatozoa with caffeine (a non-specific PDE inhibitor), thimerosal (IP_3R agonist), and thapsigargin (inhibitor of SERCA) induces hyperactivation significantly in bull sperm. However, chelating extracellular Ca^{2+} below 50nM decreases the effect of caffeine on hyperactivation greatly, whereas the ability of thapsigargin and thimerosal to induce hyperactivation persists (Ho and Suarez, 2001). This finding strongly suggests the presence of intracellular Ca^{2+} store(s) that contributes to the control of hyperactivation. Another study by Ho and Suarez, (2003) hypothesized that the redundant nuclear envelope (RNE) could function as a Ca^{2+} store by showing that IP_3R and calreticulin localizes to the RNE. Inducing hyperactivation by the voltage-gated K^+ channel blocker 4-AP also involves stored Ca^{2+} mobilization and produces the highest level of hyperactivation (Costello *et. al.,* 2010, Gu *et. al.,* 2004). Although the effect of 4-AP is well known, the molecular target(s) is less clear, making deductions from cellular responses hard. Another broad-spectrum voltage-sensitive K^+ channel blocker TEA fails to induce hyperactivation (Gu *et. al.,* 2004) suggesting that the effect of 4-AP on sperm hyperactivation is not due to block of K^+ channels, but rather from another mechanism that is not fully understood. A study by Alasmari *et. al.* (2013) showed that the Ca^{2+} from stores and extracellular influx result in different types of sperm motility patterns and functionality in human sperm. The Ca^{2+} influx from CatSper causes weak induction of hyperactivation whereas the thimerosal treatment induces strong hyperactivation levels. All of the inducers (thimerosal, NH_4Cl, and progesterone) used in the aforementioned study produced a sustained intracellular Ca^{2+} response where the CatSper inducers were sensitive to NNC55-0369 inhibition but thimerosal was not (i.e. confirms store mobilization by thimerosal). Although Ca^{2+} store mobilizer treatment results in higher levels of hyperactivation, CatSper modulators

resulted in better penetration of sperm through viscous media. This finding suggests that the source of Ca^{2+} is important to both motility and function. However, how this is achieved is not known and is highly unusual considering the amount of cytoplasm in human sperm.

1.4.4 Physiological inducers of hyperactivation

As described, hyperactivation needs to be controlled spatio-temporally in order to achieve successful fertilization. Therefore, there must be follicular fluid or other female reproductive tract factors that trigger hyperactivation *in vivo*. Follicular fluid was shown to induce hyperactivation *in vitro* (Zhu *et. al.,* 1994a). Cumulus cells secrete progesterone and it is known that it can diffuse across the fallopian tubes to reach oviduct ampulla (Ralt *et. al.,* 1991). A very recent study attempted to shed light on how progesterone controls the acrosome reaction and hyperactivation discretely. Progesterone at low concentrations (10nM and 100nM) induced sperm motility and activates tyr kinase activity whereas at higher concentrations (1-10μM) it induced hyperactivation and acrosome reaction (Sagare-Patil *et. al.,* 2012). Furthermore, photo-release of caged-progesterone stimulated hyperactivation of human sperm (Kilic *et. al.,* 2009). Although there has been some progress in our understanding of *in vivo* stimulators of hyperactivation, we still do not have a good understanding. It has been suggested that progesterone is also involved in the chemotaxis of human sperm (Oren-Benaroya *et. al.,* 2008). Furthermore, there is evidence suggesting that the hyperactivated motility is involved in setting the human sperm in the right course during chemotaxis in response to physiological concentrations of progesterone (Armon and Eisenbach, 2011).

1.5 Infertility

In order to achieve successful conception, a spermatozoon must perform almost perfectly in every aspect of sperm function. Therefore, not surprisingly, infertility is a common, significant, and a growing global problem (Sharpe and Irvine, 2004; Slama *et. al.,* 2012). There are number of reports that have raised serious concerns about the development of reproductive problems (Cadbury, 1997; Sharpe, 2012). Furthermore, there are studies that show controversial results on semen quality (Carlsen *et. al.,* 1992; Auger *et. al.,* 1995; Irvine *et. al.,* 1996).

1.5.1 Definition, prognosis, diagnosis, and treatment of male infertility

The definition of infertility itself is subject to debate. However, it is generally accepted that infertility is defined by WHO as a failure to achieve pregnancy within 12 months of regular unprotected intercourse (Cooper *et. al.,* 2010). "Normally" fertile couples anticipate pregnancy rates of approximately 30%/month with 85% of these couples achieving a pregnancy within a year (Spira, 1986; Ford *et. al.,* 2000; Thonneau *et. al.,* 1991). In men there is no sperm storage, whereas in most animals there is. Therefore, men's sperm concentration is completely dependent on the concentration of the sertoli cells, and the abstinence period. The sertoli cell concentration is fixed during development whereas the abstinence period is variable. Another factor is that even in "normal" men, only a small fraction of sperm is morphologically "normal" (5-15% depending on the criteria used) whereas in most animals 90% of spermatozoa is considered to be morphologically "normal" (i.e. pleiomorphism). Morphological assessments generally do not tell if a sperm is "normal or not". In not so frequent cases, morphological assessment can indicate the fertilization potential, especially in cases of flagella defects and globozoospermia (<0.1%, Dam *et. al.,* 2007). Furthermore, human

sperm identified as “normal” by strict morphology criteria (Kruger’s) were shown to have poor genetic quality (Ryu *et. al.*, 2001).

Over 80 million couples worldwide are infertile (Boivin *et. al.*, 1997; Slama *et. al.*, 2012). The single most common cause for infertility is male factor infertility, which accounts for 1 in 15 men of reproductive age (HFEA 2011, www.hfea.gov.uk). Despite the importance, very little is known about the factors that cause sperm dysfunction due to an incomplete understanding of sperm physiology. Our relatively limited understanding about sperm function has thus disadvantaged the development of drugs to treat male factor sub-fertility. Therefore, patients with sperm dysfunction have no treatment option, other than Assisted Reproductive Technologies (ART), which are invasive and may bypass the selection processes performed by the female reproductive tract (Holt, 2009). There are some concerns about the selection of sperm in cases of ICSI, which is used in the most severe cases of male factor infertility. However, ICSI treatment has been associated with increase in congenital birth defects (Davies *et. al.*, 2012; Tararbit *et. al.*, 2013) and imprinting disorders (Cox *et. al.*, 2002). Rather worrying, the usage of ICSI has increased dramatically and is used for 66% of total treatment cycles across Europe (Ferraretti *et. al.*, 2013). It should be noted that there are some countries, such as Turkey, which uses ICSI in 98% of total cycles (Ferraretti *et. al.*, 2012). The same scenario applies globally, as ICSI is the method of treatment in 65.6% of total cycles in Australia and New Zealand and 72.9% of total cycles in the USA (Ferraretti *et. al.*, 2013). Surprisingly, the male factor infertility diagnosis remained stable (Jain and Gupta, 2007). Therefore, increased usage of ICSI cannot be due to increased male factor infertility diagnosis. This situation is due to incorrect allocation of patients to the relevant treatment method. Supporting this statement, 53% of ICSI cycles in the USA were performed without the diagnosis of male factor infertility (CDC, 2011).

Prior to the introduction of ICSI in 1992, embryologists had to find alternative methods in order to increase the chances of a successful IVF cycle. These methods included pre-treatment of sperm with heat or pharmacological agents, including pentoxifylline (Mortimer and Mortimer, 1992; Tournaye *et. al.*, 1994). However, after ICSI was introduced into the mainstream clinical practice, embryologists now allocate this treatment for patients on the basis of sperm count, motility and/or morphology, yet without consideration of sperm function (Jain and Gupta, 2007; CDC, 2011). Therefore, it is critical to develop sperm functioning tests that are easy and efficient to perform, thus facilitating allocation of patients into the appropriate treatment methods.

Despite this importance, there are limited tools, which are available to diagnose or predict the fertilizing potential of a man. The most common method for diagnosis and prognosis is still the conventional semen analysis with the reference values provided by WHO (WHO, 2010). However, these reference values are based on statistical calculations on large populations of fertile and sub-fertile men. Furthermore, semen analysis is not an effective prognostic method for fertility, with the exception of progressive motility (Barratt *et. al.*, 1992; Barratt *et. al.*, 2011; Lefievre *et. al.*, 2007; Sanchez *et. al.*, 2013). However, there are other sperm function tests available such as the zona-binding assay, which were shown to correlate with fertilization rates (Barratt *et. al.*, 2011). Unfortunately, this test cannot be performed routinely as human material required for the test. Therefore, there is an urgent need to develop (and validate universal reference values) prognostic assays to address this very important problem, as male factor infertility is the commonest underlying cause of sub-fertility (Collins *et. al.*, 1983; Cates *et. al.*, 1985; Hull *et. al.*, 1985; Haxton and Black, 1987; Randall and Templeton, 1991; Thonneau and Spira, 1991; Schmidt *et. al.*, 1995).

1.6 Aims and objectives

The primary aim of this thesis was to re-assess the clinical significance of the hyperactivation and Ca^{2+} signalling assays. It is known that Ca^{2+} ions have pivotal role in sperm function and responsiveness of sperm in terms of Ca^{2+} signalling show relation with fertilisation success. Therefore, it was hypothesized that the ability of compounds to induce intracellular Ca^{2+} signalling can be used as a surrogate of physiological response to identify novel human sperm motility modulators. To address this, several objectives were followed:

- Assess the prognostic value of spontaneous- and agonist-induced-hyperactivation together with intracellular Ca^{2+} signalling in IVF.
- Document the intracellular Ca^{2+} signalling of Ibudilast, MMPX, Etazolate HCl, Tofisopam, and Papaverine and investigate their relationship with motility.
- Document the intracellular Ca^{2+} signalling responses of 223 compounds and categorize them accordingly to their relative responses with the progesterone response to identify the compounds causing strong Ca^{2+} influx.
- Investigate if drugs identified from the drug screening program has any effects on human sperm motility for the first time.

Chapter 2 : Investigation of Human Sperm Hyperactivation Levels and Intracellular Calcium Signalling and Their Relation with Fertilization Rates

2.1 Introduction

ICSI is the method used on the most severe cases of male factor infertility. However, allocation of patients into the correct ART method is challenging as even sperm from men with 'normal' semen parameters can show sperm dysfunction (Aitken *et. al.,* 1991). Furthermore, there is a dramatic increase in ICSI usage worldwide (see section 1.6.1 for more detail). Diagnosis as well as prognosis is done by semen analysis before fertility treatment, taking only concentration, motility, and morphology into consideration. However, these 3 parameters are poor indicators of the fertility status (see section 1.6.1 for more detail). Accordingly, there are studies, which investigated sperm functionality such as, hyaluran binding (Jakab *et. al.,* 2005; Huszar *et. al.,* 2003; Nijs *et. al.,* 2010; Sakkas, 2013), DNA fragmentation (Trisini *et. al.,* 2004; Daris *et. al.,* 2010; Lewis *et. al.,* 2013), and hyperactivation (Alasmari *et. al.,* 2013; Brenzik *et. al.,* 2013), which is believed to be better in predicting the fertilization outcome by assessing the functionality of sperm cells.

Hyperactivated motility is a directionless movement type that is critical for successful fertilization both *in vitro* and *in vivo* (see section 1.4.2 for more detail) and was proposed to be an indicator of IVF success (Alasmari *et. al.,* 2013; Brenzik *et. al.,* 2013). Hyperactivation should be tightly controlled in order to achieve successful fertilization (see section 1.4.3 for more detail). Alasmari *et. al.,* (2013) showed that spontaneous and 4-AP induced hyperactivation levels correlate significantly with fertilization rates in IVF. Another recent study demonstrated that progesterone-induced hyperactivation levels correlated significantly with fertilization rates in IVF (Brenzik *et. al.,* 2013). Furthermore, intracellular Ca^{2+} responsiveness of human sperm to 4-AP

(Alasmari *et. al.,* 2013) and progesterone (Falsetti *et. al.,* 1993; Krausz *et. al.,* 1995; Krausz *et. al.,* 1996; Alasmari *et. al.,* 2013) showed relationship with fertilization rates in IVF. However, severe cases of ICSI patients with very low sperm counts were not investigated in terms of intracellular Ca^{2+} signalling due to technical limitations. Consequently, there is no data available about the significance of Ca^{2+} defects in severe cases of ICSI patients. It is known that several compounds induce hyperactivation. Progesterone activates CatSper channels causing Ca^{2+} influx, thus hyperactivation of sperm (Lishko *et. al.,* 2011; Strunker *et. al.,* 2011; Marquez and Suarez, 2007; Chang and Suarez, 2011). Store-mobilizing agent 4-AP (a broad spectrum K^+ channel blocker, putative store mobilizer, also causes weak alkalization similar to NH_4Cl) also induce hyperactivation (Gu *et. al.,* 2004; Bedu-Addo *et. al.,* 2008). IBMX also stimulates hyperactivation through the cAMP/sAC/PKA pathway without inducing Ca^{2+} influx (Strunker *et. al.,* 2011).

In this study, progesterone, 4-AP, NH_4Cl, and IBMX were used to stimulate hyperactivation of sperm from healthy donors and sub-fertile patients. Furthermore, intracellular Ca^{2+} responses induced with progesterone and 4-AP were recorded. In this study, the clinical significance of induced hyperactivation assay and intracellular Ca^{2+} responses were re-visited by investigating a panel of patients undergoing IVF or ICSI treatment. Furthermore, severe cases of ICSI samples were tested in terms of induced hyperactivation and in terms of intracellular Ca^{2+} responses.

2.2 Materials and Methods

2.2.1 Experimental Design

Semen samples from healthy research donors, IVF patients, and ICSI patients were used in this study. Donor samples were used as a control for IVF and ICSI patients. For the sake of consistency, all of the samples were treated in the same way to enable correct comparison (see sperm preparation). Prepared samples were allowed to capacitate in capacitating medium (STF) for 2 hours. After this time, the samples were subjected to the hyperactivation assay with 4-AP, progesterone, IBMX, and NH_4Cl (see evaluation of hyperactivation) followed by the intracellular Ca^{2+} assay (see intracellular Ca^{2+} detection).

2.2.2 Media and Chemicals

Synthetic Tubal Fluid (STF) was used as the capacitating media (Mortimer, 1986). The components of STF were 4.7mM KCl, 3mM $CaCl_2$, 1mM $MgSO_4.7H_2O$, 106mM NaCl, 5.6mM D-Glucose, 1.5mM NaH_2PO_4, 1mM Na-pyruvate, 41.8mM Na lactate, 25mM $NaHCO_3$, 1.33mM Glycine, 0.68mM Glutamine, 0.07mM Taurine, Non-essential amino acids (1:100 dilution in STF) and 30mg/ml BSA. Non-Capacitating Buffer (NCB) was adapted from STF excluding the amino acids and $NaHCO_3$. The components of NCB were 5.4mM KCl, 1.8mM $CaCl_2$, 0.8mM $MgSO_4$.7H2O, 116.4mM NaCl, 5.6mM D-Glucose, 1.0mM NaH_2PO_4, 2.7mM Na-pyruvate, 41.8mM Na lactate and 25mM HEPES. The pH of NCB was adjusted to 7.4 with NaOH, and pH of STF was allowed to reach about 7.4 at 37°C and 5% CO_2 before usage. The osmolality of the buffers were checked to be between 290-320 mOsm/kg. Fresh STF and NCB were made at least weekly to avoid contamination. Experimental STF used on the FLUOstar assay was the

same as STF but lacking BSA as fura-2/AM binds to BSA resulting in background fluorescence.

4-aminopyridine (4-AP) (Sigma Aldrich, Catalogue number 275875-5G, UK) was dissolved in distilled water and used at 2mM final concentration. Progesterone (Sigma Aldrich, Catalogue number P8783-5G, UK) was dissolved in absolute ethanol and diluted with distilled water and used at 3.6µM final concentration. Ammonium chloride (NH_4Cl, Sigma Aldrich, Catalogue number 4316230J, UK) was dissolved in distilled water and used at 25mM final concentration. The Ca^{2+} indicator dye, fura-2/AM, was dissolved in DMSO and kept at -20°C at dark and used at 1µM final concentration. 1% Pluronic acid solution was made daily prior to usage.

2.2.3 Sperm Preparation

Patients were asked to produce semen samples at the Assisted Conception Unit, Ninewells Hospital on the same day of partner's egg collection. Samples were produced by masturbation into sterile plastic containers. Produced samples were allowed to liquefy at 37°C for 30 minutes. Liquefied samples were placed on to a separation density gradient (PureSperm buffered with Cook Sydney IVF Gamete Buffer, HEPES buffered media that do not support capacitation) and centrifuged at 300g for 20 minutes. The 40% fragment and majority of the 80% gradient was discarded (discarded fractions of consented patients were picked up and processed as research donors processed for the study, see below, figure 2.1). The 80% pellet was then washed with 5 ml of Cook Sydney IVF Gamete buffer for 10 minutes at 500g. If the patient was allocated to IVF, sperm from the wash stage was transferred to the Cook Sydney IVF Fertilization, bicarbonate buffered medium that supports capacitation, gassed with CO_2 and kept at room temperature for approximately 4 hours. IVF samples were then placed in incubation at 37°C and 5% CO_2 for 1 hour prior to insemination. If the patient was

allocated to ICSI, sperm from the wash stage was transferred to the Cook Sydney IVF Gamete buffer and kept at room temperature until the time of injection (approximately 4 hours).

Healthy research donors were asked to produce semen samples at home by masturbation into sterile plastic containers in 2-3 days of sexual abstinence. Samples were allowed to liquefy at 37°C for 30 minutes. If the sample was already liquefied upon arrival, then it was only incubated for 15 minutes at 37°C. 1ml of liquefied semen sample was placed on to a separation density gradient (2ml of 40% Percoll buffered with NCB on top of 2ml of 80% Percoll buffered with NCB) and centrifuged at 300g for 20 minutes. The 40% fragment and majority of the 80% gradient was discarded leaving about 2/3 of the 80% gradient on top of the 80% pellet to avoid contamination from the 40% fragment. The 80% pellet was then transferred into a 14ml Falcon tube containing 5ml of NCB and washed at 500g for 10 minutes. Washed sperm were then transferred into STF and allowed to capacitate for 2 hours at 37°C and 5% CO_2. Once the initial centrifugation done by the clinic, the surplus patient samples were collected and prepared in the same way as the donor samples were processed. Therefore, there is an additional 1 centrifugation step for the patients.

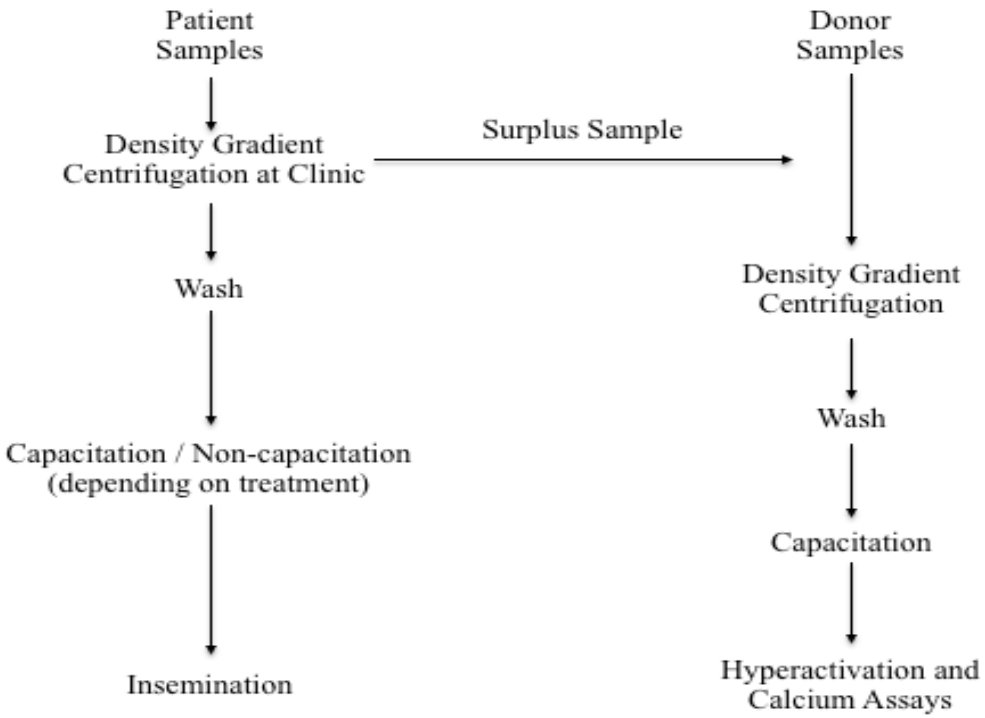

Figure 2.1: Preparation of samples. Surplus patient samples were collected from the clinic following the density gradient centrifugation. Surplus samples were then prepared as donor samples were prepared and subjected to the hyperactivation and Ca^{2+} assays.

Patients were allocated to ICSI or IVF in the light of the clinical implications and semen quality. In general, men with approximately $1x10^6$ motile cells after preparation were allocated to IVF and any men below this were allocated to ICSI.

2.2.4 Evaluation of Hyperactivation

Hamilton Thorne CASA system (Ceros, v12) was used to evaluate motility parameters including hyperactivation. The settings used for the instrument to detect human sperm were: 60 Hz; low and high size gates, 0.35 and 2.80, respectively; low and high intensity gate, 0.5 and 2 respectively; minimum number of data points, 13; non-motile head size, 6 pixels; non-motile head intensity, 160. The CASA parameters measured were as follows: the average path velocity (VAP: is the average path velocity measured in µm/s of smoothed cell path), the curvilinear velocity (VCL: is the average velocity in µm/s over the actual start-to-end track of the cell), the lateral head displacement (ALH:

is the lateral head displacement in μm), and the linearity (LIN: is the linearity of sperm path in ratio of VSL/VCL in %). The percentage of hyperactivated cells was assessed using standard criteria to identify hyperactivation: VCL ≥ 150 μm/s, linearity ≤ 50%, and ALH ≥ 7 (Mortimer *et. al.*, 1998). Progressive motility was assessed by VAP and LIN with the criteria of VAP ≥ 25 μm/s and LIN ≥ 80%. Concentration of the sperm samples was adjusted to be 20-30 million/ml during capacitation with STF to standardize all samples used for the study. At the time of analysis, sperm suspensions were homogenized gently and 4μl of sperm suspension was transferred to pre-warmed Hamilton-Thorn 2X-Cel chambers (20μm depth, Dual Sided Sperm Analysis Chamber, Hamilton Thorn Biosciences, Beverly, MA, USA) on a heated stage at 37°C. Slides were held on the heated stage for approximately 2 minutes and the motility parameters were taken. Minimum of 200 spermatozoa were analysed from 4 different chambers (i.e. 2 slides) from randomly selected fields to have statistical significance. Analysis was done under negative phase contrast trinocular optics by 10X magnification (final magnification 100X) on an Olympus CX21 light microscope with high resolution CCD camera.

Induced hyperactivation levels in response to 4-AP (putative store mobilizer), progesterone (CatSper activator), ammonium chloride (increased intracellular pH), and IBMX (AC/cAMP/PKA pathway) was detected by adding 1μl of inducer to 99μl of sperm suspension in STF. Suspensions were then kept at room temperature for 5 minutes (eppendorf tubes were tightly sealed) for the reaction to take place. After 5 minutes 4μl of sperm suspension was transferred to pre-heated slide and covered with pre-heated coverslip and allowed to reach 37°C for 2 minutes. The analysis was done as described above.

2.2.5 Intracellular Calcium Detection

Intracellular Ca^{2+} levels were measured fluorometrically using the Ca^{2+} indicator dye fura-2/AM (acetoxymethyl ester of fura-2). After the evaluation of sperm motility parameters, the concentration of sperm suspension was diluted to $6x10^6$ cells/ml with STF. 1µl of fura-2/AM was added to 500µl of sperm suspension giving a final concentration of 1µM fura-2/AM. Pluronic F-127 also added giving final concentration to 0.015% (vol/vol) and incubated at 37°C and 5% CO_2 for 40 minutes covered with foil (to ensure that the cells were not exposed to light). Following incubation, fura-2/AM was washed away by centrifugation at 500g for 10 minutes and the sperm were resuspended in Experimental STF at 37 C^o and 5% CO_2. Spermatozoa were then further incubated for 15 minutes to allow the de-esterification of fura-2/AM in dark 37C^o and 5% CO_2 incubator. Fluorescence measurements were carried out on a FLUOstar Omega device (BMG Labtech Offenburg, Germany) at 340 (Ca^{2+}-bound Fura-2) and 380nm (free Fura-2) excitation wavelength and emission at wavelength 510 nm. Aliquots of 95µl of samples were pipetted into a 96 well plate and 5µl of agonist was added after 100 seconds of data acquisition (20 readings) at the resting level (R). Following data acquisition manganese chloride at a final concentration of 10µM were injected to quench Fura-2/AM to eliminate background readings. The fluorimetric ratio between Fura-2-bound to Ca^{2+} and free Fura-2 indirectly indicates the intracellular Ca^{2+} levels. A minimum of ~150,000 cells were required per well for robust results. However, minimum of 250,000 cells were used in the assay for stronger fluorescent signals. dH_2O and ethanol were used as negative controls as 4-AP were dissolved in dH_2O and progesterone were dissolved in ethanol.

2.2.6 Definition of defective hyperactivation and Ca^{2+} response

Defective (failed) hyperactivation response was determined by standard deviation (SD), and considered to be defective where SDs were overlapping comparing basal and induced hyperactivation responses. Defective (failed) Ca^{2+} responses were determined by the cut-off values. If the maximum reading of the sample in response to 2mM 4-AP or 3.6μM progesterone fails to exceed the cut-off value, the Ca^{2+} response was considered as defective. Cut-off values for 4-AP and progesterone responses were calculated using the log transformed donor sample responses and the cut-off values were determined based on the maximum reading point around agonist injection point using SD. Using this approach, the cut-off values for progesterone and 4-AP were calculated to be 0.09 and 0.12, respectively.

2.2.7 Fertilization Rates

Fertilization rates were calculated as; fertilized number of eggs divided by the total number of inseminated eggs and multiplied by one hundred (expressed as %). Fertilization was defined as the formation of two pro-nuclei (2PN). Embryologists assessed the 2PN formation. As ICSI procedure bypasses natural means of fertilization dependent on sperm function, the fertilization rates were not taken into account in case of ICSI treatment. In order to reduce the influence of the number of eggs on the outcome of the study, only the IVF cycles with $\geq$ 4 mature oocytes were used on correlation calcuations. The average number of MII oocytes of IVF patients used in this study was 10.

2.2.8 Statistical Analysis

As majority of the data used in the study was greater than 20, it was possible to use D'agostino & Pearson test to assess the normality of the data (table 2.1). This test was

chosen, as it is the most accurate test available for normality assessment (Razali and Wah, 2011). In cases where the sample size was not enough, Shapiro-Wilk test was used, as it is an alternative test for testing the normality of the data. Correlations were assessed by Spearman (r_s; non-parametric) or Pearson (r_p; parametric) equation depending on the normality. Comparisons of groups were done with paired t-test (for normal distribution) or Wilcoxon test (for non-normal distribution). Results are expressed as the mean ± SD, median, and range for hyperactivation. All calculations were done using GraphPad Prism version 6 (GraphPad Software, La Jolla, CA, USA). Results with $p \leq 0.05$ were considered to be statistically significant. Sample powers (1-β error probability) were calculated using G*Power version 3.1 (G*Power Software, Germany) and considered to be adequate where $1-\beta > 0.80$. Sample sizes were calculated using G*Power version 3.1 software based on effect size, p value, and power (Faul *et. al.,* 2007).

Variable	Sample Size (n)	Mean	Median	Range	SD	Normality of the Data
Fertilization Rate (%)	23	59.73	60.00	0.0-100.0	26.05	Yes
IVF, Basal HA (%)	23	7.74	4.05	0.9-22.0	6.89	Yes
IVF, 4-AP induced HA (%)	22	19.50	16.38	1.4-56.5	15.00	Yes
IVF, Absolute Δ in 4-AP induced HA (%)	22	12.20	12.63	0.0-34.5	10.50	Yes
IVF, IBMX induced HA (%)	10	15.00	13.88	5.0-34.5	9.77	Yes
IVF, Absolute Δ in IBMX induced HA (%)	10	5.61	2.92	0.0-20.5	6.62	Yes
IVF, Progesterone induced HA (%)	23	12.25	12.00	0.0-35.5	8.82	Yes
IVF, NH_4Cl induced HA (%)	22	9.82	6.25	0.0-40.5	10.06	No

Table 2.1: Summary of the data used for the study. Table shows the samples size (n values), mean, median, standard deviation (SD), range, and normality of the data. D'agostino & Pearson test was used to assess normality of the data where sample size was greater than 20 and Shapiro-Wilk test used for the rest.

2.3 Results

2.3.1 Hyperactivation Levels and Efficacy of the Drugs

17 Donors, 25 IVF, and 9 ICSI patients were screened for spontaneous hyperactivation levels and induced hyperactivation levels in response to 4-AP, progesterone, ammonium chloride, and IBMX (figures 2.3-2.4-2.5). Spontaneous hyperactivation levels of IVF and ICSI patients were significantly different, with IVF patients having higher levels (p=0.0118, figure 2.2).

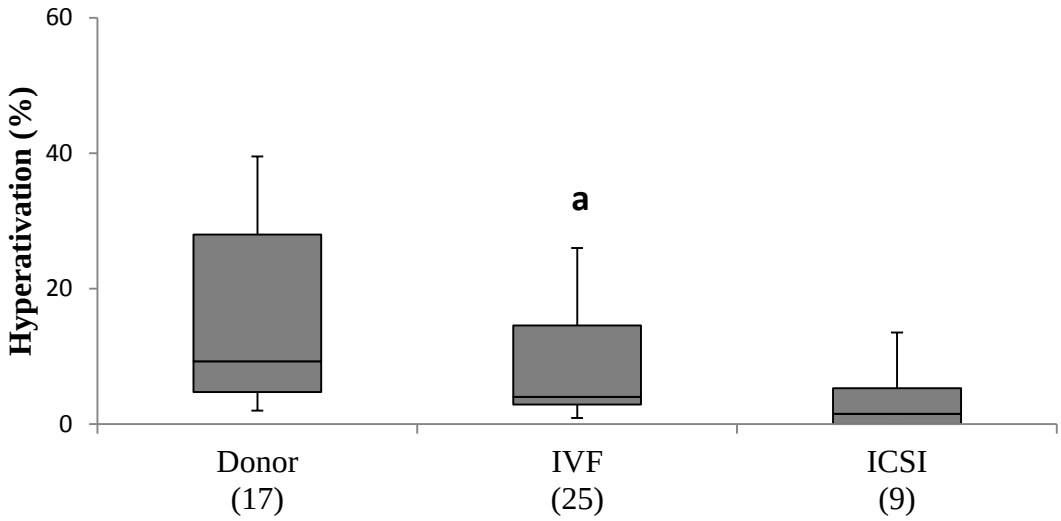

Figure 2.1: Spontaneous hyperactivation levels of donor, IVF and ICSI populations. Box and whisker plot showing the spontaneous levels of hyperactivation. Boxes represent the interquartile range and lines within them are the medians. Numbers in brackets on the x-axis are the sample size. There is significant difference between donor and ICSI populations (p=0.0004), however comparison is not scientifically ideal due to preparation differences (see sample preparation). '**a'** represents significant difference from IVF and ICSI populations (p=0.0118) assessed by paired t-test.

Among the compounds used, 4-AP was the most potent inducer of hyperactivation in the donor and IVF populations, followed by IBMX and progesterone (figures 2.3-2.4-2.5). Conversely, ammonium chloride was not an effective stimulator of hyperactivation. ICSI patients failed to respond significantly to the agonists apart from 4-AP (figure 2.5).

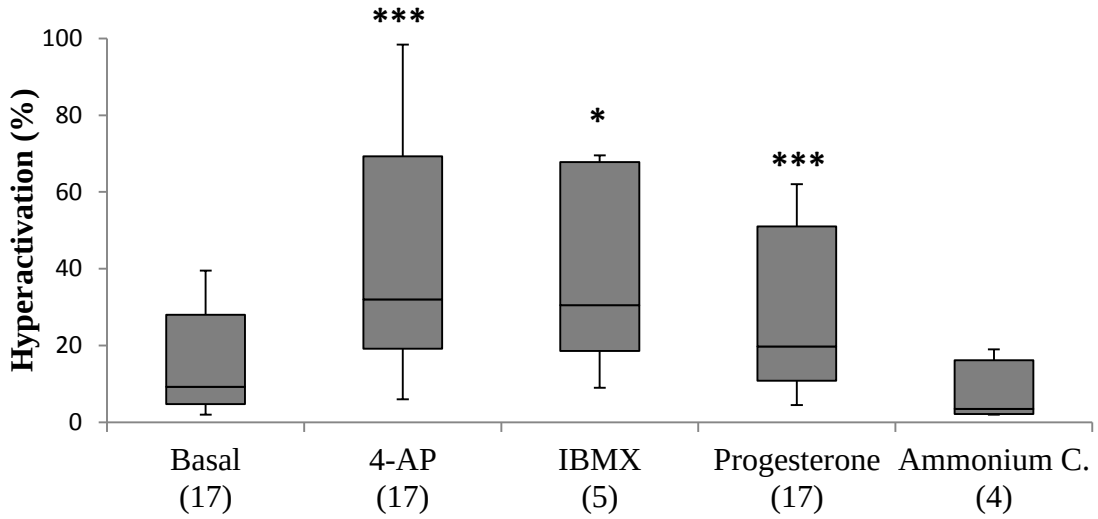

Figure 2.2: Comparison of agonists on hyperactivation levels of donors. Box and whisker plot showing basal (control) and induced levels of hyperactivation in response to 2mM 4-AP, 100µM IBMX, 3.6µM progesterone, and 25mM ammonium chloride. The boxes represent the interquartile range and lines within them are the medians. The numbers in brackets on the x-axis is the sample size. Number of asterisk (*) represents decimal place significant difference from basal hyperactivation level assessed with patired t-test for 4-AP, IBMX, and Progesterone and Wilcoxon test for ammonium chloride.

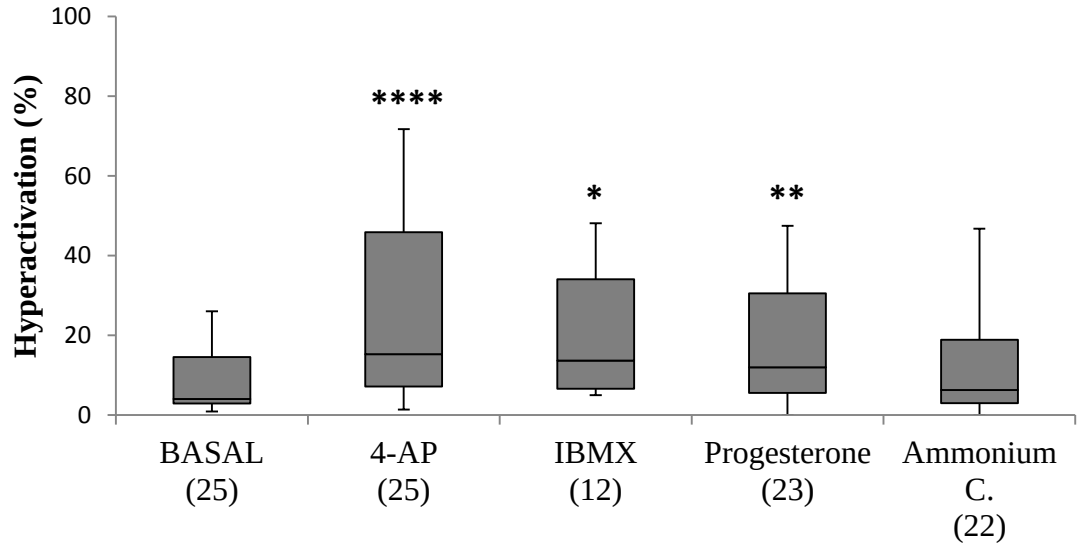

Figure 2.3: Comparison of agonists on hyperactivation levels of IVF patients. Box and whisker plot showing basal (control) and induced levels of hyperactivation in response to 2mM 4-AP, 100µM IBMX, 3.6µM progesterone, 25mM and ammonium chloride. The boxes represent the interquartile range and lines within them are the medians. The numbers in brackets on the x-axis is the sample size. Number of asterisk (*) represents decimal place significant difference from basal hyperactivation level assessed with patired t-test for 4-AP, IBMX, and Progesterone and Wilcoxon test for ammonium chloride.

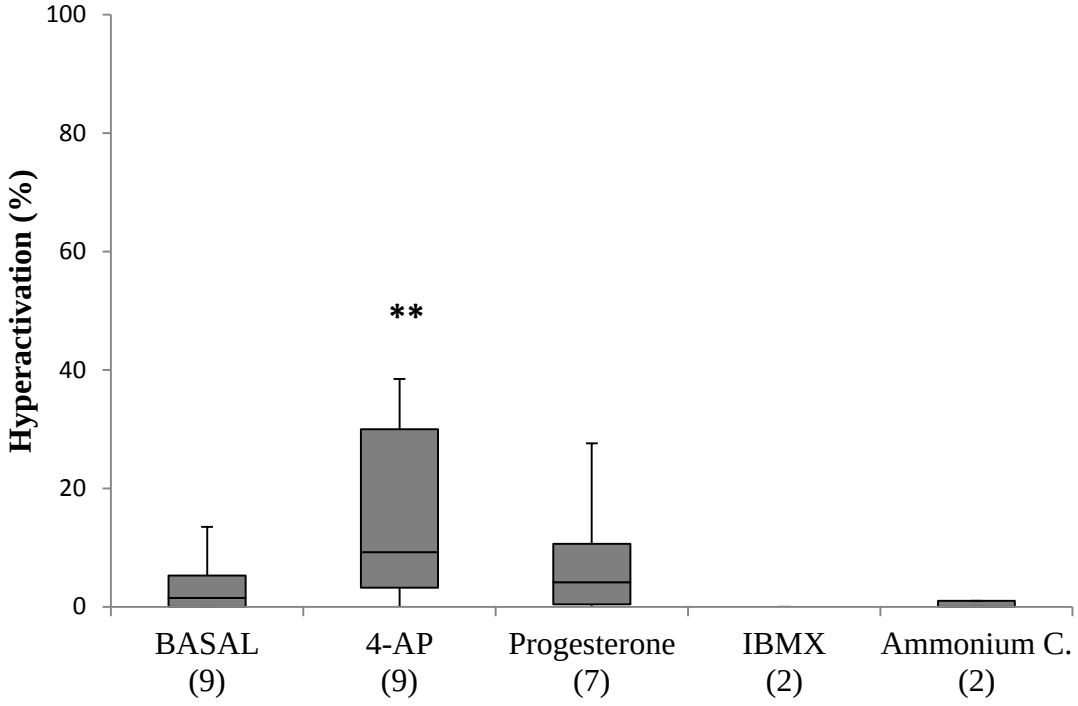

Figure 2.4: Comparison of agonists on hyperactivation levels of ICSI patients. Box and whisker plot showing the basal (control) and induced levels of hyperactivation in response to 2mM 4-AP, 100µMM IBMX, 3.6µM progesterone, 25mM and ammonium chloride. The boxes represent the interquartile range and lines within them are the medians. The numbers in brackets on the x-axis is the sample size. Number of asterisk (*) represents decimal place significant difference from basal hyperactivation level assessed with patired t-test for 4-AP, IBMX, and Progesterone and Wilcoxon test for ammonium chloride.

2.3.2 Hyperactivation Levels of IVF Patients and Relationship with Fertilization Rates

Total and progressively motile sperm levels were not correlated with fertilization rates (appendix). In order to evaluate the clinical significance of hyperactivation assay spontaneous, 4-AP-induced, progesterone-induced, ammonium chloride-induced, and IBMX-induced hyperactivation levels were checked for relationship between fertilization rates on 23 IVF cycles. Spontaneous hyperactivation levels were found to correlate with fertilization rates significantly (r_p=0.4420, p=0.0347, n=23, 1-β=0.8278, figure 2.6). The maximum hyperactivation leves in response to 4-AP as well as the increment in 4-AP-induced hyperactivation correlated significantly with fertilization

rates (r_p=0.5242, p=0.0123, n=22, 1-β=0.8869; r_p=0.4481, p=0.0365, n=22, 1-β=0.8258; respectively, figure 2.7). Another significant correlation was IBMX-induced hyperactivation levels (r_p: 0.8361, p: 0.0026, n=11, 1-β=0.9771, figure 2.8). However, IBMX-induced increment in hyperactivation was not significantly correlated with fertilization rates (ns, appendix). There was no significant relationship between progesterone- (ns, n=21, 1-β=0.7196, appendix) and ammonium chloride-induced (ns, n=19, appendix) hyperactivation levels and fertilization rates.

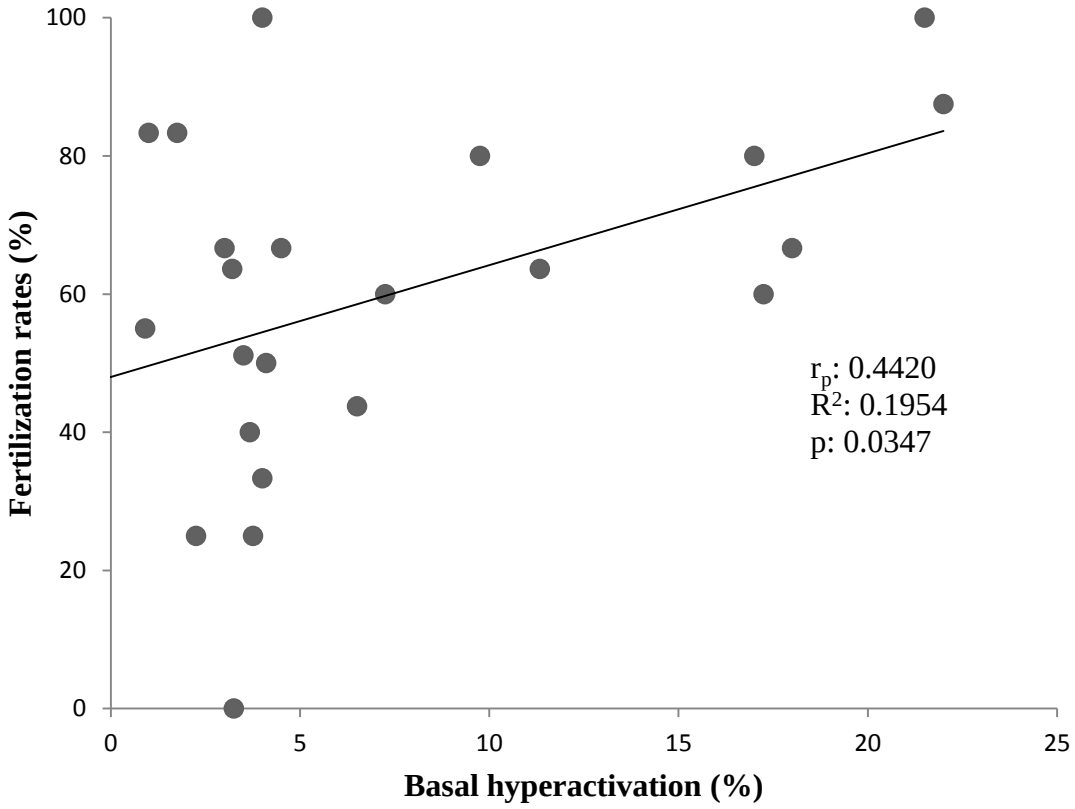

Figure 2.5: Relationship between basal hyperactivation levels and fertilization rates. Basal hyperactivation leves correlate significantly with fertilization rates (n=23). Pearson correlation coefficient (r_p), p-value, and R^2 values are shown on the figure.

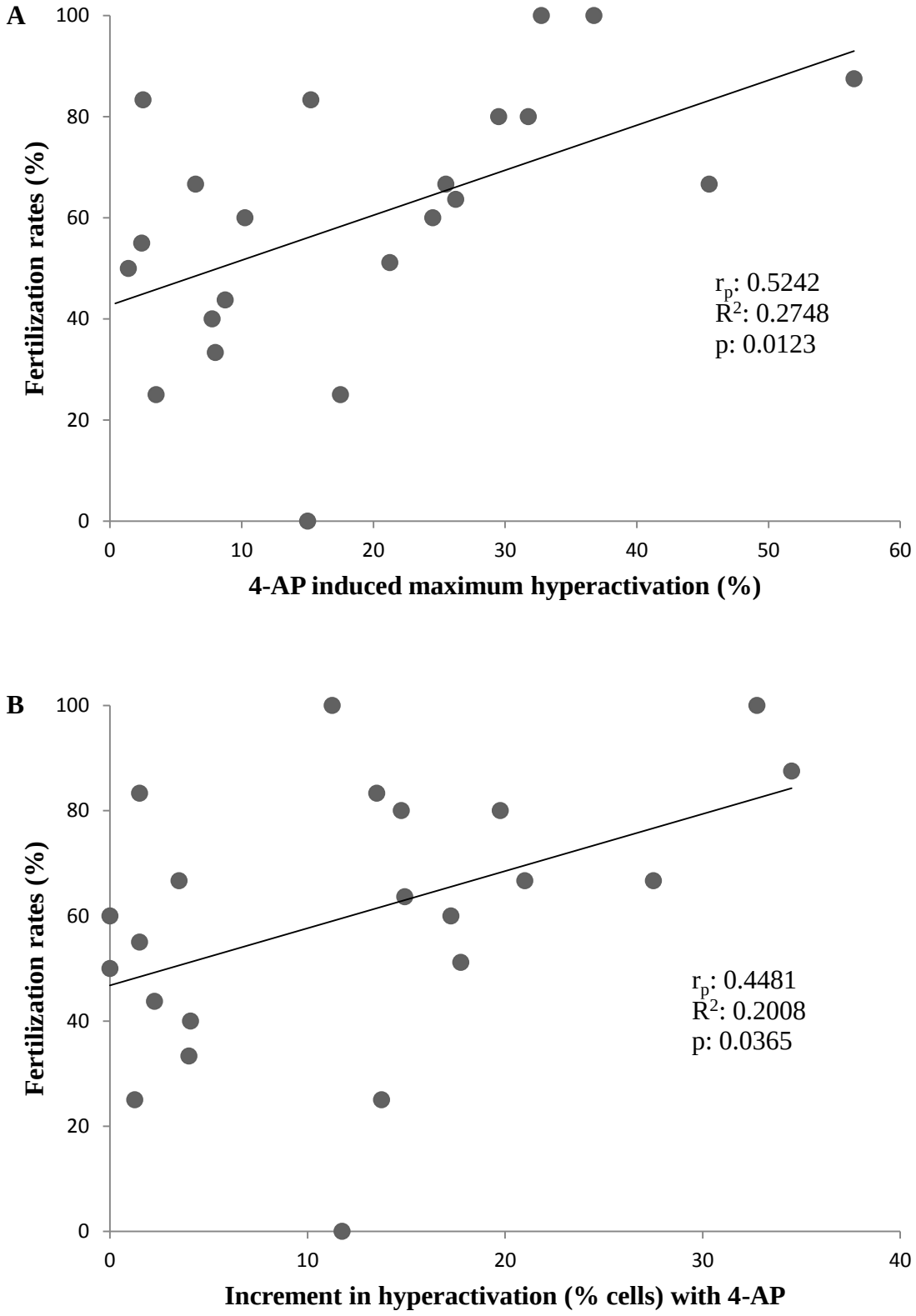

Figure 2.6: Relationship between 2mM 4-AP-induced hyperactivation (A), increment in hyperactivation with 4-AP (B) and fertilization rates. (A) 4-AP-induced hyperactivation levels correlate significantly with fertilization rates (n=22). **(B)** Increment in hyperactivation with 4-AP correlate significantly with fertilization rates (n=22). Pearson correlation (r_p), p-values, and R^2 values are shown on the figures.

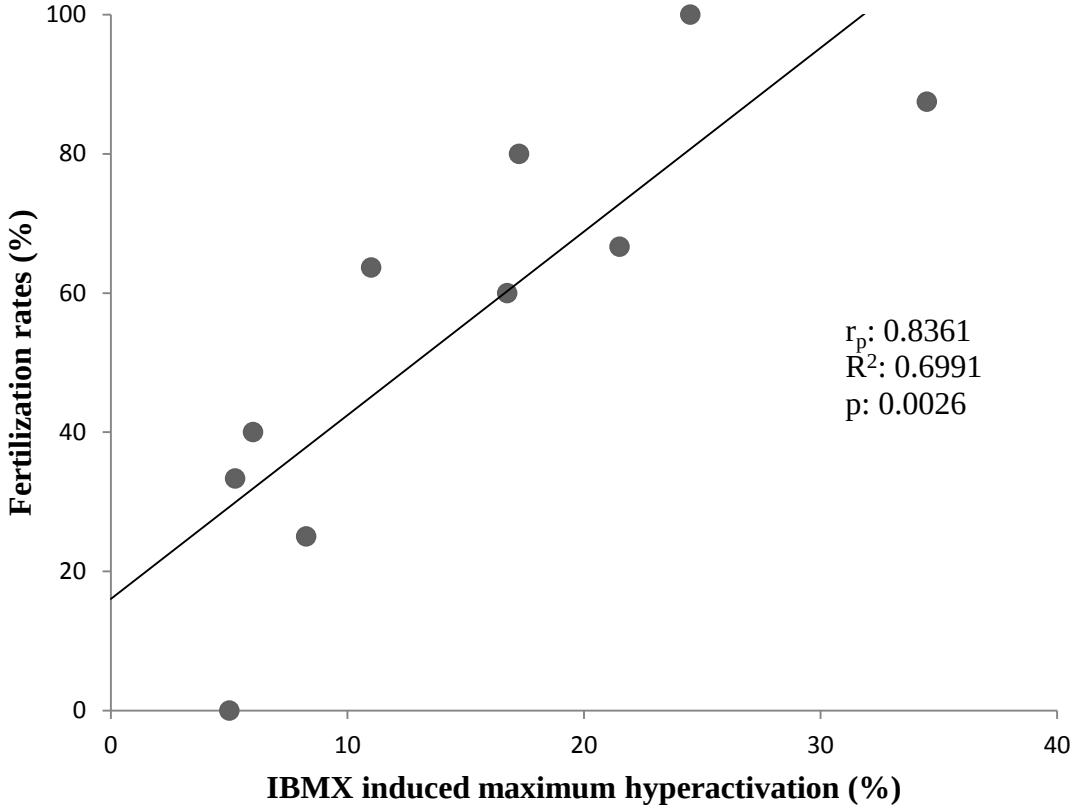

Figure 2.7: Relationship between 100µM IBMX-induced hyperactivation levels with fertilization rates. IBMX-induced hyperactivation levels correlate significantly with fertilization rates (n=11). Pearson correlation (r_p), p-value, and R^2 values are shown on the figure.

As hyperactivation criteria consist of VCL, ALH and LIN, basal and induced levels of these parameters were checked for correlation with fertilization rates. It was found that, basal ALH (r_p=0.6828, R^2=0.4800, p=0.0007, 1-β=0.9781, figure 2.9), basal VCL (r_p=0.4565, R^2=0.2084, p=0.0430, 1-β=0.8403, figure 2.10), and basal LIN (r_s=-0.7145, R^2=0.2694, p=0.0004, 1-β=0.8897, figure 2.11) levels were significantly correlated with fertilization rates. However, increments in ALH, VCL, and LIN with 4-AP or IBMX did not correlate with fertilization rates (appendix).

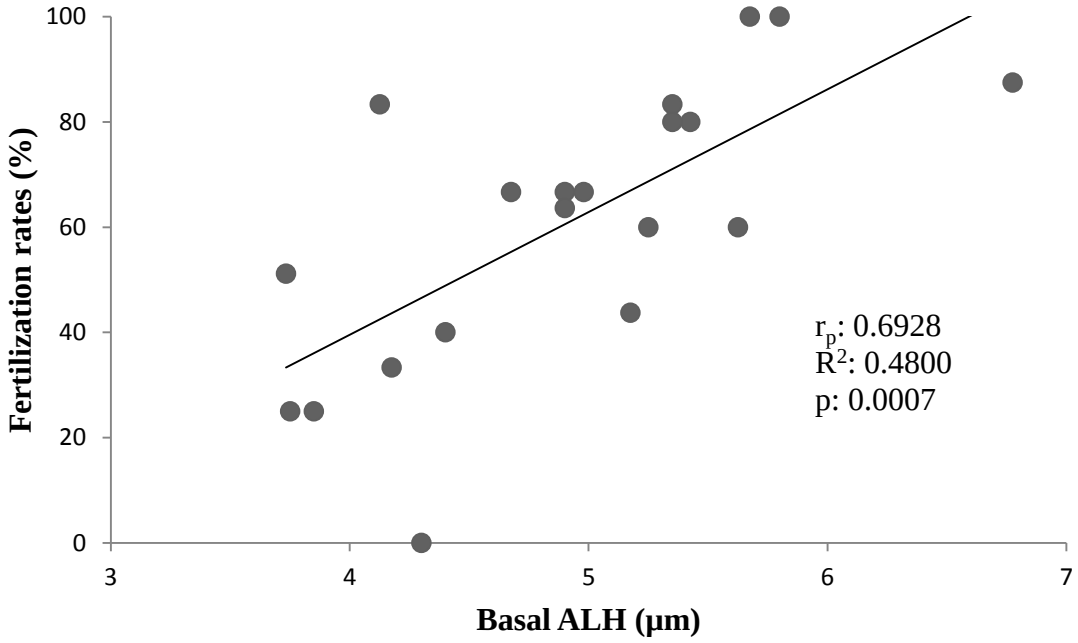

Figure 2.8: Relationship between basal ALH with fertilization rates. (A) Basal ALH levels correlate significantly with fertilization rates (n=23). Pearson correlation coefficient (r_p), p-value, and R^2 value are shown on the figure.

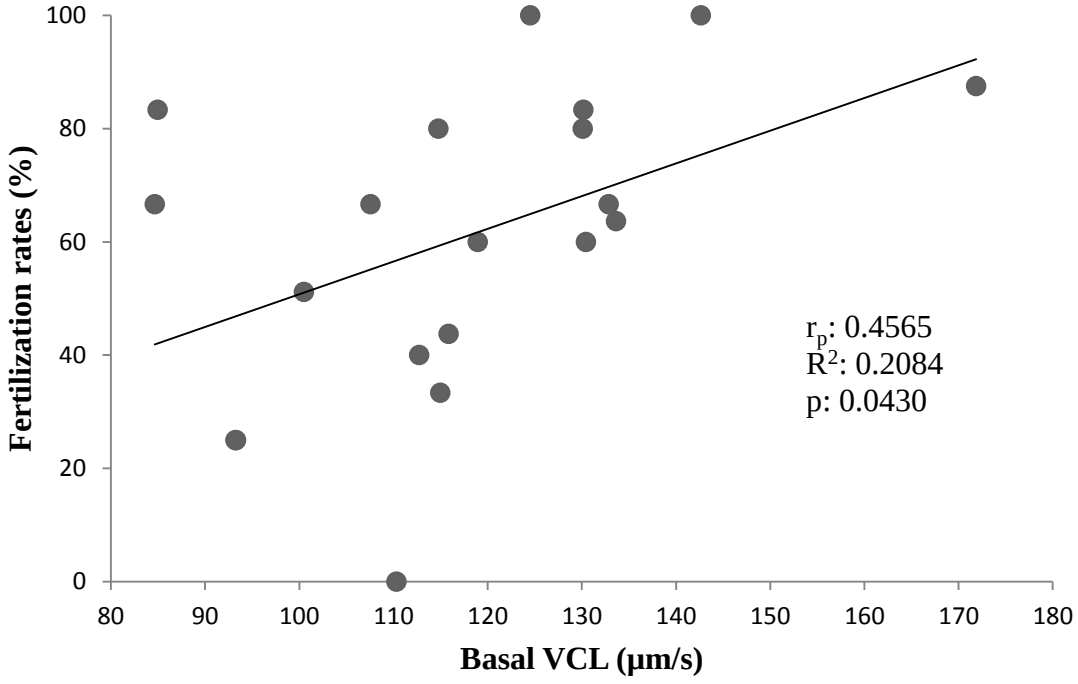

Figure 2.9: Relationship between basal VCL with fertilization rates. Basal VCL levels correlate significantly with fertilization rates (n=23). Pearson correlation coefficient (r_p), p-value, and R^2 value are shown on the figure.

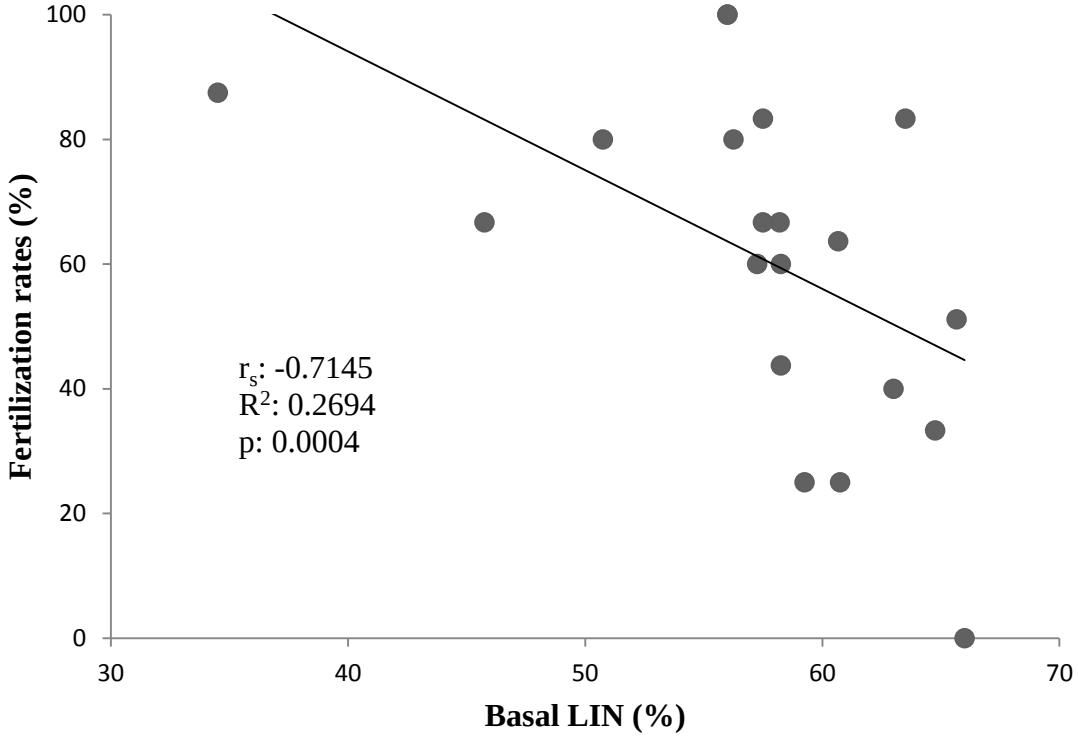

Figure 2.10: Relationship between basal LIN with fertilization rates. Basal LIN levels correlate significantly with fertilization rates (n=23). Spearman correlation coefficient (r_s), p-value, and R^2 value are shown on the figure.

2.3.3 Calcium Signalling Induction with Agonists in IVF Patients and Donors

Intracellular Ca^{2+} signalling of 11 IVF patients and 17 donors were recorded in response to 4-AP and progesterone (figure 2.12). The Ca^{2+} signalling in response to 4-AP was significantly different between IVF patients and donor populations ($p<0.05$, figure 2.12). IVF patients showed a significantly higher response to 4-AP. Furthermore, the nature of 4-AP response is different than that of donor responses (figure 2.12). On the other hand, there was no significant difference in progesterone responses of IVF and donor populations (ns, figure 2.12).

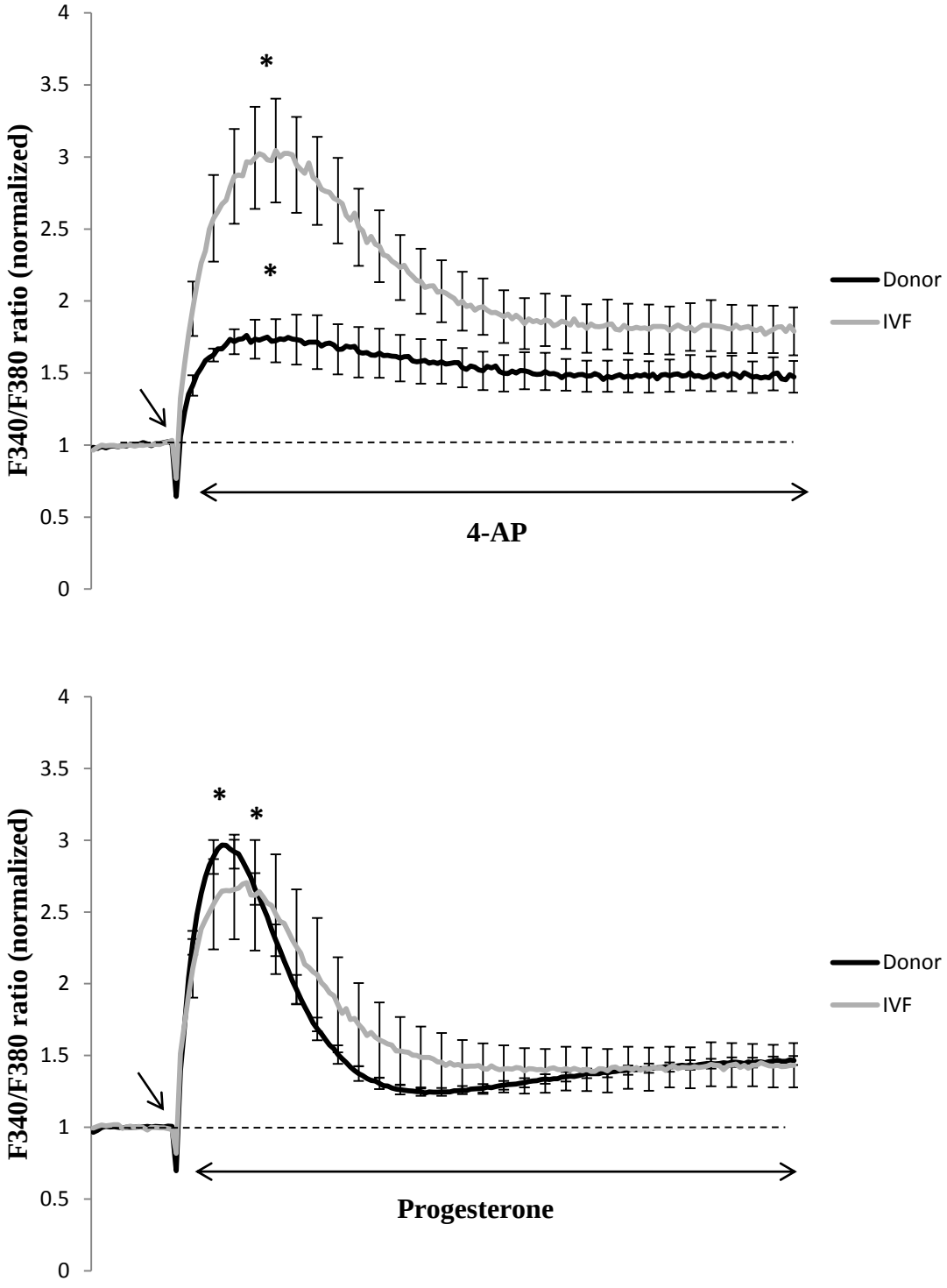

Figure 2.11: Intracellular Ca^{2+} responses to 2mM 4-AP and 3.6µM progesterone in donor and IVF patient populations. Intracellular Ca^{2+} responses induced by 4-AP and progesterone in donors (4-AP n=6, progesterone n=17) and IVF patients (4-AP n=11, progesterone n=9). * indicates significant difference from resting level Ca^{2+} ratio. Arrow indicates point of agonist injection.

The maximum reading of the peak point and sustained phase reading for both agonists were checked for relationship with fertilization rates, however, there was no such relationship. However, 4-AP induced hyperactivation levels showed a significant negative correlation with ALH levels (r_p=-0.6601, R^2=0.4357, p=0.0378, figure 2.13). This was the only relationship found with intracellular Ca^{2+} signalling and as ALH levels correlated with fertilization rates there might be a relationship.

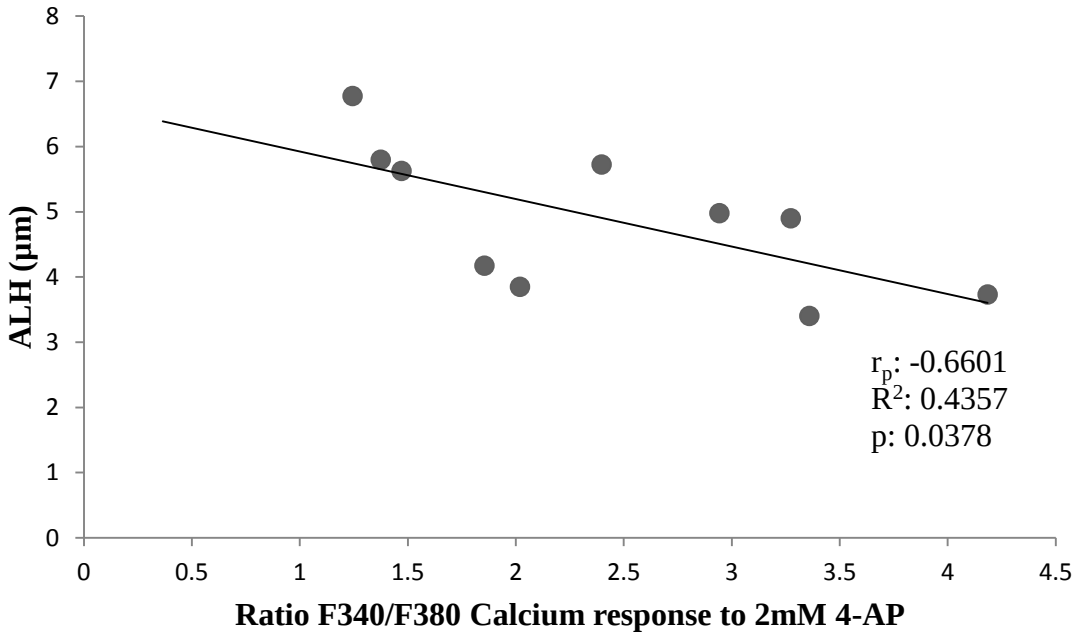

Figure 2.12: Relationship between 2mM 4-AP-induced intracellular Ca^{2+} and ALH levels. Maximal points of 4-AP-induced intracellular Ca^{2+} signaling correlate significantly with ALH levels (n=11). Pearson correlation coefficient (r_p), p-value, and R^2 values are shown on the figure.

2.3.4 Hyperactivation and Intracellular Ca^{2+} Responses of ICSI Patients

As ICSI patients had very low sperm concentration it was challenging to record intracellular Ca^{2+} signalling. Intracellular Ca^{2+} responses of only 3 out of 9 ICSI samples could be obtained (figure 2.14). 2 of the ICSI samples gave poor responses to 4-AP. However, those 2 samples that gave poor responses to 4-AP gave ‘normal’ (considering cut-off values, see materials and methods) responses to progesterone, but

the responses were significantly lower than the usual response. Of those 3 patients, only Patient 3 gave a significant response to 4-AP in terms of hyperactivation. Patient 1 responded significantly to progesterone, Patient 2 did not respond, and progesterone-induced hyperactivation for Patient 3 was not tested.

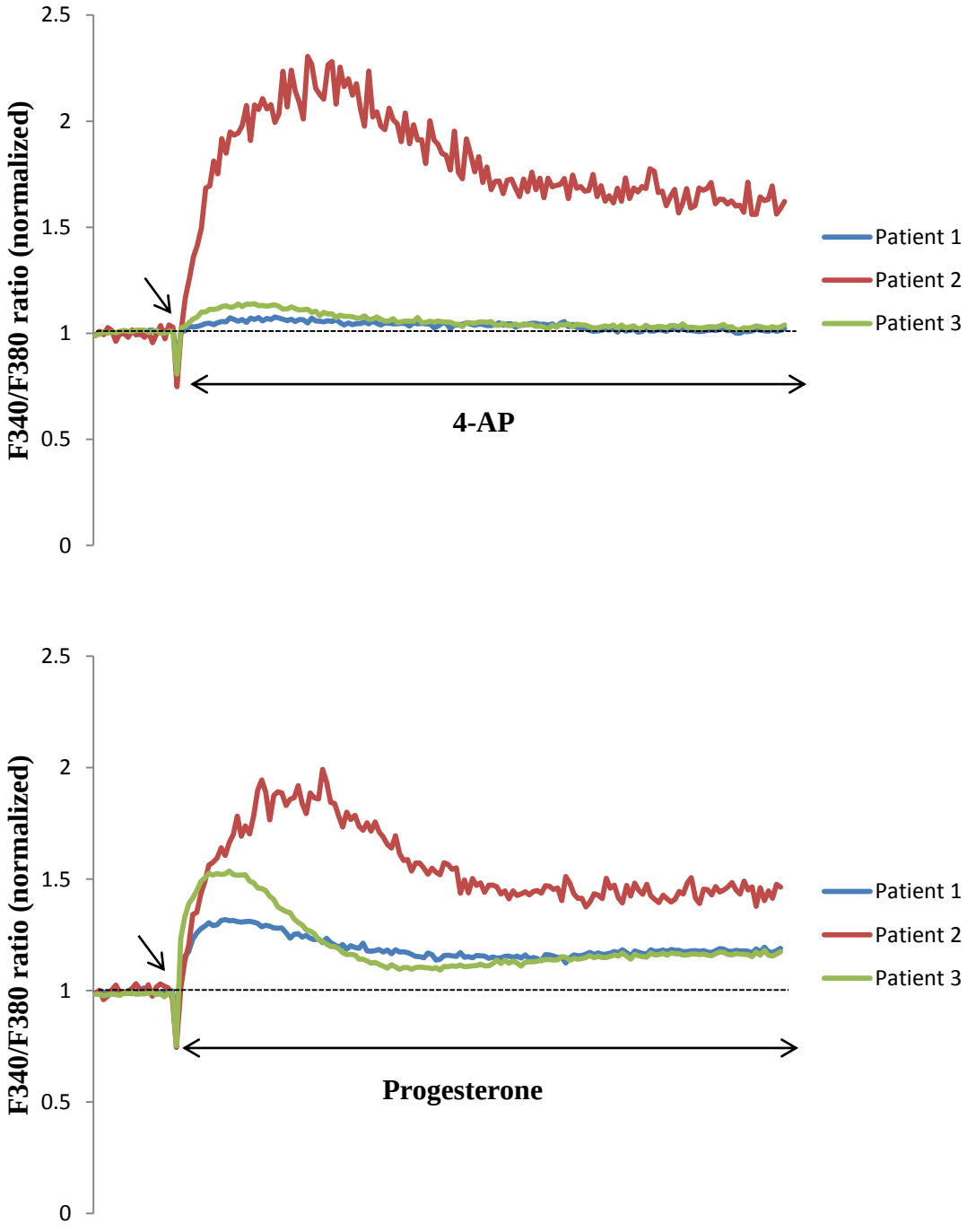

Figure 2.13: Intracellular Ca^{2+} responses to 2mM 4-AP and 3.6µM progesterone in 3 ICSI patients. Arrow indicates point of agonist injection. Patients 2 and 3 gave poor responses to 4-AP. Progesterone responses were "normal" considerin the cut-off value.

2.3.5 Defective Hyperactivation and Intracellular Ca^{2+} Responses of Different Populations

In order to understand the differences between healthy donors and sub-fertile patients, occurrence of defective hyperactivation and intracellular Ca^{2+} responses to the agonists were analysed. It was found that 12% (i.e. 2 in 17) of the donor samples gave a defective hyperactivation response to 4-AP, and 24% (i.e. 4 in 17) to progesterone. The incidence of defective hyperactivation among the IVF patients in response to 4-AP was not significantly different than that of the donor responses, 16% (i.e. 7 in 25). Similarly, the incidence of defective progesterone-induced hyperactivation levels among the IVF patients was not significantly higher than that of the donors 42% (i.e. 10 in 24) in response to progesterone. The incidence of defective hyperactivation was 33% (i.e. 3 in 9) in response to 4-AP was not significantly different than that of the donors and IVF patients. Similarly, 71% (i.e. 5 in 9) of the ICSI patients gave defective hyperactivation in response to progesterone that was not significantly different than that of the donors and IVF patients. As there was a limitation in requirement for an intracellular Ca^{2+} response detection, not all the patients could be screened for intracellular Ca^{2+} responses. However, for those patients which had the sufficient amount of cells for Ca^{2+} detection assay was assessed for their intracellular Ca^{2+} responses. None of the donors and IVF patients gave a defective intracellular Ca^{2+} response with 4-AP and progesterone. One of the ICSI patients (1 in 3) showed a defective intracellular Ca^{2+} response to 4-AP. Conversely, all of the patients gave ‘normal’ responses to progesterone.

2.4 Discussion

The aim of the study was to determine the clinical significance of hyperactivation and intracellular Ca^{2+} assays. It is clear that hyperactivation is controlled by Ca^{2+} signalling (Publicover *et. al.*, 2007). However, there are very few studies about defective hyperactivation levels in sub-fertile patients. Furthermore, the existing studies focused on the basal levels of hyperactivation (Munire *et. al.*, 2004). The control of hyperactivation is relying on extracellular stimulation from the environment. The strongest candidate for physiological external stimulation for hyperactivation is progesterone *in vivo*. Although not a potent hyperactivation inducer, progesterone is the candidate that initiates hyperactivation in mammals upon binding to CatSper in the vicinity of oocytes (Lishko *et. al.*, 2011; Strunker *et. al*, 2011). 4-AP on the other hand is much more potent inducer of hyperactivation and its effect on hyperactivation is not dependent on extracellular Ca^{2+}, suggesting the presence of intracellular Ca^{2+} store(s) (Gu *et. al.*, 2004; Bedu-Addo *et. al.*, 2008). Recently, clinical significance of the Ca^{2+} stores was evaluated (Alasmari *et. al.*, 2013). Alasmari *et. al.*, (2013) documented the prevelance of calcium store defects and highlighted the clinical significancy of calcium signalling for fertilisation at IVF.

The advantage of using the surplus patient samples is that there were no inter-ejaculate sample differences; therefore, there was a direct relationship between the sperm used for the insemination and the sperm used for the hyperactivation and Ca^{2+} assays. However, relying on surplus samples was challenging in case of samples with low sperm concentration as there is always a limit on the sperm number recovered from the samples provided from the clinic. Because of this limitation, not all the samples could be tested for all the agonists in the hyperactivation and intracellular Ca^{2+} assays. 25 IVF and 9 ICSI patients were screened. Although the sample sizes were small, the effect sizes and the sample powers indicate that data used is strong enough to make

statements (except progesterone). It was shown very clearly that; 4-AP-induced-, IBMX-induced-, and basal hyperactivation levels correlated significantly with fertilization rates (figure 2.6, figure 2.7, and figure 2.5, respectively). As hyperactivation assay shows robust repeatability (Burkman and Samrock, 1992), this study has a value in prognostic allocation of suitable treatment methods in ART. It has been suggested by Brenzik *et. al.* (2013) that the basal hyperactivation levels of sperm samples in IVF cycles is not useful. In contrast with Brenzik *et. al.* (2013), this study in agreement with Alasmari *et. al.,* (2013) shows that the basal hyperactivation levels correlated significantly with fertilization rates and it can be used together with induced levels of hyperactivation to give an idea about the IVF outcome. Again in contrast with Brenzik *et. al.,* (2013), progesterone induced hyperactivation levels did not correlate with fertilization rates in this study confirming Alasmari *et. al.,* (2013). The criteria used by Brenzik *et. al.,* (2013) for hyperactivation was; ALH ≥ 5μm, LIN ≤ 60%, and VCL ≥ 100μm/s. The criteria used in this study and Alasmari *et. al.,* (2013) was more stringent (ALH ≥ 7μm, LIN ≤ 50%, and VCL ≥ 150μm/s). Therefore, this finding could be explained by using different criterias. It is clear that the responsiveness of sperm to 4-AP in terms of hyperactivation can indicate the fertilization potential of a man (Alasmari *et. al.,* 2013; this study). However, as progesterone induced hyperactivation levels did not correlate with fertilization rates, it cannot be used as a prognostic test (Alasmari *et. al.,* 2013; this study). It was calculated to have a sample size of 51 in order to have significant results for progesterone induced hyperactivation correlating with fertilization rates.

The effects of inducers can be ranked as; 4-AP>IBMX>Progesterone>NH_4Cl (Figures 2.3, 2.4, 2.5). This ranking was similar between the different populations used. It has been suggested that progesterone-induced intracellular Ca^{2+} signalling is accompanied with a burst of hyperactivation for a short period of time (i.e. transient

period of induction, Gakamsky *et. al.,* 2009; Servin-Vences *et. al.,* 2012). However, under the experimental conditions of this study, this induction of hyperactivation was 'missed'. As a result, progesterone-induced hyperactivation levels from different populations were low and defective hyperactivation responses were frequent in all the populations used. Furthermore, IVF patients that showed failed response to progesterone also failed to respond significantly in CASA parameters (appendix). Although there are molecular weaknesses, caged-progesterone analogues could be used to test the transient Ca^{2+} period and its effect on patient samples. Furthermore, the significance of CatSper activity in hyperactivation induction in man is largely unknown (Brenker *et. al.,* 2012).

Hyperactivation is also stimulated by phosphodiesterase (PDE) inhibitors through the cAMP/PKA pathway. In order to test the significance of the cAMP pathway, IBMX was used to inhibit PDE activity and albeit increase $[cAMP]_i$ to stimulate hyperactivation (Tesarik *et. al.,* 1992). IBMX application does not stimulate Ca^{2+} influx, therefore, IBMX-induced hyperactivation is not dependent on the intra- or extra-cellular Ca^{2+}. Although, hyperactivation is controlled by Ca^{2+} not cAMP in mammals (Ho *et. al.,* 2002), in this study, it was found that the IBMX-induced hyperactivation levels showed the highest level of correlation with fertilization rates. However, it should be noted that the sample size for IBMX-induced hyperactivation levels was small (Figure 2.8). Furthermore, the increment in hyperactivation with IBMX did not correlate with fertilization rates. Therefore, it is not certain if IBMX-induced hyperactivation has a prognostic value in IVF.

IVF patients showed significantly higher Ca^{2+} response to 4-AP than research donors. There is no rational explanation for this. However, there was no correlation between the intracellular Ca^{2+} responses by agonists and fertilization rates, possibly due

to low sample sizes. Comparing the Ca^{2+} signalling between IVF and ICSI patients with independent t-test showed that the 4-AP response was significantly lower in ICSI patients (Figure 2.10 and Figure 2.12). This reflects that the ICSI patients were likely to have intracellular Ca^{2+} store deficiencies. It should be noted that the acrosome reaction was not tested for these patients and there is a possibility that these patients could have acrosome reaction problems.

In case of IVF treatment, the problem could be a female factor as well as a male factor. Therefore, it was uncertain if the patients undergoing IVF treatment had sperm dysfunction. It should be noted that the decision on using ICSI is made on the light of sperm concentration, sperm motility, and sperm morphology or the couple had a failed IVF cycle (see section 2.2.2). Therefore, there is a greater possibility that ICSI cycles were chosen due to male factor infertility. Trying IVF and failing is financially wasteful. This study demonstrates that the hyperactivation assay has potential in predicting IVF outcome and may be introduced into routine semen analysis for better allocation of patients into the correct treatment methods.

In summary it was shown that 4-AP-induced, IBMX-induced and spontaneous-hyperactivation levels correlate significantly with IVF fertilization rates. Therefore, it is proposed that the hyperactivation assay should be further investigated and clinically established reference values must be evaluated. Furthermore, hyperactivation assay along with other tests such as semen analysis, hyaluronan-binding, and sperm DNA damage could be used together to develop algorithms for predicting IVF outcome. By using these functional tests, allocation of patients to ICSI would be determined much more efficiently.

Chapter 3 : Effect of Phosphodiesterase Inhibitors on Human Sperm Motility and Calcium Signalling

3.1 Introduction

Human sperm motility is controlled through mechanisms that are dependent on cAMP and Ca^{2+} (Wennemuth *et. al.,* 2003; Publicover *et. al.,* 2007). It is known that several odorants increase cAMP content of spermatozoa that results in opening unknown Ca^{2+} channels (Spehr *et. al.,* 2003; Neuhauss *et. al.,* 2006; Veitinger *et. al.,* 2011). Supporting this finding, membrane-permeable analogues of cAMP and cGMP evoke their own Ca^{2+} signals in mouse and human sperm (Kobori *et. al.,* 2000; Ren *et. al.,* 2001; Machado-Oliveira *et. al.,* 2008). cAMP molecule itself evokes Ca^{2+} influx upon binding to CatSper on an extracellular site, making the context of Ca^{2+} signalling and its interplay with cAMP very complex (Brenker *et. al.,* 2012). cAMP and Ca^{2+} were shown to influence the flagellar beating pattern (Ishjima, 2013; Ho *et. al.,* 2002). PDE inhibitors have been used to stimulate human sperm motility through increasing intracellular cAMP content (Rees *et. al.,* 1990; Yovich *et. al.,* 1990; Pang *et. al.,* 1993). However, effects of the PDE inhibitors on Ca^{2+} signalling remain largely unknown as there are very limited studies addressing this (Nassar *et. al.,* 1998; Hong *et. al.,* 1985; Torres-Flores *et. al.,* 2008; Colas *et. al.,* 2010). There is evidence that shows hyperactivated motility is stimulated by non-specific PDE inhibitor pentoxifylline independently from Ca^{2+} induction (Nassar *et. al.,* 1998). This is particularly interesting, as it is known that hyperactivation is controlled by Ca^{2+}. It is therefore, interesting to document the effects of PDE inhibitors on Ca^{2+} signalling as Ca^{2+} ion is pivotal in sperm function.

It has been suggested that PDE type 4 is responsible for controlling motility (Fisch *et. al.,* 1998). Selective inhibitors of PDE type 4, Etazolate HCl (IC_{50}: 2µM),

Ibudilast (IC_{50}: 0.05-5µM depending on the sub-type), and Tofisopam (IC_{50}: 0.68µM) were shown to increase human sperm motility significantly (Tardif *et. al.*, unpublished data). Additionally, Papaverine (IC_{50}: 1.1µM), a non-selective PDE inhibitor that has sensitivity towards PDE type 4 also significantly increases human sperm motility (Tardif *et. al.*, unpublished data). Therefore, the effects of PDE inhibitors Ibudilast, MMPX, Tofisopam, Etazolate Hydrochloride, and Papaverine on intracellular Ca^{2+} signalling induction and its relation with motility were investigated.

3.2 Materials and Methods

3.2.1 Experimental design

Semen samples from healthy research donors were used for this study. Prepared donor samples were allowed to capacitate in the capacitating medium (STF) for 2 hours (see sperm preparation). After this time, the samples were subjected to PDE inhibition with Ibudilast, Etazolate HCL, MMPX, Tofisopam, or Papaverine at 10 different concentrations (0.1-100µM) for their motility effects (see phosphodiesterase inhibition). This range of concentration was chosen based on the IC_{50} values of these inhibitors and previous observations (Tardif *et. al.*, unpublished data). Following evaluation of motility effects, samples were subjected to the intracellular Ca^{2+} assay to evaluate the effects of the aforementioned PDE inhibitors on Ca^{2+} signalling (see intracellular Ca^{2+} detection). There is a time difference of 1 hour between motility assays and Ca^{2+} assays. Different donors were used for each experiment.

3.2.2 Media and Chemicals

NCB, STF, and Experimental STF were the same as described in Chapter 2 (see section 2.2.2). Progesterone (Sigma Aldrich, Catalogue number P8783-5G, UK) was dissolved in absolute ethanol and diluted with distilled water prior to use and used at a final concentration of 3.6µM. The Ca^{2+} indicator dye Fura-2/AM was dissolved in DMSO and kept at -20°C and used at 1µM final concentration. 1% Pluronic acid solution was made daily prior usage.

3.2.3 Sperm Preparation

Healthy research donors were asked to produce semen samples at home by masturbation into sterile plastic containers in 2-3 days of sexual abstinence. Samples were allowed to liquefy at 37°C for 30 minutes. If the sample was already liquefied upon arrival, then it

was only incubated for 15 minutes at 37°C to standardize the temperature of the samples used. Following the percoll density gradient (see section 2.2.3), the 80% fraction sperm were transferred into the STF and allowed to capacitate for 2 hours at 37°C and 5% CO_2.

3.2.4 Phosphodiesterase Inhibition

Following 2 hours of exposure to the capacitating conditions, sperm were exposed to various concentrations of different phosphodiesterase inhibitors (0.1-100µM). Selected PDE inhibitor (dissolved in DMSO) was added to the sperm suspension and mixed gently followed by a further incubation at 25°C for 5 minutes before any analysis (as Ca^{2+} assay could be only recorded up to 5 minutes). 1% DMSO was used as negative control and 3.6µM progesterone was used as positive control.

3.2.5 Evaluation of Hyperactivation

CASA settings were the same as described in Chapter 2 (see section 2.2.4). Following addition of 1µl PDE inhibitor to 99µl in STF for desired final concentration, the suspension was kept at 25°C for 5 minutes. After 5 minutes, 4µl of sperm suspension was transferred to pre-heated slide (Dual Sided Sperm Analysis Chamber, Hamilton Thorn Biosciences, Beverly, MA, USA) and covered with pre-heated coverslip and allowed to reach 37°C for 2 minutes. The analysis was done as described in section 2.2.4.

3.2.6 Intracellular Calcium Detection

The Ca^{2+} detection protocol was the same as described in Chapter 2 (see section 2.2.5). Pluronic acid was used at a final concentration of 0.005%. Minimum of $2x10^6$ cells/well were required.

3.2.7 Statistics

The general linear model was used where possible, as the sample size was small to perform other statistical calculations. Where general linear model was unable to give clear statistical results (due to wide variations in data), individual donor analysis was performed. For individual donor analysis, SD was checked with control data, and considered to be statistically significant where the SDs was not overlapping. Results with $p \leq 0.05$ were considered to be statistically significant. Sample powers ($1-\beta$ error probability) were calculated using G*Power version 3.1 (G*Power Software, Germany) and considered to be adequate where $1-\beta > 0.80$. Sample sizes were calculated using G*Power version 3.1 software based on effect size, p value, and power (Faul *et. al.*, 2007).

3.3 Results

3.3.1 Effect of PDE Inhibitors on Motility Parameters

All of the 5 PDE inhibitors tested on human sperm had significant effects on motility parameters. Whilst total motility and progressive motility were not significantly affected by PDE inhibitor treatments (ns, Figure 3.1 and 3.2), there was a significant induction in hyperactivation in spermatozoa only in response to Ibudilast (Figure 3.3). This induction was statistically significant only at 50µM and 100µM concentrations (p=0.038 and p=0.020, respectively). Due to high variation seen in the hyperactivation data (Figure 3.3) individual donors were also analysed using SD (Table 3.1-3.5).

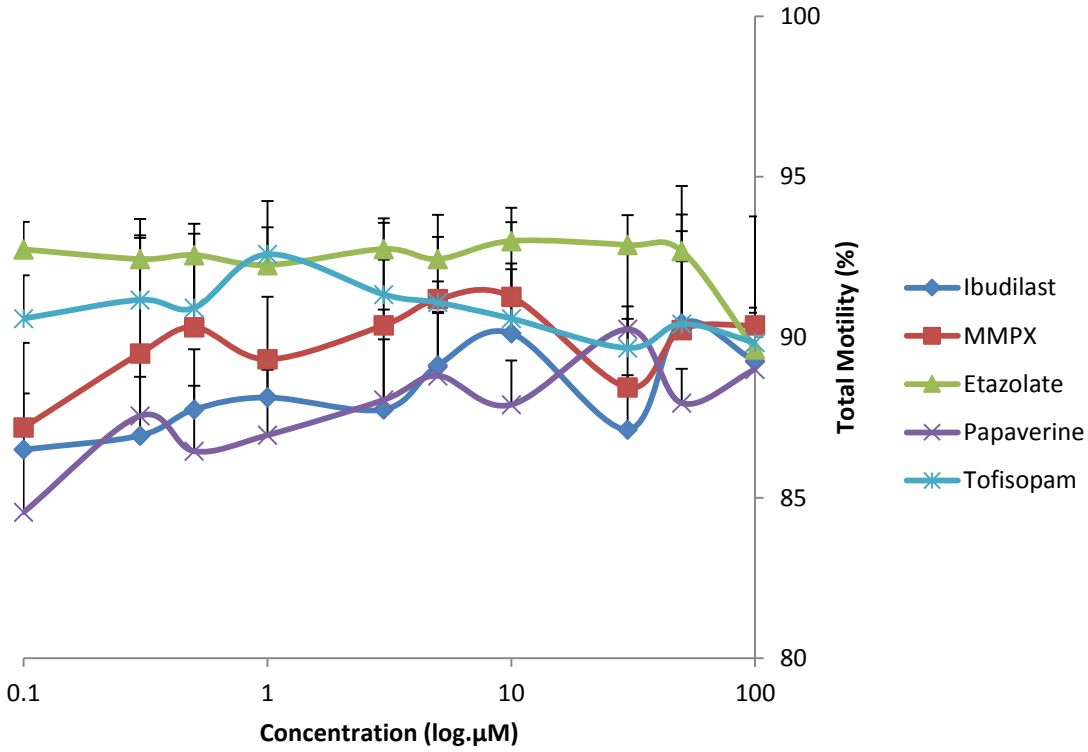

Figure 3.1: Dose responses of Ibudilast, MMPX, Etazolate, Papaverine, and Tofisopam on total motility. The scatter graph is showing a 10-point dose response of total motility of Ibudilast (n=4), MMPX (n=4), Etazolate (n=4), Papaverine (n=5), and Tofisopam (n=3). The x-axis (concentration) is on log scale. Error bars represent SEM (only plus values are shown).

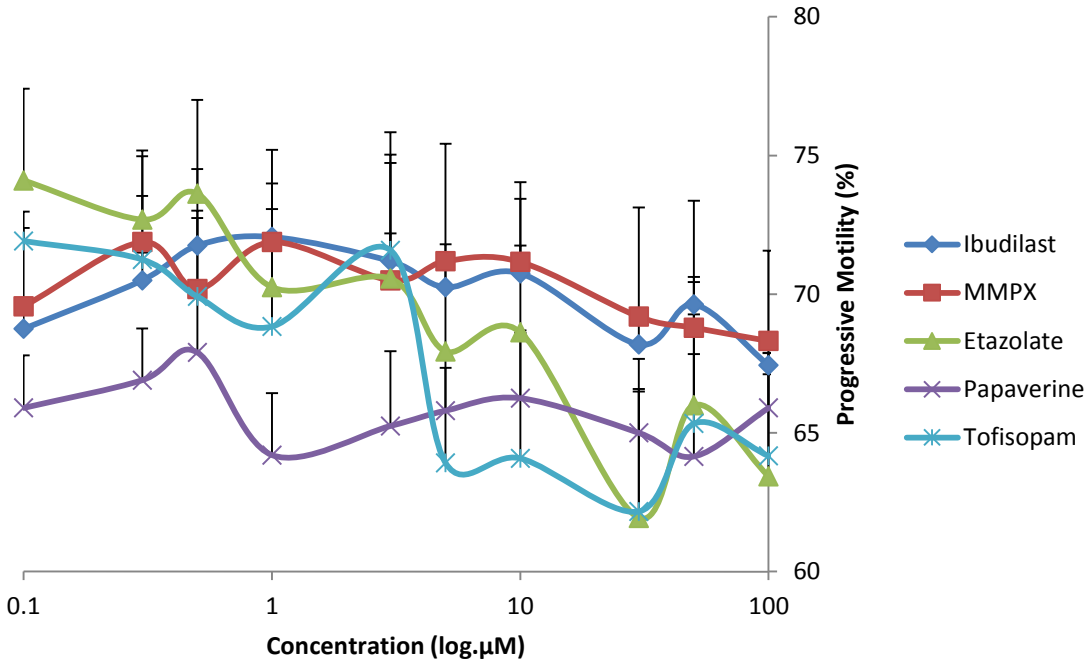

Figure 3.2: Dose responses of Ibudilast, MMPX, Etazolate, Papaverine, and Tofisopam on progressive motility. The scatter graph is showing a 10-point dose response of progressive motility of Ibudilast (n=4), MMPX (n=4), Etazolate (n=4), Papaverine (n=5), and Tofisopam (n=3). The x-axis (concentration) is on log scale. Error bars represent SEM (only plus values are shown).

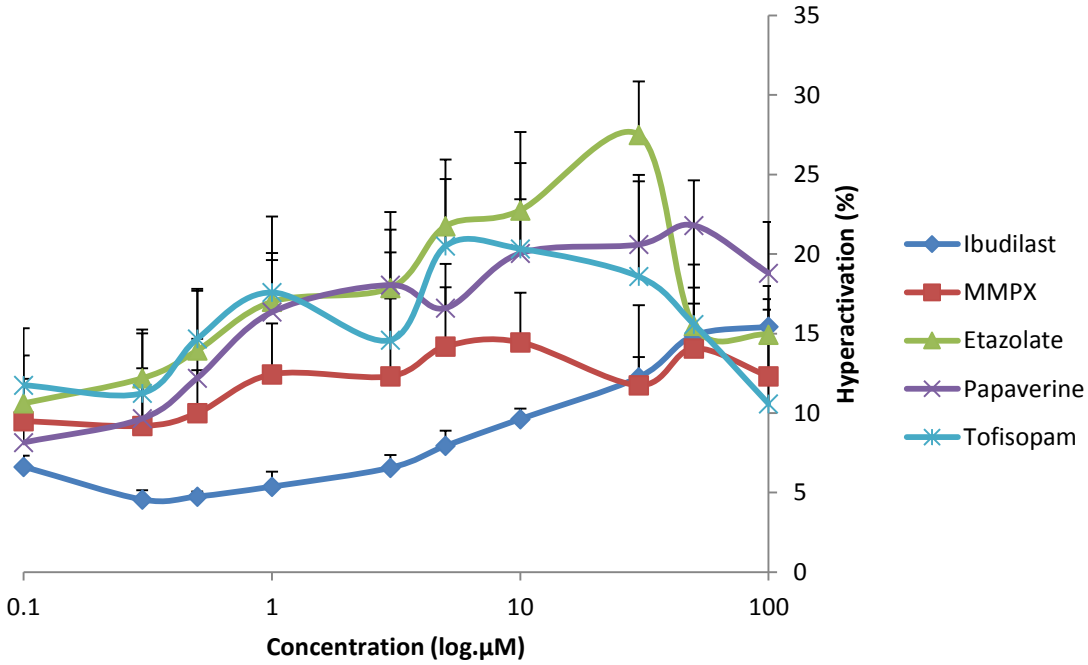

Figure 3.3: Dose responses of Ibudilast, MMPX, Etazolate, Papaverine, and Tofisopam on hyperactivation. The scatter graph is showing a 10-point dose response of hyperactivation of Ibudilast (n=4), MMPX (n=4), Etazolate (n=4), Papaverine (n=5), and Tofisopam (n=3). The x-axis (concentration) is on log scale. Error bars represent SEM (only plus values are shown).

	Concentration (µM)											
	-ve control	**0.1**	**0.3**	**0.5**	**1**	**3**	**5**	**10**	**30**	**50**	**100**	**+ve control**
D1	5.00 (1.00)	6.25 (0.50)	4.00 (0.82)	4.00 (0.00)	4.50 (1.29)	9.00* (0.82)	6.50 (1.29)	7.75 (2.22)	10.75* (0.96)	16.50* (2.89)	15.25* (0.96)	15.00* (1.15)
D2	5.00 (0.82)	8.50* (1.29)	4.75 (0.96)	6.75 (2.36)	5.75 (0.50)	6.25 (1.26)	6.75* (0,50)	11.75* (0.96)	11.75* (1.89)	20.25* (1.50)	23.25* (2.63)	17.00* (2.58)
D3	4.50 (0.87)	5.25 (0.63)	4.00 (0.71)	2.00 (0.00)	3.50 (0.29)	3.75 (0.75)	9.00* (1.47)	6.50* (0.87)	7.75* (0.48)	6.50* (0.50)	6.25* (0.48)	5.25 (1.18)
D4	8.00 (2.71)	6.50 (3.00)	5.50 (1.00)	6.25 (0.96)	7.75 (1.71)	7.25 (1.71)	9.50 (1.29)	12.50 (2.38)	18.75* (3.59)	16.25* (4.99)	17.00* (2.58)	21.75* (3.10)

Table 3.1: Effect of Ibudilast on hyperactivation. Table shows the effect of Ibudilast on hyperactivation as 10 different concentrations on 4 different donors. The numbers in brackets are standard deviation. Asterix (*) indicates that standard deviations are not overlapping compared to control (i.e. statistically significant). Negative (1% DMSO) and positive (3.6µM progesterone) controls are shown on the table.

	Concentration (µM)											
	-ve control	**0.1**	**0.3**	**0.5**	**1**	**3**	**5**	**10**	**30**	**50**	**100**	**+ve control**
D1	2.00 (2.45)	3.50 (2.38)	4.50 (2.38)	6.5 (4.04)	5.50 (1.73)	9.50* (2.65)	9.75* (2.22)	4.25 (2.63)	5.25 (3.20)	3.50 (1.91)	7.50 (6.66)	11.75 (6.29)
D2	3.25 (0.50)	2.75 (0.96)	3.25 (0.96)	1.75 (0.50)	2.25 (1.50)	3.50 (1.29)	7.25* (2.22)	5.25* (0.96)	7.50* (1.73)	10.00* (2.16)	11.25* (2.22)	10.00* (2.44)
D3	15.50 (3.42)	20.75 (6.34)	15.75 (3.40)	13.25 (3.30)	27.50* (3.11)	24.00* (2.31)	23.25 (5.90)	27.80* (3.42)	24.75* (5.12)	29.75* (5.32)	21.00 (4.08)	22.25 (4.72)
D4	8.50 (0.29)	11.00* (0.58)	13.25* (0.63)	18.50* (1.19)	14.50* (0.96)	12.25* (1.25)	16.50* (1.55)	20.50* (1.76)	9.50 (2.25)	13.00* (1.00)	9.50* (0.29)	21.00* (5.52)

Table 3.2: Effect of MMPX on hyperactivation. Table shows the effect of MMPX on hyperactivation as 10 different concentrations on 4 different donors. The numbers in brackets are standard deviation. Asterix (*) indicates that standard deviations are not overlapping compared to control (i.e. statistically significant). Negative (1% DMSO) and positive (3.6µM progesterone) controls are shown on the table.

	Concentration (µM)											
	-ve control	**0.1**	**0.3**	**0.5**	**1**	**3**	**5**	**10**	**30**	**50**	**100**	**+ve control**
D1	8.75 (3.10)	13.25 (2.99)	10.25 (2.06)	14.25 (3.59)	15.00***** (2.45)	24.25***** (4.79)	25.75***** (3.30)	27.75***** (3.30)	29.25***** (8.26)	18.75***** (3.29)	19.25***** (3.59)	40.00* (5.48)
D2	19.5 (4.80)	18.75 (5,62)	25.00 (3.26)	20.25 (6.29)	32.00***** (6.38)	26.50 (5.26)	33.25***** (8.46)	29.00***** (3.16)	33.25***** (3.77)	17.75 (4.92)	17.50 (3.70)	38.00* (3.74)
D3	2.75 (1.71)	2.20 (1.30)	4.25 (0.96)	4.00 (1.41)	5.50 (1.29)	5.25 (1.50)	6.25***** (1.71)	12.00***** (1.83)	14.5***** (3.42)	10.75***** (1.71)	7.25 (2.87)	9.50* (1.29)
D4	11.75 (3.86)	8.25 (3.59)	9.25 (2.63)	17.25 (6.85)	15.5 (5.20)	15.50 (7.05)	21.75 (6.95)	22.25***** (2.22)	33.00***** (12.25)	14.75 (2.50)	15.75 (9.95)	22.50 (9.04)

Table 3.3: Effect of Etazolate on hyperactivation. Table shows the effect of Etazolate on hyperactivation as 10 different concentrations on 4 different donors. The numbers in brackets are standard deviation. Asterix (*) indicates that standard deviations are not overlapping compared to control (i.e. statistically significant). Negative (1% DMSO) and positive (3.6µM progesterone) controls are shown on the table.

	Concentration (µM)											
	-ve control	**0.1**	**0.3**	**0.5**	**1**	**3**	**5**	**10**	**30**	**50**	**100**	**+ve control**
D1	3.25 (0.50)	1.75 (0.50)	3.25 (0.96)	3.75 (0.96)	4.25 (0.50)	9.25***** (0.96)	6.75***** (0.96)	11.25***** (0.96)	11.75***** (1.71)	17.50***** (3.11)	15.00***** (2.94)	19.75* (4.50)
D2	9.25 (0.63)	11.00***** (0.41)	10.00 (1.22)	11.00***** (0.41)	20.50***** (0.96)	22.50***** (1.04)	25.00***** (1.08)	18.75***** (1.44)	28.75***** (1.44)	24.00***** (1.22)	20.25***** (1.25)	19.25* (1.44)
D3	9.75 (0.75)	14.00***** (0.82)	15.75***** (0.75)	21.75***** (1.11)	25.25***** (1.44)	23.00***** (1.91)	21.00***** (1.00)	32.25***** (1.11)	24.00***** (0.91)	30.00***** (0.41)	25.25***** (0.75)	27.75* (0.85)
D4	4.75 (1.71)	3.50 (0.58)	5.00 (0.00)	7.25 (0.98)	15.50***** (1.29)	13.75***** (3.30)	10.75***** (1.26)	12.50***** (1.73)	18.75***** (4.99)	11.75***** (0.96)	10.25***** (2.87)	17.25* (0.98)
D5	13.00 (1.15)	10.50 (2.38)	14.25 (1.26)	17.25***** (2.50)	16.25***** (1.89)	21.75***** (1.89)	19.50***** (1.29)	25.50***** (2.08)	19.75***** (1.50)	25.75***** (3.50)	23.25***** (2.06)	19.25* (1.50)

Table 3.4: Effect of Papaverine on hyperactivation. Table shows the effect of Papaverine on hyperactivation as 10 different concentrations on 5 different donors. The numbers in brackets are standard deviation. Asterix (*) indicates that standard deviations are not overlapping compared to control (i.e. statistically significant). Negative (1% DMSO) and positive (3.6µM progesterone) controls are shown on the table.

	Concentration (µM)											
	-ve control	**0.1**	**0.3**	**0.5**	**1**	**3**	**5**	**10**	**30**	**50**	**100**	**+ve control**
D1	17.75 (9.88)	14.50 (4.93)	15.00 (2.94)	22.75 (4.79)	27.75 (4.99)	21.50 (5.20)	28.25 (12.42)	34.00***** (3.46)	30.75 (10.10)	24.25 (7.27)	17.75 (5.90)	42.25* (8.46)
D2	6.50 (1.91)	19.25***** (3.40)	16.00***** (3.16)	20.00***** (3.74)	22.75***** (5.12)	19.50***** (4.12)	28.00***** (9.56)	23.75***** (2.99)	23.25***** (3.95)	20.25***** (6.29)	12.00 (9.76)	34.75* (3.10)
D3	0.50 (1.00)	1.50 (1.73)	2.75 (1.26)	1.25 (0.50)	2.25 (1.26)	2.75***** (0.96)	5.25***** (1.5)	3.25 (1.89)	1.75 (1.26)	2.25 (1.71)	2.00 (1.41)	4.50 (3.11)

Table 3.5: Effect of Tofisopam on hyperactivation. Table shows the effect of Tofisopam on hyperactivation as 10 different concentrations on 3 different donors. The numbers in brackets are standard deviation. Asterix (*) indicates that standard deviations are not overlapping compared to control (i.e. statistically significant). Negative (1% DMSO) and positive (3.6µM progesterone) controls are shown on the table.

Comparison between individual donor responses indicates that all 5 inhibitors were effective inducers of hyperactivation. However, their effective concentration on stimulating hyperactivation varies as expected. Among the 5 PDE inhibitors examined, Papaverine had the broadest concentration spectrum on hyperactivation; above 0.5µM concentration, all of the donors showed a significant increase in hyperactivated cells in response to Papaverine (Table 3.6). Rest of the inhibitors had narrower concentration spectrum on hyperactivation. Ibudilast (IC_{50}: 0.05-5µM depending on the sub-type) was effective between 10-100µM, MMPX (IC_{50}: 5.2µM) was effective between 3-100µM, Etazolate (IC_{50}: 2µM) was effective between 5-30µM, and Tofisopam (IC_{50}: 0.68µM) was found to be most effective at 10µM (Table 3.6). Furthermore, the increment in hyperactivation in response to PDE inhibitors was found to be lower at 100µM (Figure 3.3).

	Concentration (µM)										
Drug	**0.1**	**0.3**	**0.5**	**1**	**3**	**5**	**10**	**30**	**50**	**100**	**+ve control**
Ibudilast	1/4	0/4	0/4	1/4	2/4	2/4	2/4	4/4	4/4	4/4	3/4
MMPX	1/4	1/4	1/4	2/4	3/4	3/4	3/4	2/4	3/4	2/4	2/4
Etazolate	0/4	0/4	0/4	2/4	1/4	3/4	4/4	4/4	2/4	1/4	3/4
Papaverine	2/5	1/5	3/5	5/5	5/5	5/5	5/5	5/5	5/5	5/5	5/5
Tofisopam	1/3	1/3	1/3	1/3	2/3	1/3	2/3	1/3	1/3	0/3	2/3

Table 3.6: Table shows the number of donors showing significant responses to 5 PDE inhibitors on hyperactivation 10 different concentrations. Ibudilast (n=4), MMPX (n=4), Etazolate (n=4), Papaverine (n=5), Tofisopam (n=3). Progesterone at 3.6µM is used as +ve control. Siginificancy was determined by examining SD compared to –ve control (1% DMSO, not shown).

As the spermatozoa used in these experiments were highly motile, it was hypothesized that the intracellular cAMP concentration was maximal (Tash and Means,

1983). Therefore, further increment in intracellular cAMP concentration may not have been possible in response to the PDE inhibitors, hence no significant difference observed in total motility and progressive motility. To examine this, further analysis was performed on individual donors on specific motility parameters, namely VAP, VCL, VSL, and ALH (Appendix). It was found that all PDE inhibitors used increased these parameters.

3.3.2 Effect of PDE Inhibitors on Calcium Signalling and Its Relation with Motility

Intracellular Ca^{2+} signals of research donors in response to 5 PDE inhibitors at 10µM to 100µM were recorded. This range of concentration was determined in the light of IC_{50} values to have 100% inhibition of PDEs and previous observations by Tardif *et. al.,* (unpublished data) suggesting that above 100µM concentration these PDE inhibitors become toxic to human sperm cells. All of the PDE inhibitors tested evoked their own Ca^{2+} signals at higher concentrations (50-100µM, Figure 3.8-3.22) and showed no significant relationship with motility. However, these signals were not strong and statistically insignificant. At 100µM Papaverine evoked 14% (± 0.82%, ns, n=4, Figure 3.20) of response that of progesterone response. MMPX showed the highest response at 100µM as it showed 21% (± 18, ns, n=4, Figure 3.12) of response that of progesterone response. However, this was due to an unusual response of 1 donor, which showed 73% response that of progesterone.

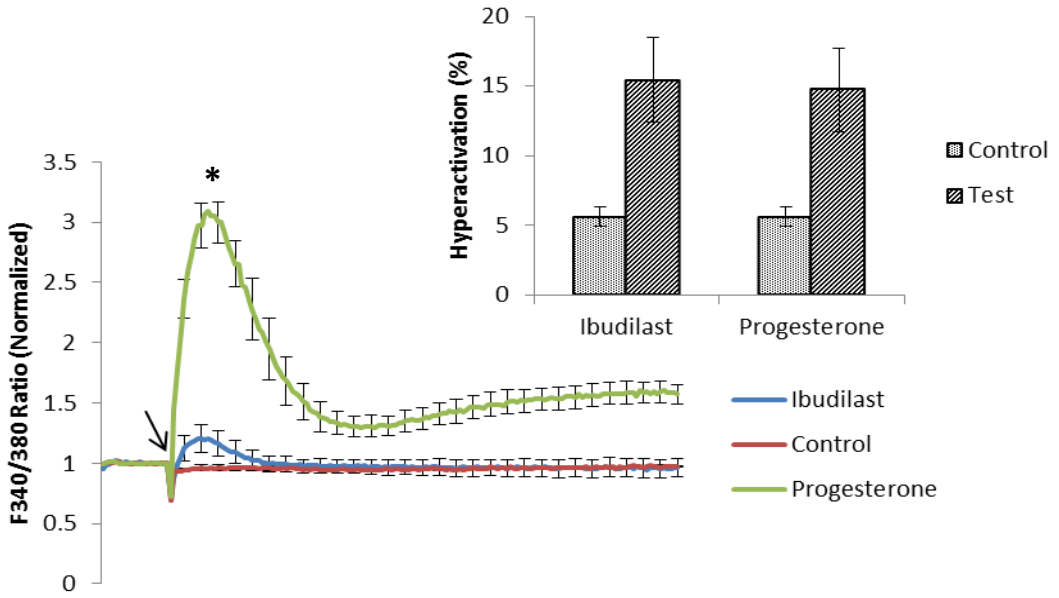

Figure 3.4: Relationship between intracellular Ca^{2+} signalling and hyperactivation in response to 100µM Ibudilast. Intracellular Ca^{2+} signals were evaluated upon stimulation with Ibudilast (n=4) at 100µM final concentration, and both +ve (progesterone at 3.6µM final concentration, n=4) and –ve (1% DMSO, n=4) controls after 100sec (20 readings) of data acquisition at resting level indicated by arrow. Inset shows %hyperactivation in response to 100µM Ibudilast (n=4) and 3.6µM progesterone (n=4). Error bars represent SEM. Asterisk "*" indicates significancy at $p<0.05$.

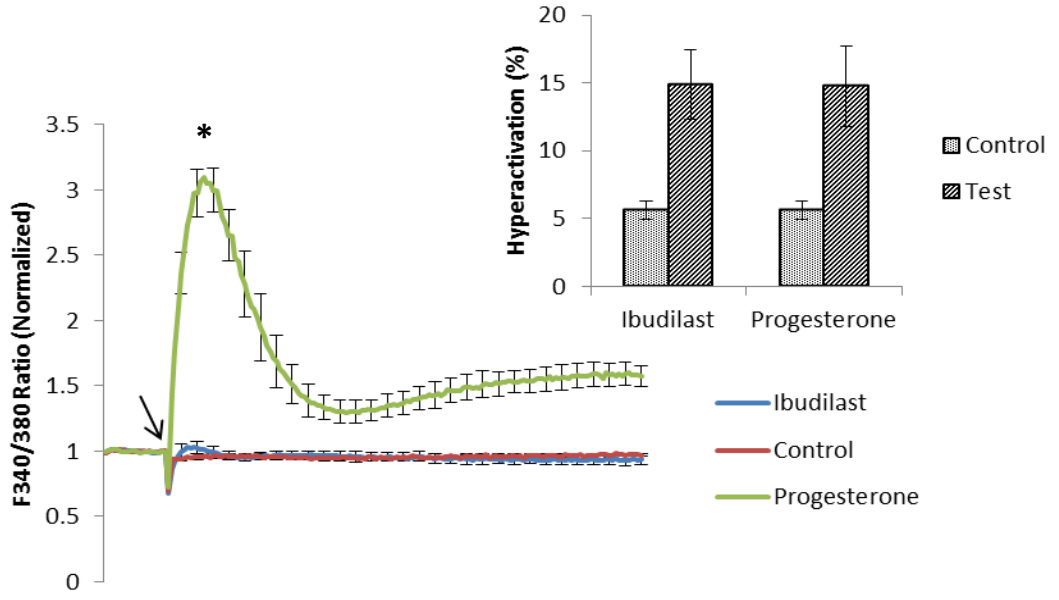

Figure 3.5: Relationship between intracellular calcium signalling and hyperactivation in response to 50µM Ibudilast. Intracellular Ca^{2+} signals were evaluated upon stimulation with Ibudilast (n=4) at 50µM final concentration, and both +ve (progesterone at 3.6µM final concentration, n=4) and –ve (1% DMSO, n=4) controls after 100sec (20 readings) of data acquisition at resting level indicated by arrow. Inset shows %hyperactivation in response to 50µM Ibudilast (n=4) and 3.6µM progesterone (n=4). Error bars represent SEM. Asterisk "*" indicates significance at $p<0.05$.

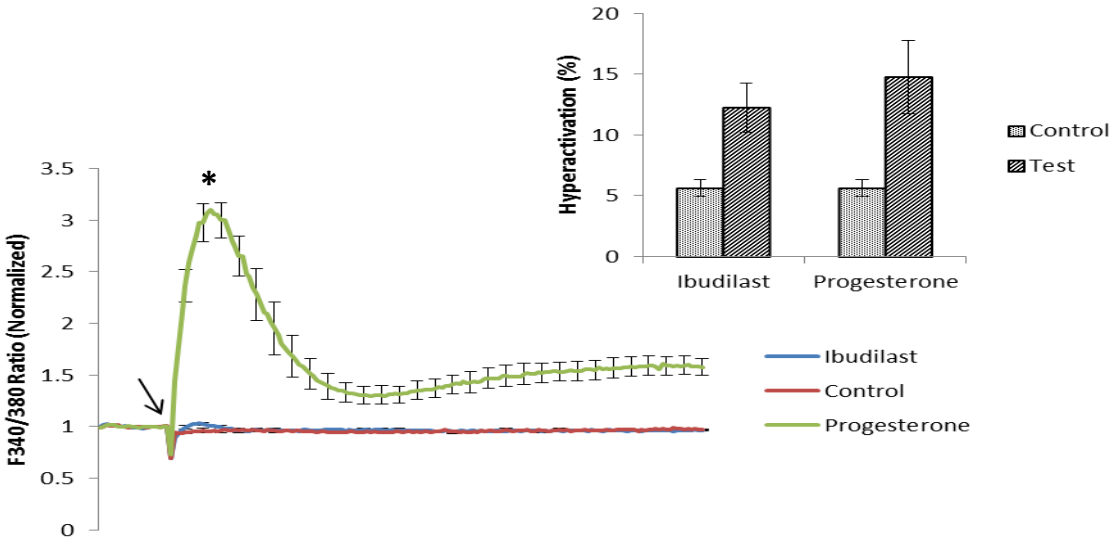

Figure 3.6: Relationship between intracellular calcium signalling and hyperactivation in response to 30µM Ibudilast. Intracellular Ca^{2+} signals were evaluated upon stimulation with Ibudilast (n=3) at 30µM final concentration, and both +ve (progesterone at 3.6µM final concentration, n=3) and –ve (1% DMSO, n=3) controls after 100sec (20 readings) of data acquisition at resting level indicated by arrow. Inset shows %hyperactivation in response to 30µM Ibudilast (n=3) and 3.6µM progesterone (n=3). Error bars represent SEM. Asterisk "*" indicates significance at $p<0.05$.

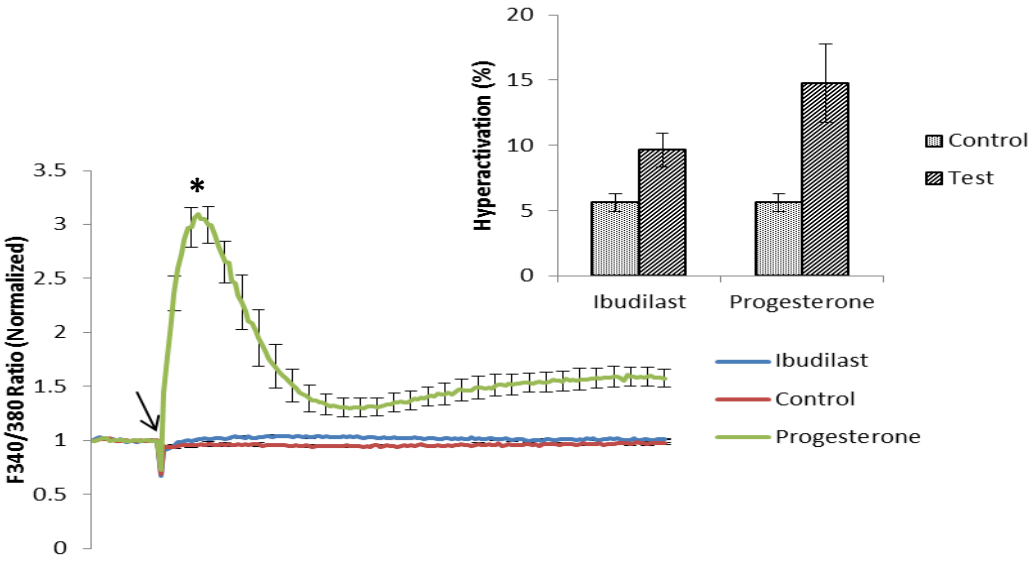

Figure 3.7: Relationship between intracellular calcium signalling and hyperactivation in response to 10µM Ibudilast. Intracellular Ca^{2+} signals were evaluated upon stimulation with Ibudilast (n=3) at 10µM final concentration, and both +ve (progesterone at 3.6µM final concentration, n=3) and –ve (1% DMSO, n=3) controls after 100sec (20 readings) of data acquisition at resting level indicated by arrow. Inset shows %hyperactivation in response to 10µM Ibudilast (n=3) and 3.6µM progesterone (n=3). Error bars represent SEM. Asterisk "*" indicates significance at $p<0.05$.

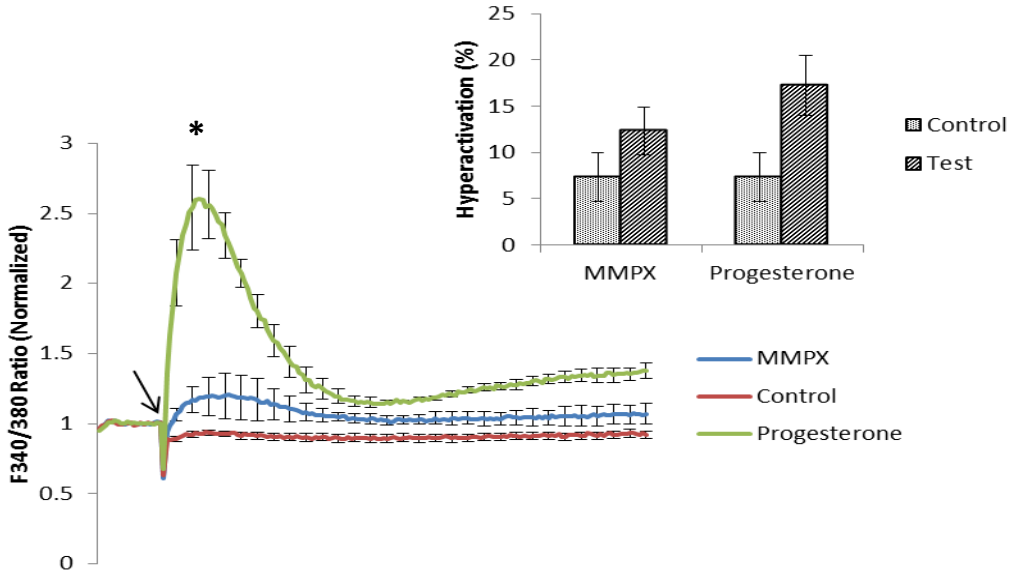

Figure 3.8: Relationship between intracellular calcium signalling and hyperactivation in response to 100µM MMPX. Intracellular Ca^{2+} signals were evaluated upon stimulation with MMPX (n=4) at 100µM final concentration, and both +ve (progesterone at 3.6µM final concentration, n=4) and –ve (1% DMSO, n=4) controls after 100sec (20 readings) of data acquisition at resting level indicated by arrow. Inset shows %hyperactivation in response to 100µM MMPX (n=4) and 3.6µM progesterone (n=4). Error bars represent SEM. Asterisk "*" indicates significance at $p<0.05$.

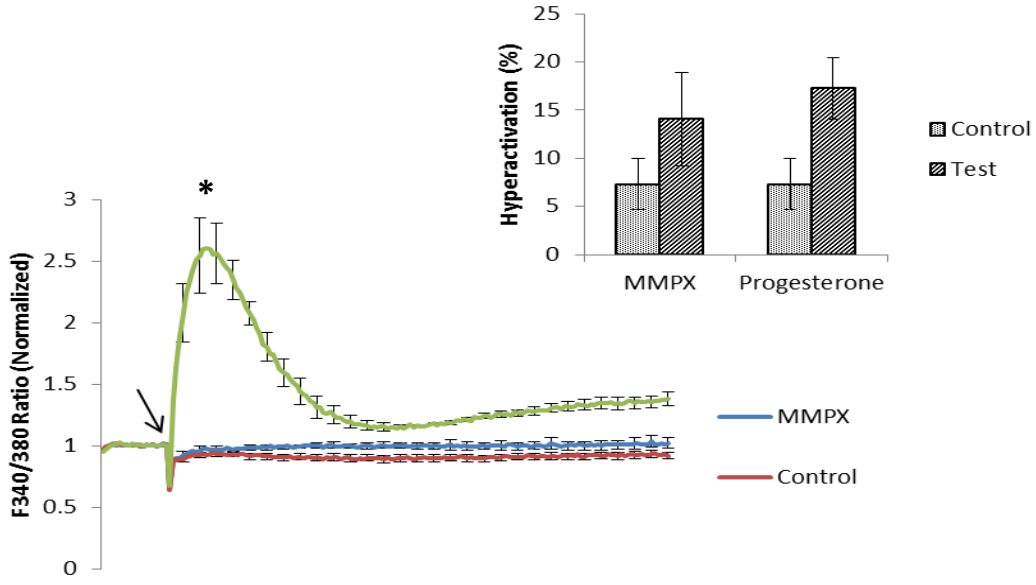

Figure 3.9: Relationship between intracellular calcium signalling and hyperactivation in response to 50µM MMPX. Intracellular Ca^{2+} signals were evaluated upon stimulation with MMPX (n=4) at 50µM final concentration, and both +ve (progesterone at 3.6µM final concentration, n=4) and –ve (1% DMSO, n=4) controls after 100sec (20 readings) of data acquisition at resting level indicated by arrow. Inset shows %hyperactivation in response to 50µM MMPX (n=4) and 3.6µM progesterone (n=4). Error bars represent SEM. Asterisk "*" indicates significance at $p<0.05$.

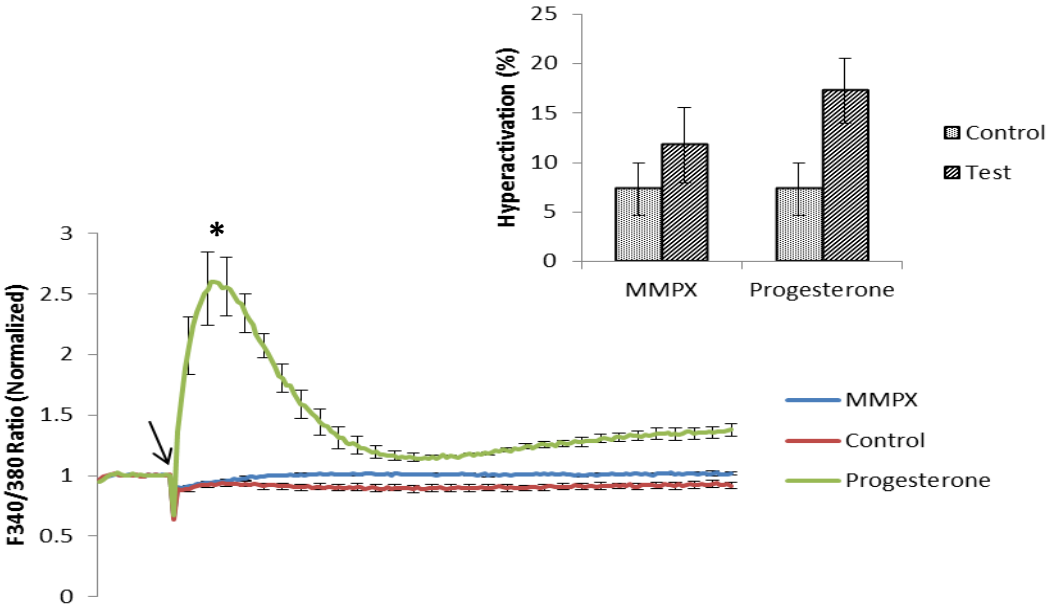

Figure 3.10: Relationship between intracellular calcium signalling and hyperactivation in response to 30µM MMPX. Intracellular Ca^{2+} signals were evaluated upon stimulation with MMPX (n=4) at 30µM final concentration, and both +ve (progesterone at 3.6µM final concentration, n=4) and –ve (1% DMSO, n=4) controls after 100sec (20 readings) of data acquisition at resting level indicated by arrow. Inset shows %hyperactivation in response to 30µM MMPX (n=4) and 3.6µM progesterone (n=4). Error bars represent SEM. Asterisk "*" indicates significance at $p<0.05$.

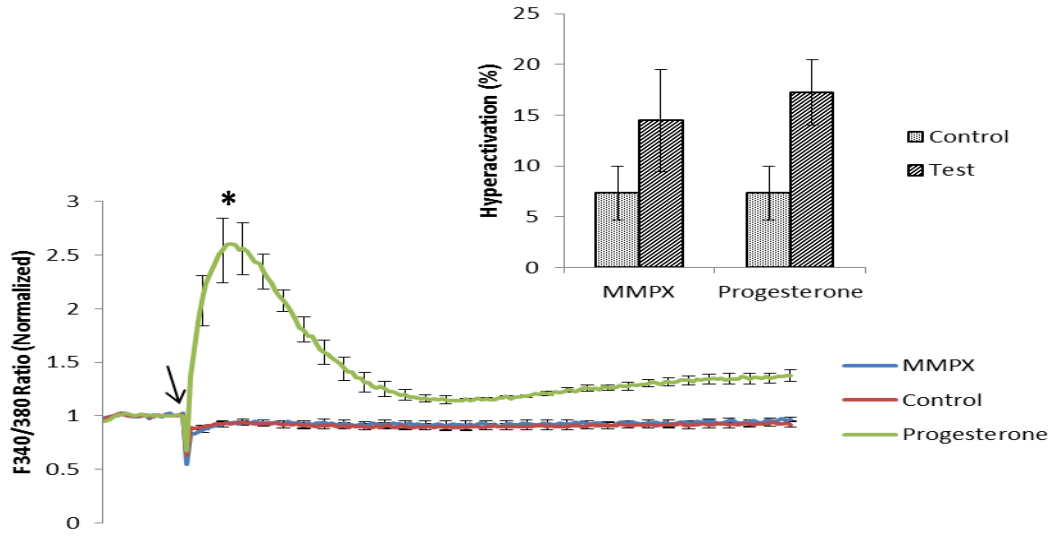

Figure 3.11: Relationship between intracellular calcium signalling and hyperactivation in response to 10µM MMPX. Intracellular Ca^{2+} signals were evaluated upon stimulation with MMPX (n=4) at 10µM final concentration, and both +ve (progesterone at 3.6µM final concentration, n=4) and –ve (1% DMSO, n=4) controls after 100sec (20 readings) of data acquisition at resting level indicated by arrow. Inset shows %hyperactivation in response to 10µM MMPX (n=4) and 3.6µM progesterone (n=4). Error bars represent SEM. Asterisk "*" indicates significance at $p<0.05$.

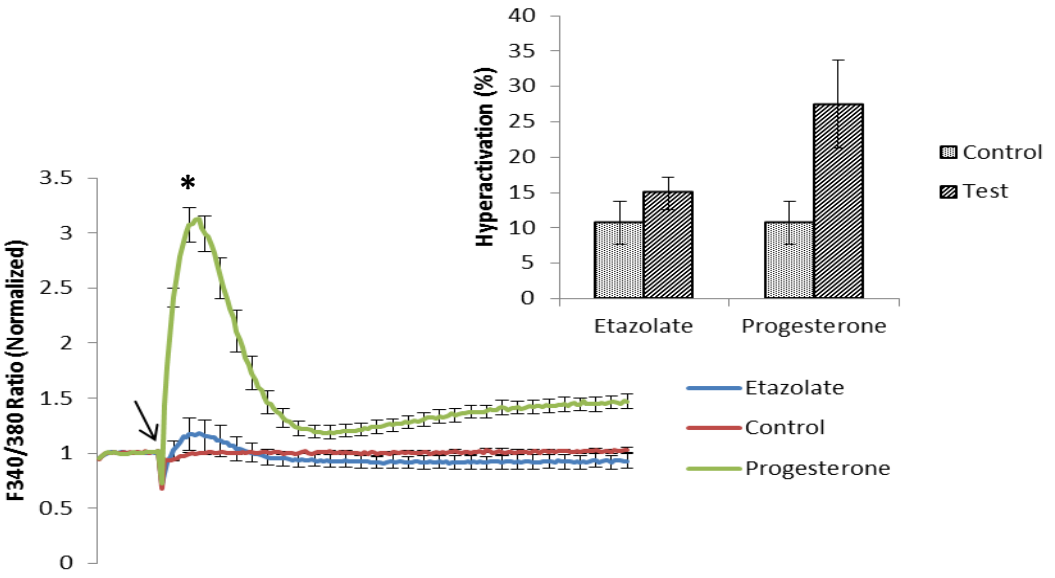

Figure 3.12: Relationship between intracellular calcium signalling and hyperactivation in response to 100µM Etazolate. Intracellular Ca^{2+} signals were evaluated upon stimulation with Etazolate (n=4) at 100µM final concentration, and both +ve (progesterone at 3.6µM final concentration, n=4) and –ve (1% DMSO, n=4) controls after 100sec (20 readings) of data acquisition at resting level indicated by arrow. Inset shows %hyperactivation in response to 100µM Etazolate (n=4) and 3.6µM progesterone (n=4). Error bars represent SEM. Asterisk "*" indicates significance at $p<0.05$.

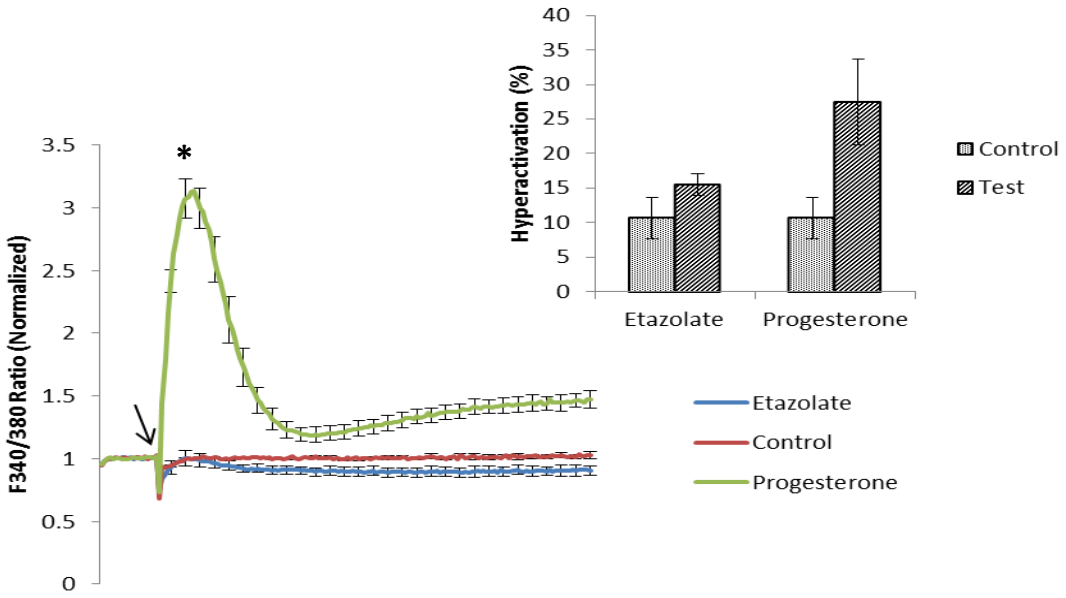

Figure 3.13: Relationship between intracellular calcium signalling and hyperactivation in response to 50µM Etazolate. Intracellular Ca^{2+} signals were evaluated upon stimulation with Etazolate (n=4) at 50µM final concentration, and both +ve (progesterone at 3.6µM final concentration, n=4) and –ve (1% DMSO, n=4) controls after 100sec (20 readings) of data acquisition at resting level indicated by arrow. Inset shows %hyperactivation in response to 50µM Etazolate (n=4) and 3.6µM progesterone (n=4). Error bars represent SEM. Asterisk "*" indicates significance at $p<0.05$.

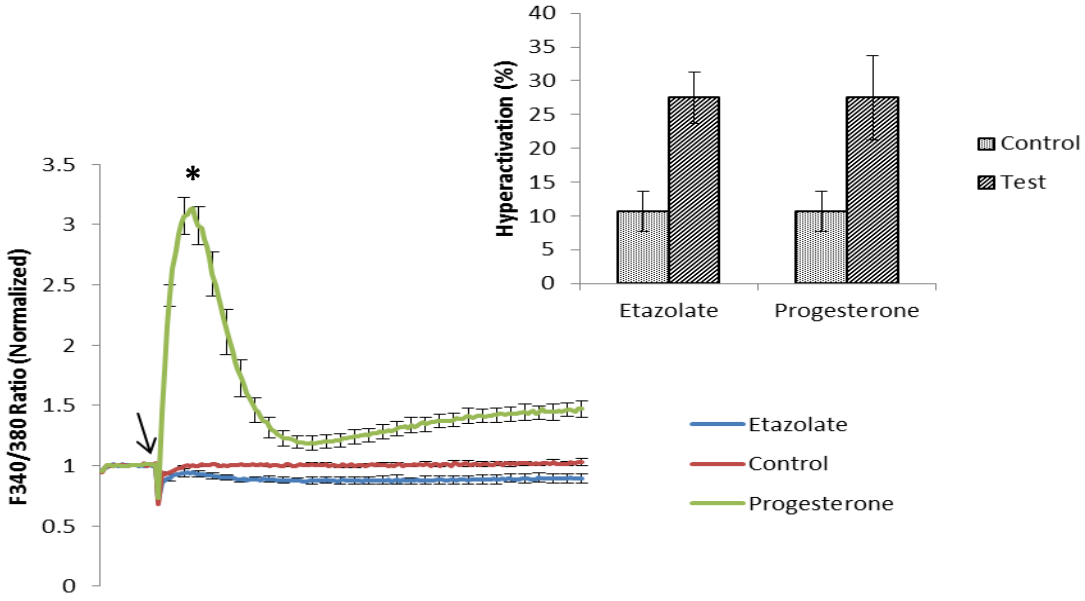

Figure 3.14: Relationship between intracellular calcium signalling and hyperactivation in response to 30µM Etazolate. Intracellular Ca^{2+} signals were evaluated upon stimulation with Etazolate (n=4) at 30µM final concentration, and both +ve (progesterone at 3.6µM final concentration, n=4) and –ve (1% DMSO, n=4) controls after 100sec (20 readings) of data acquisition at resting level indicated by arrow. Inset shows %hyperactivation in response to 30µM Etazolate (n=4) and 3.6µM progesterone (n=4). Error bars represent SEM. Asterisk "*" indicates significance at $p<0.05$.

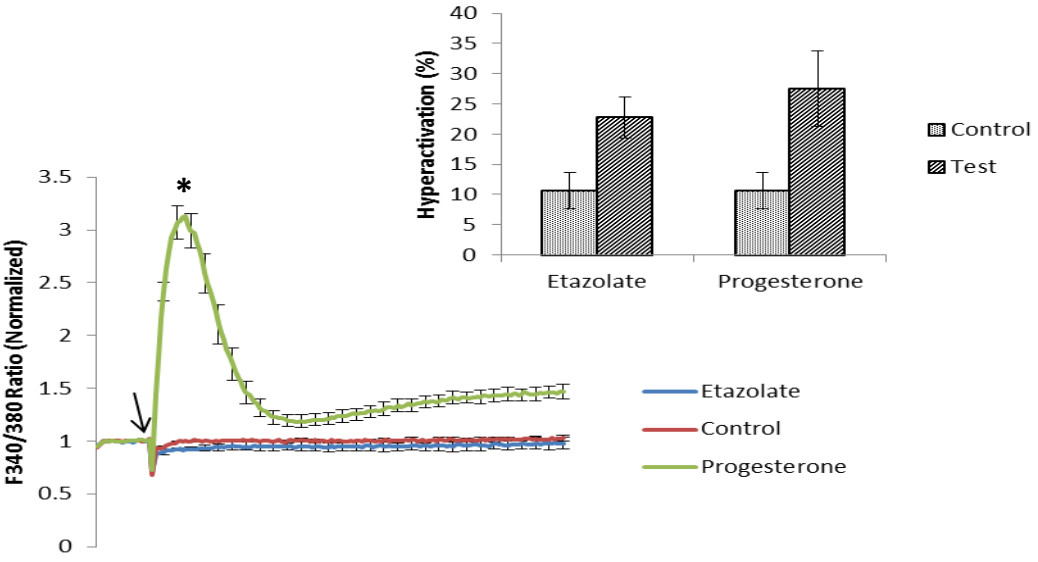

Figure 3.15: Relationship between intracellular calcium signalling and hyperactivation in response to 10µM Etazolate. Intracellular Ca^{2+} signals were evaluated upon stimulation with Etazolate (n=4) at 10µM final concentration, and both +ve (progesterone at 3.6µM final concentration, n=4) and –ve (1% DMSO, n=4) controls after 100sec (20 readings) of data acquisition at resting level indicated by arrow. Inset shows %hyperactivation in response to 10µM Etazolate (n=4) and 3.6µM progesterone (n=4). Error bars represent SEM. Asterisk "*" indicates significance at $p<0.05$.

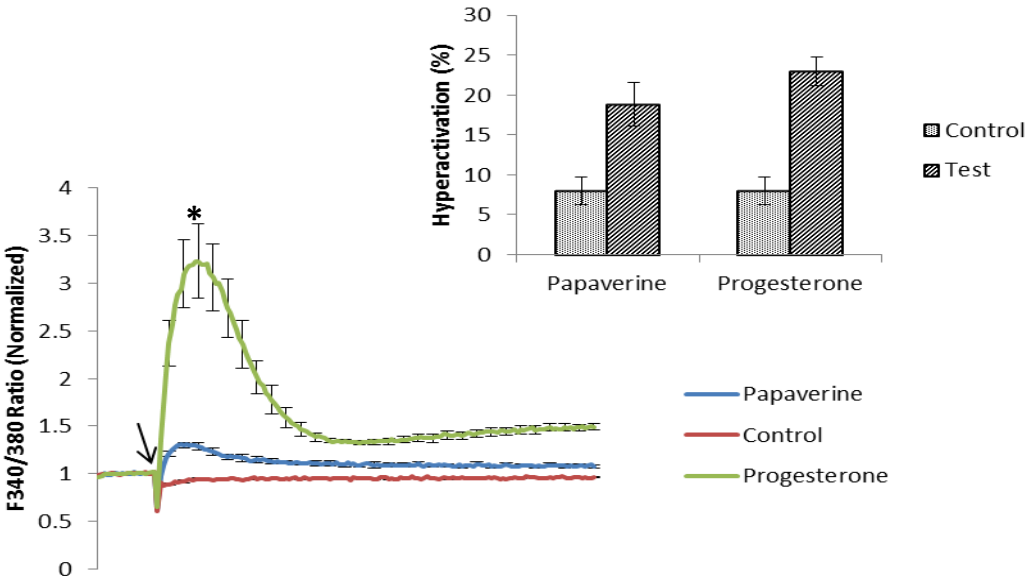

Figure 3.16: Relationship between intracellular calcium signalling and hyperactivation in response to 100µM Papaverine. Intracellular Ca^{2+} signals were evaluated upon stimulation with Papaverine (n=4) at 100µM final concentration, and both +ve (progesterone at 3.6µM final concentration, n=4) and –ve (1% DMSO, n=4) controls after 100sec (20 readings) of data acquisition at resting level indicated by arrow. Inset shows %hyperactivation in response to 100µM Etazolate (n=4) and 3.6µM progesterone (n=4). Error bars represent SEM. Asterisk "*" indicates significance at $p<0.05$.

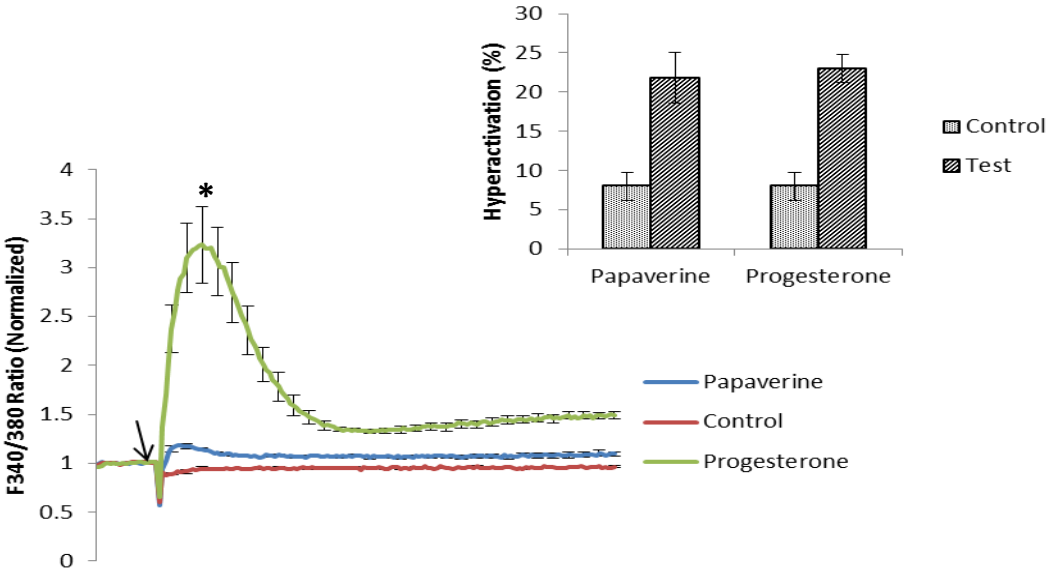

Figure 3.17: Relationship between intracellular calcium signalling and hyperactivation in response to 50µM Papaverine. Intracellular Ca^{2+} signals were evaluated upon stimulation with Papaverine (n=4) at 50µM final concentration, and both +ve (progesterone at 3.6µM final concentration, n=4) and –ve (1% DMSO, n=4) controls after 100sec (20 readings) of data acquisition at resting level indicated by arrow. Inset shows %hyperactivation in response to 50µM Etazolate (n=4) and 3.6µM progesterone (n=4). Error bars represent SEM. Asterisk "*" indicates significance at $p<0.05$.

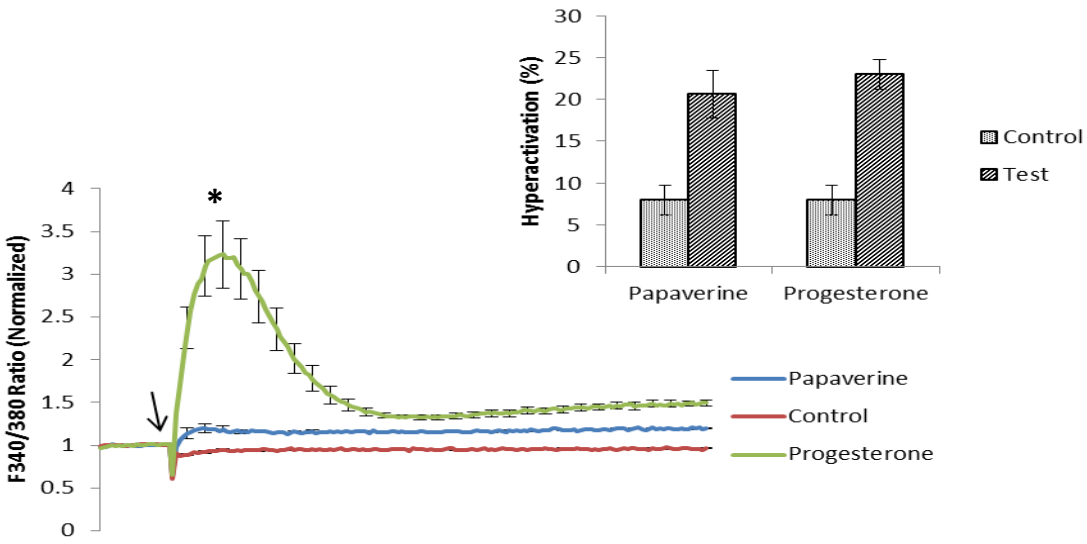

Figure 3.18: Relationship between intracellular calcium signalling and hyperactivation in response to 30µM Papaverine. Intracellular Ca^{2+} signals were evaluated upon stimulation with Papaverine (n=4) at 30µM final concentration, and both +ve (progesterone at 3.6µM final concentration, n=4) and –ve (1% DMSO, n=4) controls after 100sec (20 readings) of data acquisition at resting level indicated by arrow. Inset shows %hyperactivation in response to 30µM Etazolate (n=4) and 3.6µM progesterone (n=4). Error bars represent SEM. Asterisk "*" indicates significance at $p<0.05$.

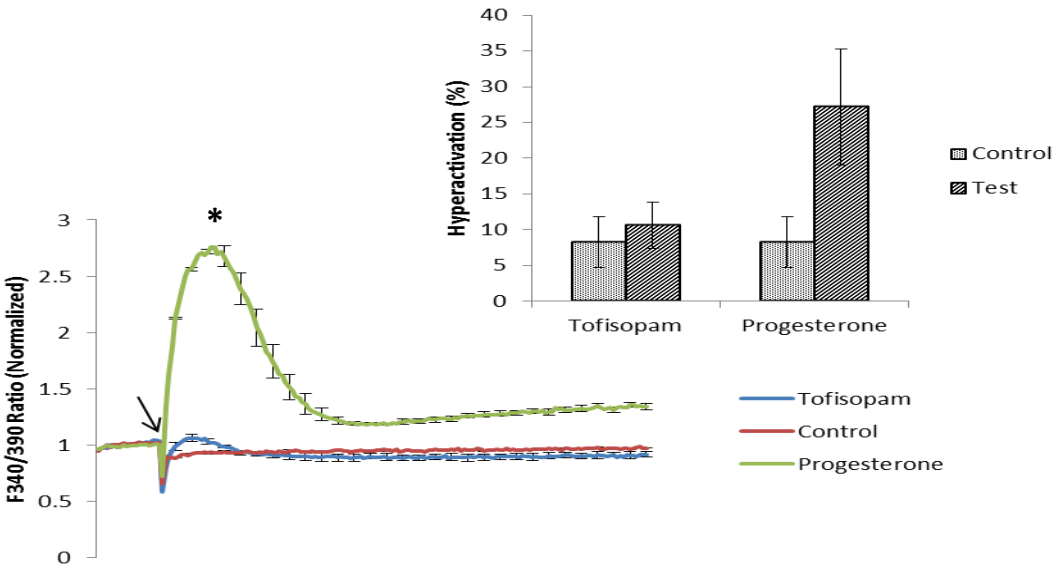

Figure 3.19: Relationship between intracellular calcium signalling and hyperactivation in response to 100µM Tofisopam. Intracellular Ca^{2+} signals were evaluated upon stimulation with Tofisopam (n=2) at 100µM final concentration, and both +ve (progesterone at 3.6µM final concentration, n=2) and –ve (1% DMSO, n=2) controls after 100sec (20 readings) of data acquisition at resting level indicated by arrow. Inset shows %hyperactivation in response to 100µM Tofisopam (n=3) and 3.6µM progesterone (n=3). Error bars represent SEM. Asterisk "*" indicates significance at $p<0.05$.

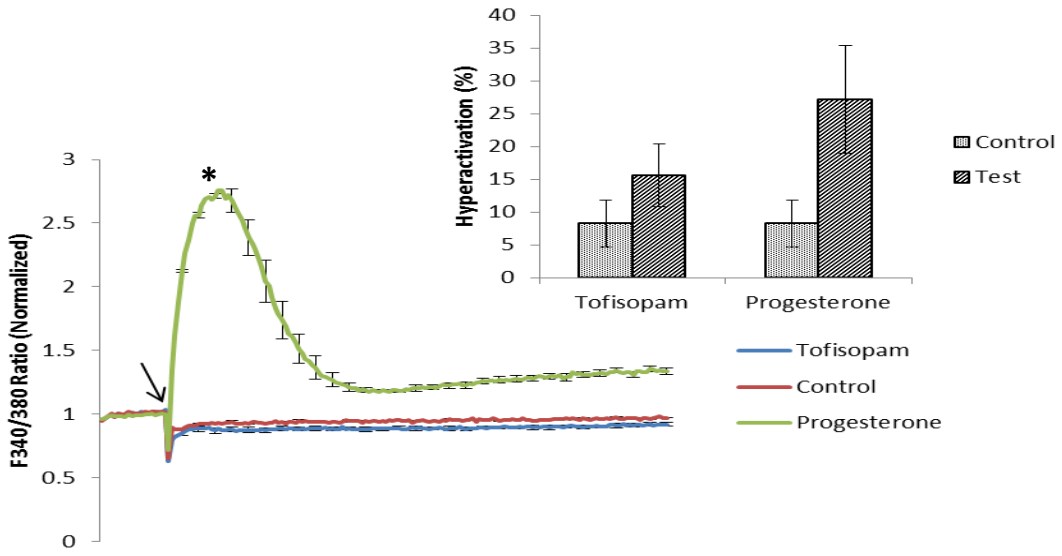

Figure 3.20: Relationship between intracellular calcium signalling and hyperactivation in response to 50µM Tofisopam. Intracellular Ca^{2+} signals were evaluated upon stimulation with Tofisopam (n=2) at 50µM final concentration, and both +ve (progesterone at 3.6µM final concentration, n=2) and –ve (1% DMSO, n=2) controls after 100sec (20 readings) of data acquisition at resting level indicated by arrow. Inset shows %hyperactivation in response to 50µM Tofisopam (n=3) and 3.6µM progesterone (n=3). Error bars represent SEM. Asterisk "*" indicates significance at $p<0.05$.

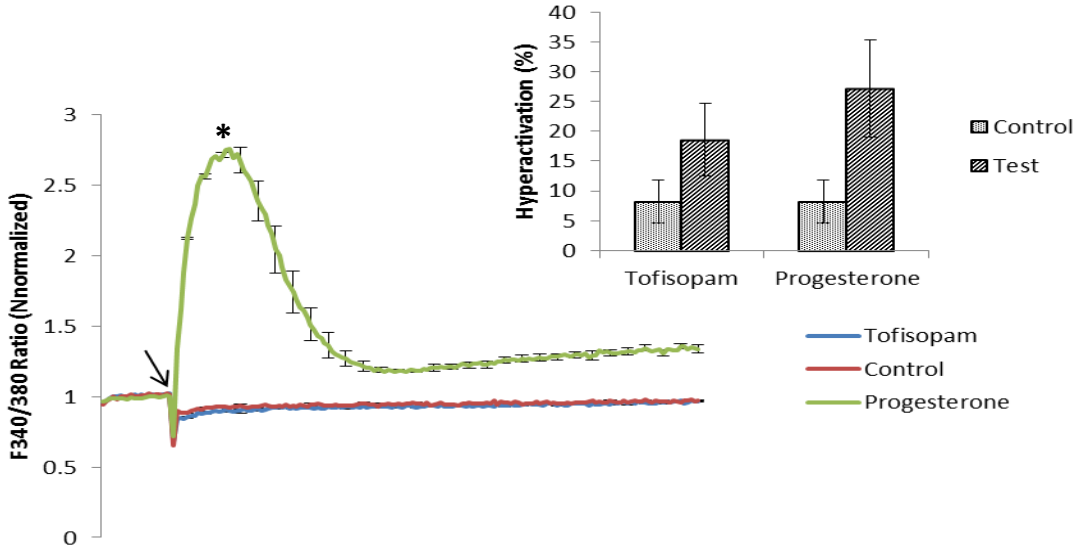

Figure 3.21: Relationship between intracellular calcium signalling and hyperactivation in response to 30µM Tofisopam. Intracellular Ca^{2+} signals were evaluated upon stimulation with Tofisopam (n=2) at 30µM final concentration, and both +ve (progesterone at 3.6µM final concentration, n=2) and –ve (1% DMSO, n=2) controls after 100sec (20 readings) of data acquisition at resting level indicated by arrow. Inset shows %hyperactivation in response to 30µM Tofisopam (n=3) and 3.6µM progesterone (n=3). Error bars represent SEM. Asterisk "*" indicates significance at $p<0.05$.

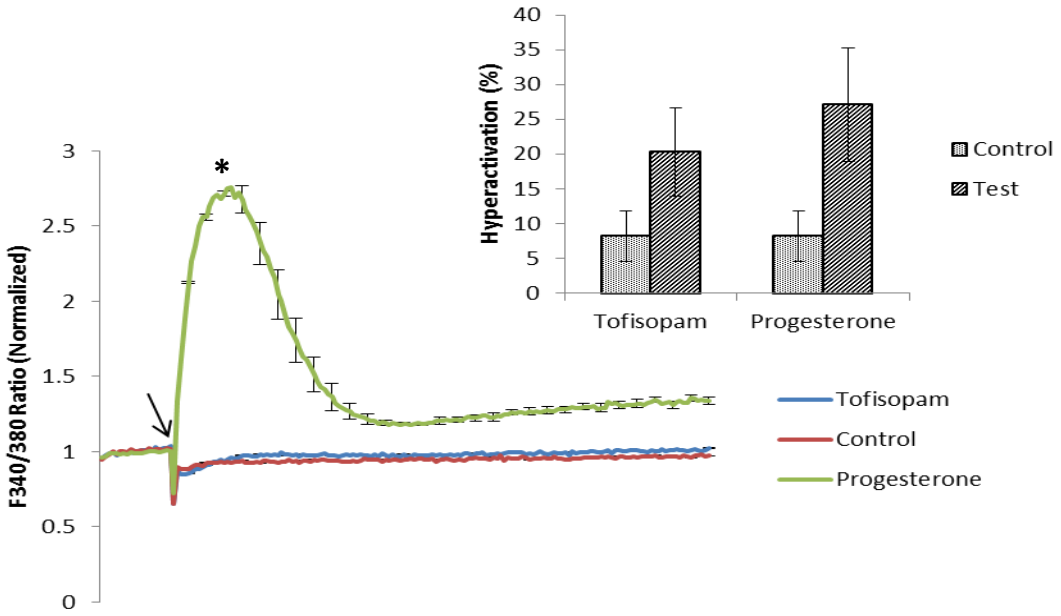

Figure 3.22: Relationship between intracellular calcium signalling and hyperactivation in response to 10µM Tofisopam. Intracellular Ca^{2+} signals were evaluated upon stimulation with Tofisopam (n=2) at 10µM final concentration, and both +ve (progesterone at 3.6µM final concentration, n=2) and –ve (1% DMSO, n=2) controls after 100sec (20 readings) of data acquisition at resting level indicated by arrow. Inset shows %hyperactivation in response to 10µM Tofisopam (n=3) and 3.6µM progesterone (n=3). Error bars represent SEM. Asterisk "*" indicates significance at $p<0.05$.

3.4 Discussion

The aim of the study was to document the intracellular Ca^{2+} responses of 5 different PDE inhibitors (Ibudilast, MMPX, Etazolate, Papaverine and Tofisopam) and to investigate their relationship with motility. Pentoxifylline, a well defined, first generation non-specific PDE inhibitor was shown to increase human sperm motility, induce hyperactivation, and induce acrosome reaction (Tesarik *et. al.,* 1992; De Jonge *et. al.,* 1991; Nassar *et. al.,* 1998). Surprisingly, the effect of pentoxifylline on both acrosome reaction and hyperactivation is not induced by Ca^{2+} influx (Nassar *et. al.,* 1998). This finding suggests that there are different mechanisms that control the acrosome reaction and hyperactivation other than Ca^{2+} signalling. However, the effects of specific PDE inhibitors on Ca^{2+} signalling have never been tested before.

In this study, it was shown that selective PDE inhibitors Ibudilast, MMPX, Etazolate, Tofisopam, and non-selective PDE inhibitor Papaverine failed to induce significant Ca^{2+} influx in human sperm at any concentration. Therefore, their effects on motility occur through mechanisms other than Ca^{2+} signalling. All compounds tested stimulated hyperactivation and CASA parameters VAP, VCL, VSL, and ALH. The effects of inhibitors tested on hyperactivation appear to be more effective on lower concentrations (1-10µM), with the exception of Papaverine. Conversely, all of the inhibitors tested had effects on Ca^{2+} signalling on higher concentrations (50-100µM). Based on the IC_{50} values of PDE inhibitors used, it was concluded that the induction in Ca^{2+} signalling is due to non-specific interactions of the drugs used. It has been showed that CatSper is a polymodal channel that can be activated by various compounds (Brenker *et. al.,* 2012). Furthermore, Trequinsin HCl, an ultra-potent PDE type 4 inhibitor also activates CatSper, such that the ionic current is indistinguishable from the progesterone activation (see chapter 4 and 5; Mansell *et. al.,* unpublished data). Therefore, Ca^{2+} signals induced by these 5 PDE inhibitors tested in this study could

influx through CatSper channels as well as through opening of unknown Ca^{2+} channels or through store mobilization. However, none of these Ca^{2+} signals were statistically significant. These chemicals were required in high quantities for each Ca^{2+} assay and due to financial limitations, the compounds were in limited supply. Consequently, the sample sizes of the study were small. Therefore, more repeats are required in order to have more significant results. All compounds evoked the highest Ca^{2+} signals at 100µM concentration. Therefore, sample powers for each compound at 100µM were calculated and checked with the sample power of the positive control (3.6µM progesterone). Sample powers for the compounds were; Ibudilast (1-β=0.7753), MMPX (1-β=0.6982), Etazolate (1-β=0.7201), Papaverine (1-β=0.7424), and Tofisopam (1-β=0.7664). Positive control 3.6µM progesterone oppositely showed 1-β > 0.99 on each case. Based on the statistical power and significancy of the positive control, it was concluded that the statistics applied were working. Required sample sizes in order to have significant results were calculated based these findings to be 13 for Ibudilast, 20 for MMPX, 18 for Etazolate, 15 for Papaverine, and 9 for Tofisopam in order to have significant results. Therefore, it was concluded that evaluating intracellular Ca^{2+} responses of these compounds would be impractical using FLUOstar and it is suggested to use Flexstation for future experiments. Nevertheless, the sample sizes were sufficient enough to conclude that the effects of these PDE inhibitors on both hyperactivation and Ca^{2+} signalling were repeatable.

As these PDE inhibitors are effective human sperm motility inducers (Tardif *et. al.*, unpublished data; this study), the value of screening possible drug candidates for human sperm motility using Ca^{2+} responses could also be investigated. It can be said that these effective drugs would not be identified from the drug screening program for further investigation as none of the inhibitors evoked sufficient Ca^{2+} signals in order to be considered as a hit compound (see chapter 4). The Ca^{2+} signals in this study were

evaluated for 5 minutes, whereas, in the drug screening Flexstation assay, the signals were only evaluated for 100 seconds at a single point screen at 40µM. Comparing the closest concentration of PDE inhibtors on the Ca^{2+} assays in this study (30µM and 50µM) suggests that only Papaverine would be identified as a responding compound and would be categorized to respond 8-10% response that of the progesterone response which is below the criteria considered as a hit compound. Nevertheless, drug-screening program still possesses importance as it already identified a novel compound that increases human sperm motility (see chapters 4 and 5). Additionally, it is possible that some compounds that cause Ca^{2+} influx may still alter human sperm motility.

In conclusion, it was shown that Ibudilast, MMPX, Etazolate, Papaverine, and Tofisopam are effective human sperm motility inducers. However, their effects on hyperactivation are through mechanisms other than intracellular Ca^{2+} signalling.

Chapter 4 : Screening a Chemogenomics Library Using Calcium as a Surrogate

4.1 Introduction

Despite the unmet need for therapeutic options for male factor sub-fertility, there is limited progress in our understanding of sperm physiology that controls human sperm function thus, hampering novel drug design/discovery. However, sperm motility and intracellular Ca^{2+} signalling of human sperm are known to correlate with fertilization success *in vitro* and *in vivo* (Publicover and Barratt, 2011; Alasmari *et. al.,* 2012; Brenzik *et. al.,* 2013). Changes in intracellular Ca^{2+} concentration controls human sperm function such as hyperactivation, acrosome reaction, and chemotaxis (Publicover *et. al.,* 2007; Publicover and Barratt, 2011; Darzson *et. al.,* 2011; Eisenbach and Giojalas, 2006). For this reason, a chemogenomics library consisting of 223 compounds (from Drug Discovery Unit, University of Dundee, College of Life Science) was subjected to high throughput screening (HTS) using intracellular Ca^{2+} signalling as a surrogate for physiological response in order to identify potential pro-motility compounds for human sperm. Although it was shown that effective motility stimulators are ineffective Ca^{2+} influx inducers (see chapter 3), it is still possible that compounds that cause Ca^{2+} influx can also alter sperm function. Clearly, using CASA would be the ideal method for screening motility modulators. However, screening large number of compounds using CASA would be methodologically impractical and inefficient. Promisingly, there is evidence suggesting CatSper functioning as a polymodal channel indicating that there are possibilities of finding novel CatSper agonists (Brenker *et. al.,* 2012). As both intracellular Ca^{2+} signalling and hyperactivation correlates with fertilization success *in vitro* and *in vivo*, it was hypothesized that HTS screening compounds would lead to the discovery of novel compounds (possible drug candidates) for human sperm motility induction as well as helping us to understand and unravel the

control mechanisms of human sperm physiology and motility. Therefore, a chemogenomics library consisting of 223 compounds aiming at a broad range of physiological targets was screened using intracellular Ca^{2+} signalling as a surrogate of physiological response. Compounds were ranked and categorized according to their Ca^{2+} responses. Subsequently, identified hit compounds with intense intracellular Ca^{2+} signalling were tested on motility in order to confirm the hypothesis in the next chapter (see chapter 5).

4.2 Materials and Methods

4.2.1 Experimental design

Semen samples from research donors were used for this study. Prepared samples were allowed to capacitate for 2½ hours (see sperm preparation). Following capacitation, sperm samples were prepared for Flexstation screening (see Flexstation assay).

4.2.2 Media and Chemicals

STF and NCB were the same as described in Chapter 2 (see section 2.2.2) with the exception of BSA, which is used at 0.3% final concentration in both STF and NCB. Fresh STF and NCB were made 1 day before the experiment to avoid contamination. All of the chemicals were purchased from Sigma. The Flexstation assay buffer consists of 1X HBSS (Invitrogen Cat No 14065-049) supplemented with 20mM HEPES (4.766g/l), 0.5mM probenecid (Sigma Cat No P8761) and the pH was adjusted to 7.4 with NaOH. Calcium 3 (Molecular Devices R8090) and Calcium 5 (Molecular Devices R8186) dyes were reconstituted at a 2X concentration in Flexstation assay buffer, as described by the manufacturer. Fluo-3/AM (Invitrogen Cat No F14242) was re-constituted in solution B (100mg/ml pluronic F-127 (Sigma, Cat No. P2443) dissolved in 0.1% acetic acid in dry DMSO) to a concentration of 10mM and stored at -20°C. The dye was subsequently diluted in Flexstation assay buffer to a final concentration of 20μM in assay buffer, prior to the Flexstation assay. Solution B was made of 100mg/ml pluronic F-127 dissolved in 0.1% acetic acid in dry DMSO.

4.2.3 Sperm Preparation

Semen samples were prepared as described in Chapter 2 (see section 2.2.3). Prepared samples were allowed to capacitate for 2½ hours.

4.2.4 Flexstation Assay

Following the capacitation, cells were diluted with the Flexstation assay buffer to 5 x 10^6 cells / ml and equal volume of Ca^{2+} sensitive dye was added and incubated at 37ºC for 40 minutes. Following the incubation, Ca^{2+} sensitive dye was washed away by centrifugation at 700g for 5 minutes at room temperature (25ºC). Cells were then resuspended at a concentration of $5x10^6$ cells/ml in flexstation buffer and aliquoted 50µl ($0.25x10^6$ cells) of cells into individual wells of a 384 well black walled, clear bottom assay plate. The assay plate was then centrifuged at 700g for 5 minutes at room temperature (25ºC) to ensure that the cells were located at the base of the plate. Assay plate, agonist/compound plate, and tips were placed into the appropriate chambers of the flexstation device and started the chosen protocol. Resting levels of fluorescence were evaluated for 20 seconds followed by agonist injection. Cells were stimulated by the addition of 12.5µl progesterone giving a final concentration of 30µM or other agonists giving final concentration of 40µM and fluorescence signals were evaluated for 100 seconds.

4.3 Results

The chemogenomics library consisted of a broad spectrum of compounds aimed at a wide range of molecular targets. Total of 223 compounds were screened on a single plate and single point concentration were used (40μM). Hits were divided into 3 categories (>25% effect, >50% effect, and >75% effect) according to their relative signal strength compared to progesterone (positive control) to identify the compunds evoking strong Ca^{2+} influx. 11.2% (25 compounds), 6.3% (14 compounds), and 3.1% (7 compounds) gave putative hit effect of >25% effect, >50% effect, and >75% effect respectively (Table 4.1 and 4.2).

Output	Result	As % of total
Total number of compounds	223	-
Putative hit >25% effect	25	11.2
Putative hit >50% effect	14	6.3
Putative hit >75% effect	7	3.1

Table 4.1: Output chemogenomics library on flexstation assay. Compounds were categorized (colour coded) accordingly with their relative responses to progesterone.

Compound Name	Primary Action	Increase in Fluorescence (%)
JX 401	Potent, reversible p38α inhibitor	115
PHA 665752	Potent and selective MET inhibitor	111
Lylamine hydrochloride	CB1 agonist	108
Trequinsin hydrochloride	Ultrapotent inhibitor of PDE3	91
Y 29794 oxalate	Prolyl endopeptidase inhibitor	88
NVP 231	Potent, selective and reversible CerK inhibitor	77
FPL 64176	Potent activator of Ca2+ channels (L-type)	75
GW 9508	Potent and selective FFA1 (GPR40) agonist	67
UK 78282 hydrochloride	Blocker of KV1.3 and KV1.4 channels	66
Ciglitazone	Selective PPARg agonist	64
SANT-1	Inhibitor of hedgehog (Hh) signalling; antagonizes smoothened activity	57
U 89843A	Positive allosteric modulator of GABAA receptors	57
AS 1949490	SH2 domain-containing inositol 5'-phosphatase 2 (SHIP2) inhibitor	54
Calcipotriol	Vitamin D3 analogue	51
BRL 50481	Selective PDE7 inhibitor	49
IKK 16	Selective inhibitor of IKK	47
BI 78D3	Selective, competitive JNK inhibitor	45
EO 1428	Selective inhibitor of p38α and p38b2	39
Repaglinide	KATP channel blocker	38
SANT-2	Inhibitor of hedgehog (Hh) signalling; antagonizes smoothened activity	36
SD 208	Potent ATP-competitive TGFbRI inhibitor	34
NNC 55-0396 dihydrochloride	Highly selective Ca2+ channel blocker (T-type)	32
GP 1a	Highly selective CB2 agonist	32
EHT 1864	Potent inhibitor of Rac family GTPases	32
RO-3	Selective P2X3 and P2X2/3 antagonist	26
SB 218078	Inhibitor of checkpoint kinase 1 (Chk1)	25

Table 4.2: 25 compounds identified as hit compounds. Table shows 25 compounds that gave a response ≥25% response that of progesterone. Compounds are colour coded according to their relative response compared to progesterone (increase in fluorescence expressed as percentage compared to resting level fluorescence). All of the compounds were tested on single point concentration (40μM) on a single plate (n=1).

4.4 Discussion

The aim of the study was to document the intracellular Ca^{2+} responses of 223 compounds, categorize them according to their relative responses (that of progesterone), and further investigate their effects on human sperm motility (see chapter 5). High throughput screening protocol was designed by Sarah Martins Da Silva (University of Dundee, Ninewells Hospital) and Anthony Hope (University of Dundee, College of Life Sciences) and utilized on human sperm for the first time (Da Silva *et. al.*, 2012). This method was developed as it is a highly time, effort, and material efficient way of screening the effect of a large number of compounds on human sperm Ca^{2+} signalling. This screening program was aimed at human sperm motility, as asthenozoospermia is the main male factor infertility (Van der Steeg *et. al.*, 2011). However, testing hundreds of compounds on human sperm motility is time consuming and financially wasteful. Therefore, HTS was utilized using Ca^{2+} signalling as a surrogate for physiological response. The compounds library consisting of 223 compounds (some commercially available) were aimed at broad spectrum of targets ranging from ion channels to PDEs. Therefore, a wide range of compounds with different primary actions was documented in their ability to induce Ca^{2+} influx.

Using single point concentration has both advantages and disadvantages. The advantage was as screening was performed at low concentration (40μM) compared to Tardif *et. al.*, (unpublished data); only the compounds that induce Ca^{2+} influx at (relatively) lower concentrations were detected. On the other hand, compounds that would normally induce Ca^{2+} influx at higher concentrations would be "missed". This would be highly appropriate in case of compounds showing sigmoidal response curves. HTS screening on Flexstation showed good repeatability (Da Silva *et. al.*, unpublished data). The vast majority (96%) of the compounds identified were novel Ca^{2+} influx

inducers. There are, however, compounds that were known to induce Ca^{2+} influx. NNC 55-0369 is used as a potent CatSper channel blocker, which also induces its own Ca^{2+} signals at concentrations greater than 10µM (Strunker *et. al*, 2011). Vitamin D analogue, calcipotriol, also stimulated Ca^{2+} influx. Vitamin D itself induces Ca^{2+} signalling in human sperm and has positive effect on human sperm motility (Jensen *et. al.,* 2011). It is known that vitamin D receptor (VDR) is present in human sperm, therefore, it could be possible that calcipotriol induces Ca^{2+} through its action on VDR (Jensen *et. al.,* 2010; Jensen *et. al.,* 2011). Both CB1 and CB2 receptors are found in human sperm (Rosatto *et. al.,* 2005; Agirregoitia *et. al.,* 2010). Furthermore, stimulation through CB1 and CB2 were shown to modulate sperm motility, acrosome reaction, and capacitation (Rosatto *et. al.,* 2005; Aquila *et. al.,* 2009; Aquila *et. al.,* 2010). Therefore, GP1a and Lylamine HCl identified in this study have potential in modulating sperm function(s). GABA receptor modulation was shown to induce acrosome reaction in bull sperm (Puente *et. al.,* 2011). This indicates a possible role for U 89843A. However, species differences should not be neglected. PPARg were shown to be present in human and pig sperm and agonists of this receptor were shown to increase sperm motility and capacitation (Santoro *et. al.,* 2013; Aquila *et. al.,* 2006). Therefore, selective PPARg agonist Ciglitazone identified in this study may alter some of the sperm function(s).

The transient component of the progesterone Ca^{2+} response was at its maximal within 100 seconds (Strunker *et. al.,* 2011). Therefore, the maximum peak point of the transient component of the progesterone response was not missed in the screening. This enabled us to examine the compounds on the Ca^{2+} signalling kinetics in comparison with the progesterone response. However, it was hard to comment on the kinetics, therefore, this section of the analysis should be considered preliminarily. In order to have much clearer findings about the kinetics of the compounds, a 10-point concentration curve should be evaluated. None of the compounds evoked Ca^{2+} influx as

rapid as progesterone with the exception of PHA 665752. PHA 665752 evoked Ca^{2+} signalling instantaneously that the maximal stimulation was reached within 2 seconds and sustained over the period of readings (i.e. 100 seconds) and produced a signal that is greater than the progesterone signal (110% response that of progesterone response). Trequinsin HCl evoked Ca^{2+} influx that was almost linear throughout the period of data acquisition. This observation, also applies to Lylamine HCl, GP 1a, SB 218078, IKK 16, NNC 55-0396, UK 78282, AS 1949490, EO 1428, RO-3, and Y 29784 although the signal magnitudes showed variation. Other inhibitors, namely; Ciglitazone, BRL 50481, FPL 64176, JX 401, BI 78D3, Repaglinide, NVP 231, SD 208, SANT-2 and Calcipotriol showed plateau responses. The natures of the Ca^{2+} signals evoked by these compounds should be investigated for longer period of time and at various concentrations in order to have a better understanding.

Some PDE inhibitors also identified as hit compounds. It is known that several odorants increase intracellular cAMP concentration of sperm that consequently opens unknown voltage-gated Ca^{2+} channels (Spehr *et. al.,* 2003; Neuhauss *et. al.,* 2006; Veitinger *et. al.,* 2011). Supporting this, membrane-permeable analogues of cAMP induce Ca^{2+} influx as well (Kobori *et. al.,* 2000; Ren *et. al.,* 2001; Machado-Oliveira *et. al.,* 2008). Therefore, it can be deduced that PDE inhibitors could induce Ca^{2+} influx. There are several PDE inhibitors identified as hit compounds, namely; Trequinsin HCl (ultrapotent inhibitor of PDE type 3, IC_{50}: 250pM), and BRL 50481 (selective PDE type 7 substrate competitor, K_i: 180nM). However, there is no data available in the literature on Trequinsin HCl and BRL 50481 about their effects on sperm cells. Trequinsin HCl induced Ca^{2+} influx almost as strong as progesterone (91% response that of progesterone). This induction cannot be explained by the opening of unknown voltage-gated Ca^{2+} channels via cAMP stimulation as other PDE inhibitors do not stimulate Ca^{2+} signalling at this magnitude (see chapter 3). Therefore, it is possible that there

might be other mechanisms responsible for Ca^{2+} signalling in response to the PDE inhibitors.

It is highly important to test all of these compounds on human sperm as some of the targets of these compounds have been reported to alter sperm function. It should be noted that Ca^{2+} measurements on Flexstation are from populations of spermatozoa. Therefore, further experiments must be performed for better understanding the actions of the drugs on Ca^{2+} signalling (i.e. patch-clamping and single-cell imaging). Furthermore, although there are exceptions, effective motility inducers are either poor Ca^{2+} stimulators or do not stimulate Ca^{2+} at all (see appendix for a list of compounds). Therefore, there is a possibility that the hit compounds would be ineffective on human sperm motility induction.

Chapter 5 : Effect of Drugs Identified from Drug Screening on Human Sperm Motility

5.1 Introduction

There are different types of phosphodiesterases found in human sperm that control sperm functions spatio-temporally including the control of sperm motility (Fisch *et. al.,* 1996; Wennemuth *et. al.,* 2002). In a simple way, using PDE inhibitors to increase the number of functional spermatozoa for either IUI or IVF is a logical approach to increase the success rates. Consequently, there are studies which investigated the effects of methylxanthines pentoxifylline, IBMX, and caffeine on human sperm motility *in vitro*. However, these drugs fail in clinical trials, as they do not increase the fertilization rates in ART unless used at high concentrations (1-10mM; Tesarik *et. al.,* 1992; Lanzafame *et. al.,* 1994; Tesarik *et. al.,* 1992a; Terriou *et. al.,* 2000). The reason of failure was because these drugs lack the specificity, as they are non-specific inhibitors of PDEs. Due to non-specific inhibition, acrosome reaction is also stimulated. Although it is known that acrosome reacted rabbit (Kuzan *et. al.,* 1984) and mouse (Inoue *et. al.,* 2011) sperm are able to fertilize oocytes, human sperm have never been tested for this ability. Consequently, it is considered that acrosome reacted human sperm cannot fertilize oocytes. Therefore, it is important to find/develop specific drugs to stimulate only the sperm motility in order to be useful in the ART field. However, there has been a lack of research in this area, especially in terms of developing/finding third generation PDE inhibitors (Publicover and Barratt, 2011). It is clear that further research is required in order to develop/find specific PDE inhibitors to be used clinically for increasing the fertilizing potential of men. Therefore, Trequinsin HCl (PDE type 3 specific ultrapotent inhibitor) and BRL 50481 (PDE type 7 specific competitive inhibitor), 2 of the PDE inhibitors identified from the drug-screening program (see chapter 4) were tested on human spermatozoa motility using CASA.

5.2 Materials and Methods

5.2.1 Experimental design

Semen samples from healthy research donors were used for this study. Following density gradient centrifugation, both the 40% and the 80% fraction of the samples were aliquoted into 4. 2 aliquots (one for control and one for test) were subjected to non-capacitating conditions, and 2 aliquots (one for control and one for test) were subjected to capacitating conditions. The 40% fraction sperm were used as putative surrogates of patient samples as they were previously shown to have similar profile in terms of motility, morphology, and DNA status to men with male factor infertility (O'Connell et al., 2003; Glenn et al., 2007). Effect of drugs on motility was also investigated under non-capacitating conditions as these are commonly used in clinics for IUI. Prepared donor samples were allowed to capacitate (or not to capacitate in non-capacitating buffer) in capacitating medium (STF) for 2½ hours (see sperm preparation). After this time, samples were subjected to drug administration with either of Trequinsin or BRL 50481 for 2 hours (see phosphodiesterase inhibition).

5.2.2. Chemicals and Solutions

STF and NCB used were the same as described in Chapter 2 (see section 2.2.2) with the exception 0.3% BSA final concentration in both STF and NCB. Trequinsin hydrochloride (T2057 sigma) and BRL 50481 (0936 sigma) were dissolved in DMSO and stored at 4 C^{o}.

5.2.3 Sperm Preparation

Semen samples were prepared as described in Chapter 2 (see section 2.2.3). Prepared samples were allowed to capacitate for 2½ hours.

5.2.4 Drug Administration

After 2½ hours of capacitation or non-capacitation, spermatozoa were aliquoted in round-bottomed tubes and trequinsin/BRL 50481/DMSO were added giving final concentration of trequinsin or BRL 50481 (test) at 10µM final concentration or 1% DMSO (control) followed by mixing gently. Motility parameters of treated spermatozoa were taken over 2 hours period at; 20 min, 40 min, 60 min, 90 min, and 120 min time intervals.

5.2.5 Sperm Motility Detection

CASA settings are the same as described in Chapter 2 (see section 2.2.4). In addition to CASA parameters described in section 2.2.4, the velocity on a straight line (VSL: is the velocity of sperm over the actual start-to-end track of cell in µm/s) and the beat cross-frequency (BCF: is the frequency of sperm head crossing the sperm average path velocity in Hz) were also evaluated.

5.2.6 Statistics

Normality of the data was checked using Kolmogorov-Smirnov test. Paired t-test was used to evaluate significance. Data shown are the means with the error bars representing SEM unless stated otherwise.

5.3 Results

5.3.1 Effects of Trequinsin and BRL 50481 Treatment on 40% Fraction Spermatozoa

5.3.1.1 Under Non-Capacitating Conditions

The 40% fraction spermatozoa from normozoospermic research donors were treated with DMSO (vehicle control), 10µM Trequinsin (test) or 10µM BRL 50481 (test) under non-capacitating conditions. Following 20 min incubation with 10µM Trequinsin, total motility increased by 20% (±7%, p=0.009, n=4; figure 5.1) under non-capacitating conditions. However, there was no increase observed on spermatozoa treated with 10µM BRL 50481 in any of the motility parameters (Appendix). Progressive motility was also stimulated following 20 min incubation with 10µM Trequinsin by 26% (±13%, p=0.026, n=4; figure 5.2) under non-capacitating conditions. There was no significant increase in hyperactivated cells in response to 10µM Trequinsin under non-capacitating conditions.

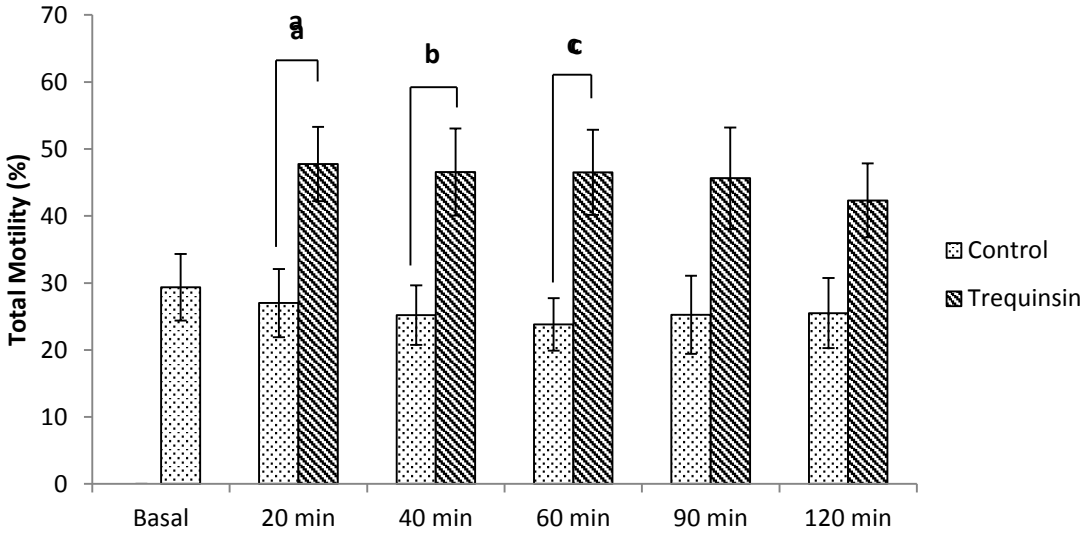

Figure 5.1: Effect of 10 µM Trequinsin on the 40% fraction spermatozoa under non-capacitating conditions on total motility (n=4). Letters above the bars represents p values (a: 0.009, b: 0.029, c: 0.015) and error bars represent SEM.

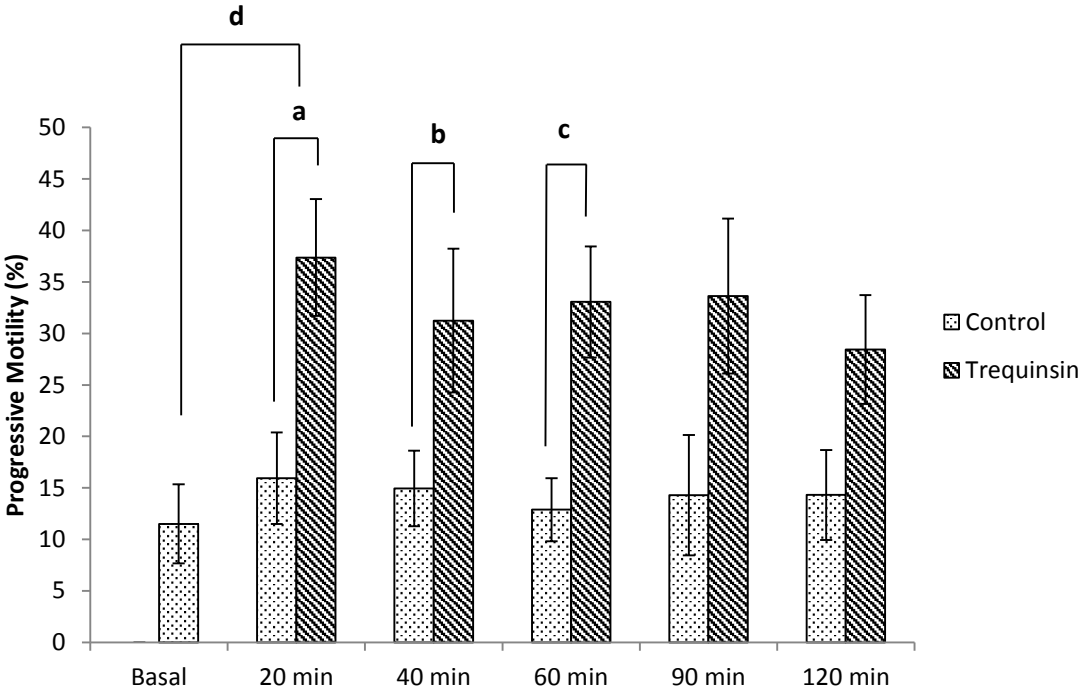

Figure 5.2: Effect of 10 µM Trequinsin on the 40% fraction spermatozoa under non-capacitating conditions on progressive motility (n=4). Letters above the bars represents p values (a: 0.003, b: 0.033, c: 0.015, d: 0.026) and error bars represent SEM.

Trequinsin at 10µM stimulated motility parameters under non-capacitating conditions. In order to further investigate the motility stimulation, average values for individual motility parameters were evaluated, namely; ALH (amplitude of lateral head displacement), VCL (curvilinear velocity), VSL (velocity on a straight line), VAP (average path velocity), LIN (linearity), and BCF (beat cross frequency). Non-capacitated spermatozoa showed significant increases in their VAP, VSL, VCL, LIN and BCF (Table 5.1).

Treatment	Movement Parameters					
	VAP (µm/s)	VSL (µm/s)	VCL (µm/s)	ALH (µm)	LIN (%)	BCF (Hz)
20 min control	41.01 ± 1.99	34.43 ± 2.10	67.14 ± 1.87	3.59 ± 0.09	50.25 ± 1.93	22.69 ± 0.86
20 min trequinsin	53.54 ± 1.61 *	47.19 ± 2.32 *	81.83 ± 1.42 *	3.35 ± 0.21	59.13 ± 3.39 *	27.20 ± 0.73 *
40 min control	42.11 ± 2.54	35.39 ± 2.55	67.86 ± 2.52	3.56 ± 0.13	51.31 ± 1.87	22.03 ± 0.65
40 min trequinsin	51.23 ± 1.75 *	44.48 ± 2.78 *	80.11 ± 0.59 *	3.55 ± 0.16	56.38 ± 3.72	26.02 ± 0.85 *
60 min control	40.05 ± 2.76	33.34 ± 2.69	65.02 ± 3.58	3.66 ± 0.04	50.13 ± 1.45	21.33 ± 1.01
60 min trequinsin	52.19 ± 2.83 *	45.11 ± 3.13 *	82.37 ± 1.93 *	3.58 ± 0.08	55.44 ± 2.81	25.99 ± 0.84 *
90 min control	39.15 ± 3.12	32.75 ± 3.49	63.89 ± 2.94	3.56 ± 0.09	50.04 ± 2.80	22.94 ± 0.72
90 min trequinsin	51.93 ± 2.57 *	44.77 ± 3.45 *	82.15 ± 1.24 *	3.62 ± 0.11	55.63 ± 3.45 *	25.45 ± 0.82
120 min control	41.36 ± 2.94	34.64 ± 2.88	67.78 ± 2.94	3.74 ± 0.11	50.00 ± 2.26	21.91 ± 0.49
120 min trequinsin	49.59 ± 2.29 *	41.99 ± 3.01 *	80.55 ± 1.23 *	3.71 ± 0.12	52.63 ± 3.02	24.93 ± 0.95 *

Table 5.1: Effect of 10µM Trequinsin on movement characteristics of the 40% fraction spermatozoa under non-capacitating conditions (n=4). ± values are SEM. * indicates $p<0.05$.

5.3.1.2 Under Capacitating Conditions

The 40% fraction spermatozoa from normozoospermic research donors were treated with DMSO (vehicle control), 10µM Trequinsin (test) or 10µM BRL 50481 (test) under capacitating conditions. Following 60 min incubation with Trequinsin at 10µM, total motilility increased by 15% (±5%, p=0.009, n=4, figure 5.3). Progressive motility was also stimulated following 40 min incubation with 10µM Trequinsin by 11% (±6%, p=0.046, n=4, figure 5.4) under capacitating conditions. Only capacitated spermatozoa treated with Trequinsin showed a significant increase in hyperactivated cells by 6% (±3%, p=0.025, n=4, figure 5.5) following 40 min incubation.

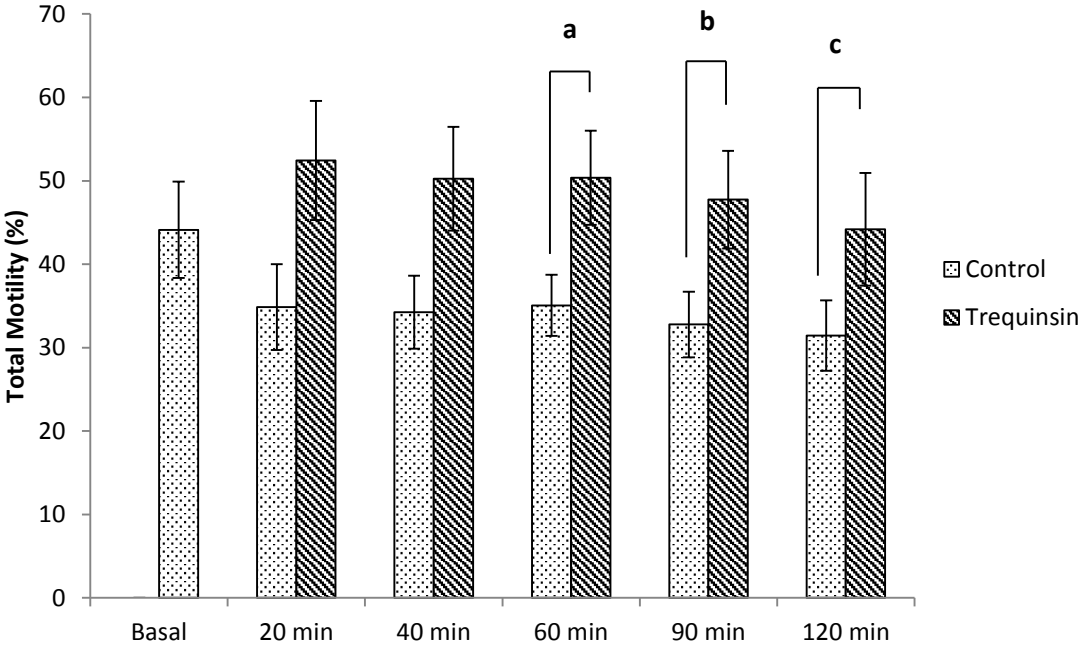

Figure 5.3: Effect of 10 µM Trequinsin on the 40% fraction spermatozoa under capacitating conditions on %total motility (n=4). Letters above the bars represents p values (a: 0.009, b: 0.02, c: 0.04) and error bars represent SEM.

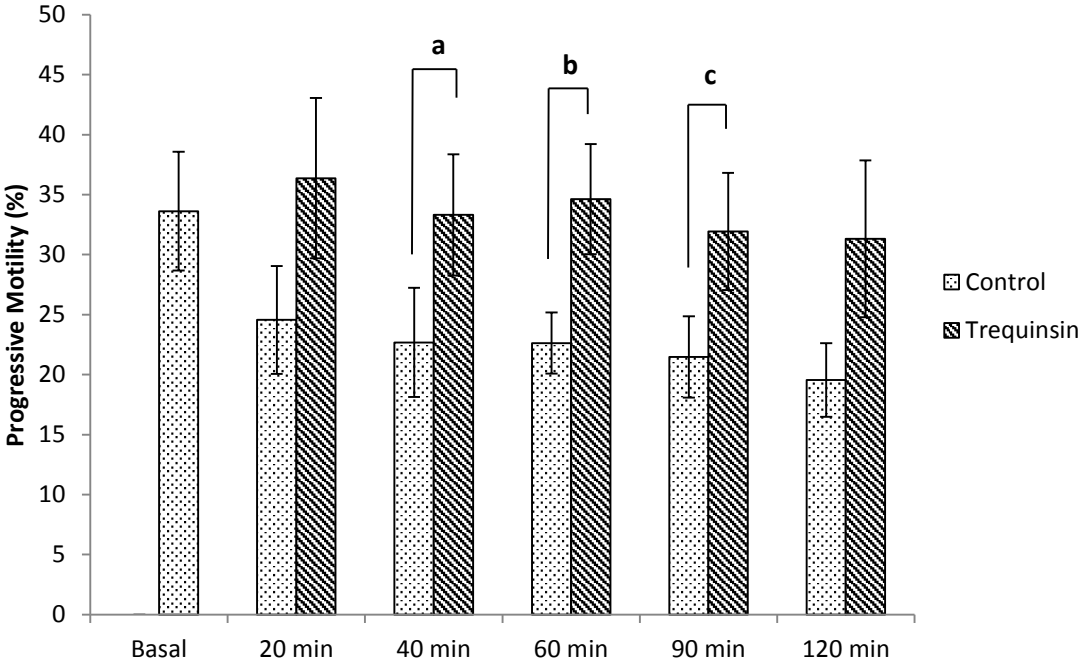

Figure 5.4: Effect of 10 µM Trequinsin on the 40% fraction spermatozoa under capacitating conditions on progressive motility (n=4). Letters above the bars represents p values (a: 0.046, b: 0.012, c: 0.013) and error bars represent SEM.

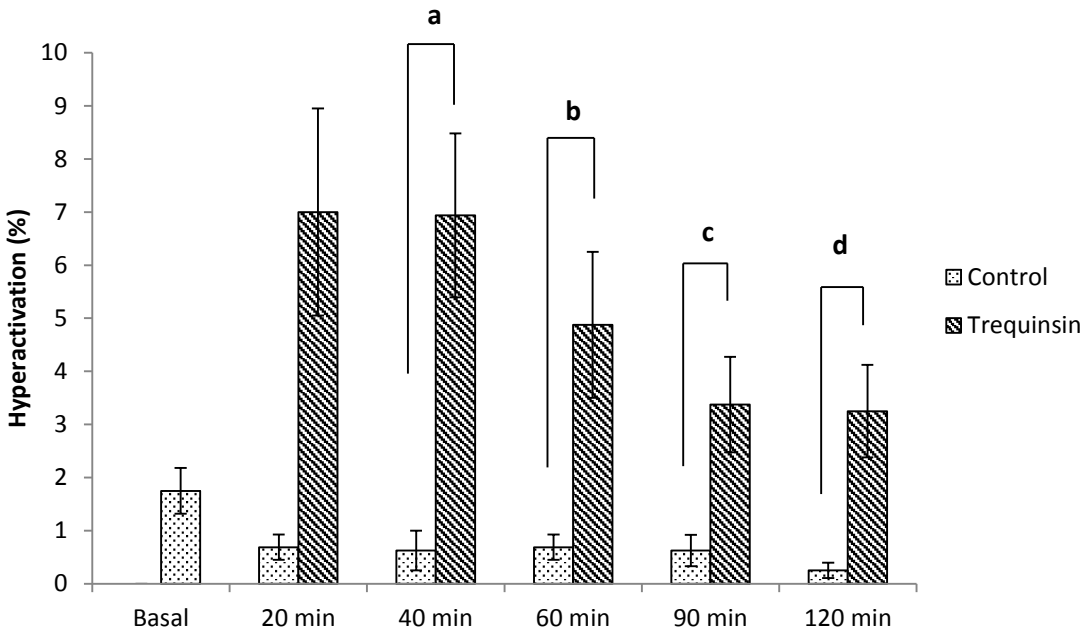

Figure 5.5: Effect of 10 µM Trequinsin on the 40% fraction spermatozoa under capacitating conditions on hyperactivation (n=4). Letters above the bars represent p values (a: 0.025, b: 0.041, c: 0.043, d: 0.048) and error bars represent SEM.

Trequinsin at 10µM stimulated motility parameters under capacitating conditions. In order to further investigate the motility stimulation, average values for individual motility parameters were evaluated, namely; ALH, VCL, VSL, VAP, LIN, and BCF. Capacitated spermatozoa showed increase in their VAP, VSL, VCL, and ALH (Table 5.2). The magnitude of increase in motility parameters was higher than that of non-capacitated spermatozoa.

Treatment	Movement Parameters					
	VAP (µm/s)	**VSL (µm/s)**	**VCL (µm/s)**	**ALH (µm)**	**LIN (%)**	**BCF (Hz)**
20 min control	48.71 ± 2.07	42.83 ± 2.36	74.36 ± 2.79	3.59 ± 0.10	56.25 ± 2.03	24.54 ± 1.10
20 min trequinsin	64.16 ± 1.73 *	53.79 ± 3.05 *	104.40 ± 3.49 *	4.48 ± 0.38	53.75 ± 4.62	27.48 ± 1.10
40 min control	48.68 ± 2.45	42.66 ± 2.89	74.09 ± 1.83	3.53 ± 0.08	56.25 ± 2.46	24.93 ± 0.79
40 min trequinsin	61.83 ± 1.93 *	51.70 ± 2.96 *	102.22 ± 1.10 *	4.59 ± 0.22 *	52.19 ± 3.37 *	26.54 ± 0.76
60 min control	47.59 ± 2.19	41.60 ± 2.37	72.63 ± 1.95	3.46 ± 0.16	55.94 ± 2.54	25.14 ± 0.91
60 min trequinsin	62.18 ± 2.46 *	52.74 ± 3.53 *	101.31 ± 1.53 *	4.56 ± 0.27 *	53.31 ± 3.55	25.83 ± 1.22
90 min control	47.29 ± 3.66	41.44 ± 3.73	71.13 ± 2.48	3.41 ± 0.10	57.63 ± 3.95	24.60 ± 0.63
90 min trequinsin	59.48 ± 3.59 *	50.19 ± 4.22 *	98.19 ± 2.69 *	4.69 ± 0.15 *	51.63 ± 3.00 *	25.28 ± 1.31
120 min control	44.81 ± 2.06	38.58 ± 1.98	68.63 ± 2.15	3.44 ± 0.11	54.63 ± 1.56	24.16 ± 0.63
120 min trequinsin	57.60 ± 3.44 *	49.46 ± 4.06 *	94.28 ± 3.78 *	4.52 ± 0.17 *	52.63 ± 3.12	24.29 ± 1.36

Table 5.2: Effect of 10µM Trequinsin on movement characteristics of 40% fraction spermatozoa under capacitating conditions (n=4). ± values are SEM. * indicates $p<0.05$.

5.3.2 Effects of Trequinsin Treatment on 80% Fraction Spermatozoa

5.3.2.1 Under non-capacitating conditions

The 80% fraction spermatozoa from healthy normozoospermic research donors were treated with DMSO (vehicle control), 10µM Trequinsin or 10µM BRL 50481 and under non-capacitating conditions. BRL 50481 was found to be not effective in stimulating any of the motility parameters under non-capacitating conditions (Appendix). 10µM Trequinsin failed to stimulate total motility significantly under non-capacitating conditions (Figure 5.6). However, progressive motility showed 23% (±12%, p=0.029, n=4, figure 5.7) increase following 20 min incubation under non-capacitating conditions.

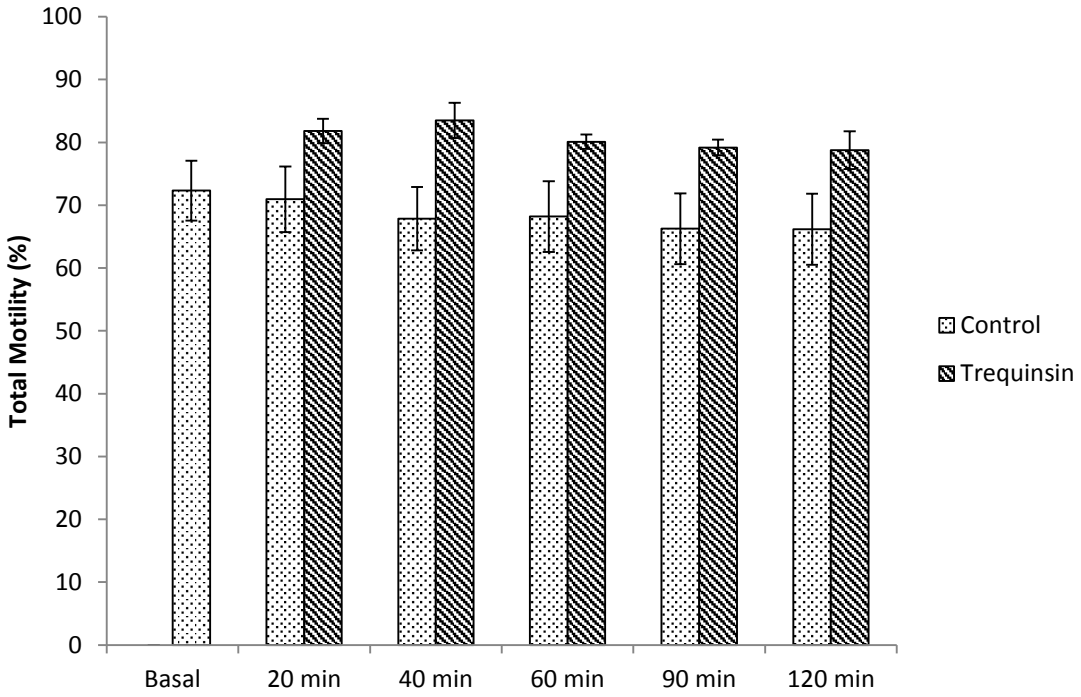

Figure 5.6: Effect of 10 µM Trequinsin on the 80% fraction spermatozoa under non-capacitating conditions on %total motility (n=4). There is no significant increase in %total motility. Error bars represent SEM.

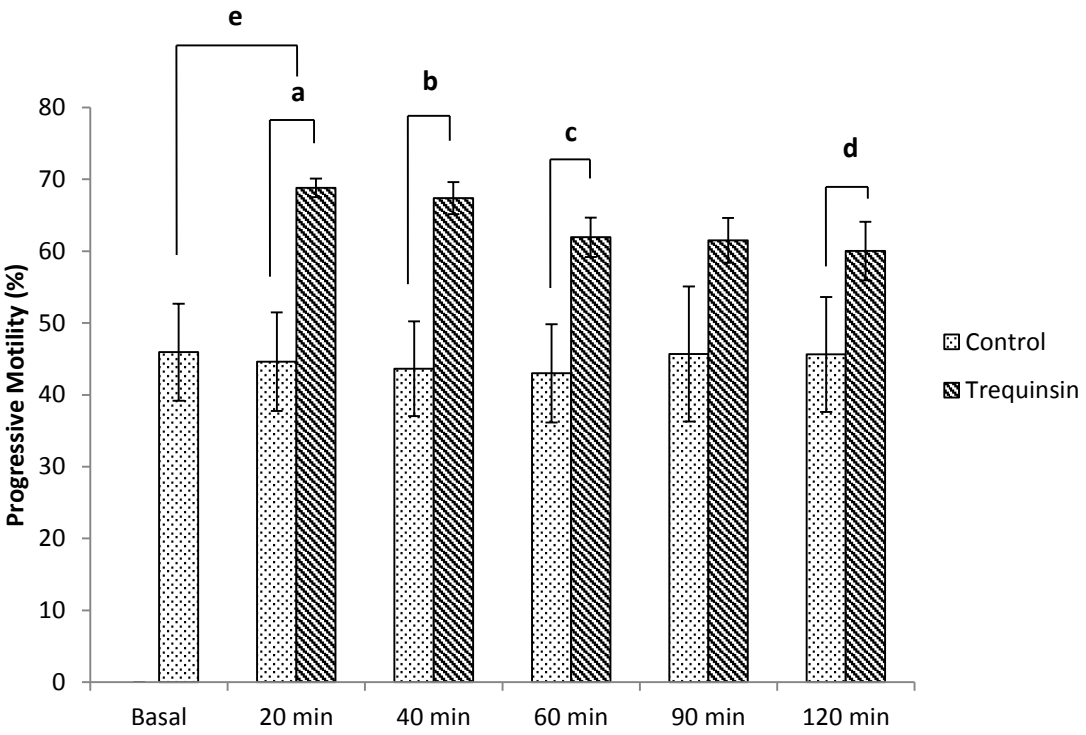

Figure 5.7: Effect of 10 µM Trequinsin on the 80% fraction spermatozoa under non-capacitating conditions on %progressive motility (n=4). Letters above the bars represents p values (a: 0.026, b: 0.046, c: 0.04, d: 0.044, e: 0.029) and error bars represent SEM

Trequinsin at 10µM stimulated motility parameters under both capacitating and non-capacitating conditions. In order to further investigate the motility stimulation, average values for individual motility parameters were evaluated, namely; ALH, VCL, VSL, VAP, LIN, and BCF. Non-capacitated spermatozoa showed increase in their VAP, VSL, VCL, ALH, and BCF (Table 5.3).

Treatment	Movement Parameters					
	VAP (µm/s)	VSL (µm/s)	VCL (µm/s)	ALH (µm)	LIN (%)	BCF (Hz)
20 min control	55.03 ± 4.17	49.71 ± 4.67	82.16 ± 3.01	3.59 ± 0.13	59.88 ± 3.59	24.94 ± 1.32
20 min trequinsin	66.42 ± 2.82 *	59.92 ± 3.54 *	97.10 ± 1.72 *	3.71 ± 0.28	63.25 ± 4.09	28.11 ± 1.58 *
40 min control	52.84 ± 4.25	46.69 ± 4.55	81.08 ± 3.22	3.69 ± 0.16	57.00 ± 3.34	23.80 ± 0.96
40 min trequinsin	63.18 ± 1.89 *	55.94 ± 2.53 *	96.95 ± 1.53 *	3.96 ± 0.17	59.50 ± 2.80	26.31 ± 1.47 *
60 min control	51.89 ± 4.69	45.89 ± 4.95	78.91 ± 3.97	3.59 ± 0.10	57.31 ± 3.23	23.96 ± 1.33
60 min trequinsin	62.61 ± 2.53 *	54.34 ± 3.44 *	96.26 ± 0.93 *	3.98 ± 0.19	58.15 ± 3.22	25.76 ± 1.61
90 min control	50.91 ± 4.90	45.11 ± 5.18	77.69 ± 4.31	3.68 ± 0.12	57.13 ± 3.50	23.60 ± 1.16
90 min trequinsin	61.25 ± 3.16 *	53.74 ± 3.74 *	96.44 ± 2.16 *	4.21 ± 0.16 *	56.69 ± 2.48	24.81 ± 1.94
120 min control	49.98 ± 4.07	44.06 ± 4.32	77.07 ± 3.66	3.63 ± 0.10	56.25 ± 2.96	23.85 ± 0.92
120 min trequinsin	59.66 ± 3.26 *	52.23 ± 4.05 *	96.38 ± 1.62 *	4.37 ± 0.15 *	54.90 ± 3.19	24.37 ± 1.58

Table 5.3: Effect of 10µM Trequinsin on movement characteristics of 80% fraction spermatozoa under non-capacitating conditions (n=4). ± values are SEM. * indicates $p<0.05$.

5.3.2.2 Under capacitating conditions

The 80% fraction spermatozoa from healthy normozoospermic research donors were treated with DMSO (vehicle control), 10µM Trequinsin or 10µM BRL 50481 and capacitating conditions. BRL 50481 was found to be not effective in stimulating any motility parameters under capacitating conditions (Appendix). 10µM Trequinsin failed to stimulate total motility, progressive motility, and hyperactivation under capacitating conditions significantly (ns, Figure 5.8, 5.9, and 5.10, respectively).

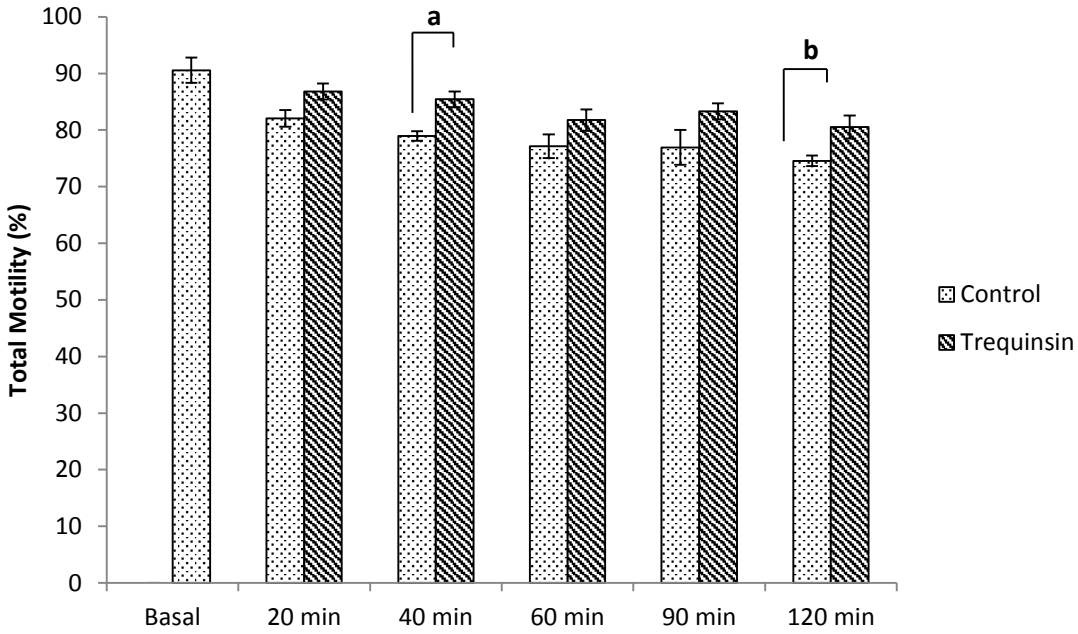

Figure 5.8: Effect of 10 µM Trequinsin on the 80% fraction spermatozoa under capacitating conditions on %total motility (n=4). Error bars represent SEM.

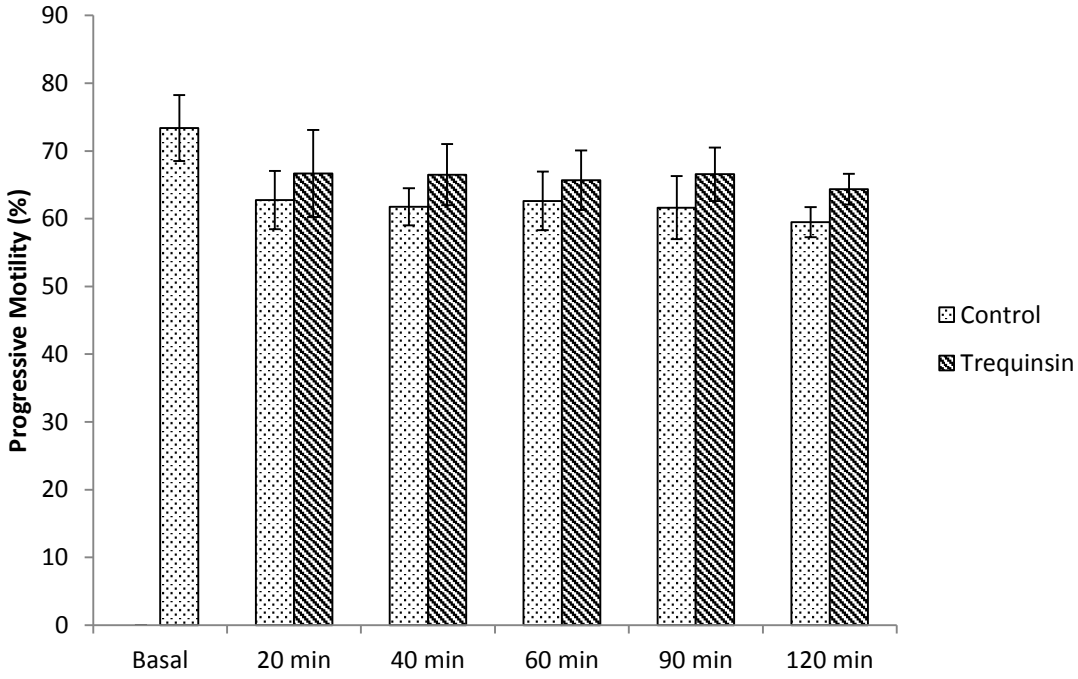

Figure 5.9: Effect of 10 µM Trequinsin on the 80% fraction spermatozoa under capacitating conditions on %progressive motility (n=4). There is no significant response. Error bars represent SEM.

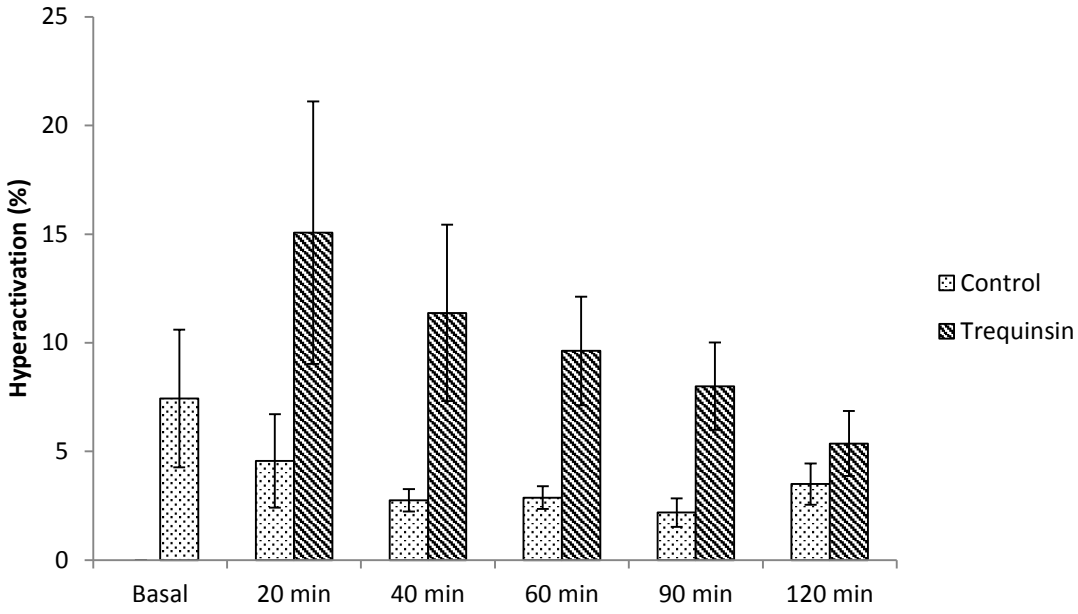

Figure 5.10: Effect of 10 µM Trequinsin on the 80% fraction spermatozoa under capacitating conditions on hyperactivation (n=4). There is no significant response. Error bars represent SEM.

Trequinsin at 10µM stimulated motility parameters under both capacitating and non-capacitating conditions. In order to further investigate the motility stimulation, average values for individual motility parameters were evaluated, namely; ALH, VCL, VSL, VAP, LIN, and BCF. Capacitated spermatozoa showed increase in their VAP, VSL, VCL, and ALH and decrease in their LIN and BCF (Table 5.4).

Treatment	Movement Parameters					
	VAP (µm/s)	VSL (µm/s)	VCL (µm/s)	ALH (µm)	LIN (%)	BCF (Hz)
20 min control	64.06 ± 3.88	56.86 ± 4.63	96.68 ± 4.06	4.01 ± 0.21	59.94 ± 4.11	26.73 ± 1.31
20 min trequinsin	79.29 ± 2.88 *	67.61 ± 4.56 *	130.36 ± 4.45 *	5.65 ± 0.41 *	54.44 ± 4.99	25.44 ± 1.56
40 min control	64.43 ± 2.18	57.45 ± 2.95	94.14 ± 1.60	3.88 ± 0.17	61.25 ± 3.02	27.06 ± 1.27
40 min trequinsin	75.68 ± 3.02 *	65.52 ± 4.05 *	123.44 ± 3.22 *	5.56 ± 0.39 *	54.94 ± 4.02 *	24.06 ± 1.78 *
60 min control	64.88 ± 5.15	58.28 ± 5.63	94.54 ± 3.45	3.89 ± 0.12	61.81 ± 3.45	26.39 ± 0.93
60 min trequinsin	75.94 ± 3.86 *	65.89 ± 4.29	124.90 ± 2.18 *	5.86 ± 0.22 *	53.75 ± 3.03 *	23.65 ± 1.53 *
90 min control	64.53 ± 5.01	58.41 ± 5.31	93.78 ± 5.01	3.92 ± 0.16	61.94 ± 2.87	26.64 ± 1.84
90 min trequinsin	75.86 ± 4.06 *	66.09 ± 4.90 *	123.89 ± 4.07 *	5.93 ± 0.29 *	53.94 ± 3.26 *	23.24 ± 1.75 *
120 min control	64.51 ± 5.83	57.86 ± 6.02	96.33 ± 6.06	4.08 ± 0.17	60.19 ± 2.93	25.82 ± 1.58
120 min trequinsin	72.06 ± 4.67	63.38 ± 5.21	116.48 ± 4.34 *	5.53 ± 0.23 *	54.50 ± 2.94 *	23.45 ± 1.69 *

Table 5.4: Effect of 10µM Trequinsin on movement characteristics of 80% fraction spermatozoa under capacitating conditions (n=4). ± values are SEM. * indicates $p<0.05$.

5.3.3 Trequinsin Stimulates 40% Fraction Motility of Failed Fertilization ICSI Patient

In order to eliminate speculations about using the 40% fraction from healthy research donors as a surrogate of poorly motile spermatozoa, 40% fraction spermatozoa from a patient is also tested with 10µM Trequinsin. The 40% fraction spermatozoa from a failed fertilization ICSI patient were tested with 10µM Trequinsin as a time-course experiment for 2 hours. It was found that total motility and progressive motility increased significantly (increase is considered significant as standard deviation error bars is not overlapping).

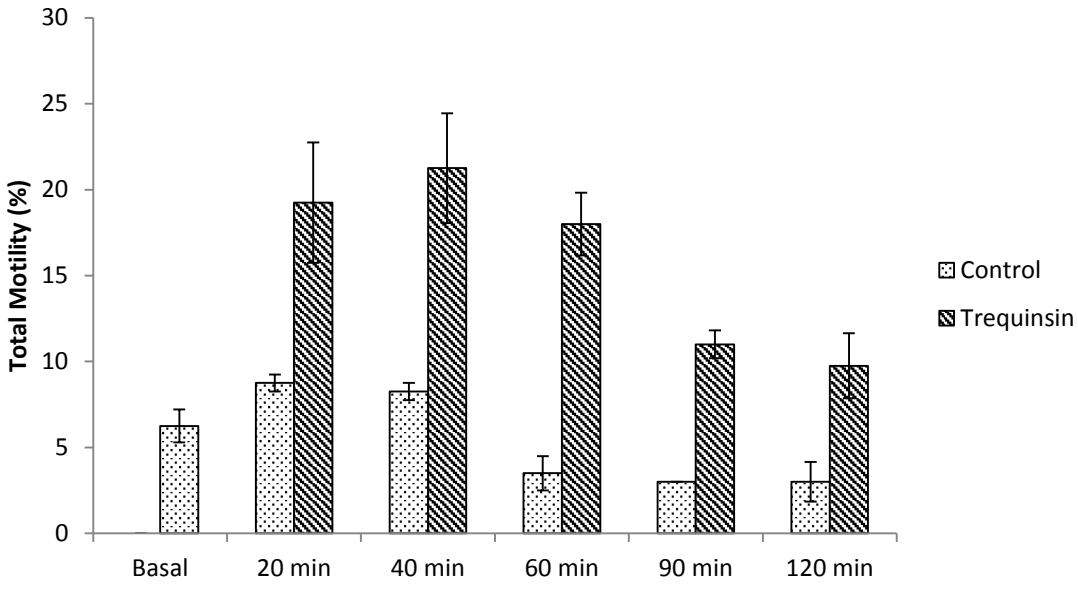

Figure 5.11: Effect of 10µM Trequinsin on total motility of failed fertilization ICSI patient under non-capacitating conditions. Error bars represent standard deviation (SD).

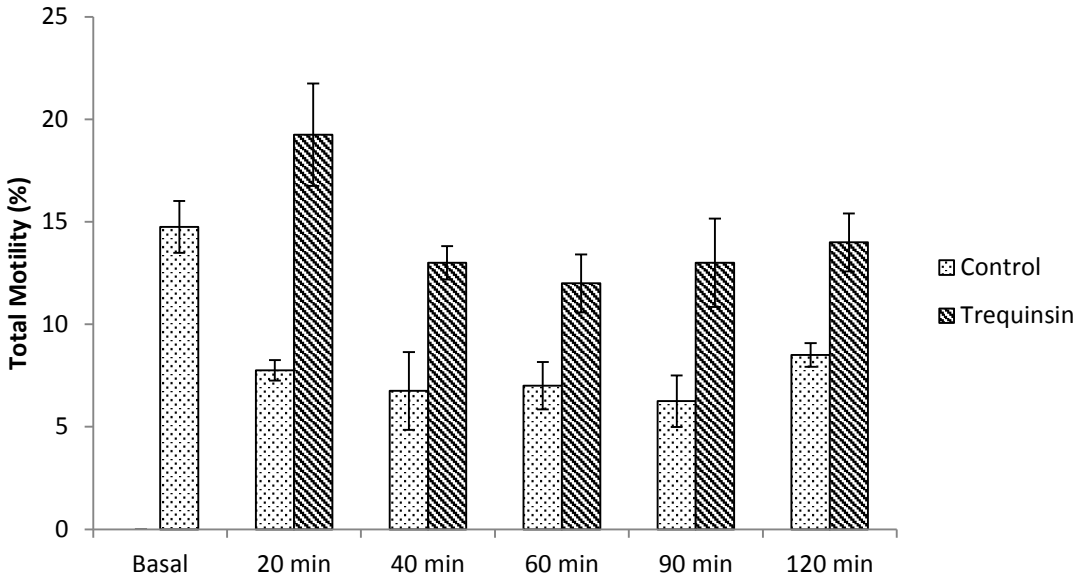

Figure 5.12: Effect of 10µM Trequinsin on total motility of failed fertilization ICSI patient under capacitating conditions. Error bars represent standard deviation (SD).

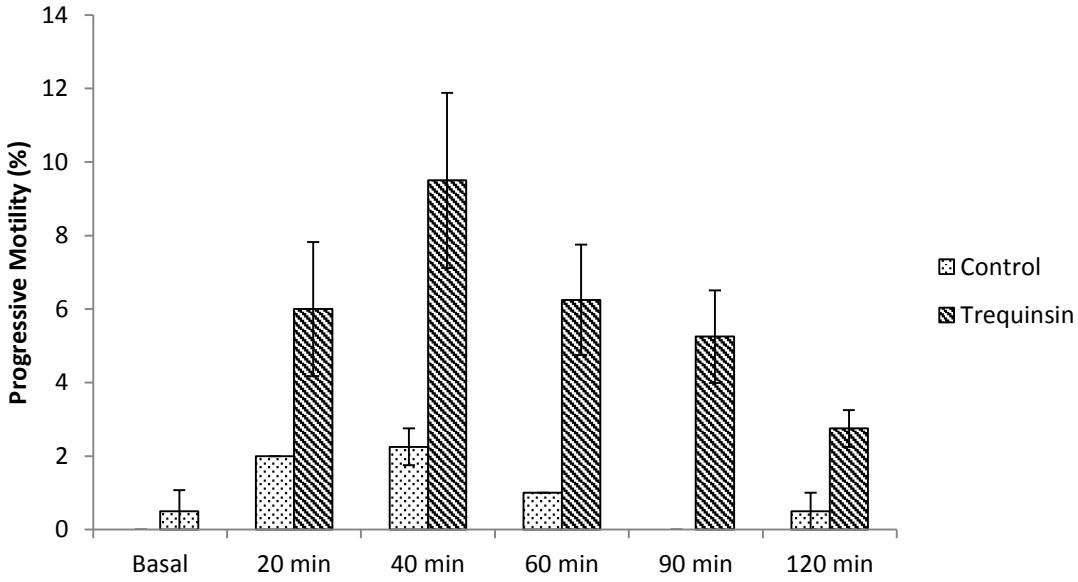

Figure 5.13: Effect of 10µM Trequinsin on progressive motility of failed fertilization ICSI patient under non-capacitating conditions. Error bars represent standard deviation (SD).

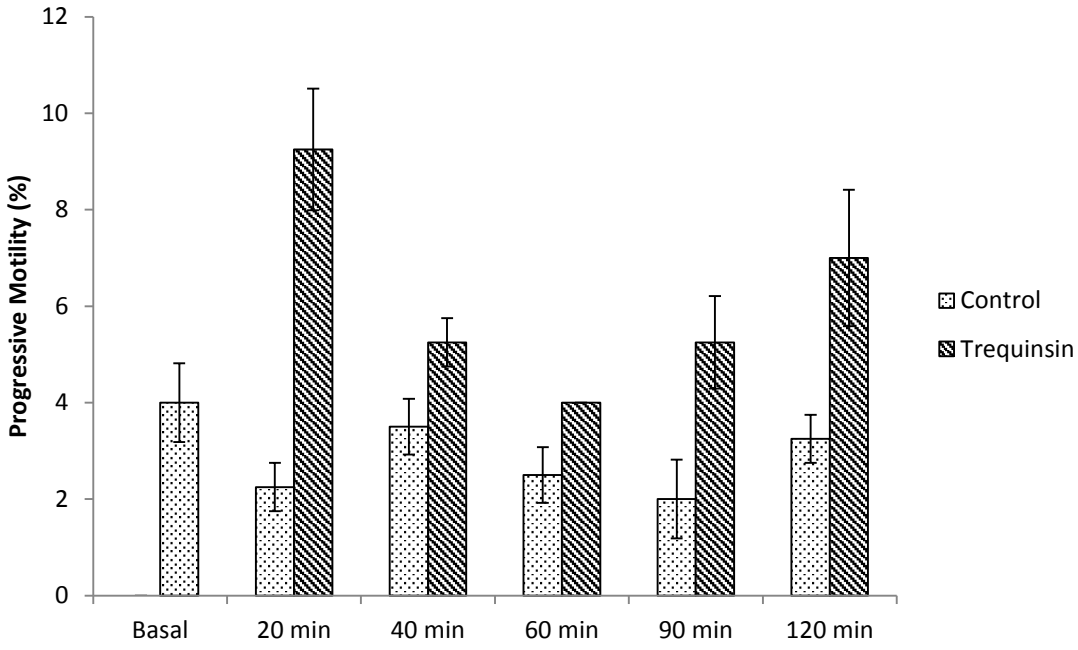

Figure 5.14: Effect of 10µM Trequinsin on progressive motility of failed fertilization ICSI patient under capacitating conditions. Error bars represent standard deviation (SD).

5.4 Discussion

Trequinsin (IC_{50}: 250pM, a type 3 PDE inhibitor) and BRL 50481 (K_i: 180nM, a type 7 PDE substrate competitor) are both potent and specific PDE inhibitors (O'Donnell and Frith, 1999; Kurjak *et. al.,* 1999; Reid, 1999; Smith *et. al.,* 2004) as well as inducers of intracellular Ca^{2+} influx of human spermatozoa (see chapter 4). Another type 3 specific PDE inhibitor, milrinone at 50µM (IC_{50}: 0.5µM) increase intracellular cAMP concentration by 15% without any alterations in sperm function (Lefievre *et. al.,* 2002). Trequinsin is clearly effective at a concentration of 10µM in stimulating motility parameters of both the 40% and the 80% fractions under both capacitating and non-capacitating conditions. Conversely, BRL 50481 was ineffective at this concentration. However, the initial Flexstation was done at 40µM concentration, so further experiments were performed to examine the effects of BRL 50481 on human sperm motility. However, the results were shown to be the same under both capacitating and non-capacitating conditions (Appendix). Therefore, it was confirmed that BRL 50481 is ineffective in stimulating human sperm motility.

Using 40% fraction sperm as a surrogate for poorly motile patient sperm has limitations. These cells are known to be the "bad" fraction sperm of "good" sperm sample. However, as even the testicular sperm can be used for ICSI with successful outcomes (Schlegel *et. al.,* 1997) it can be said that even these cells have the genetic requirements for fertilising oocytes, although the 40% fraction sperm would not be able to reach the site of fertilisation *in vivo*. As this is also the case with patient samples with poor motility, it can be assumed that there are better chances of mimicking the poorly motile patient samples.

The main effect of 10µM Trequinsin on motility parameters was to increase; VAP, VCL, VSL, and in the case of capacitated spermatozoa, increase in ALH as well

(Table 5.1-5.4). These alterations in the motility parameters appear not to be dependent on the capacitation (apart from ALH) and the population of spermatozoa used.

Trequinsin were effective in increasing total motility and progressive motility in the 40% fraction under both capacitating and non-capacitating conditions. However, total motility was found to be not significantly different from control under capacitating conditions for the 80% fraction spermatozoa. Progressive motility on the other hand, was found to be responding to the drug. This finding on total motility can be explained. The 80% fraction spermatozoa were highly motile prior to Trequinsin treatment. Therefore, these spermatozoa probably had maximal PKA stimulation already, which any further increase in $[cAMP]_i$ is non-beneficial (Tash and Means, 1983).

Trequinsin appears not to be stimulating hyperactivation significantly. CASA was set to detect hyperactivation using VCL, LIN, and ALH (see section 2.2.4 for details). As ALH was not stimulated under the non-capacitating conditions only the capacitated spermatozoa showed an increase in hyperactivation levels. Therefore, frequency distribution graphs evaluated to examine the effect of Trequinsin on hyperactivation (Figure 5.15-5.17, see appendix for the rest of the CASA parameters). It is clear that Trequinsin stimulates VCL towards the hyperactive sperm criteria range. However, stimulation of ALH appears to be the limiting factor as Trequinsin fails to increase ALH beyond 7μm (Figure 5.16). As clearly seen on figure 5.10 stimulation of hyperactivation is maximal at 20min incubation point. Trequinsin treatment increases VCL beyond the criteria for hyperactivation (≥150 μm/s) but both LIN and ALH fails to reach hyperactivation criteria levels of this study (≤50% and ≥7 μm, respectively, Figure 5.15-5.17).

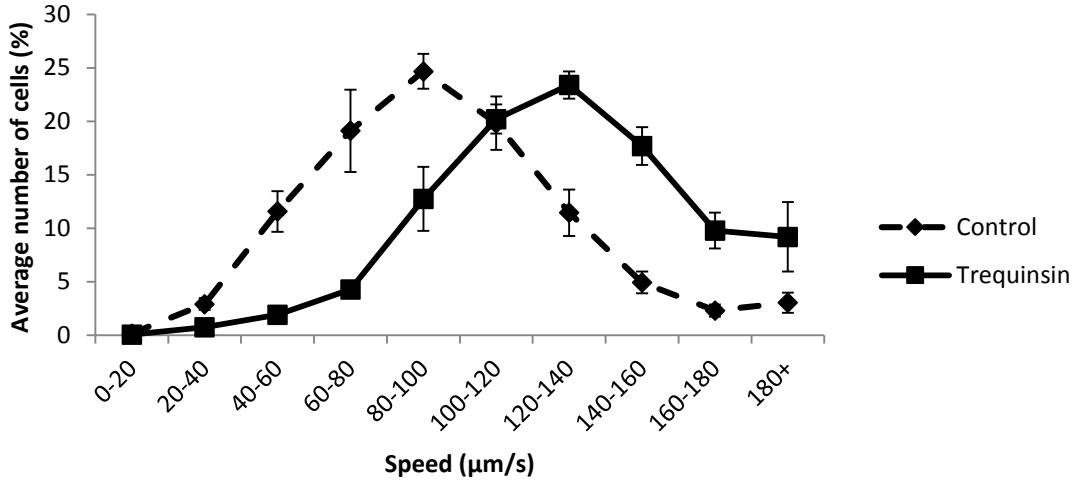

Figure 5.15: Effect of 10µM Trequinsin on 80% fraction spermatozoa under capacitating conditions on VCL after 20min treatment (n=4). Error bars represent SEM.

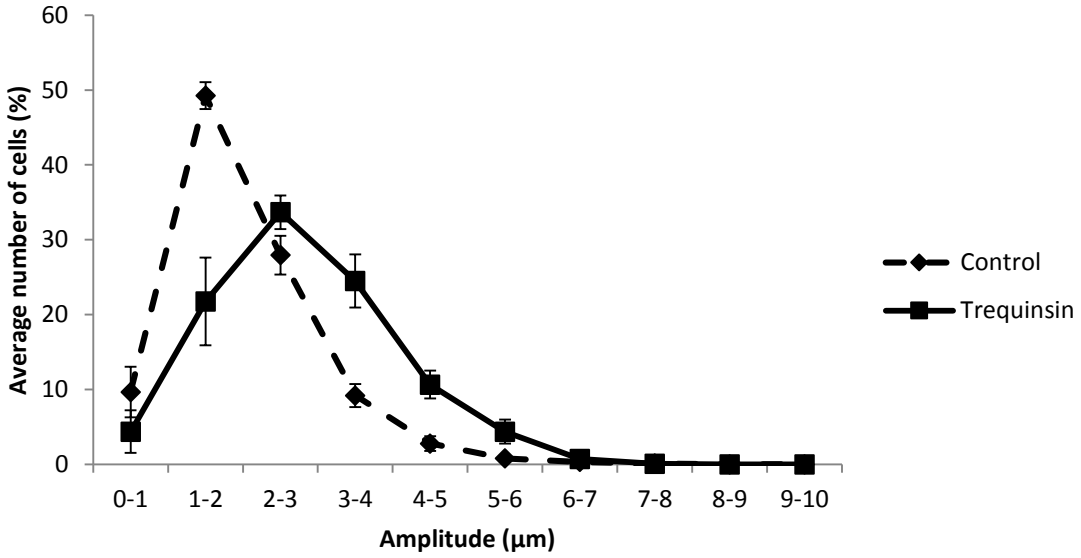

Figure 5.16: Effect of 10µM Trequinsin on 80% fraction spermatozoa under capacitating conditions on ALH after 20min treatment (n=4). Error bars represent SEM.

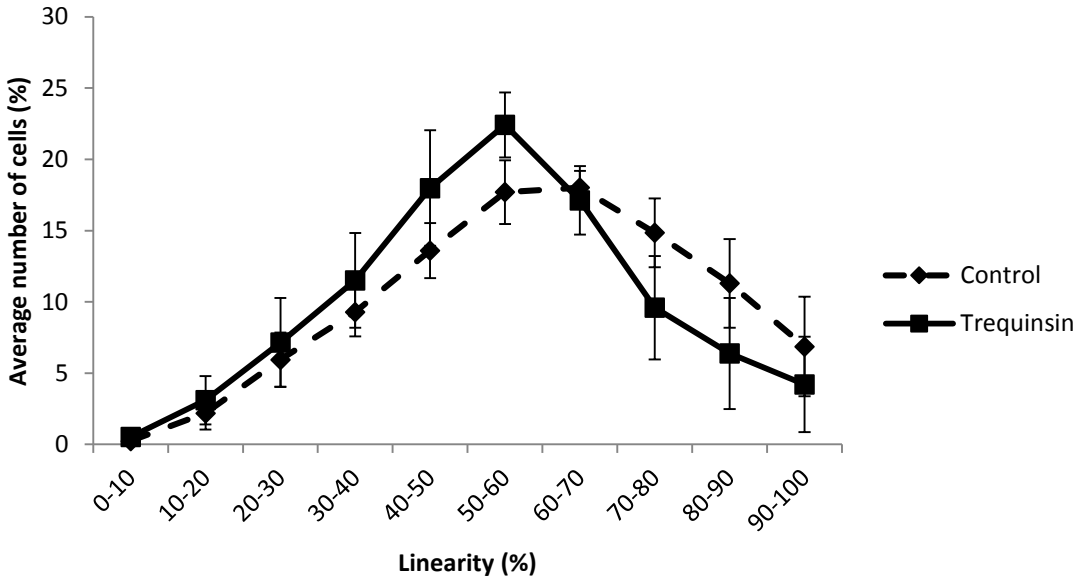

Figure 5.17: Effect of 10µM Trequinsin on 80% fraction spermatozoa under capacitating conditions on LIN after 20min treatment (n=4). Error bars represent SEM.

As human sperm motility was significantly stimulated by 1 of the 25 drugs identified as hit compounds, the drug-screening program using Ca^{2+} as a surrogate has potential in identifying pro-motility compounds. However, it should be noted that the remaining 23 compounds were not tested on human sperm motility due to time limitations. Nevertheless, motility assay was the second stage of the screening program and it was expected that some of the compounds would be filtered throughout the process. Therefore, identifying 1 compound (for now) out of 223 compounds is a good outcome considering other drug screening programs from other fields.

In summary, Trequinsin is a novel and effective motility stimulator at 10µM concentration. Trequinsin's effectiveness at low concentration is important, because, theoretically, selectivity of the drug is preserved at this concentration. This is important, as other PDE inhibitors have found to be ineffective in clinical aspects of the field due to lack of selectivity (Lanzafame *et. al.,* 1994). Further experiments are required in

order to have a better idea about the drug. The effect of Trequinsin on sperm metabolism must be tested, as alterations on sperm motility undoubtedly require energy. Acrosome reaction must be tested as Trequinsin might also be stimulating acrosome reaction. Furthermore, preliminary patch-clamping studies by Mansell *et. al.*, (unpublished data) showed that Trequinsin is activating CatSper channels in a manner that is indistinguishable from progesterone activation. Therefore, motility studies together with CatSper blocking agents could be useful in understanding the effect of Ca^{2+} induction on motility in response to Trequinsin.

Chapter 6 : General discussion

In chapter 2, it was clearly shown that the hyperactivation assay has clinical value. It is possible that mobilizing stored Ca^{2+} has a significant role in determining fertilizing capacity of sperm *in vitro* as putative store-mobilizing agent 4-AP gave the highest increment in hyperactivation and showed a significant correlation with fertilization rates. The role of CatSper-induced-hyperactivation in fertilization is not clear; even though CatSper deficient males are infertile and show disrupted CatSper activity in response to progesterone (Smith *et. al.,* 2013). Progesterone- or NH_4Cl-induced hyperactivation levels did not correlate with fertilization rates (see chapter 2). Alasmari *et. al.,* (2013) showed that Ca^{2+} originating from store(s) resulted in higher level of hyperactivation but Ca^{2+} originating from CatSper resulted in better penetration into viscous media *in vitro*. However, clinical studies on stored Ca^{2+} suggest the opposite (Alasmari *et. al.,* 2013; this study). This can be explained as 4-AP used at high concentration (2mM) possibly depletes the stored Ca^{2+} giving a burst in hyperactivation, however, it is possible that stored Ca^{2+} may be released at a lower rate or used for oscillations to support penetration of zona pellucida or viscous media *in vivo*. However, definitive conclusions cannot be made, as the molecular mechanism(s) of 4-AP on human sperm hyperactivation remains largely unknown. An interesting experiment to further investigate Ca^{2+} deficiencies on IVF or ICSI patients would be to use single-cell imaging technologies to record intracellular Ca^{2+} responses from individual sperm cells of patients, especially the poor responding patients. These single-cell-imaging experiments could be taken a step forward using experiments together with oocytes, cumulus cells, and the isthmic epithelial cells could be performed. Such experiments would be highly valuable in understanding the *in vivo* significance of human sperm hyperactivation and intracellular Ca^{2+} signalling. Lacking a standard definition of hyperactivation makes interpretation of the literature data difficult (Robertson *et. al.,*

1988; Mortimer and Mortimer, 1990; Grunert *et. al.*, 1990; Burkman, 1991; Zhu *et. al.*, 1994b; Sukcharoen *et. al.*, 1995; Mortimer and Swan, 1995). Therefore, there is a need for setting a defined and universally accepted hyperactivation criteria for using this easy and valuable prognostic test effectively.

Male factor infertility accounts for the majority of infertility cases (HFEA 2011, www.hfea.gov.uk). These men have to rely on ART without a guarantee of success. Therefore, it is now a necessity to find/develop drugs to target male factor infertility in order to reduce the usage of ART as well as to increase the success rates of ART. Based on the fact that Ca^{2+} signalling is pivotal in sperm function (Publicover *et. al.*, 2007), the clinical findings (Brenzik *et. al.*, 2013, Alasmari *et. al.*, 2013; and see chapter 2), and CatSper being a polymodal chemosensor (Brenker *et. al.*, 2012), it was hypothesized that screening compounds using Ca^{2+} as a surrogate for physiological responses would identify novel compounds for male infertility. This hypothesis was addressed prior to the HTS experiments with known motility inducers (PDE inhibitors), namely; MMPX, Tofisopam, Papaverine, Etazolate HCl, and Ibudilast (see chapter 3). It was found that these 5 compounds are poor inducers of Ca^{2+} influx therefore they would not be identified with the drug screening program. This supports the null hypothesis and findings by Nassar *et. al.*, (1998) suggesting no relation in motility modulation with Ca^{2+} signalling. Nevertheless, HTS was utilized using the Flexstation and 223 compounds were screened using intracellular Ca^{2+} signalling as a surrogate of the physiological response (see chapter 4). Promisingly, some hit compounds identified from the screening program had previously been suggested to modulate sperm function (either positive or negative; see chapter 4). However, the fact that effective motility inducers are either poor Ca^{2+} inducers or do not stimulate Ca^{2+} influx questions the logic of screening. That said, it is possible that some human sperm motility stimulators may induce Ca^{2+} influx as well (such as Trequinsin). Nevertheless, HTS is by far the best

method available that is efficient enough to be utilized to screen large number of compounds. 2 of the 25 hit compounds were tested for their ability to induce human sperm motility. It was found that 1 of the 2 compounds, Trequinsin, is an effective motility inducer under both capacitating and non-capacitating conditions on both 40% and 80% fraction spermatozoa (see chapter 5). Furthermore, patch-clamping studies performed by Mansell *et. al.,* (unpublished data) indicate that Trequinsin activates CatSper channels in a manner that is indistinguishable from the progesterone activation. Therefore, a novel human sperm motility inducer was identified using HTS using intracellular Ca^{2+} signalling as a surrogate. This finding is in agreement with Brenker *et. al.,* (2012) that supports CatSper being a polymodal channel. It is possible that an increase in intracellular Ca^{2+} results in motility induction (Publicover *et. al.,* 2007). However, without performing intracellular cAMP measurement and CatSper blocking agent experiments it cannot be confirmed, as Trequinsin is a type 3 selective PDE inhibitor. Further experiments are required for clearer results on Trequinsin. As acrosome reaction and chemotaxis are also controlled through Ca^{2+} influx, effects of Trequinsin on acrosome reaction and chemotaxis must be investigated. Another interesting experiment would be to test Trequinsin on different species such as mice. There are crucial species differences between mice and human sperm, such that mouse CatSper is not responsive to progesterone whereas human CatSper is highly responsive (Lishko *et. al.,* 2011). Therefore, it would be interesting to perform motility experiments with Trequinsin on mice sperm and test if Trequinsin activates CatSper, and if so, CatSper knockout mice sperm would shed light on the underlying mechanisms of Trequinsin stimulation.

On a broader aspect, derivatives of identified compounds could be produced by changing the molecular composition slightly (i.e. changing the structure of identified compounds) in order to have a better understanding of the structure-activity relationship

(SAR). This could potentially shed light on the binding site(s) of CatSper in the case of Trequinsin. If this would be achieved, it would be very important, as CatSper has never been crystalized in order to perform x-ray crystallography studies. Another possible outcome from screening library would be to find a sperm specific contraceptive that could immobilize/kill spermatozoa (possibly through Ca^{2+} homeostasis disruption). It is known that human sperm intracellular Ca^{2+} levels are kept around 200nM (Irvine and Aitken, 1986). Therefore, excessive intracellular Ca^{2+} should be effluxed or stored in intracellular store(s) (i.e. acrosome, Dorval *et. al.*, 2002) in order to maintain Ca^{2+} homeostasis. Disrupting Ca^{2+} homeostasis would consequently result in increased energy requirements. Therefore, it is possible that compounds that cause excessive Ca^{2+} influx can deplete ATP levels, consequently adversely affecting sperm function. Candidates for this would be Lylamine HCl (which also evoked Ca^{2+} influx greater than progesterone response) and GP1a (CB1 and CB2 agonists, respectively) which both CB1 and CB2 modulation had been proposed to had negative effects on sperm motility and viability (Whan *et. al.*, 2006).

Results of this thesis demonstrate that systematical drug screening can be utilized for sperm physiology research, and can help to understand the control mechanisms of human sperm motility. It is clear that understanding sperm physiology from production of sperm to function and unlocking the mysteries on signalling pathways that controls sperm function will lead to finding alternative treatment method(s) for male factor infertility other than ART, as well as providing safe contraception. Applying known research methods such as HTS, or even succeeding to accomplish *in vitro* spermiogenesis for knockout studies on human cells would result in a breakthrough. It is hoped that results of this study would ignite a spark to drive continuous studies to find/develop specific drugs for the global infertility problem.

Nevertheless, it is almost certain that ART usage is inevitable, especially ICSI, but for sure it could be reduced or used appropriately.

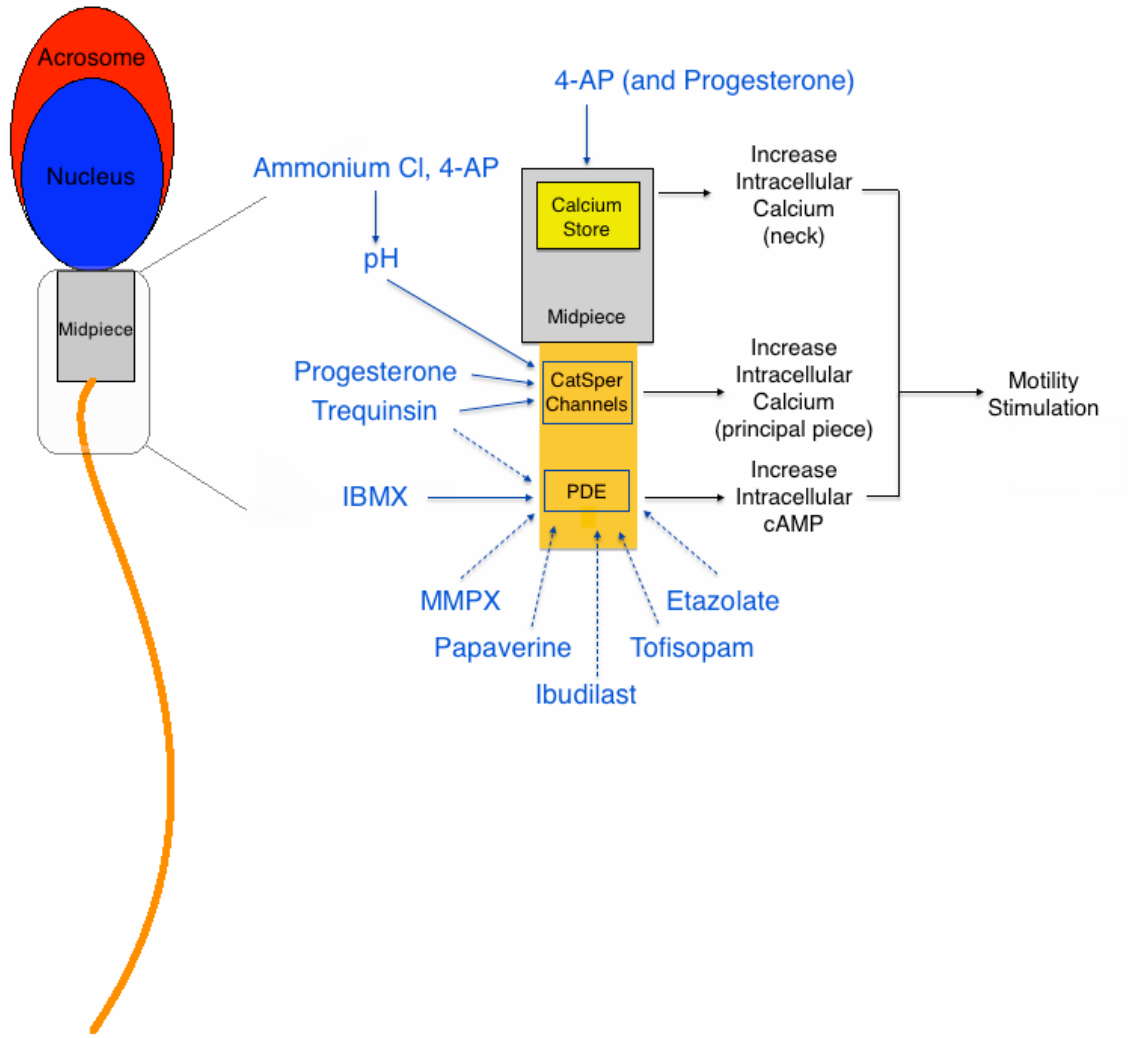

Figure 6.1: Model for controlling human sperm motility in this study. Progesterone directly binds and activates the CatSper channels. Trequinsn HCl activates the CatSper channels (Steven Mansell, unpublished data). Ammonium chloride and 4-AP increase intracellular pH that results in activation of CatSper channels. Activation of CatSper channels results in increased intracellular Ca^{2+} levels in the principal piece that results in hyperactivation and penetration into viscous media (Alasmari *et. al.*, 2013). 4-AP (putatively) mobilizes stored Ca^{2+} in the neck region that results in hyperactivation. IBMX inhibits PDEs resulting in increased intracellular cAMP levels that promote hyperactivated motility through AC/cAMP/PKA pathway. MMPX, Papaverine, Ibudilast, Tofisopam, and Etazolate inhibit PDE(s) (types of PDEs are to be confirmed) and promote hyperactivation. Effect of Trequinsin HCl on human sperm PDEs is yet to be confirmed. Solid lines indicate the mechanism of action. Dashed lines indicate mechanism(s) of action(s) yet to be confirmed.

Chapter 7 : Appendix

7.1 Supplementary figures and tables for chapter 2

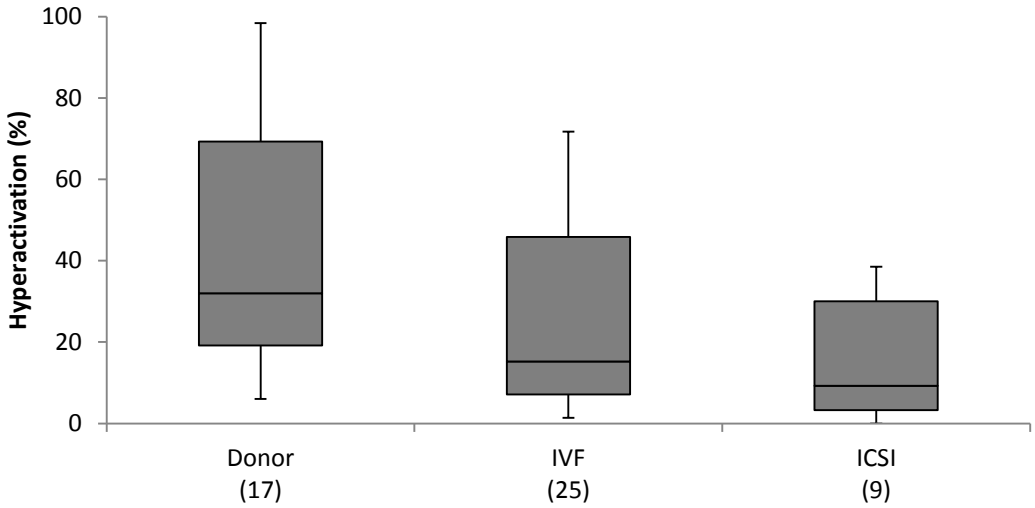

Figure 7.1: Effect of 2mM 4-AP-induced hyperactivation levels on donor, IVF and ICSI populations. Box and whisker plot showing 4-AP-induced hyperactivation levels. The boxes represent the interquartile range and lines within them are the medians. The numbers in brackets on the x-axis are the sample size.

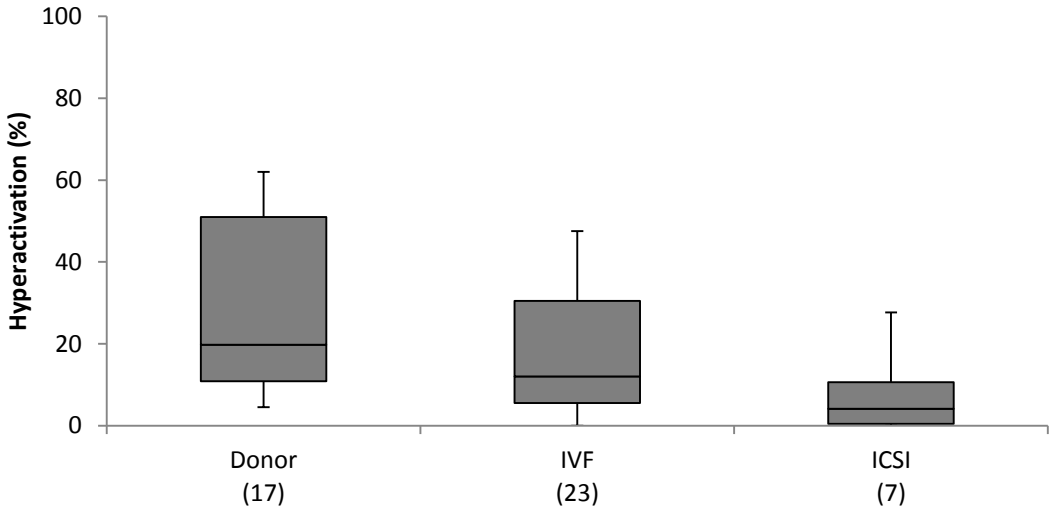

Figure 7.2: Effect of 3.6µM progesterone-induced hyperactivation levels on donor, IVF and ICSI populations. Box and whisker plot showing progesterone-induced hyperactivation levels. The boxes represent the interquartile range and lines within them are the medians. The numbers in brackets on the x-axis are the sample size.

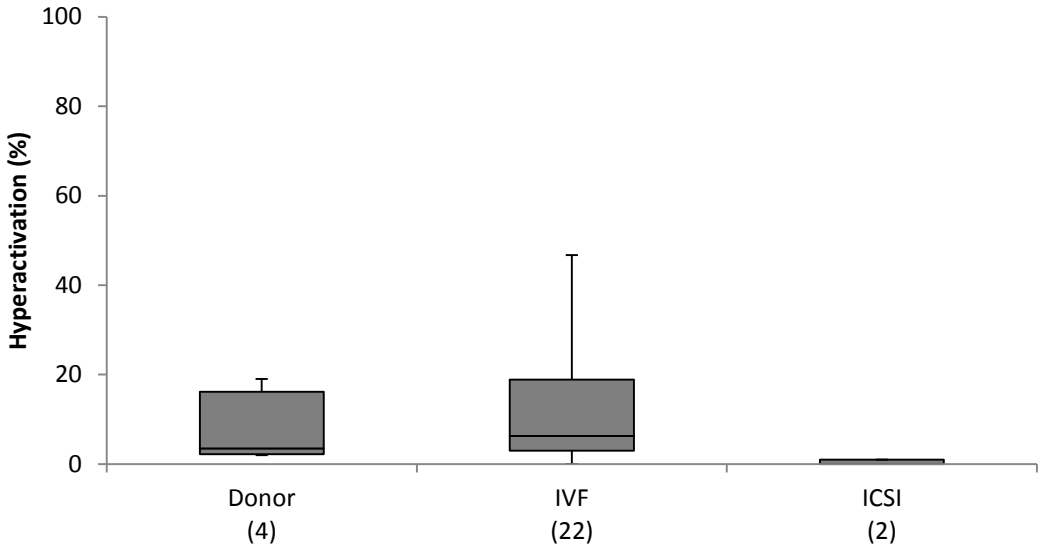

Figure 7.3: Effect of 25mM NH_4Cl-induced hyperactivation levels on donor, IVF and ICSI populations. Box and whisker plot showing NH_4Cl-induced hyperactivation levels. The boxes represent the interquartile range and lines within them are the medians. The numbers in brackets on the x-axis are the sample size.

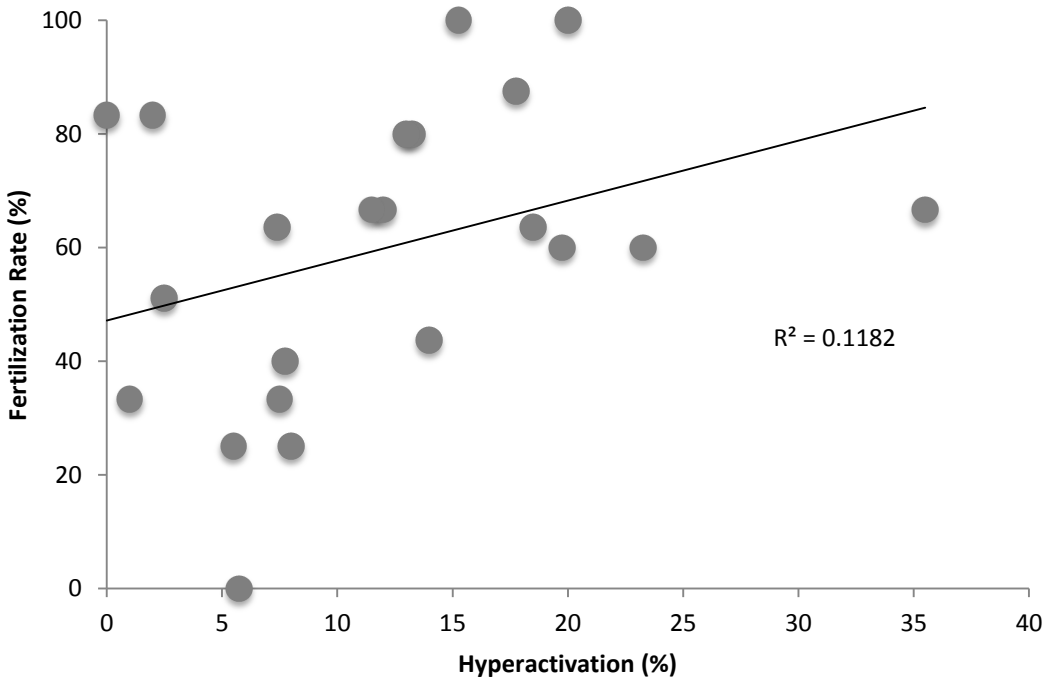

Figure 7.4: Relationship between progesterone-induced hyperactivation and fertilization rates. There is no correlation with fertilization rates. Pearson correlation coefficient (r_p), p value (p), and R^2 values are shown on graph.

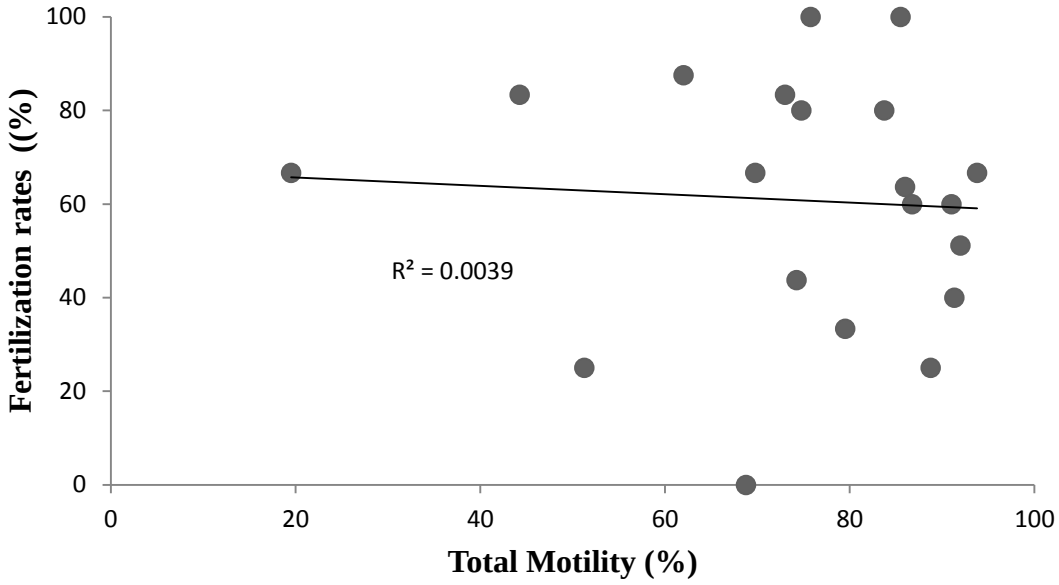

Figure 7.4: Relationship between total motility and fertilization rates. There is no correlation with fertilization rates. Spearman correlation coefficient (r_s), p value (p), and R^2 values are shown on graph.

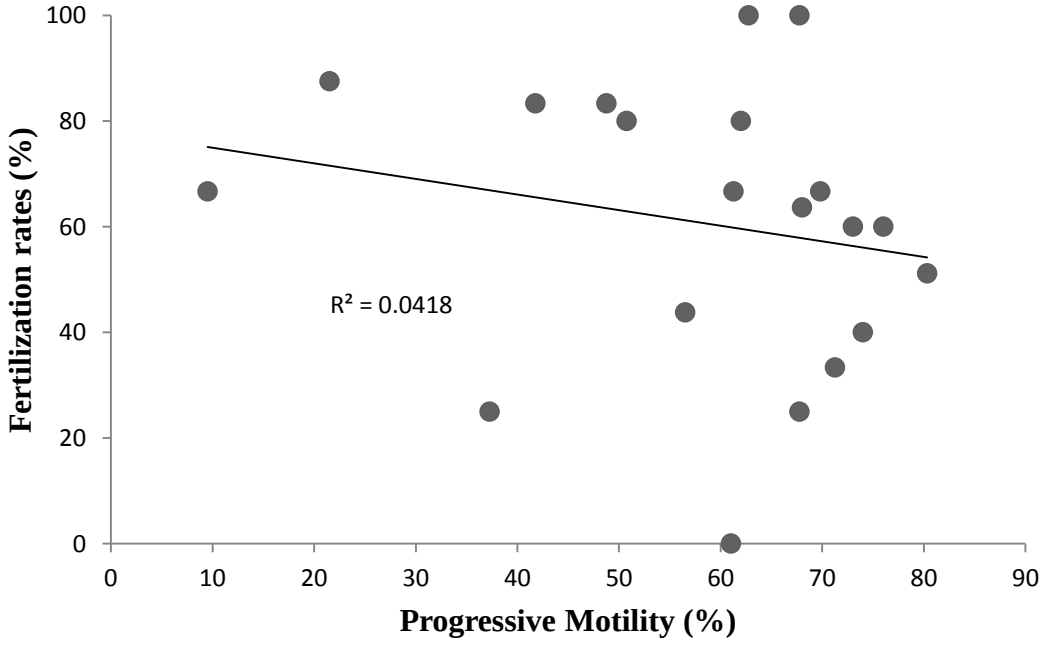

Figure 7.5: Relationship between total motility and fertilization rates. There is no correlation with fertilization rates. Spearman correlation coefficient (r_s), p value (p), and R^2 values are shown on graph.

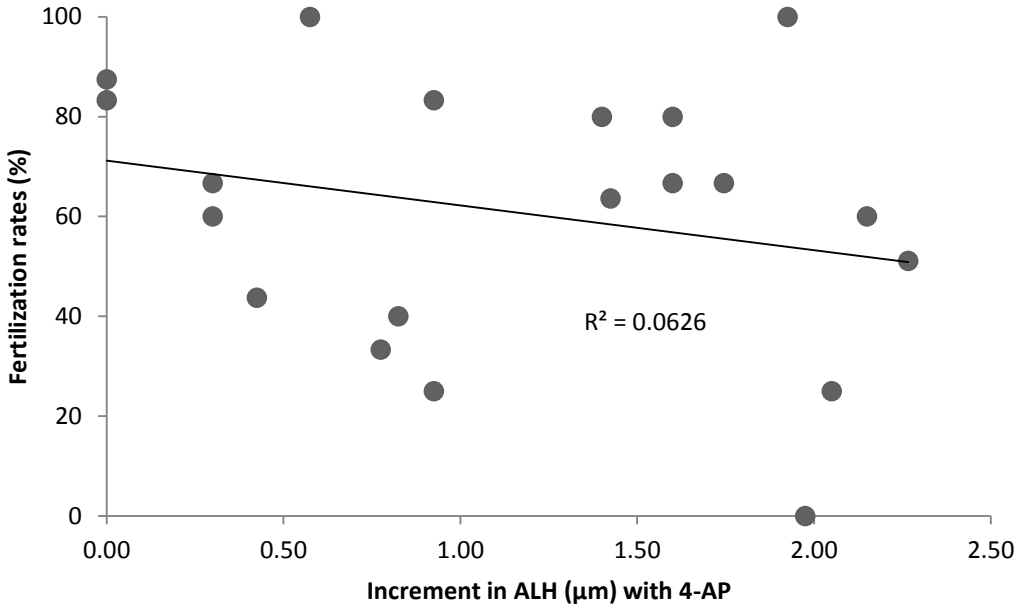

Figure 7.6: Relationship betweeen 2mM 4-AP-induced increment in ALH and fertilization rates in IVF. There is no correlation with fertilization rates. Pearson correlation coefficient (r_p), p value (p), and R^2 values are shown on graph.

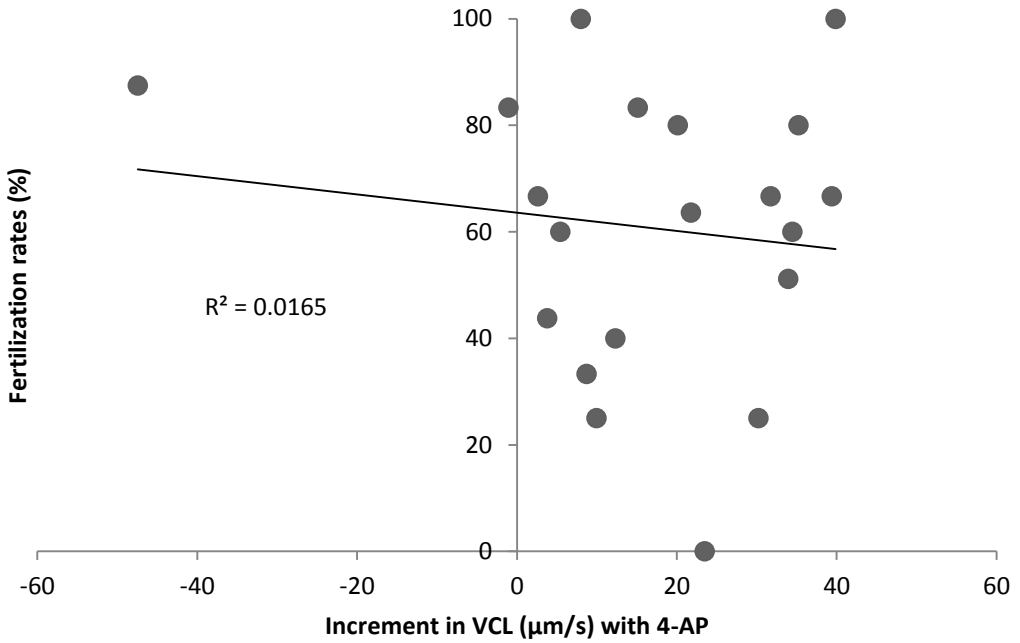

Figure 7.7: Relationship betweeen 2mM 4-AP-induced increment in VCL and fertilization rates in IVF. There is no correlation with fertilization rates. Spearman correlation coefficient (r_s), p value (p), and R^2 values are shown on graph.

Patient	VCL (µm/s)	ALH (µm)	LIN (%)	HA (%)
1- Control	90.90 ± 1.70	3.9 ± 0.08	63.00 ± 0.00	1.00 ± 0.00
Progeterone	94.98 ± 1.18	4.32 ±0.05	57.25 ± 0.50	1.00 ± 0.00
2- Control	142.63 ± 8.21	5.68 ± 0.50	56.00 ± 2.00	21.50 ± 5.26
Progeterone	128.65 ± 3.59	5.40 ± 0.14	54.50 ± 1.00	15.25 ±2.06
3- Control	114.78 ± 3.91	5.43 ± 0.05	50.75 ± 1.50	9.75 ± 2.22
Progeterone	130.93 ± 3.59	6.23 ± 0.15	51.25 ± 1.89	13.25 ± 2.36
4- Control	130.18 ± 4.74	5.25 ± 0.19	63.50 ± 3.00	1.75 ± 3.50
Progeterone	112.40 ± 4.81	6.30 ± 0.35	48.33 ± 2.31	0.00 ± 0.00
5- Control	130.43 ± 6.10	5.63 ± 0.41	58.25 ± 2.06	17.25 ± 6.24
Progeterone	132.85 ± 6.47	6.70 ± 0.36	52.25 ± 1.50	19.75 ± 4.25
6- Control	171.85 ± 3.95	6.78 ± 0.66	34.50 ± 1.29	22.00 ± 4.97
Progeterone	121.88 ± 2.55	5.85 ± 0.10	46.25 ± 1.50	17.75 ± 3.20
7- Control	130.10 ± 10.12	5.35 ± 0.62	56.25 ± 4.19	17.00 ± 5.60
Progeterone	130.55 ± 4.18	5.33 ± 0.24	59.50 ± 1.00	13.00 ± 1.83
8- Control	83.63 ± 1.27	3.40 ± 0.12	59.00 ± 0.82	2.75 ± 0.50
Progeterone	95.18 ± 2.07	4.00 ± 0.14	59.25 ± 0.50	3.50 ± 1.29
9- Control	93.28 ± 2.61	3.85 ± 0.06	60.75 ± 0.96	3.75 ± 1.26
Progeterone	93.10 ± 2.89	4.33 ± 0.13	55.25 ± 1.71	5.50 ± 0.58
10- Control	100.50 ± 0.86	3.73 ± 0.08	65.67 ± 0.82	3.50 ± 0.58
Progeterone	104.65 ± 2.39	4.33 ± 0.10	62.75 ± 1.50	2.50 ± 0.58

Table 7.1: CASA parameters in 10 IVF patients with failed respose to 3.6µM progesterone. Data are presented as average ± standard deviation (SD).

7.2 Supplementary figures and tables for chapter 3

	Concentration (µM)											
	-ve control	**0.1**	**0.3**	**0.5**	**1**	**3**	**5**	**10**	**30**	**50**	**100**	**+ve control**
D1	89.73 (0.49)	90.15 (1.59)	91.38* (0.67)	93.08* (1.60)	94.50* (1.61)	98.00* (1.81)	99.88* (0.62)	101.70* (2.00)	104.95* (1.42)	101.35* (1.78)	101.03* (1.14)	110.10* (0.88)
D2	69.35 (1.68)	68.75 (1.47)	67.03 (1.17)	69.45 (0.71)	70.88 (0.36)	69.05 (0.96)	70.83 (1.61)	78.33* (0.93)	95.58* (8.69)	85.90* (2.64)	88.00* (1.75)	85.83* (2.22)
D3	70.80 (0.57)	69.65 (1.33)	68.78 (1.77)	66.20 (2.10)	77.88* (2.43)	72.68 (3.80)	78.38* (2.23)	70.40 (2.52)	79.75* (1.31)	75.03* (2.48)	80.93* (1.91)	72.23 (3.08)
D4	66.45 (0.42)	69.00 (3.63)	70.28* (1.13)	68.83* (1.54)	70.80* (1.87)	70.53* (1.37)	71.83* (1.23)	75.60* (1.35)	77.45* (3.33)	73.63* (3.69)	77.58* (0.96)	80.85* (4.39)

Table 7.2: Effect of Ibudilast on VAP. Table shows effect of Ibudilast on VAP as 10 different concentrations on 4 different donors. The numbers in brackets are standard deviation. Asterix (*) indicates that standard deviations are not overlapping compared to -ve control (i.e. statistically significant). Negative (1% DMSO) and positive (3.6µM progesterone) controls are shown on the table.

	Concentration (µM)											
	-ve control	**0.1**	**0.3**	**0.5**	**1**	**3**	**5**	**10**	**30**	**50**	**100**	**+ve control**
D1	81.43 (0.12)	81.90 (1.43)	84.38* (0.59)	85.95* (1.88)	86.30* (1.26)	89.45* (1.04)	91.23* (1.14)	91.95* (1.21)	94.40* (0.85)	88.43* (1.28)	87.65* (1.43)	97.78* (1.20)
D2	61.33 (2.20)	59.33 (0.83)	59.05 (0/90)	61.70 (0.88)	62.45 (0.31)	61.15 (0/90)	62.05 (1.51)	68.53* (0.88)	81.68* (6.95)	73.03* (2.15)	74.10* (0.91)	72.53* (1.27)
D3	65.68 (1.63)	63.40 (1.61)	63.60 (1.90)	61.90 (2.04)	72.68* (2.46)	66.63 (3.24)	70.60* (1.43)	64.28 (1.65)	72.30* (0.81)	68.25 (3.08)	75.13* (2.05)	65.70 (2.46)
D4	55.68 (1.07)	59.10 (2.49)	59.55* (1.23)	58.40* (1.14)	59.18* (1.34)	59.93* (1.36)	59.28* (1.00)	61.10* (1.57)	62.25* (3.18)	59.95* (1.80)	60.70* (1.64)	62.98* (2.10)

Table 7.3: Effect of Ibudilast on VSL. Table shows effect of Ibudilast on VSL as 10 different concentrations on 4 different donors. The numbers in brackets are standard deviation. Asterix (*) indicates that standard deviations are not overlapping compared to -ve control (i.e. statistically significant). Negative (1% DMSO) and positive (3.6µM progesterone) controls are shown on the table.

	Concentration (µM)											
	-ve control	**0.1**	**0.3**	**0.5**	**1**	**3**	**5**	**10**	**30**	**50**	**100**	**+ve control**
D1	120.43 (1.56)	122.38 (1.99)	120.75 (1.35)	120.95 (2.11)	126.95* (2.75)	135.85* (3.86)	134.18* (0.57)	141.10* (4.51)	145.95* (2.42)	147.00* (9.55)	143.73* (2.79)	162.20* (1.42)
D2	102.98 (1.52)	106.35 (3.11)	102.23 (2.36)	104.90 (2.60)	106.55 (1.65)	104.63 (2.39)	105.13 (1.65)	118.23* (1.50)	147.78* (12.91)	138.48* (4.03)	144.70* (3.48)	138.68* (5.59)
D3	97.88 (3.46)	99.68 (2.01)	93.525 (1.20)	88.13 (1.91)	104.83 (3.42)	98.40 (6.07)	114.13* (4.75)	98.40 (5.04)	115.15* (2.77)	108.65* (1.52)	110.85* (2.35)	102.25 (8.90)
D4	109.40 (3.01)	109.63 (7.97)	111.78 (2.69)	109.88 (2.67)	115.13 (4.52)	113.48 (2.83)	115.50 (2.43)	126.15* (2.61)	131.68* (6.85)	126.28* (8.33)	132.53* (4.01)	138.25* (7.68)

Table 7.4: Effect of Ibudilast on VCL. Table shows effect of Ibudilast on VCL as 10 different concentrations on 4 different donors. The numbers in brackets are standard deviation. Asterix (*) indicates that standard deviations are not overlapping compared to -ve control (i.e. statistically significant). Negative (1% DMSO) and positive (3.6µM progesterone) controls are shown on the table.

	Concentration (µM)											
	-ve control	**0.1**	**0.3**	**0.5**	**1**	**3**	**5**	**10**	**30**	**50**	**100**	**+ve control**
D1	4.400 (0.000)	4.325 (0.096)	4.350 (0.058)	4.125 (0.096)	4.475 (0.050)	4.875* (0.189)	4.650* (0.100)	4.950* (0.173)	5.000* (0.082)	5.075* (0.613)	4.825* (0.275)	6.050* (0.129)
D2	4.375 (0.050)	4.600 (0.183)	4.425 (0.126)	4.325 (0.189)	4.300 (0.141)	4.225 (0.050)	4.150 (0.100)	4.725* (0.096)	5.350* (0.058)	5.575* (0.263)	6.050* (0.129)	5.700* (0.231)
D3	3.400 (0.216)	3.550 (0.129)	3.400 (0.082)	3.025 (0.050)	3.650 (0.208)	3.425 (0.263)	3.925* (0.096)	3.300 (0.216)	4.150* (0.208)	3.975* (0.287)	3.725* (0.096)	3.825 (0.411)
D4	4.875 (0.171)	4.900 (0.356)	4.975 (0.171)	4.675 (0.096)	4.975 (0.250)	4.850 (0.173)	4.775 (0.096)	5.375* (0.171)	5.700* (0.316)	5.475* (0.330)	5.700* (0.258)	6.050* (0.129)

Table 7.5: Effect of Ibudilast on ALH. Table shows effect of Ibudilast on ALH as 10 different concentrations on 4 different donors. The numbers in brackets are standard deviation. Asterix (*) indicates that standard deviations are not overlapping compared to -ve control (i.e. statistically significant). Negative (1% DMSO) and positive (3.6µM progesterone) controls are shown on the table.

	Concentration (µM)											
	-ve control	**0.1**	**0.3**	**0.5**	**1**	**3**	**5**	**10**	**30**	**50**	**100**	**+ve control**
D1	60.18 (1.77)	65.00* (1.72)	69.60* (1.37)	67.58* (2.82)	71.03* (1.16)	71.95* (1.58)	73.63* (1.93)	67.40* (2.24)	67.95* (2.42)	65.55* (2.95)	66.45 (5.08)	72.73* (4.01)
D2	76.28 (2.68)	78.55 (0.40)	78.38 (1.95)	78.53 (1.20)	80.80* (0.81)	83.95* (3.53)	89.20* (1.79)	87.43* (3.18)	90.88* (3.76)	88.48* (2.99)	87.95* (3.50)	94.15* (0.68)
D3	80.83 (1.11)	85.28 (4.68)	80.53 (3.87)	82.18 (1.89)	85.08* (3.01)	84.88* (2.09)	85.13 (4.12)	85.30* (1.85)	82.20 (2.44)	83.85 (1.99)	79.83 (2.80)	82.60 (1.56)
D4	73.55 (1.20)	75.40 (0.95)	74.50 (0.32)	83.95* (1.57)	87.10* (0.65)	79.75* (1.77)	83.90* (1.78)	84.45* (0.70)	90.53* (0.05)	82.20* (0.95)	78.53* (0.27)	90.90* (1.77)

Table 7.6: Effect of MMPX on VAP. Table shows effect of MMPX on VAP as 10 different concentrations on 4 different donors. The numbers in brackets are standard deviation. Asterix (*) indicates that standard deviations are not overlapping compared to -ve control (i.e. statistically significant). Negative (1% DMSO) and positive (3.6µM progesterone) controls are shown on the table.

	Concentration (µM)											
	-ve control	**0.1**	**0.3**	**0.5**	**1**	**3**	**5**	**10**	**30**	**50**	**100**	**+ve control**
D1	52.40 (1.60)	56.68* (1.16)	60.58* (1.39)	56.75 (3.25)	61.28* (1.64)	60.55* (1.71)	62.53* (1.72)	57.35* (0.99)	57.63* (1.82)	54.93 (2.14)	54.00 (2.70)	60.70* (2.94)
D2	69.70 (2.90)	71.43 (0.68)	72.48 (2.49)	71.98 (1.86)	74.75* (1.34)	76.73* (2.20)	80.95* (2.28)	80.23* (3.34)	82.68* (2.88)	79.60* (1.87)	78.23* (2.82)	84.95* (0.60)
D3	68.4 (0.97)	71.73 (4.15)	67.95 (4.31)	70.98 (1.72)	69.58 (3.75)	70.10 (1.80)	70.98 (3.88)	70.12 (3.09)	66.85 (2.61)	67.68 (1.97)	64.90 (3.14)	66.75 (0.95)
D4	64.83 (1.43)	67.20 (0.94)	65.63 (0.71)	73.35* (1.87)	78.35* (0.75)	70.43* (1.46)	74.50* (1.92)	73.48* (0.80)	81.80* (0.33)	74.60* (0.79)	71.75* (0.15)	83.75* (0.15)

Table 7.7: Effect of MMPX on VSL. Table shows effect of MMPX on VSL as 10 different concentrations on 4 different donors. The numbers in brackets are standard deviation. Asterix (*) indicates that standard deviations are not overlapping compared to -ve control (i.e. statistically significant). Negative (1% DMSO) and positive (3.6µM progesterone) controls are shown on the table.

	Concentration (µM)											
	-ve control	**0.1**	**0.3**	**0.5**	**1**	**3**	**5**	**10**	**30**	**50**	**100**	**+ve control**
D1	96.35 (4.60)	103.53 (5.63)	111.35* (2.68)	112.15* (8.70)	114.25* (2.02)	120.58* (3.11)	123.63* (4.48)	108.38* (5.04)	112.48* (5.75)	107.70 (6.56)	114.58* (11.96)	123.65* (8.67)
D2	106.40 (4.33)	107.50 (1.43)	106.43 (2.99)	106.03 (2.02)	108.28 (1.24)	114.33 (6.29)	122.68* (3.10)	118.75* (3.15)	127.90* (7.79)	126.08* (6.87)	128.25* (6.03)	135.53* (4.98)
D3	128.63 (1.07)	141.40* (7.62)	129.80 (4.12)	129.95 (1.89)	145.65* (3.07)	142.10* (2.62)	140.53* (7.70)	144.56* (4.85)	139.53* (4.07)	146.43* (5.08)	135.48* (2.91)	138.95* (2.81)
D4	113.35 (2.00)	114.33 (1.13)	115.88 (1.24)	134.75* (2.56)	134.70* (0.80)	121.53* (3.77)	127.75* (2.16)	134.95* (1.70)	139.00* (1.31)	126.77* (0.88)	116.15 (1.06)	129.75* (2.16)

Table 7.8: Effect of MMPX on VCL. Table shows effect of MMPX on VCL as 10 different concentrations on 4 different donors. The numbers in brackets are standard deviation. Asterix (*) indicates that standard deviations are not overlapping compared to -ve control (i.e. statistically significant). Negative (1% DMSO) and positive (3.6µM progesterone) controls are shown on the table.

	Concentration (µM)											
	-ve control	**0.1**	**0.3**	**0.5**	**1**	**3**	**5**	**10**	**30**	**50**	**100**	**+ve control**
D1	4.300 (0.140)	4.500 (0.420)	4.825* (0.190)	4.775 (0.440)	4.825* (0.130)	5.125* (0.150)	5.325* (0.240)	4.600 (0.320)	5.025* (0.300)	4.650* (0.210)	5.100* (0.560)	5.600* (0.270)
D2	3.750 (0.250)	3.775 (0.130)	3.725 (0.130)	3.650 (0.190)	3.650 (0.190)	3.825 (0.220)	3.925 (0.100)	3.800 (0.080)	4.175 (0.380)	4.125 (0.340)	4.175 (0.330)	4.650* (0.310)
D3	5.125 (0.130)	5.875* (0.380)	5.375 (0.250)	5.250 (0.170)	6.200* (0.140)	5.900* (0.360)	5.775* (0.220)	5.900* (0.390)	5.950* (0.310)	6.125* (0.210)	5.650* (0.170)	5.750* (0.260)
D4	4.375 (0.060)	4.150 (0.030)	4.525 (0.120)	5.175* (0.170)	4.950* (0.030)	4.375 (0.210)	4.575 (0.160)	4.950* (0.120)	5.150* (0.060)	4.733* (0.030)	4.175 (0.130)	4.375 (0.210)

Table 7.9: Effect of MMPX on ALH. Table shows effect of MMPX on ALH as 10 different concentrations on 4 different donors. The numbers in brackets are standard deviation. Asterix (*) indicates that standard deviations are not overlapping compared to -ve control (i.e. statistically significant). Negative (1% DMSO) and positive (3.6µM progesterone) controls are shown on the table.

	Concentration (µM)											
	-ve control	**0.1**	**0.3**	**0.5**	**1**	**3**	**5**	**10**	**30**	**50**	**100**	**+ve control**
D1	68.58 (2.27)	76.65* (2.49)	75.60* (0.99)	76.45* (0.01)	75.63* (1.94)	80.38* (3.45)	82.43* (3.65)	82.60* (3.01)	81.28* (0.83)	74.58* (2.86)	76.63* (2.94)	86.55* (4.07)
D2	83.38 (2.20)	86.18 (3.58)	85.05 (1.67)	85.63 (2.22)	88.80 (3.42)	86.90 (2.54)	87.63 (3.61)	83.25 (2.02)	84.05 (0.79)	75.30 (2.01)	73.65 (2.25)	92.30* (1.63)
D3	81.93 (3.96)	81.68 (1.36)	87.45 (1.65)	88.70 (2.82)	90.73* (2.43)	92.43* (4.38)	90.88* (1.30)	98.23* (3.35)	93.75* (2.62)	90.45* (0.62)	80.23 (2.53)	96.15* (3.28)
D4	76.33 (3.03)	76.43 (1.78)	79.95 (5.61)	81.35 (2.72)	81.83 (3.01)	82.65 (3.83)	81.53 (4.34)	80.40 (2.09)	80.05 (4.51)	74.43 (3.61)	70.45 (3.39)	87.63* (2.37)

Table 7.10: Effect of Etazolate on VAP. Table shows effect of Etazolate on VAP as 10 different concentrations on 4 different donors. The numbers in brackets are standard deviation. Asterix (*) indicates that standard deviations are not overlapping compared to -ve control (i.e. statistically significant). Negative (1% DMSO) and positive (3.6µM progesterone) controls are shown on the table.

	Concentration (µM)											
	-ve control	**0.1**	**0.3**	**0.5**	**1**	**3**	**5**	**10**	**30**	**50**	**100**	**+ve control**
D1	60.08 (3.05)	66.90* (0.76)	66.78* (1.58)	66.35* (2.24)	65.28* (1.86)	66.35* (1.71)	67.98 (4.11)	69.05* (2.57)	64.90 (1.92)	62.48 (2.74)	64.00 (3.37)	69.70* (1.88)
D2	68.90 (2.25)	72.40 (2.76)	69.90 (1.79)	72.25 (0.92)	70.33 (1.59)	70.88 (1.96)	70.05 (3.02)	65.78 (1.92)	64.15 (1.65)	59.03 (0.97)	58.13 (2.45)	72.80* (0.82)
D3	74.95 (4.01)	75.48 (1.91)	79.90 (1.86)	81.70 (2.48)	82.90* (2.30)	84.55* (3.82)	82.90* (1.82)	88.85* (3.98)	81.98 (2.32)	80.70* (0.93)	71.78 (2.61)	86.60* (3.44)
D4	65.93 (2.90)	67.325 (3.63)	69.55 (4.13)	69.95 (2.26)	71.05 (2.56)	70.85 (4.60)	68.53 (4.53)	67.53 (1.34)	63.40 (0.70)	62.00 (2.51)	58.43 (2.64)	74.88* (1.94)

Table 7.11: Effect of Etazolate on VSL. Table shows effect of Etazolate on VSL as 10 different concentrations on 4 different donors. The numbers in brackets are standard deviation. Asterix (*) indicates that standard deviations are not overlapping compared to -ve control (i.e. statistically significant). Negative (1% DMSO) and positive (3.6µM progesterone) controls are shown on the table.

	Concentration (µM)											
	-ve control	**0.1**	**0.3**	**0.5**	**1**	**3**	**5**	**10**	**30**	**50**	**100**	**+ve control**
D1	107.23 (5.20)	120.23* (6.58)	115.10 (2.57)	121.23* (2.47)	119.80* (3.60)	135.10* (9.06)	139.20* (3.61)	139.45* (7.18)	143.85* (7.58)	126.60* (6.71)	128.88* (4.34)	153.90* (8.35)
D2	135.50 (3.42)	139.30 (9.39)	142.38 (6.23)	139.00 (8.22)	152.00* (8.58)	146.20 (6.77)	151.28* (9.44)	143.88 (4.75)	146.70* (3.36)	129.88 (5.03)	129.23 (5.05)	162.58* (4.04)
D3	109.35 (3.81)	107.36 (1.98)	116.70* (2.60)	118.08* (3.65)	120.70* (3.29)	125.45* (8.67)	123.10* (1.24)	139.68* (3.16)	136.95* (6.44)	130.90* (2.40)	118.23 (5.71)	135.53* (5.20)
D4	122.55 (5.83)	119.15 (2.34)	124.75 (8.84)	132.13 (8.32)	133.20 (7.14)	135.03* (5.17)	139.03* (8.38)	137.90* (5.02)	145.95* (15.05)	125.00 (4.24)	122.00 (10.69)	145.98* (9.61

Table 7.12: Effect of Etazolate on VCL. Table shows effect of Etazolate on VCL as 10 different concentrations on 4 different donors. The numbers in brackets are standard deviation. Asterix (*) indicates that standard deviations are not overlapping compared to -ve control (i.e. statistically significant). Negative (1% DMSO) and positive (3.6µM progesterone) controls are shown on the table.

	Concentration (µM)											
	-ve control	**0.1**	**0.3**	**0.5**	**1**	**3**	**5**	**10**	**30**	**50**	**100**	**+ve control**
D1	4.150 (0.130)	4.750* (0.370)	4.475 (0.210)	4.650* (0.100)	4.600* (0.140)	5.350* (0.700)	5.500* (0.240)	5.750* (0.330)	5.975* (0.450)	5.100* (0.410)	5.450* (0.240)	6.500* (0.450)
D2	5.425 (0.130)	5.525 (0.390)	5.725 (0.190)	5.575 (0.320)	6.025 (0.530)	5.950 (0370)	6.175* (0.220)	5.775 (0.220)	6.125* (0.340)	5.550 (0.100)	5.900 (0.330)	6.600* (0.290)
D3	3.575 (0.170)	3.56 (0.090)	3.775 (0.210)	3.800 (0.120)	3.850 (0.170)	4.025 (0.400)	3.900* (0.00)	4.575* (0.170)	4.550* (0.310)	4.375* (0.130)	4.250* (0.260)	4.650* (0.260)
D4	5.225 (0.340)	5.000 (0.350)	5.075 (0.300)	5.425 (0.330)	5.425 (0.300)	5.675 (0.430)	5.875 (0.390)	5.950* (0.640)	6.575* (0.640)	5.425 (0.150)	5.600 (0.470)	6.075* (0.450)

Table 7.13: Effect of Etazolate on ALH. Table shows effect of Etazolate on ALH as 10 different concentrations on 4 different donors. The numbers in brackets are standard deviation. Asterix (*) indicates that standard deviations are not overlapping compared to -ve control (i.e. statistically significant). Negative (1% DMSO) and positive (3.6µM progesterone) controls are shown on the table.

	Concentration (µM)											
	-ve control	**0.1**	**0.3**	**0.5**	**1**	**3**	**5**	**10**	**30**	**50**	**100**	**+ve control**
D1	64.10 (0.29)	65.15 (0.90)	68.78* (0.84)	74.38* (0.47)	77.05* (1.50)	79.10* (0.36)	80.60* (1.73)	80.55* (1.38)	78.43* (0.79)	82.15* (0.90)	77.03* (1.05)	79.00* (2.79)
D2	73.88 (0.11)	79.03* (0.39)	81.25* (0.25)	80.35* (0.85)	85.83* (0.31)	87.15* (0.34)	88.75* (0.88)	87.78* (0.41)	88.50* (0.58)	89.05* (0.65)	81.93* (0.54)	87.33* (0.60)
D3	70.25 (0.45)	79.73* (0.22)	77.80* (1.60)	88.05* (0.50)	83.40* (0.51)	87.70* (0.44)	86.85* (0.50)	90.08* (0.57)	85.00* (0.80)	88.23* (0.58)	84.00* (0.86)	86.55* (0.94)
D4	61.13 (1.16)	63.28 (1.52)	71.33* (0.36)	72.60* (0.67)	78.68* (0.43)	80.23* (1.01)	76.75* (0.57)	75.73* (1.53)	79.35* (1.19)	75.23* (2.00)	75.03* (1.00)	82.35* (1.01)
D5	83.98 (0.80)	86.40 (2.38)	83.80 (1.14)	90.75* (0.65)	83.03 (1.19)	89.98* (2.20)	89.53* (1.71)	85.53 (0.88)	84.93 (1.14)	85.35 (0.70)	84.68 (0.15)	87.98* (2.20)

Table 7.14: Effect of Papaverine on VAP. Table shows effect of Papaverine on VAP as 10 different concentrations on 4 different donors. The numbers in brackets are standard deviation. Asterix (*) indicates that standard deviations are not overlapping compared to -ve control (i.e. statistically significant). Negative (1% DMSO) and positive (3.6µM progesterone) controls are shown on the table.

	Concentration (µM)											
	-ve control	**0.1**	**0.3**	**0.5**	**1**	**3**	**5**	**10**	**30**	**50**	**100**	**+ve control**
D1	57.68 (0.32)	60.08* (0.57)	62.93* (0.43)	68.35* (0.76)	70.78* (1.61)	72.25* (0.24)	73.83* (1.73)	72.33* (1.52)	70.40* (1.06)	72.18* (0.33)	68.30* (0.89)	66.60* (1.27)
D2	63.38 (0.48)	67.73* (0.83)	70.78* (0.71)	69.75* (1.32)	71.70* (0.24)	70.53* (1.24)	72.10* (1.32)	74.78* (0.79)	70.78* (0.50)	72.88* (0.15)	67.08* (0.92)	72.93* (0.65)
D3	61.53 (0.64)	66.68* (0.99)	65.23 (3.36)	73.28* (0.70)	65.23* (0.46)	71.75* (0.69)	72.08* (0.36)	71.20* (0.93)	68.40* (1.00)	71.75* (0.53)	69.45* (1.34)	68.95* (1.67)
D4	54.15 (1.68)	55.45 (1.75)	62.85* (0.33)	63.83* (0.10)	65.55* (0.56)	68.35* (0.13)	65.65* (0.26)	65.35* (1.70)	66.43* (0.54)	63.05* (2.37)	65.20* (0.27)	65.25* (0.10)
D5	73.20 (0.58)	75.98* (1.92)	72.50 (0.96)	77.85* (1.28)	71.73 (1.00)	76.55* (1.11)	76.00* (1.35)	73.45 (0.65)	73.25 (1.10)	72.30* (1.16)	70.83 (0.92)	74.55* (0.65)

Table 7.15: Effect of Papaverine on VSL. Table shows effect of Papaverine on VSL as 10 different concentrations on 4 different donors. The numbers in brackets are standard deviation. Asterix (*) indicates that standard deviations are not overlapping compared to -ve control (i.e. statistically significant). Negative (1% DMSO) and positive (3.6µM progesterone) controls are shown on the table.

	Concentration (µM)											
	-ve control	**0.1**	**0.3**	**0.5**	**1**	**3**	**5**	**10**	**30**	**50**	**100**	**+ve control**
D1	97.73 (1.88)	93.40 (1.32)	101.38 (2.14)	107.63* (0.68)	115.18* (2.89)	118.08* (0.97)	117.58* (2.84)	126.13* (0.49)	122.03* (1.80)	134.38* (5.59)	124.33* (3.28)	136.03* (7.99)
D2	111.75 (0.93)	120.25* (0.73)	121.85* (2.18)	119.88* (1.48)	134.45* (1.88)	140.50* (1.47)	144.88* (2.27)	136.20* (1.96)	149.68* (2.33)	146.38* (2.16)	136.13* (2.54)	137.13* (2.08)
D3	105.65 (0.39)	125.33* (1.22)	124.45* (2.06)	142.98* (0.99)	140.98* (2.08)	142.48* (1.16)	139.23* (1.13)	151.93* (0.86)	141.58* (1.17)	149.28* (1.36)	138.85* (0.92)	144.28* (1.36)
D4	98.55 (0.67)	100.03 (0.73)	109.90* (1.08)	113.03* (1.77)	129.88* (2.72)	129.90* (4.83)	121.60* (2.08)	122.93* (1.96)	130.03* (4.22)	121.88* (2.90)	119.93* (3.04)	136.23* (1.77)
D5	132.08 (2.32)	134.68 (4.70)	134.10 (1.61)	146.93* (2.24)	137.28* (1.39)	147.58* (4.42)	147.48* (4.17)	145.33* (0.87)	140.33* (1.52)	147.08* (2.29)	143.75* (1.89)	149.08* (0.87)

Table 7.16: Effect of Papaverine on VCL. Table shows effect of Papaverine on VCL as 10 different concentrations on 4 different donors. The numbers in brackets are standard deviation. Asterix (*) indicates that standard deviations are not overlapping compared to -ve control (i.e. statistically significant). Negative (1% DMSO) and positive (3.6µM progesterone) controls are shown on the table.

	Concentration (µM)											
	-ve control	**0.1**	**0.3**	**0.5**	**1**	**3**	**5**	**10**	**30**	**50**	**100**	**+ve control**
D1	4.050 (0.058)	3.600 (0.000)	3.925 (0.096)	3.975 (0.050)	4.450* (0.129)	4.375* (0.050)	4.200 (0.115)	4.875* (0.096)	4.725* (0.222)	5.175* (0.299)	5.000* (0.183)	5.725* (0.330)
D2	4.150 (0.050)	4.550* (0.029)	4.400* (0.122)	4.400* (0.041)	4.950* (0.132)	5.150* (0.104)	5.475* (0.125)	5.000* (0.091)	5.500* (0.158)	5.600* (0.147)	5.025* (0.111)	5.400* (0.041)
D3	4.025 (0.048)	4.875* (0.149)	4.950* (0.065)	5.425* (0.025)	5.825* (0.125)	5.425* (0.063)	5.225* (0.048)	5.750* (0.065)	5.375* (0.063)	5.850* (0.029)	5.325* (0.025)	5.875* (0.085)
D4	4.450 (0.100)	4.675 (0.096)	4.600 (0.000)	4.850* (0.129)	5.550* (0.173)	5.425* (0.250)	5.050* (0.100)	5.050* (0.129)	5.325* (0.126)	5.025* (0.171)	4.825* (0.189)	5.575* (0.173)
D5	5.550 (0.191)	5.725 (0.189)	5.875 (0.050)	6.500* (0.216)	6.250* (0.129)	6.275* (0.126)	6.400* (0.216)	6.725* (0.050)	6.300* (0.081)	6.675* (0.171)	6.575* (0.096)	6.625* (0.129)

Table 7.17: Effect of Papaverine on VCL. Table shows effect of Papaverine on VCL as 10 different concentrations on 4 different donors. The numbers in brackets are standard deviation. Asterix (*) indicates that standard deviations are not overlapping compared to -ve control (i.e. statistically significant). Negative (1% DMSO) and positive (3.6µM progesterone) controls are shown on the table.

	Concentration (µM)											
	-ve control	**0.1**	**0.3**	**0.5**	**1**	**3**	**5**	**10**	**30**	**50**	**100**	**+ve control**
D1	82.18 (5.25)	92.08 (3.77)	84.50 (3.29)	88.28 (1.26)	91.08 (4.76)	93.45* (1.63)	89.45 (5.23)	85.93 (3.51)	85.20 (3.97)	81.20 (3.21)	78.43 (2.23)	97.45* (3.92)
D2	77.38 (4.85)	81.88 (3.18)	80.05* (2.04)	82.20* (2.37)	82.10* (2.55)	81.75* (3.19)	81.83* (3.76)	77.80* (2.17)	76.60* (1.98)	77.98 (1.80)	72.00 (5.42)	83.53* (2.93)
D3	58.28 (1.35)	61.45 (4.48)	66.38 (5.47)	65.88 (0.94)	70.28 (2.80)	67.88 (2.00)	68.38 (2.39)	62.88 (1.94)	62.80 (1.69)	58.40 (4.30)	56.48 (1.74)	67.30 (2.54)

Table 7.18: Effect of Tofisopam on VAP. Table shows effect of Tosfisopam on VAP as 10 different concentrations on 4 different donors. The numbers in brackets are standard deviation. Asterix (*) indicates that standard deviations are not overlapping compared to -ve control (i.e. statistically significant). Negative (1% DMSO) and positive (3.6µM progesterone) controls are shown on the table.

	Concentration (µM)											
	-ve control	**0.1**	**0.3**	**0.5**	**1**	**3**	**5**	**10**	**30**	**50**	**100**	**+ve control**
D1	69.45 (2.47)	80.48* (4.20)	73.25 (1.87)	75.93* (0.79)	75.43 (5.10)	80.48* (0.96)	75.40* (1.62)	70.78 (3.21)	69.18 (0.98)	67.25 (1.58)	66.00 (3.07)	77.85* (4.55)
D2	67.53 (4.84)	68.43 (3.76)	66.08 (1.94)	67.15 (2.03)	65.70 (2.11)	67.10 (2.74)	62.93 (1.95)	61.53 (1.51)	59.08 (2.38)	62.08 (3.19)	56.85 (3.17)	63.75 (3.53)
D3	52.90 (1.66)	55.93 (4.15)	60.98 (6.23)	60.65* (0.79)	65.28* (2.43)	62.33* (1.85)	61.70* (1.96)	56.48* (1.21)	56.85* (1.67)	51.93 (3.96)	50.20 (1.94)	59.20* (2.92)

Table 7.19: Effect of Tofisopam on VSL. Table shows effect of Tosfisopam on VSL as 10 different concentrations on 4 different donors. The numbers in brackets are standard deviation. Asterix (*) indicates that standard deviations are not overlapping compared to -ve control (i.e. statistically significant). Negative (1% DMSO) and positive (3.6µM progesterone) controls are shown on the table.

	Concentration (µM)											
	-ve control	**0.1**	**0.3**	**0.5**	**1**	**3**	**5**	**10**	**30**	**50**	**100**	**+ve control**
D1	134.28 (15.44)	142.90 (6.88)	134.85 (7.07)	146.05 (4.36)	153.73 (5.22)	151.23 (6.00)	150.45 (14.03)	151.60 (6.35)	152.23 (14.56)	139.43 (8.50)	133.20 (6.13)	171.10* (10.85)
D2	116.70 (3.97)	132.93* (2.41)	130.30* (3.50)	132.43* (4.92)	137.23* (3.49)	136.25* (5.37)	143.73* (12.09)	136.10* (5.22)	135.05* (5.99)	133.18* (3.33)	121.90 (12.42)	145.28* (6.23)
D3	84.85 (1.52)	88.15 (7.25)	94.45* (4.06)	91.53* (2.46)	97.20* (3.21)	94.68* (2.94)	101.38* (4.41)	96.35* (5.85)	93.13* (2.70)	90.13 (6.56)	86.88 (3.17)	100.53* (6.73)

Table 7.20: Effect of Tofisopam on VCL. Table shows effect of Tosfisopam on VCL as 10 different concentrations on 4 different donors. The numbers in brackets are standard deviation. Asterix (*) indicates that standard deviations are not overlapping compared to -ve control (i.e. statistically significant). Negative (1% DMSO) and positive (3.6µM progesterone) controls are shown on the table.

	Concentration (µM)											
	-ve control	**0.1**	**0.3**	**0.5**	**1**	**3**	**5**	**10**	**30**	**50**	**100**	**+ve control**
D1	5.750 (0.968)	5.750 (0.342)	5.550 (0.351)	6.000 (0.283)	6.400 (0.271)	6.200 (0.337)	6.375 (0.562)	6.750 (0.208)	6.725 (0.629)	6.325 (0.386)	5.975 (0.330)	7.300* (0.469)
D2	4.575 (0.206)	5.475* (0.222)	5.175* (0.171)	5.250* (0.311)	5.525* (0.050)	5.575* (0.263)	5.750* (0.681)	5.625* (0.263)	5.650* (0.208)	5.650* (0.191)	5.275* (0.403)	5.800* (0.316)
D3	3.300 (0.183)	3.400 (0.216)	3.525 (0.096)	3.300 (0.200)	3.450 (0.129)	3.350 (0.129)	3.775* (0.171)	3.800 (0.337)	3.600 (0.141)	3.550 (0.191)	3.350 (0.238)	3.925* (0.287)

Table 7.21: Effect of Tofisopam on ALH. Table shows effect of Tosfisopam on ALH as 10 different concentrations on 4 different donors. The numbers in brackets are standard deviation. Asterix (*) indicates that standard deviations are not overlapping compared to -ve control (i.e. statistically significant). Negative (1% DMSO) and positive (3.6µM progesterone) controls are shown on the table.

7.2 Supplementary figures and tables for chapter 4

#	Compound	Author	Species	Concentration	Effect on Mot.	Ca2+ effect
1	Arecoline	Yuan et. al.	Human	300µg/ml	Negative	N/A
2	Arecaidine	Yuan et. al.	Human	300µg/ml	Negative	N/A
3	Guvacine	Yuan et. al.	Human	300µg/ml	Negative	N/A
4	HerbOshield	Singh et. al.	Rat	100mg/ml	Immobil.	N/A
5	NIM-76	Singh et. al.	Rat			N/A
6	Zeralenone	Filannino et. al.	Stallion	0.1mM	Slowed	N/A
7	α-zeralenone	Filannino et. al.	Stallion	0.1mM	Negative	N/A
8	β-zeralenone	Filannino et. al.	Stallion	0.1mM	Slowed	N/A
9	Relaxin	Ferlin et. al.	Human	100nM	HA	Positive
10	Butan-1-ol	Itach et. al.	Mice	0.1%-0.5%	Negative	N/A
11	L-arginine	Keller et. al.	Human	0.004M	Positive	N/A
12	Theophylline	Ebner et. al.	Human		Positive	N/A
13	Remifantil	Xu et. al.	Human	0.1-100µg/L	Negative	N/A
14	Biotin	Kathur et. al.	Human	10nM	Negative	N/A
15	Propranolol	Peterson et al	Human	0.8mM	Negative	N/A
16	Sotalol	Peterson et al	Human	10mM	Negative	N/A
17	Chlorpromazine	Peterson et al	Human	0.2mM	Negative	N/A
18	Lidocaine	Peterson et al	Human	12mM	Negative	N/A
19	Diphahydramine	Peterson et al	Human	2mM	Negative	N/A
20	Atropine	Peterson et al	Human	7.5mM	Negative	N/A
21	Seopolamine	Peterson et al	Human	10mM	Negative	N/A
22	Benztropine	Peterson et al	Human	0.1mM	Negative	N/A
23	Phentolamine	Peterson et al	Human	2mM	Negative	N/A
24	Phenoxybenzamine	Peterson et al	Human	5mM	Negative	N/A
25	T. fetus extracellular prod.	Riberio et. al.	Bull	N/A	Negative	N/A
26	SEMG1	O'Rand et. al.	Human		Negative	Negative
27	Anti-eppin	O'Rand et. al.	Human		Negative	Negative
28	L-carnitine	Banihani et. al.	Human	0.5mg/ml	Positive	N/A
29	N,N′-Dithiobisphthalimide	Florez et. al.	Human	24µM	Immobil.	N/A
30	Kilikrein	Schill et. al.	Human		Positive	N/A
31	Adenosine	Brenker et. al.	Human	50µM	N/A	N/A
32	SQ22536	Brenker et. al.	Human	500µM	N/A	N/A
33	MDL12330a	Brenker et. al.	Human	100µM	N/A	N/A
34	U73122	Brenker et. al.	Human		N/A	N/A
35	Bourgeonal	Brenker et. al.	Human	10µM	N/A	Positive
36	Undeacanal	Brenker et. al.	Human	3µM	N/A	Positive
37	NNC	Brenker et. al.	Human	10µM	N/A	Negative
38	Mibefradil	Brenker et. al.	Human	30µM	N/A	Negative

Table 7.22: Table shows the effect of 102 compounds on sperm motility and Ca^{2+} signaling. The literature was screened and 102 compounds were found that effect sperm motility and/or Ca^{2+} signaling. Effective concentration and organism of the studies are shown on the table. Table continues over-page.

#	Compound	Author	Species	Concentration	Effect on Mot.	Ca2+ effect
39	Calcitonin	Brenker et. al.	Human	1.5µM	N/A	N/A
40	Angiotensin II	Brenker et. al.	Human	10µM	N/A	N/A
41	FFP	Brenker et. al.	Human	100µM	N/A	N/A
42	Diltiazem	Hong et. al.	Human	7.5µM	Positive	Negative
43	Flunarizine	Hong et. al.	Human	5µM	Positive	Negative
44	Verapamil	Hong et. al.	Human	0.25µM	Positive	Negative
45	Caffeine	Hong et. al.			Positive	Positive
46	IBMX	Fisch et. al.	Human	100µM	Positive	N/A
47	RS-25344	Fisch et. al.	Human	10µM	Positive	N/A
48	Rolipram	Fisch et. al.	Human	20µM	Positive	N/A
49	Sildenafil	Glenn et. al.	Human	0.67µM	Positive	N/A
50	Thapsigargin	Blackmore	Human	10µM	HA	Positive
51	Pentoxifylline	Nassar et. al.	Human	1mg/ml	Positive	Negative
52	Progesterone	Blackmore et. al.	Human	31.8nM	Positive	Positive
53	17α-Hydroxyprogesterone	Blackmore et. al.	Human	30.3nM	N/A	Positive
54	11β-Hydroxyprogesterone	Blackmore et. al.	Human	30.3nM	N/A	Positive
55	5α-Pregnane-3,20-dione	Blackmore et. al.	Human	31.6nM	N/A	Positive
56	Androstendione	Blackmore et. al.	Human	34.9nM	N/A	Positive
57	Pregnendione	Blackmore et. al.	Human	31.4nM	N/A	Positive
58	Corticosterone	Blackmore et. al.	Human	28.9nM	N/A	Positive
59	20α Hydroxypregnen-3-onc	Blackmore et. al.	Human	31.6nM	N/A	Positive
60	β-Estradiol	Blackmore et. al.	Human	36.7nM	N/A	Positive
61	Testosterone	Blackmore et. al.	Human	34.7nM	N/A	Positive
62	Estrone	Blackmore et. al.	Human	37nM	N/A	Positive
63	Dehydroepiandrosterone	Blackmore et. al.	Human	34.7nM	N/A	Positive
64	Abamectin	Ozenci et. al.	Human		N/A	N/A
65	Nonoxynol-9	Nithya et. al.	Rat	250µg/ml	Immobil.	N/A
66	DBZ	Reddy et. al.	Human	0.05mM	Negative	Positive
67	Ouabain	Peris et. al.	Ram	0.1mM	Negative	N/A
68	Calmidazolium	Garcia et. al.	Human		N/A	Negative
69	Pimozode	Garcia et. al.	Human		N/A	Negative
70	Acetylcholine	Bray et. al.	Human	200µM	N/A	Positive
71	Sodium hexachloro-platina	Eberl et. al.	Human	1mM	Negative	N/A
72	Tetraamineplatinuim-II-chl	Eberl et. al.	Human	1mM	Negative	N/A
73	Quinine	Yeung and Cooper	Human	20µmol/L	↓VCL LIN ALH	N/A
74	Tamoifen Citrate	Saberwal et. al.	Rat	0.4mg/kg/day	↓ Forward ↑circ.	Positive
75	SAMMA	Anderson at. al.	Human	2µg/ml	N/A	Dysregula.
76	FSH	Arienti et. al.	Human	98ng/ml	N/A	Positive

Table 7.22 (continued): Table shows the effect of 102 compounds on sperm motility and Ca^{2+} signaling. The literature was screened and 102 compounds were found that effect sperm motility and/or Ca^{2+} signaling. Effective concentration and organism of the studies are shown on the table. Table continues over-page.

#	Compound	Author	Species	Concentration	Effect on Mot.	Ca2+ effect
78	ATP	Edwards et. al.	Human	2.5mM	Positive	No effect
79	Thimerosal	Ho and Suarez	Bull	20µM	HA	Positive
80	Vitamin D	Jensen et. al.	Human	(serum conc)	Positive	Positive
81	Lindane	Silvestroni et. al.	Human	40µM	N/A	Positive
82	4-AP	Gu et. al.	Human	2mM	HA	Positive
83	PGE2	Schaefer et. al.	Human	1µM	N/A	Positive
84	PGE1	Schaefer et. al.	Human	1µM	N/A	Positive
85	NONOate	M-Oliveira et. al.	Human	100µM	Flagella Modula.	Positive
86	GSNO	M-Oliveira et. al.	Human	100µM	N/A	Positive
87	Dithiothreitol	M-Oliveira et. al.	Human	1mM	N/A	(Negative)
88	CCCP	M-Oliveira et. al.	Human	10µM	N/A	Positive
89	Mifepristone (RU486)	Yang et. al.	Human	10µM	Negative	Negative
90	RU39009	Yang et. al.	Human	10µM	N/A	Negative
91	RU41291	Yang et. al.	Human	10µM	N/A	Positive
92	RU39411	Yang et. al.	Human	10µM	N/A	Negative
93	Estradiol	Yang et. al.	Human	10µM	N/A	Positive
94	R5020	Yang et. al.	Human	10µM	N/A	Positive
95	Leuhistin	Subiran et. al.	Human	100µM	Positive/HA	N/A
96	Thiorphan	Subiran et. al.	Human	1µM	Positive	N/A
97	LY294002	Nauc et. al.	Human	30µM	N/A	Positive
98	ZP3	Brewis et. al.	Human	20X conc. Solution	N/A	Positive
99	KN62	M-Briggiler et. al.	Human	60µM	Negative	N/A
100	KN93	M-Briggiler et. al.	Human	60µM	Negative	N/A
101	PACAP	Brubel et. al.	Human	100nmol	Positive	N/A
102	Imidazole	Garbers et. al.	Bovine	75 mM or 107 mM	Inhibition	N/A

Table 7.22 (continued): Table shows the effect of 102 compounds on sperm motility and Ca^{2+} signaling. The literature was screened and 102 compounds were found that effect sperm motility and/or Ca^{2+} signaling. Effective concentration and organism of the studies are shown on the table.

7.3 Supplementary figures and tables for chapter 5

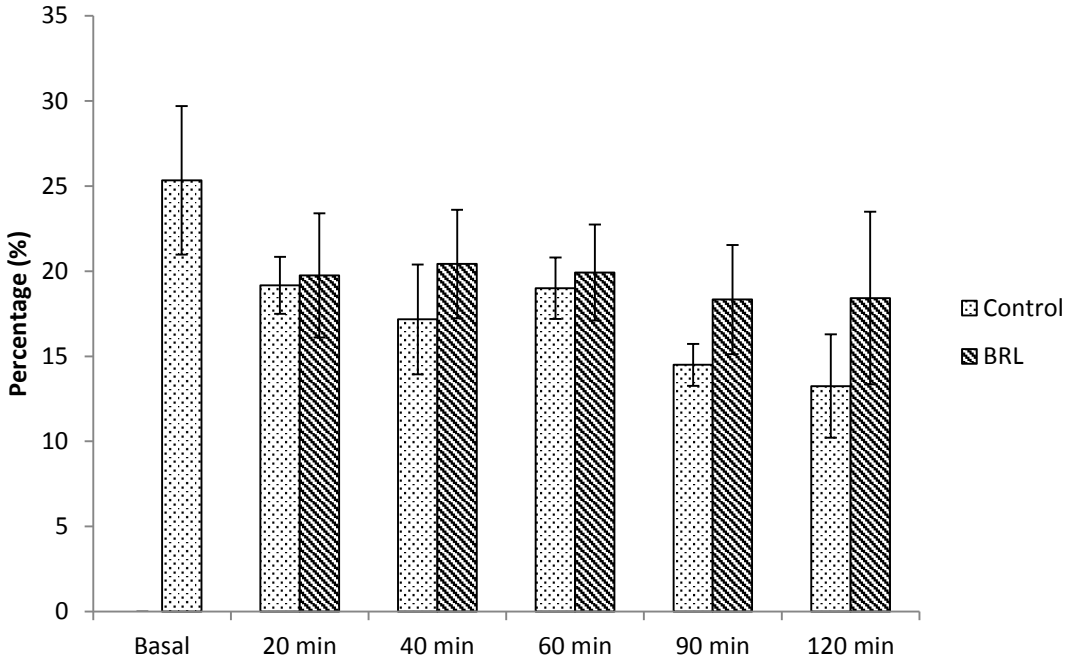

Figure 7.8: Effect of 10µM BRL 50481 on 40% fraction spermatozoa under non-capacitating conditions on total motility (n=4). There is no significant response. Error bars represent SEM.

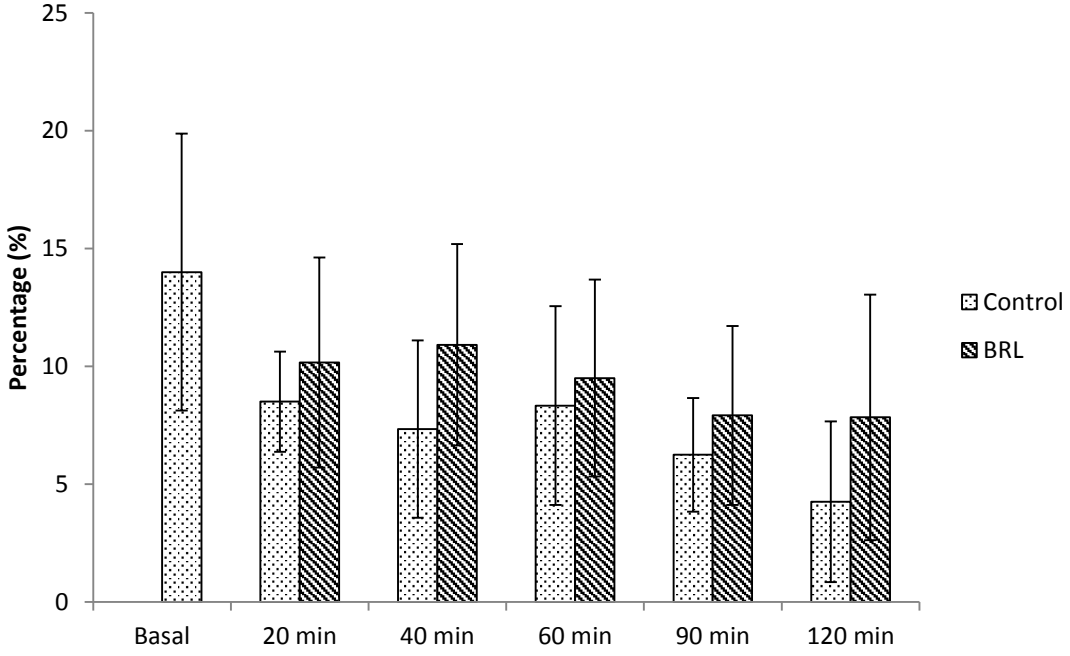

Figure 7.9: Effect of 10µM BRL 50481 on 40% fraction spermatozoa under non-capacitating conditions on progressive motility (n=4). There is no significant response. Error bars represent SEM.

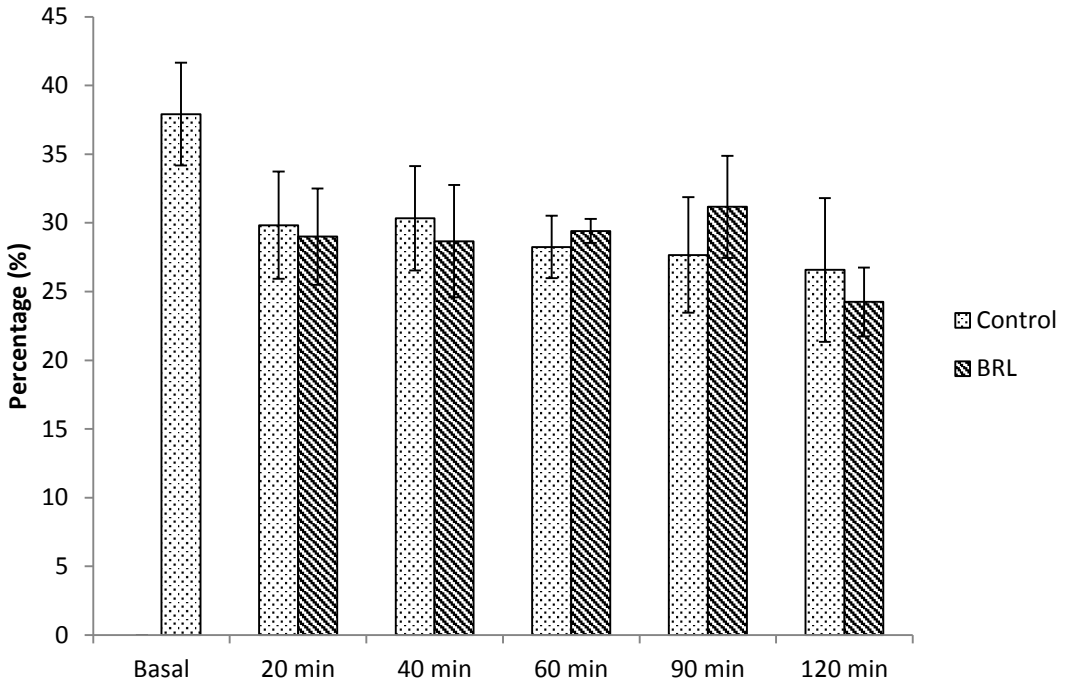

Figure 7.10: Effect of 10µM BRL 50481 on 40% fraction spermatozoa under capacitating conditions on total motility (n=4). There is no significant response. Error bars represent SEM.

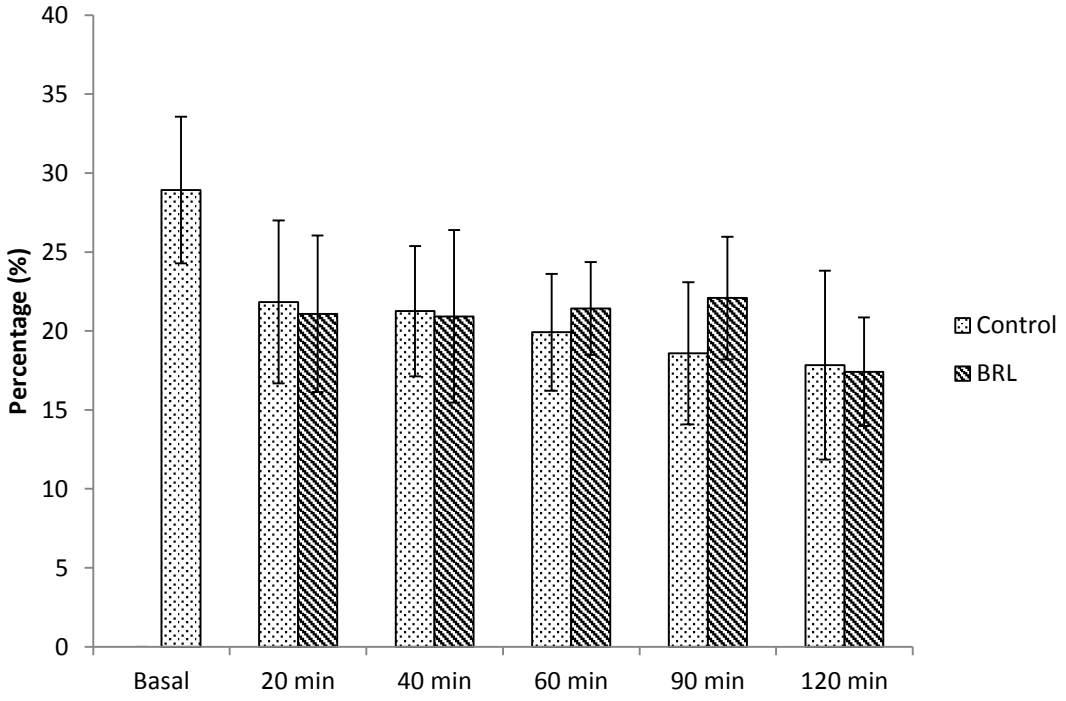

Figure 7.11: Effect of 10µM BRL 50481 on 40% fraction spermatozoa under capacitating conditions on progressive motility (n=4). There is no significant response. Error bars represent SEM.

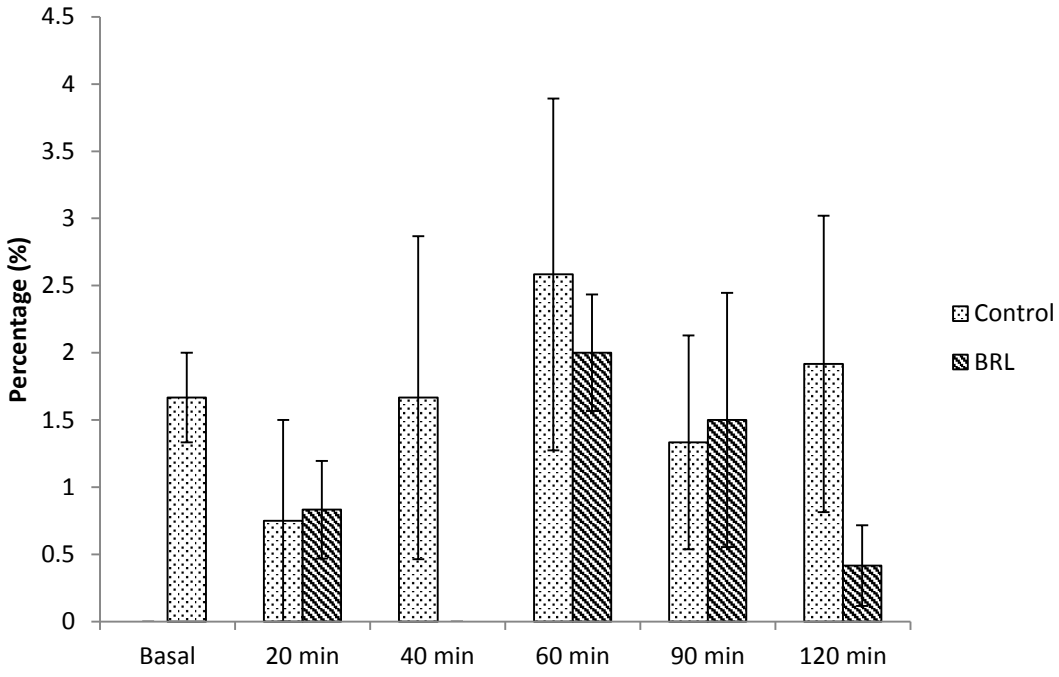

Figure 7.12: Effect of 10µM BRL 50481 on 40% fraction spermatozoa under capacitating conditions on hyperactivation (n=4). There is no significant response. Error bars represent SEM.

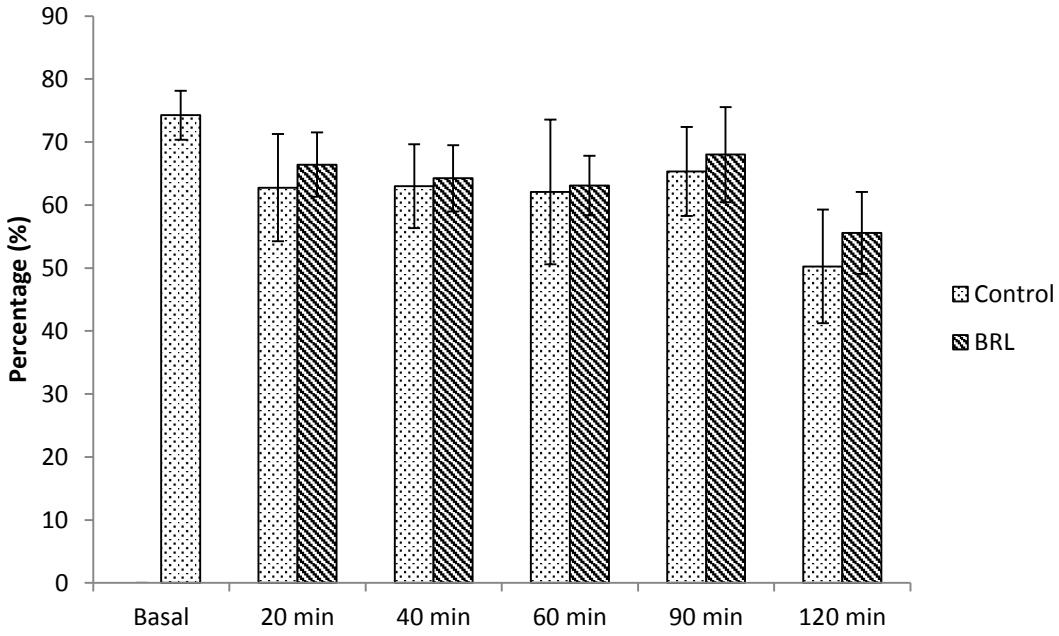

Figure 7.13: Effect of 10µM BRL 50481 on 80% fraction spermatozoa under non-capacitating conditions on total motility (n=4). There is no significant response. Error bars represent SEM.

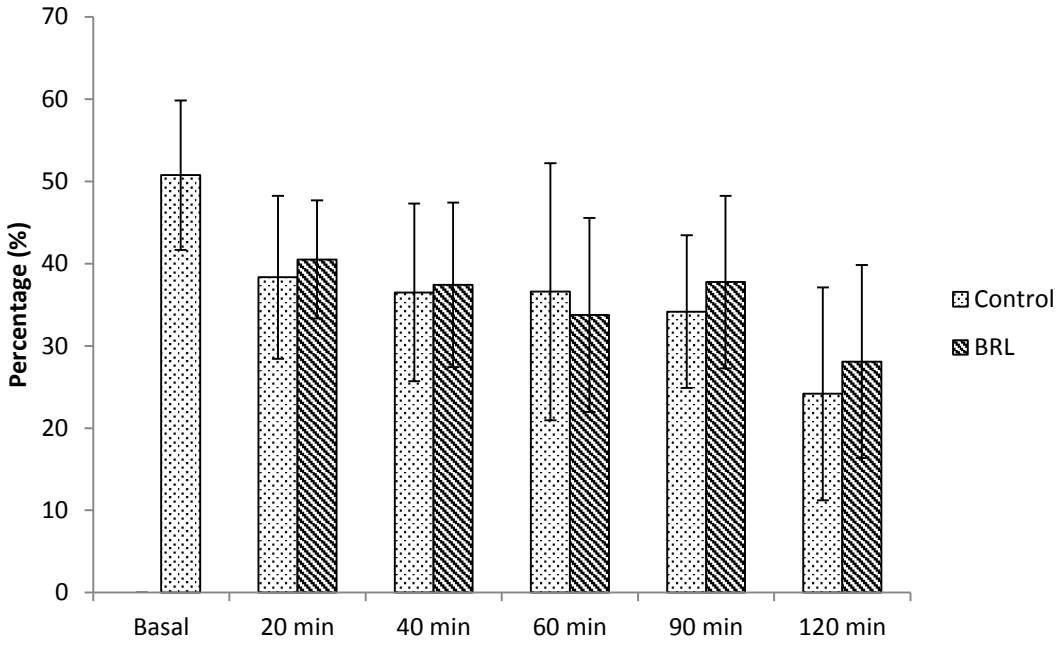

Figure 7.14: Effect of 10µM BRL 50481 on 80% fraction spermatozoa under non-capacitating conditions on progressive motility (n=4). There is no significant response. Error bars represent SEM.

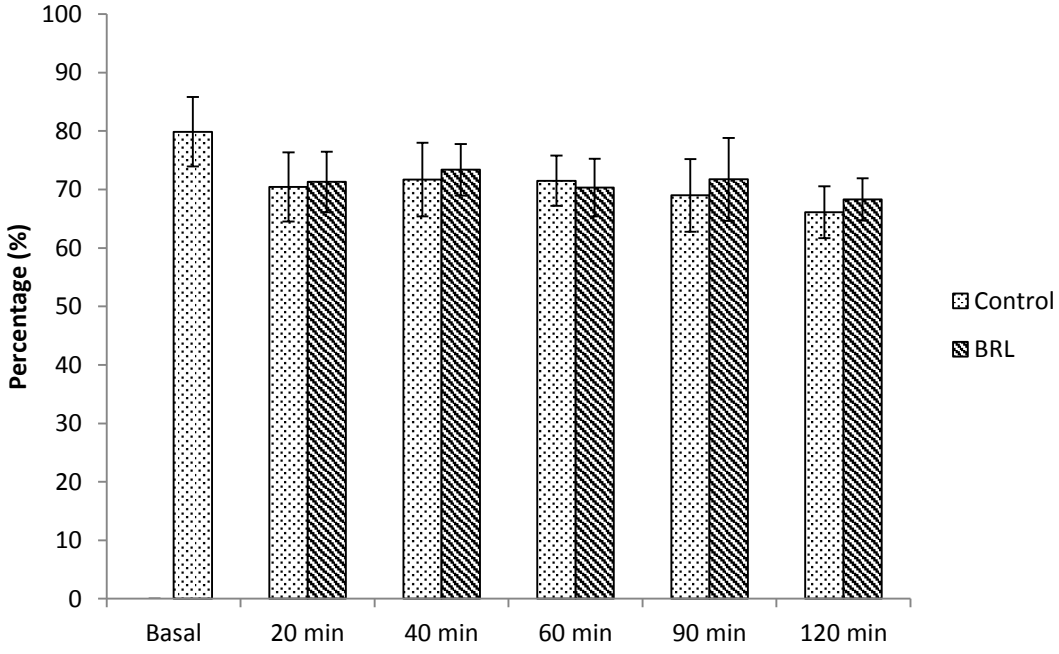

Figure 7.15: Effect of 10µM BRL 50481 on 80% fraction spermatozoa under capacitating conditions on total motility (n=4). There is no significant response. Error bars represent SEM.

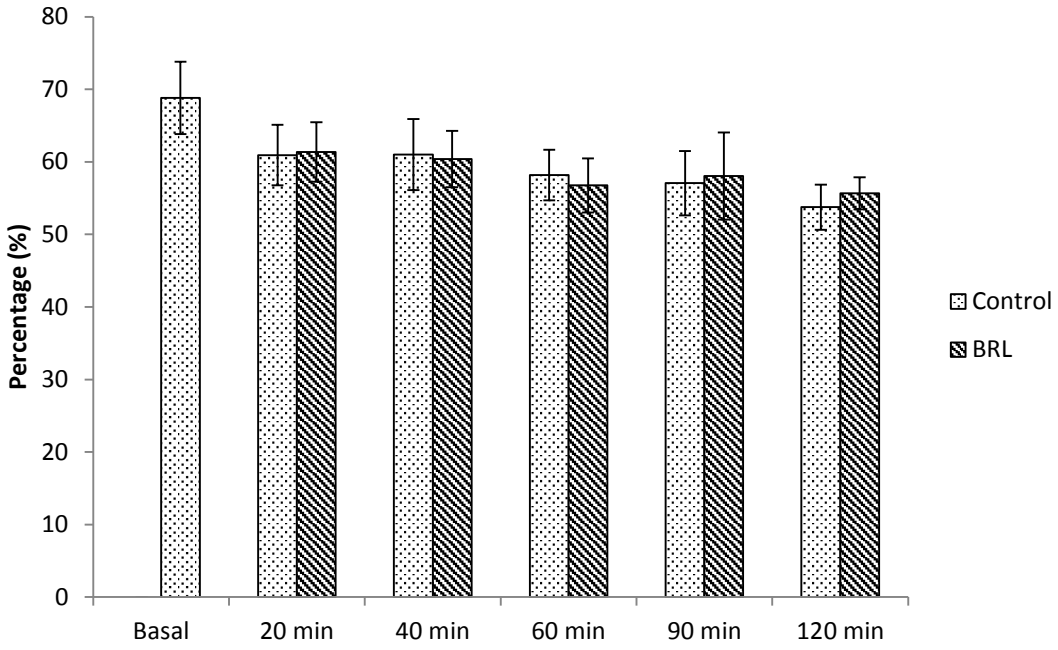

Figure 7.16: Effect of 10µM BRL 50481 on 80% fraction spermatozoa under capacitating conditions on progressive motility (n=4). There is no significant response. Error bars represent SEM.

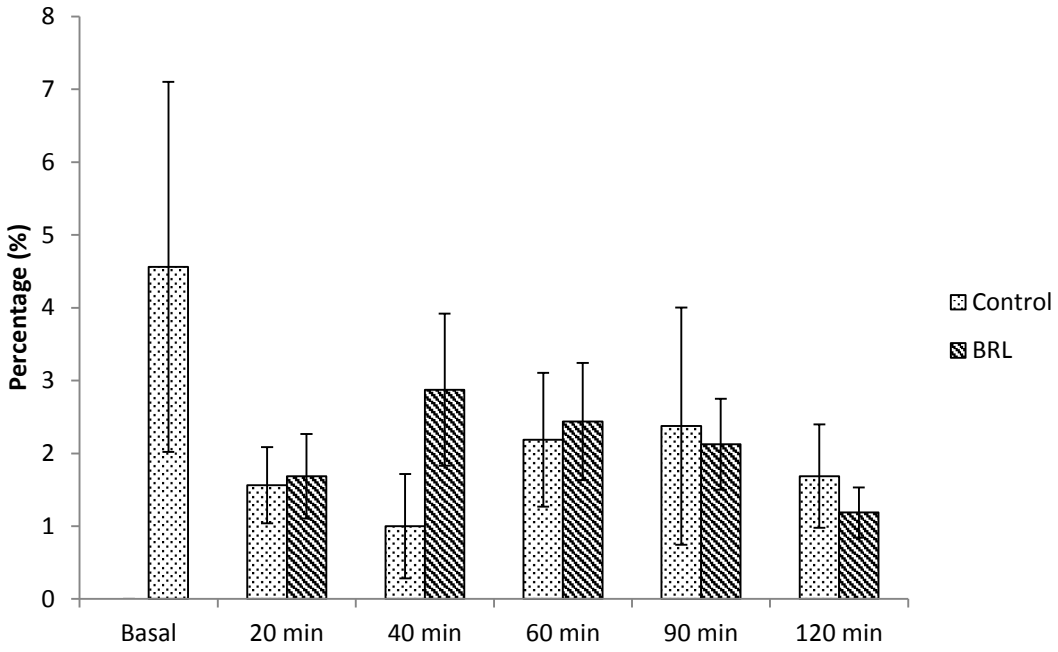

Figure 7.17: Effect of 10µM BRL 50481 on 80% fraction spermatozoa under capacitating conditions on hyperactivation (n=4). There is no significant response. Error bars represent SEM.

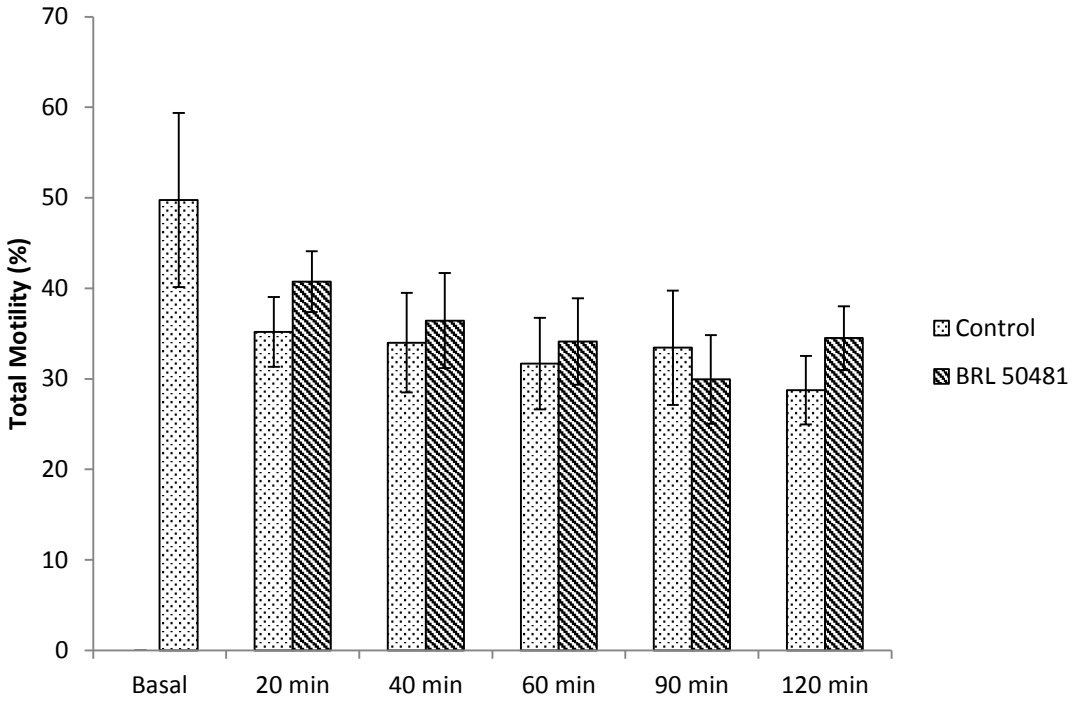

Figure 7.18: Effect of 40µM BRL 50481 on 40% fraction spermatozoa under capacitating conditions on total motility (n=4). There is no significant response. Error bars represent SEM.

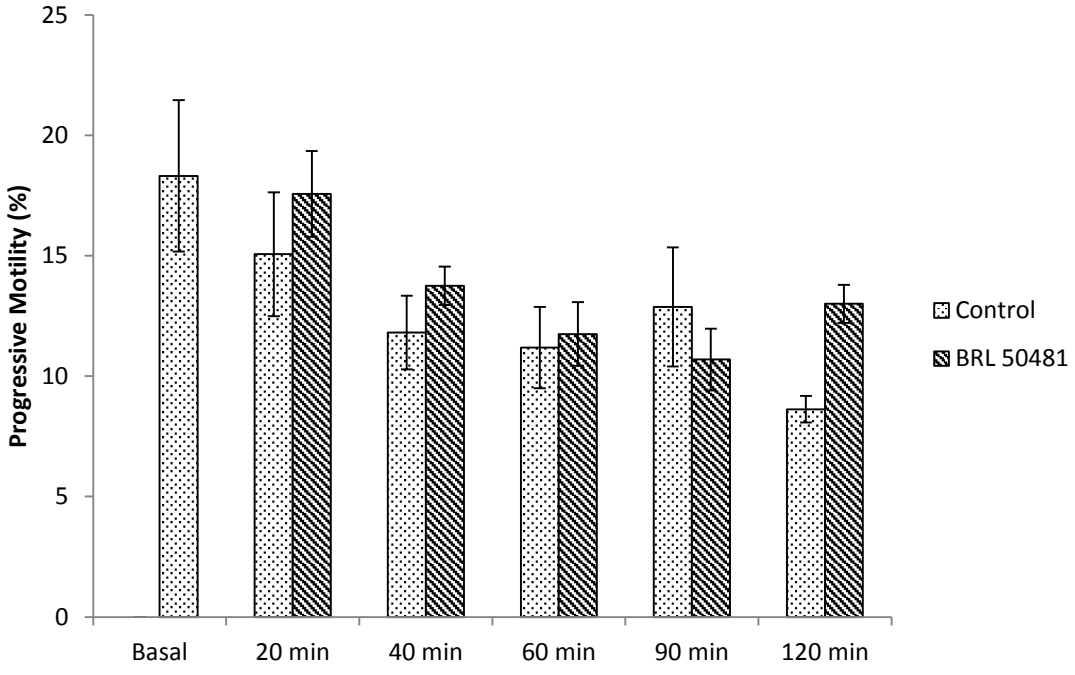

Figure 7.19: Effect of 40µM BRL 50481 on 40% fraction spermatozoa under capacitating conditions on progressive motility (n=4). There is no significant response. Error bars represent SEM.

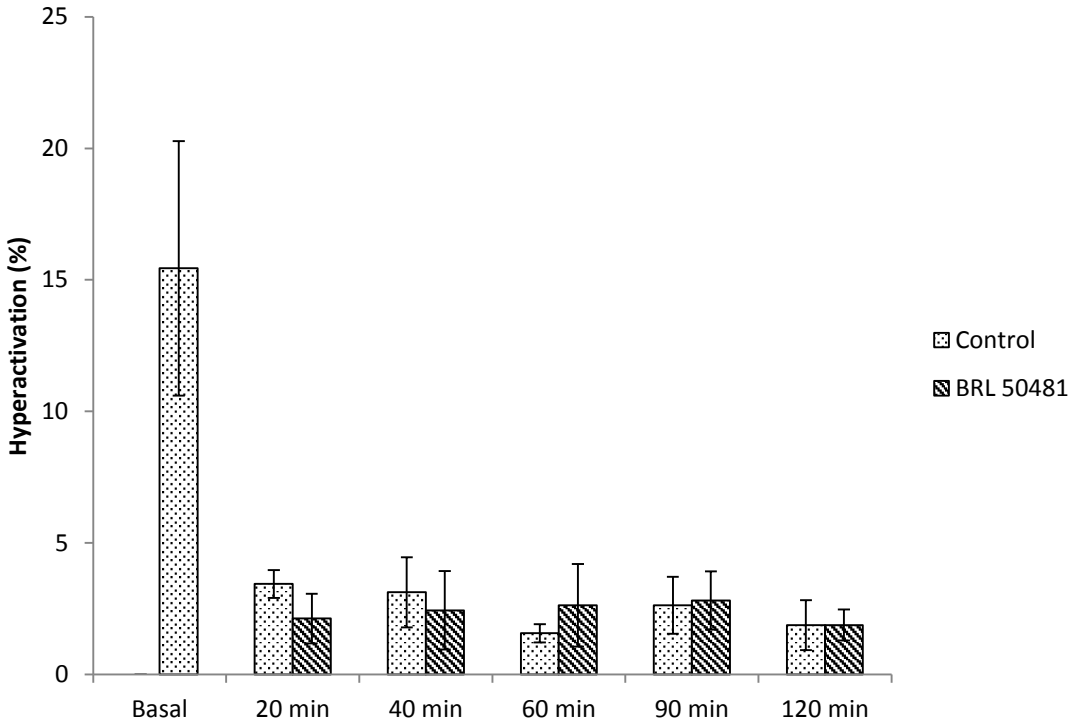

Figure 7.20: Effect of 40µM BRL 50481 on 40% fraction spermatozoa under capacitating conditions on hyperactivation (n=4). There is no significant response. Error bars represent SEM.

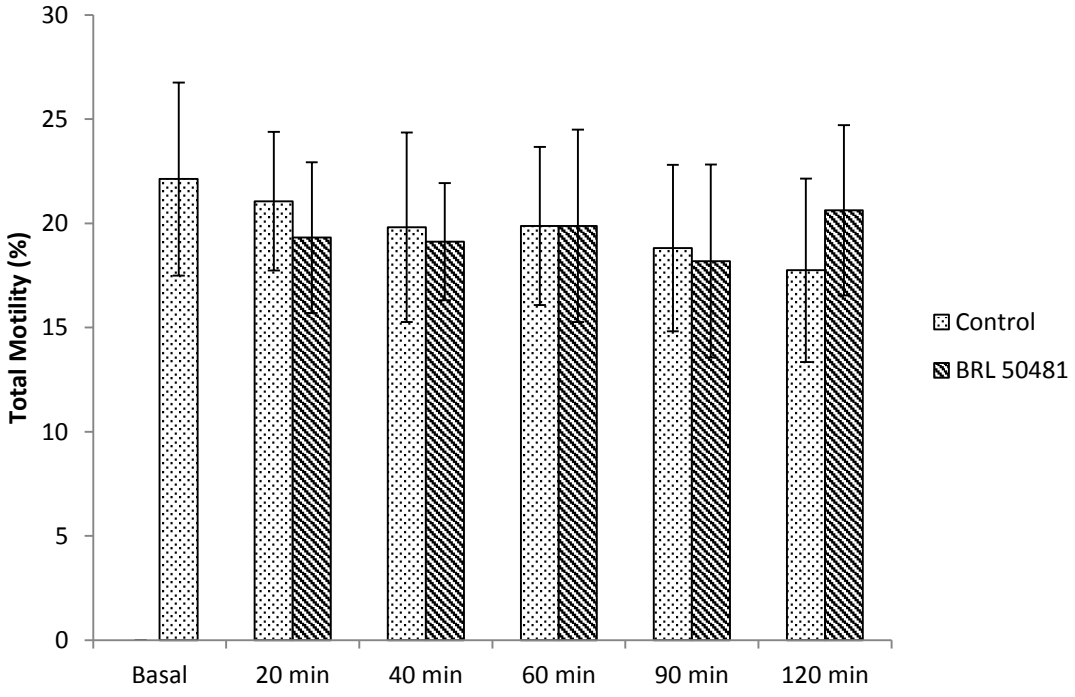

Figure 7.21: Effect of 40µM BRL 50481 on 40% fraction spermatozoa under non-capacitating conditions on total motility (n=4). There is no significant response. Error bars represent SEM.

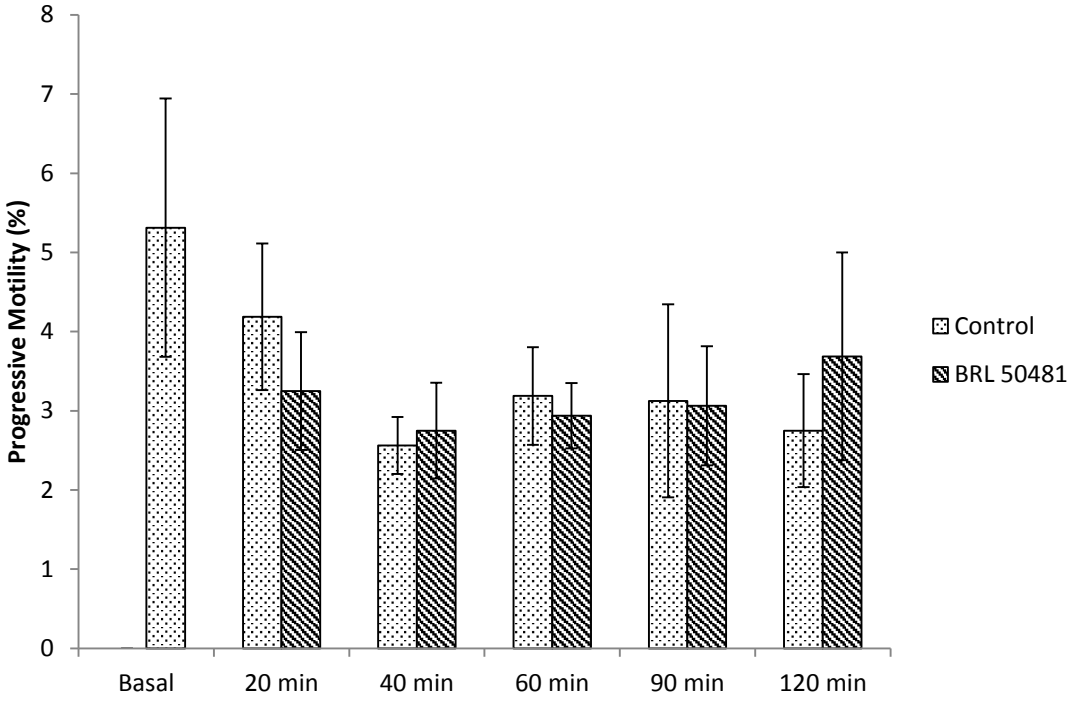

Figure 7.22: Effect of 40µM BRL 50481 on 40% fraction spermatozoa under non-capacitating conditions on progressive motility (n=4). There is no significant response. Error bars represent SEM.

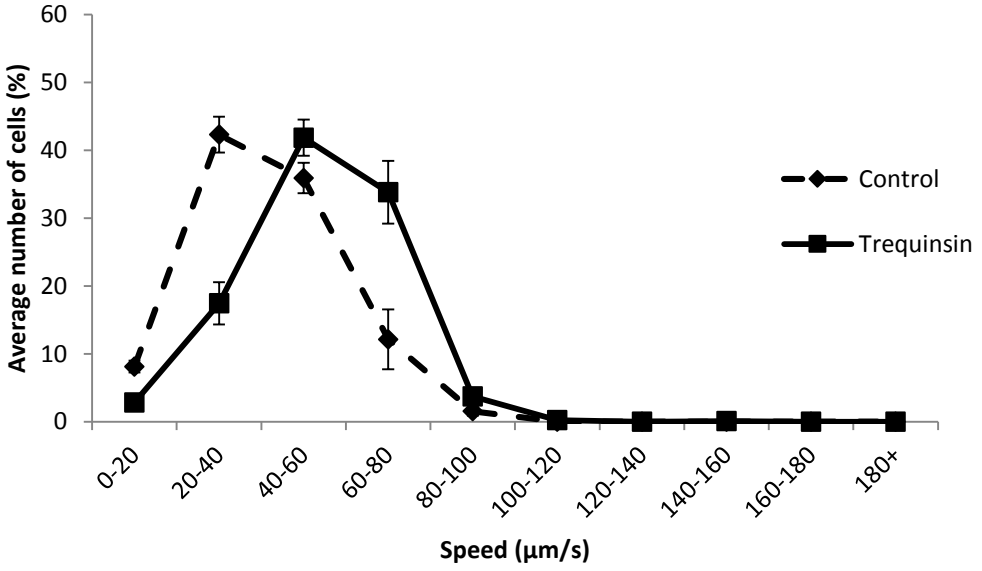

Figure 7.23: Effect of 10µM Trequinsin on 40% fraction spermatozoa under non-capacitating conditions on VAP after 20min treatment (n=4). Error bars represent SEM.

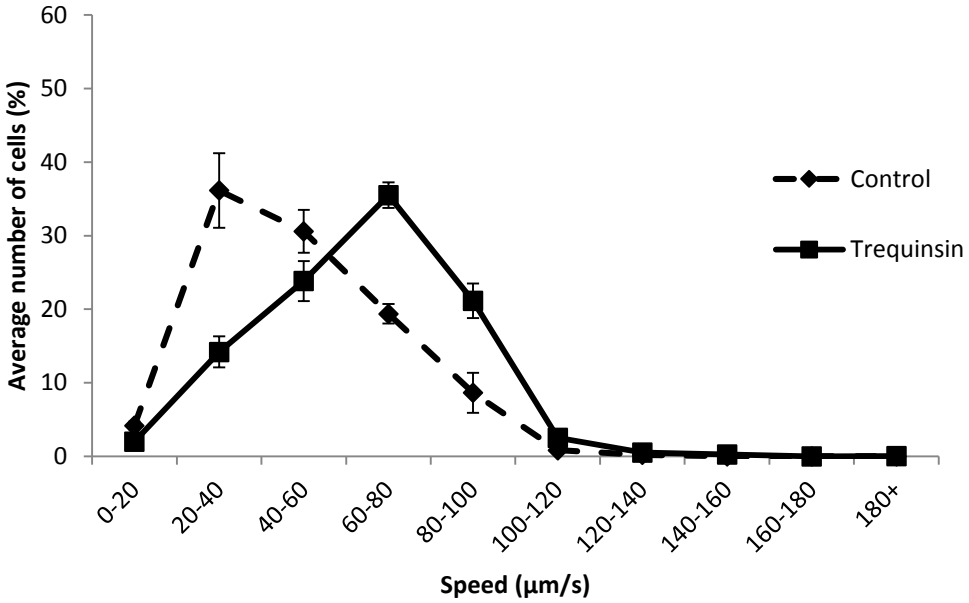

Figure 7.24: Effect of 10µM Trequinsin on 40% fraction spermatozoa under capacitating conditions on VAP after 20min treatment (n=4). Error bars represent SEM.

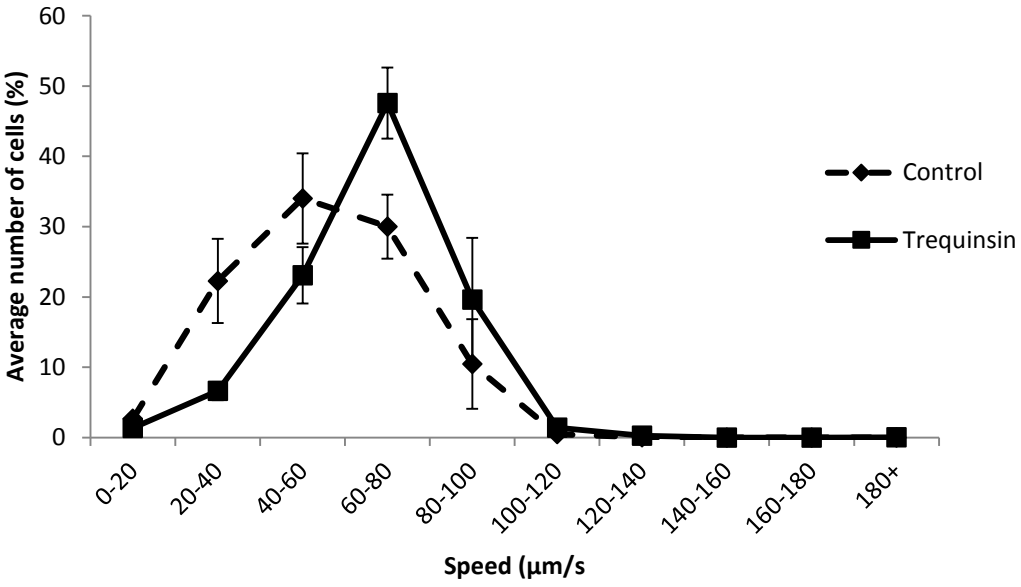

Figure 7.25: Effect of 10µM Trequinsin on 80% fraction spermatozoa under non-capacitating conditions on VAP after 20min treatment (n=4). Error bars represent SEM.

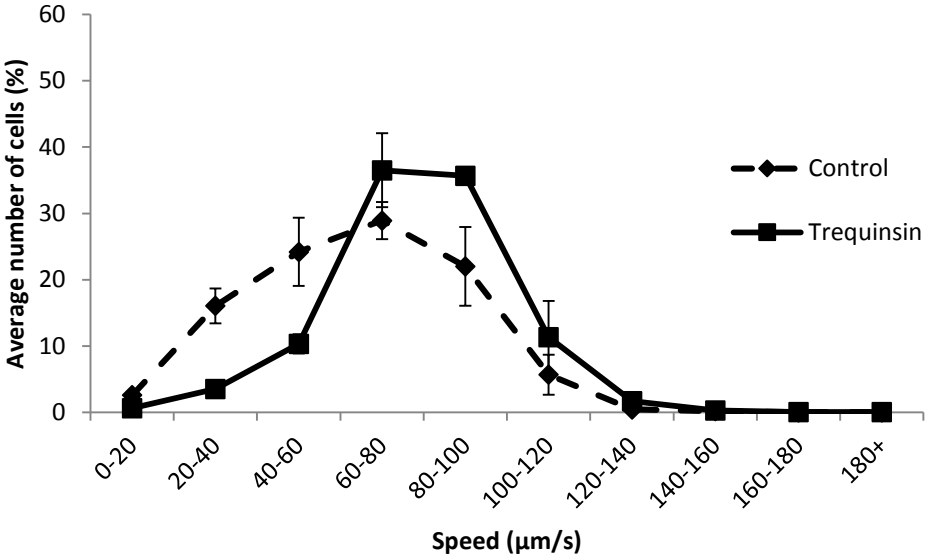

Figure 7.26: Effect of 10µM Trequinsin on 80% fraction spermatozoa under capacitating conditions on VAP after 20min treatment (n=4). Error bars represent SEM.

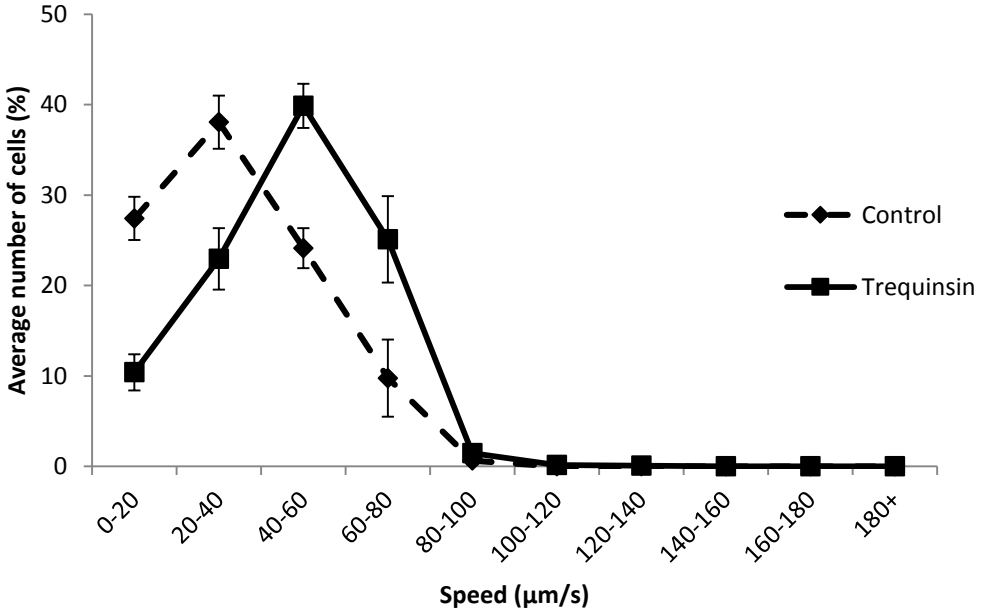

Figure 7.27: Effect of 10µM Trequinsin on 40% fraction spermatozoa under non-capacitating conditions on VSL after 20min treatment (n=4). Error bars represent SEM.

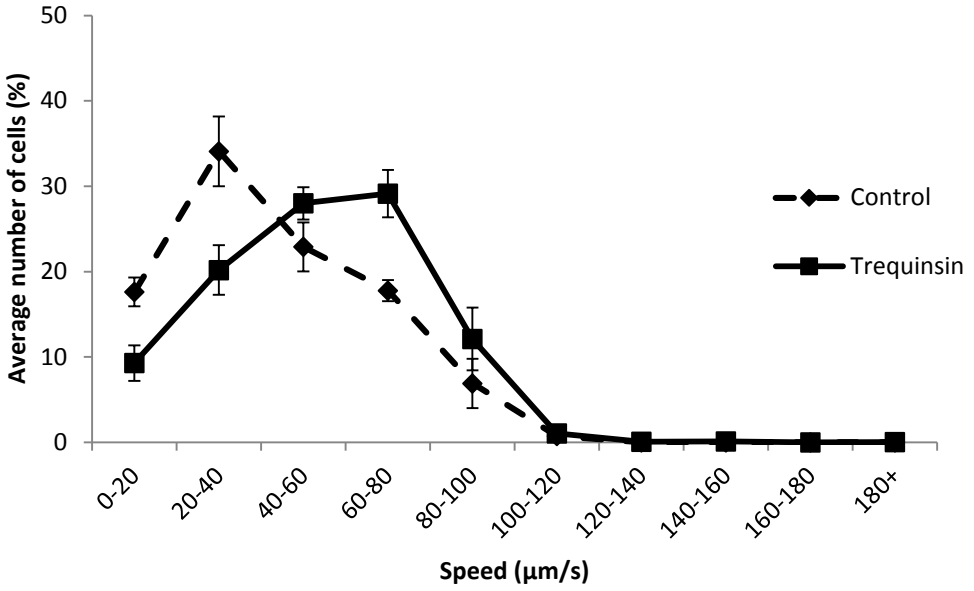

Figure 7.28: Effect of 10µM Trequinsin on 40% fraction spermatozoa under capacitating conditions on VSL after 20min treatment (n=4). Error bars represent SEM.

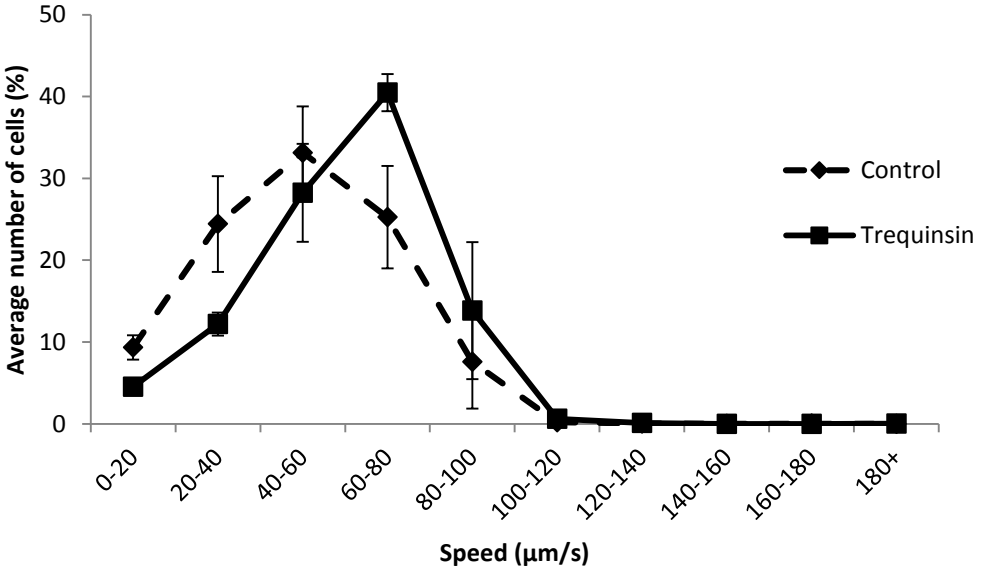

Figure 7.29: Effect of 10µM Trequinsin on 80% fraction spermatozoa under non-capacitating conditions on VSL after 20min treatment (n=4). Error bars represent SEM.

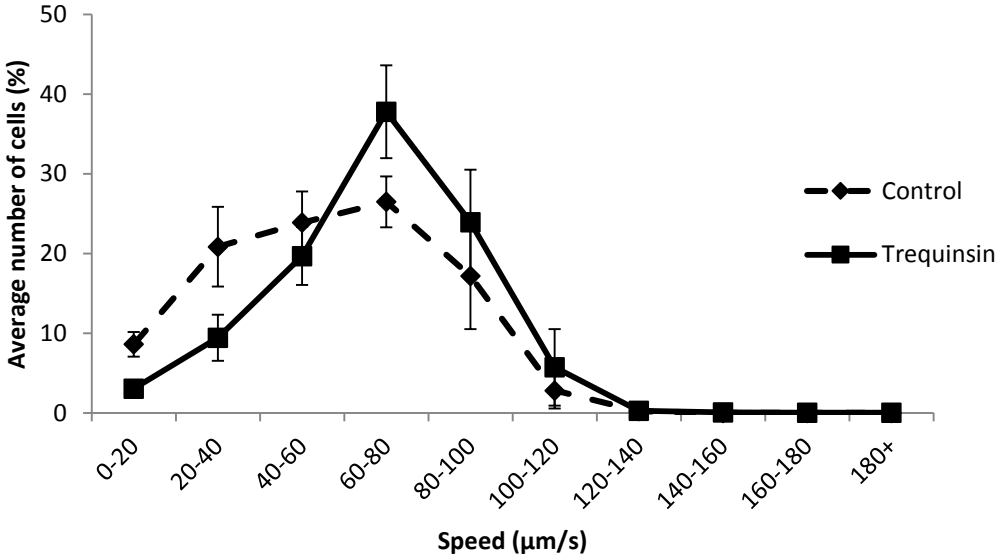

Figure 7.30: Effect of 10µM Trequinsin on 80% fraction spermatozoa under capacitating conditions on VSL after 20min treatment (n=4). Error bars represent SEM.

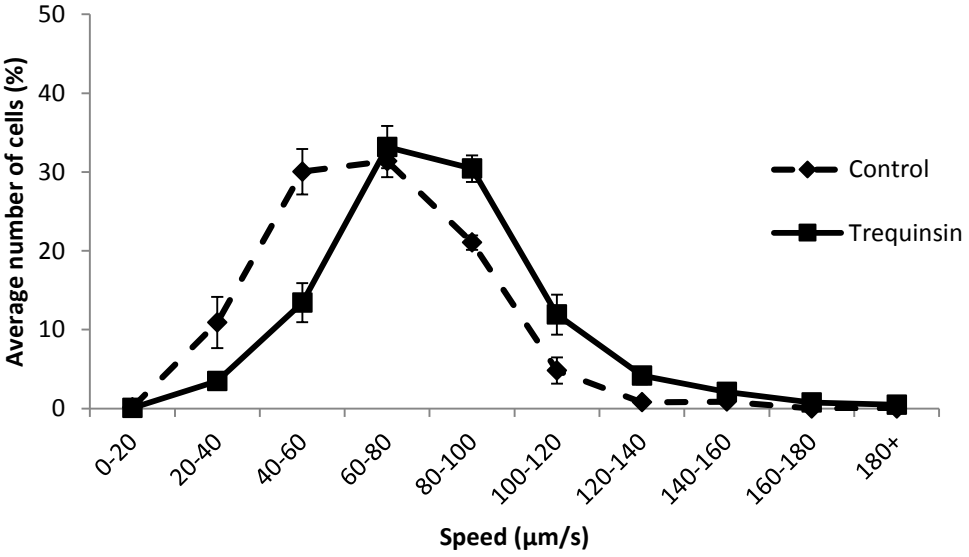

Figure 7.31: Effect of 10µM Trequinsin on 40% fraction spermatozoa under non-capacitating conditions on VCL after 20min treatment (n=4). Error bars represent SEM.

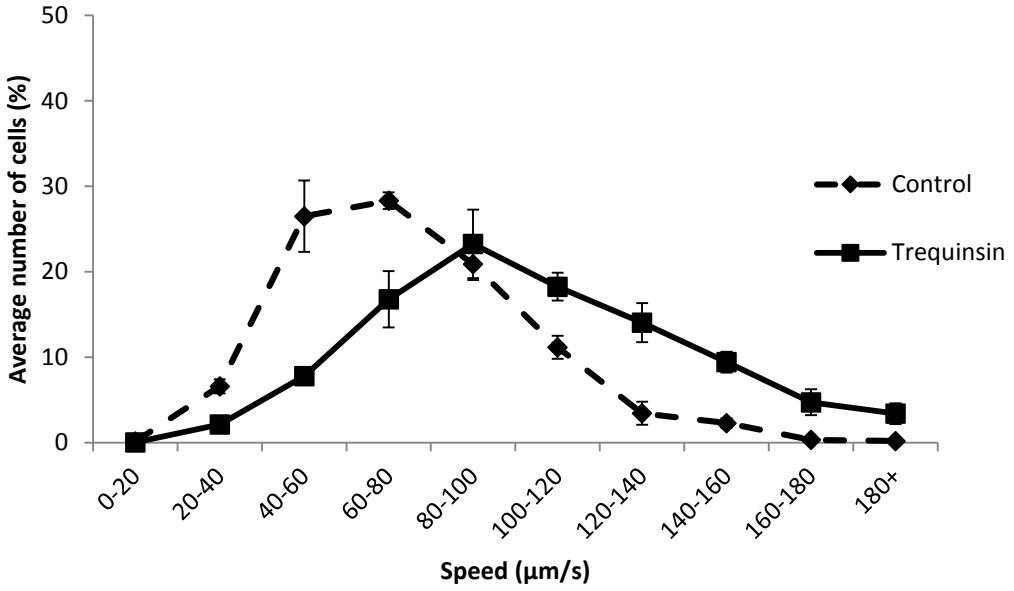

Figure 7.32: Effect of 10µM Trequinsin on 40% fraction spermatozoa under capacitating conditions on VCL after 20min treatment (n=4). Error bars represent SEM.

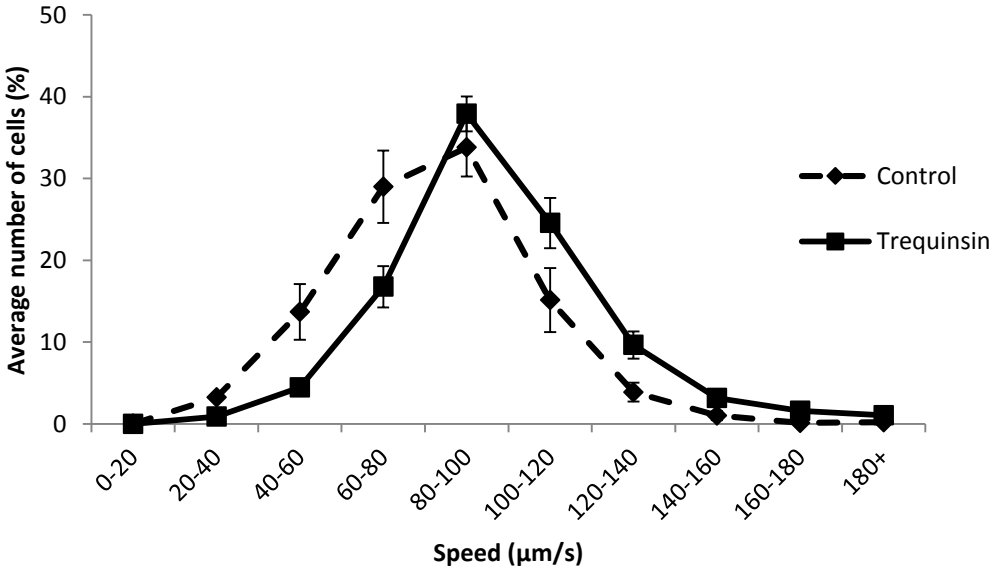

Figure 7.33: Effect of 10µM Trequinsin on 80% fraction spermatozoa under non-capacitating conditions on VCL after 20min treatment (n=4). Error bars represent SEM.

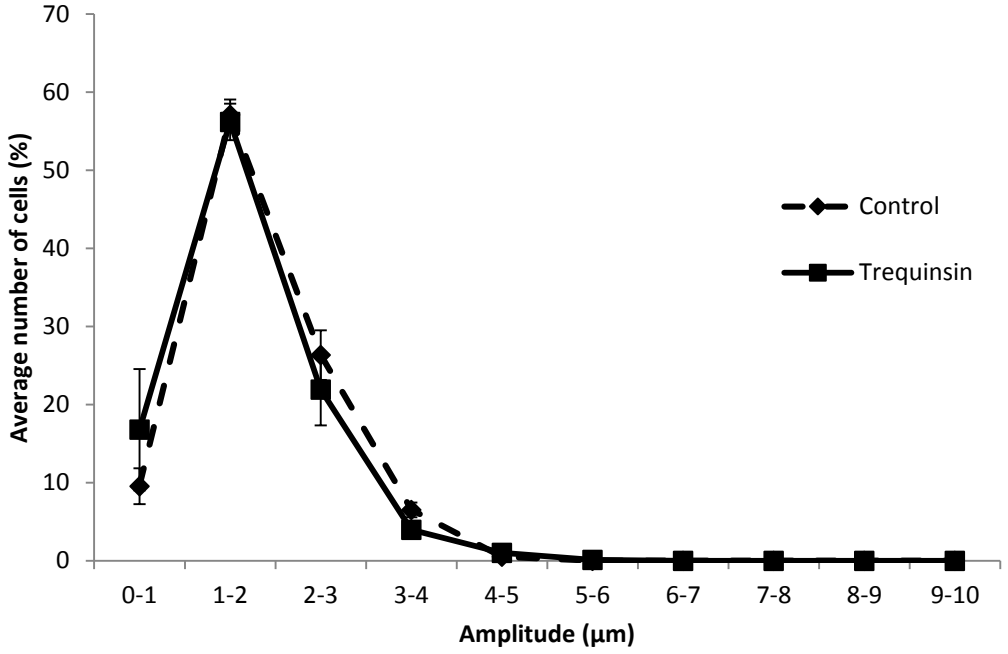

Figure 7.34: Effect of 10µM Trequinsin on 40% fraction spermatozoa under non-capacitating conditions on ALH after 20min treatment (n=4). Error bars represent SEM.

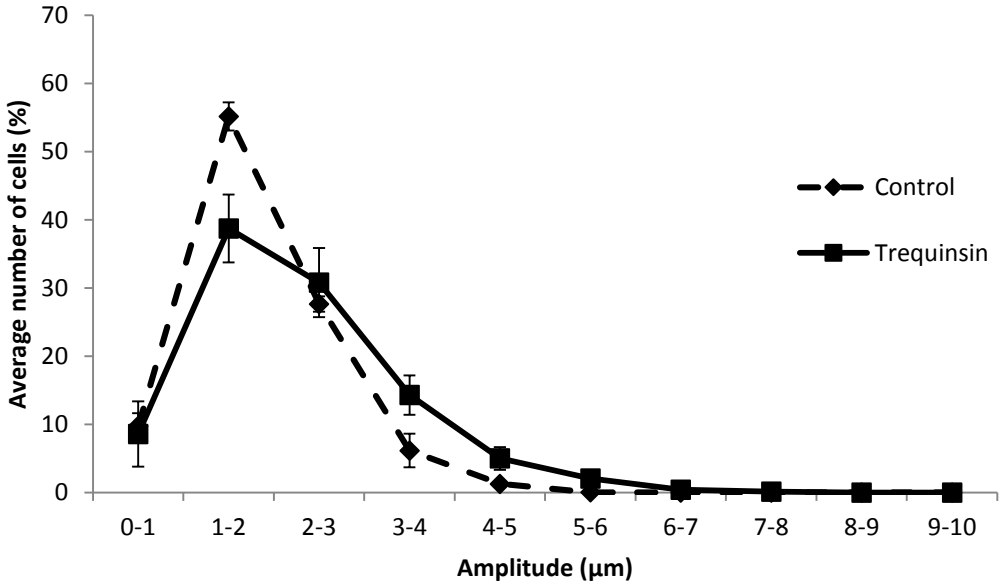

Figure 7.35: Effect of 10µM Trequinsin on 40% fraction spermatozoa under capacitating conditions on ALH after 20min treatment (n=4). Error bars represent SEM.

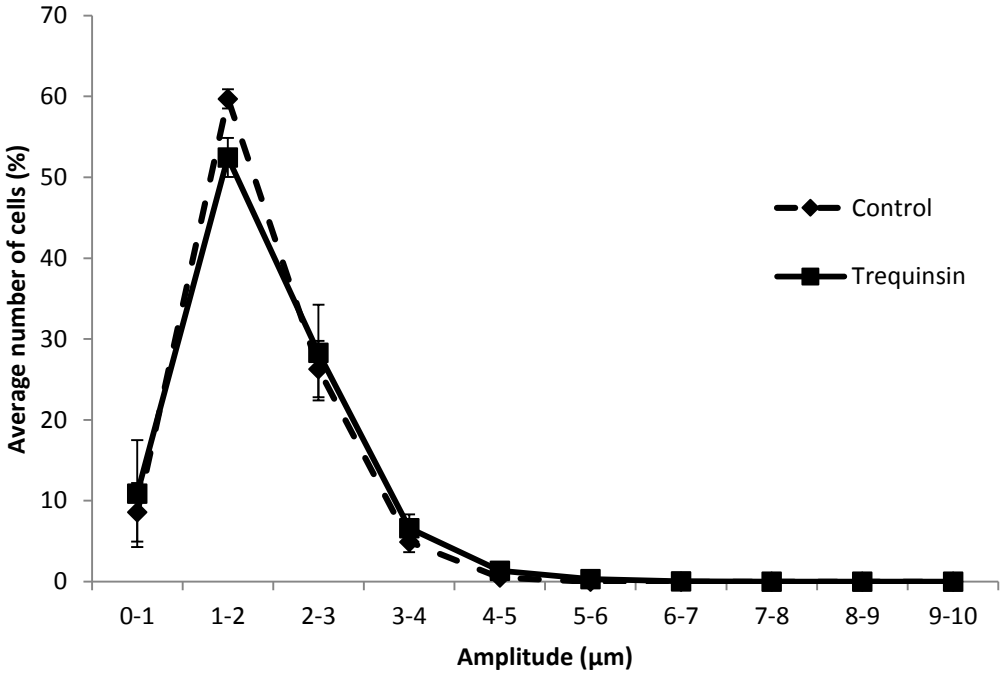

Figure 7.36: Effect of 10µM Trequinsin on 80% fraction spermatozoa under non-capacitating conditions on ALH after 20min treatment (n=4). Error bars represent SEM.

References

Agirregoitia E, Carracedo A, Subiran N, Valdivia A, Agirregoitia N, Peralta L, Velasco G and Irazusta J (2010) The CB2 cannabinoid receptor regulates human sperm cell motility. *Fertil Steril.* **93**: 1378-1387.

Aitken RJ, Harkiss D, Knox W, Paterson M and Irvine S (1998) On the cellular mechanisms by which the bicarbonate ion mediates the extragenomic action of progesterone on human spermatozoa. *Biol. Reprod.* **58:** 186-196.

Aitken RJ, Harkiss D, Knox W, Paterson M and Irvine S (1998)A novel signal transduction cascade in capacitating human spermatozoa characterized by a redox-regulated, cAMP-mediated induction of tyrosine phosphorylation. *J. Cell Sci.* **111:** 645-656.

Aitken RJ and Nixon B (2013) Sperm capacitation: a distant landscape glimpsed but unexplored. *Mol. Hum. Reprod.* **26**:1-9

Alasmari W, Barratt CLR, Publicover SJ, Whalley KM, Foster E, Kay V, da Silva SM, Oxenham SK (2013) The clinical significance of calcium-signalling pathways mediating human sperm hyperactivation. *Hum. Reprod.* **28:** 866-876.

Amann RP and Hammerstedt RH (1993) *In vitro* evaluation of sperm quality – an opinion. *J. Androl.* **14:** 397-406.

Arias JM, Murbartian J and Perez-Reyes E (2003) Cloning of a novel one-repeat calcium channel-like gene. *Biochem. Biophys. Res. Commun.* **303**: 31-36.

Armon L and Eisenbach M (2011) Behavioural mechanism during human sperm chemotaxis: involvement of hyperactivation. *PLoS* **6:** 1-9.

Auger J, Kunstmann JM, Czygik F and Jouannet P (1995) Decline in semen quality among fertile men in Paris during the past 20 years. *New Eng. J. Med.* **332:** 281-285.

Austin CR (1951) Observations on the penetration of the sperm in mammalian egg. *Aust. J. Sci. Res*. **(B)4:** 581-596

Avenarius MR, Hildebrand MS, Zhang Y, Meyer NC, Smith LL, Kahrizi K, Najmabadi H and Smith RJ (2009) Human male infertility caused by mutations in the CATSPER1 channel protein. *Am. J. Hum. Genet* **84:** 505-510.

Avidan N, Tamary H, Dgany O, Cattan D, Pariente A, Thulliez M, Borot N, Moati L, Barthelme A, Shalmon L, Krasnov T, Ben-Asher E, Olender T, Khen M, Yaniv I, Zaizov R, Shalev H, Delaunay J, Fellous M, Lancet D and Beckmann JS (2003) CATSPER2, a human autosomal nonsyndromic male infertility gene. *Eur. Gen. Hum. Genet.* **11:** 497-502.

Aparicio NJ, Schwarzstein L and De Turner EA (1980) Pentoxifylline by oral administration in the treatment of asthenozoospermia. *Andrologia* **12:** 228-231.

Aquila S, Guido C, Santoro A, Gazzerro P, Laezza C, Baffa MF, Ando S and Bifulco M (2010) Rimonabant (SR141716) induces metabolism and acquisition of fertilizing ability in human sperm. *Br. J. Pharmacol.* **159:** 831-841.

Baillie HS, Pacey AA, Warren MA, Scudamore IW and Barratt CL (1997) Greater numbers of spermatozoa associate with endosalpingeal cells derived from the isthmus compared with those from the ampulla. *Hum. Reprod.* **12:** 1985-1992.

Baker MA, Hetherington L and Aitken RJ (2006) Identification of SRC as a key PKA-stimulated tyrosine kinase involved in the capacitation-associated hyperactivation of murine spermatozoa. *J. Cell. Sci.* **119:** 3182-3192.

Barratt CL, Kay V and Oxenham SK (2009) The human spermatozoon – a stripped down but refined machine. *J. Biol.* **8:** 63.2-63.4.

Barratt CL, McLeod ID, Dunpy BC and Cooke ID (1992) Prognostic value of two putative sperm function tests: hypo-osmotic swelling and bovine sperm mucus penetration test (Penetrak). *Hum. Reprod.* **7:** 1240-1244.

Barratt CLR., Mansell S., Beaton C., Tardiff S., Oxenham S. (2011) Diagnostic tools in male infertility- The question of sperm dysfunction. *Asian Journal of Andrology* **13:** 53-58.

Battistone MA, Da Ros VG, Salicioni AM, Navarrete FA, Krapf D, Visconti PE and Cuasnicu PS (2013) Functional human sperm capacitation requires both bicarbonate-dependent PKA activity and down-regulation of Ser/Thr phosphatases by Src family kinases. *Mol. Hum. Reprod.* **19:** 570-580.

Beavo J (1995) Cyclic nucleotide phosphodiesterases: functional implications of multiple isoforms. *Am. J. Physiol.* **75:** 725-748.

Bedu-Addo K, Barratt CL, Kirkman-Brown JC, and Publicover SJ (2007) Patterns of [Ca2+](i) mobilization and cell response in human spermatozoa exposed to progesterone. *Dev. Biol.* **302:** 324-332.

Bedu-Addo K, Costello S, Harper C, Machado-Oliveira G, Lefievre L, Ford C, Barratt C and Publicover S (2008) Mobilization of stored calcium in the neck region of human sperm – a mechanism for regulation of flagellar activity. *Int. J. Dev. Biol.* **52:** 615-626.

Boatman DE and Robbins RS (1991) Bicarbonate: carbon-dioxide regulation of sperm capacitation, hyperactivated motility, and acrosome reactions. *Biol. Reprod*. **44:** 806-813.

Bozkurt HH and Wooley DM (1993) Morphology of nexin links in relation to interdoublet sliding in the sperm flagellum. *Cell Motil. Cytoskeleton* **24:** 109-118.

Brenzik PB., Kovacic B., Vlaisavlievic V. (2013). Are sperm DNA fragmentation, hyperactivation, and hyaluronan-binding ability predictive for fertilization and embryo development in in vitro fertilization and intracytoplasmic sperm injection? *Fertil. Steril.* **99:** 1233-1241

Buck J, Sinclair M and Levin LR (2001) Purification of soluble adenylyl cyclase. In: Hildebrant, ed. Methods in Enzymology. San Diego, CA, USA: Academic Press.

Burkman LJ (1991) Discrimination nonhyperactivated and classical hyperactivated motility in human spermatozoa using computerized analysis. *Fertil. Steril.* **55:** 363-371.

Burkman L and Samrock R (1992). Sperm hyperactivation (HA) assay: values are repeatable within individual men (abstract). *Fertil Steril (Program Suppl.)* **186**

Bjorndahl L, Mortimer D, Barratt C, Castilla J, Menkveld R, Kvist U, Alvertz J and Haugen T (2010) A Practical Guide to Basic Laboratory Andrology. Cambridge University Press.

Brenker C, Goodwin N, Weyand I, Kashikar ND, Naruse M, Krahling M, Muller A, Kaupp UB and Strunker T (2012) The CatSper channel: a polymodal chemosensor in human sperm. *EMBO* **31:** 1654-1665.

Brenzik PB, Kovacic B and Vlaisavlievic V (2013) Are sperm DNA fragmentation, hyperactivation, and hyaluronan-binding ability predictive for fertilization and embryo development in in vitro fertilization and intracytoplasmic sperm injection? *Fertil. Steril.* **99:** 1233-1241.

Brewer L., Corzett M. and Balhorn R (2002) Condensation of DNA by spermatid basic nuclear proteins. *J. Biol. Chem.* **277:** 38895-38900.

Brokaw CJ (2009) Thinking about flagellar oscillation. *Cell Motil. Cytoskeleton* **66:** 425-436.

Brokaw CJ and Kamiya R (1987) Bending patterns of Chlamydomonas flagella: IV. Mutantas with defects in inner and outer dynein arms indicate differences in dynein arm and function. *Cell Motil. Cytoskeleton* **8:** 68-75.

Brokaw CJ, Josslin R and Bobrow L (1974) Calcium ion regulation of flagellar beat symmetry in reactivated sea urchin spermatozoa. *Bichem. Biophys. Res. Commun.* **58:** 795-800.

Cadbury D (1997) The feminization of nature: our future at risk. London: Hamish Hamilton Ltd.

Calogero AE, Fishel S, Hall J, Ferrara E, Vicari E, Green S, Hunter A, Burello N, Thornton S and D'Agata R (1998) Correlation between intracellular cAMP content, kinematic parameters and hyperactivation of human spermatozoa after incubation with pentoxifylline. *Hum Reprod* **13:** 911-915.

Carlsen E, Giwercman A, Keiding N and Skakkebaek NE (1992) Evidence for decreasing quality of semen during past 50 years. *Brit. Med. J.* **305**: 609-613.

Carlson AE, Westenbroek RE, Quill T, Ren D, Clapham DE, Hille B, Garbers DL and Babcock DF (2003) CatSper1 required for evoked Ca2+ entry and control of flagellar function in sperm. *Proc. Natl. Acad. Sci.* **100:** 14864-14868.

Carlson AE, Hille B and Babcock DF (2007) External Ca^{2+} acts upstream of adenylyl cyclase SACY in the bicarbonate signaled activation of sperm motility. *Dev. Biol.* **312:** 183-192.

Carr DW, Usselman MC and Acott Ts (1985) Effects of pH, lactate, and viscoelastic drag on sperm motility: a species comparison. *Biol. Reprod.* **33:** 588-595.

Carrera A, Moos J, Ning XP, Gerton GL, Tesarik J, Kopf GS and Moss SB (1996) Regulation of protein tyrosine phosphorylation in human sperm by a calcium/calmodulin-dependent mechanism: identification of A kinase anchor proteins as major substrates for tyrosine phosphorylation. *Dev. Biol.* **180:** 284-296.

Cates W, Farley TM and Rowe PJ (1985) Worldwide patterns of infertility: is Africa different? *Lancet* **2:** 596-598.

CDC, Centres for Disease Control and Prevention. Reproductive Health. Assissted Reproductive Technology. National Summary and Fertility Clinic Reports 2009. November 2011 at http://www.cdc.gov/ART/ART2009.

Chang MC (1951) Fertilizing capacity of spermatozoa deposited into the fallopian tubes. *Nature* **168:** 697-698.

Chang MC and Suarez SS (2011) Two distinct Ca^{2+} signaling pathways modulate flagellar beating patterns in mice. *Biol. Reprod.* **85**: 296-305.

Chen Y, Cann MJ, Litvin TN, Iourgenko V, Sinclair ML, Levin LR and Buck J (2000) Soluble adenylyl cyclase as an evolutionarily conserved bicarbonate sensor [and comments]. *Science* **289:** 625-628.

Chen X, Zhang W, Luo Y, Long X and Sun X (2009) Predictive value of semen parameters in in vitro fertilization pregnancy outcome. *Andrologia* **41:** 111-117.

Chung JJ, NNavarro B, Krapivinsky G, Krapivinsky L and Clapham DE (2011) A novel gene required for male fertility and functional CATSPER channel formation in spermatozoa. *Nature Commun*. **2:** 153.

Colas C, Cebrian-Perez JA and Muino-Blanco T (2010) Caffeine induces ram sperm hyperactivation independent of cAMP-dependent protein kinase. *Int. J. Androl.* **33:** e187-e197.

Conti M, Nemoz G, Sette C and Vicini E (1995) Recent progress in understanding the hormonal regulation of phosphodiesterases. *Endocrin. Rev.* **16:** 370-389.

Cooper TG, Noonan E, Von Eckardstein S, Auger J, Baker HW, Behre HM, Haugen TB, Kruger T, Wang C, Mbizvo MT and Vogelsong KM (2010) World Health Organization reference values for human semen characteristics. *Hum. Reprod. Update* **16:** 231-45.

Collins JA, Wrixon W, Janes LB and Wilson EH (1983) Treatment-independent pregnancy among infertile couples. *N. Engl. J. Med.* **309:** 1201-1206.

Costello S., Michelangeli F., Nash K., Lefievre L., Morris J., Machado-Oliveria G., Barratt C., Kirkman-Brown J., Publicover S. (2009). Calcium stores in sperm: their identities and functions. *Reproduction* **138:** 425-437

Cox GF, Burger J, Lip V, Mau UA, Sperling K, Wu BL and Horsthemke B (2002) Intracytoplasmic sperm injection may increase the risk of imprinting defects. *Am. J. Hum. Genet*. **71:**162-164.

Croxatto HB (1995) Gamete transport. In *Reproductive Endocrinology, Surgery and Technology*, ed. Adashi J and Rosewaks Z, 395-398. New York: Raven.

Da Silva SJM, Hope AG, Gray DW and Barratt CLR (2012) Validation of a novel High Throughput Screening assay to assess calcium responses in human sperm. *ASRM abstract.*

Dadoune JP (2003) Expression of mammalian spermatozoal nucleoproteins. *Micros. Res. Tech.* **61:** 56-75.

Dam AHDM, Freenstra I, Westphal JR, Ramos L, van Golde RJT and Kremer JAM (2007) Globozoospermia revisited. *Hum. Reprod. Update* **13:** 63-75.

Daris B, Goropevsek A, Hojnik N and Vlaisavljevic V (2010) Sperm morphological abnormalities as indicator of DNA fragmentation in ICSI. *Arch. Gynecol. Obstet.* **281:** 363-367.

Davies MJ, Moore VM, Willson KJ, Essen VP, Priest K, Scott H, Haan EA, and Chan A (2012) Reproductive technologies and the risk of birth defects. *N Engl J Med* **366:** 1803-1813.

Darzson A, Nishigaki T, Beltran C and Trevino CL (2011) Calcium channels in the development, maturation, and function of spermatozoa. *Physiol. Rev.* **91:** 1305-1355.

De Jonge C (2005) Biological basis for human capacitation. *Human Reproduction Update* **11:** 205-214.

De Jonge C and Barratt C (2006) The Sperm Cell, Cambridge University Press.

Demarco IA, Espinosa F, Edwards J, Sosnik J, De La Vega-Beltran JL, Hockensmith JW, Kopf GS, Darszon A and Visconti PE (2003) Involvement of a Na^+/HCO_3 cotransporter in mouse sperm capacitation. *J. Biol. Chem.* **278:** 7001-7009.

Demott RP and Suarez SS (1992) Hyperactivated sperm progress in the mouse oviduct. *Biol. Reprod.* **46:** 779-785.

Devi KU, Jha K and Shivaji S (1999) Plasma membrane-associated protein tyrosine phosphatase activity in hamster spermatozoa. *Mol. Reprod. Dev.* **53:** 42-50.

Di Bella LM and King SM (2001) Dynein motors of the Chlamydomonas flagellum. *Int. Rev. Cytol*. **210:** 227-268.

Dorval V, Dufour M and Leclerc P (2002) Regulation of phosphotyrosine content of human sperm proteins by intracellular Ca^{2+}: Role of Ca^{2+}-adenosine triphosphatases. *Biol. Reprod.* **67:** 1538-1545.

Drobnis EZ, Yudin AI, Cherr GN and Katz DF (1988) Kinematics of hamster sperm during penetration of the cumulus matrix. *Gamete Res.* **21:** 367-383.

Ecroyd H, Asquith KL, Jones RC and Aitken RJ (2004) The development of signal transduction pathways during epididymal maturation is calcium dependent. *Dev. Biol.* **268:** 53-63.

Eddy EM, Toshimori K and O'Brien DA (2003) Fibrous sheath of mammalian spermatozoa. *Microsc. Res. Tech.* **61:** 103-115.

Eisenbach M (1999) Sperm chemotaxis. *Rev. Reprod.* **4:** 55-66.

Eisenbach M and Giojalas LC (2006) Sperm guidance in mammals – an unpaved road to the egg. *Nature Rev.* **7:** 276-286.

Esposito G, Jaiswal BS and Xie F (2004) Mice deficient for soluble adenylyl cyclase are infertile because of a severe sperm-motility defect. *Proc. Narl. Acd. Sci.* **101:** 2993-2998.

Fauci LJ and Dillon R (2006) Biofluidmechanics of Reproduction. *Annu. Rev. Fluid Mech.* **38:** 371-394.

Fazeli A, Nabeel AA, Hubank M and Holt WV (2004) Sperm-induced modification of the oviduct gene expression profile after natural insemination in mice. *Biol. Reprod.* **71:** 60-65.

Ferraretti AP, Goossens V, Kupka M, Bhattacharya S, de Mouzon J, Castilla JA, Erb K, Korsak V and Nyboe Andersen A (2013) Assissted reproductive technology in Europe, 2009: results generated from European registers by ESHRE. *Hum. Reprod.* **28:** 2318-2331.

Ferraretti AP, Goossens V, Kupka M, Bhattacharya S, de Mouzon J, Castilla JA, Erb K, Korsak V and Nyboe Andersen A (2012) Assissted reproductive technology in Europe, 2008: results generated from European registers by ESHRE. *Hum. Reprod.* **27**: 2571-2585.

Fisch JD, Behr B and Conti M (1998) Enhancement of motility and acrosome reaction in human spermatozoa: differential activation by type-specific phosphodiesterase inhibitors. *Hum. Reprod.* **13:** 1248-1254.

Flesch FM, Brouwers JF, Nievelstein PF, Verkleij AJ, Van Golde LM, Colenbrander B and Gadella BM (2001) Bicarbonate stimulated phospholipid scrambling induces cholesterol redistribution in the sperm plasma membrane. *J. Cell. Sci.* **114:** 3543-3555.

Florman HM, Arnoult C, Kazam IG, Li C and O'Toole CM (1998) A perspective on the control of mammalian fertilization by egg-activated ion channels in sperm: a tale of two channels. *Biol. Reprod.* **59:** 12-16.

Foo JYA and Lim CS (2008) Biofluid mechanics of the human reproductive process: modeling of the complex interaction and pathway to the oocytes. *Zygote* **16:** 343-354

Ford WC, North K, Taylor H, Farrow A, Hull MG and Golding J (2000) Increasing paternal age is associated with delayed conception in a large population of fertile couples: evidence for declining fecundity in older men. The ALSPAC Study Team (Avon Longitudinal Study of Pregnancy and Childhood). *Hum. Reprod.* **15:** 1703-8.

Gadella BM and Harrison RA (2000) The capacitating agent bicarbonate induces protein kinase A-dependent changes in phospholipid transbilayer behavior in the sperm plasma membrane. *Development* **127:** 2407-2420.

Gadella BM, Miller NG, Colenbrander BB, Van Golde LM and Harrison RA (1999) Flow cytometric detection of transbilayer movement of fluorescent phospholipid analogues across the boar sperm plasma membrane: elimination of labeling artifacts. *Mol. Reprod. Dev.* **53:** 108-125.

Gagnon C, White D, Cosson J, Huitorel P, Edde B, Desbruyeres E, Paturle-Lafanechere L, Multinger L, Job D and Cibert C (1996) The polyglutamylated lateral chain of alpha-tubulin plays a key role in flagellar motility. *J. Cell. Sci.* **109:** 1545-1553.

Gakamsky A, Armon L and Eisenbach M (2009) Behavioural response of human spermatozoa to a concentration jump of chemoattractants or intracellular cyclic nucleotides. *Hum. Reprod.* **24:** 1152-1163.

Galantino-Homer HL, Visconti PE and Kopf GS (1997) Regulation of protein tyrosine phosphorylation during bovine sperm capacitation by a cyclic adenosine 3’5’-monophosphate-dependent pathway. *Biol. Reprod.* **56:** 707-719.

Gandella BM and Harrison RA (2002) Capacitation induces cyclic adenosine 3’,5’-monophosphate-dependent, but apoptosis-unrelated, exposure of aminophospholipids at the apical head plasma membrane of boar sperm cells. *Biol. Reprod.* **67:** 340-350.

Garbers DL, Tubb DJ and Hyne RV (1982) A requirement of bicarbonate for Ca2+ - induced elevations of cyclic AMP in guinea pig spermatozoa. *J. Biol. Chem.* **257:** 8980-8984.

Garty NB and Salomon Y (1987) Stimulation of partially purified adenylate cyclase from bull sperm by bicarbonate. *FEBS Lett.* **218:** 148-152.

Glenn DRJ, McVicar CM, McClure N and Lewis SE (2007) Sildenafil citrate improves sperm motility but causes a premature acrosome reaction in vitro. *Fertil. Steril.* **87:** 1064-1070.

Gnaratne HJ and Vacquier VD (2006) Evidence for a secretory pathway Ca^{2+}-ATPase in sea urchin spermatozoa. *FEBS Lett*. **580:** 3900-3904.

Gobet I, Lippai M, Tomkowiak M, Durocher Y, Leclerc Y, Moreau M and Guerrier P (1995) 4-aminopyridine acts as a weak base and a calcium mobilizing agent in triggering oocytes meiosis reinitiation and activation in the Japanese clam Ruditapes philippinarum. *Int. J. Dev. Biol.* **39:** 485-491.

Gross MK, Toscano DG and Toscano Jr WA (1987) Calmodlin-mediated adenylate cyclase from mammalian sperm. *J. Biol. Chem*. **262:** 8672-8676.

Grunert JH, De Geyter C and Nieschlag E (1990) Objective identification of hyperactivated human spermatozoa by computerized sperm motion analysis with the Hamilton-Thorn sperm motility analyzer. *Hum. Reprod.* **5:** 593-599.

Gu Y, Kirkman-Brown JC, Korchev Y, Barratt CLR and Publicover SJ (2004). Multi-state, 4-aminopyridine-sensitive ion channels in human spermatozoa. *Dev. Biol.* **274:** 308-317.

Harper C, Wootton L, Michalengeli F, Lefievre L, Barratt C and Publicover S (2005) Secretory pathway Ca^{2+}-ATPase (SPCA1) and Ca^{2+}-pumps, nor SERCAs, regulate complex $[Ca^{2+}]_i$ signals in human spermatozoa. *J. Cell Sci.* **118:** 1673-1685.

Harrison RA (2004) Rapid PKA-catalyzed phosphorylation of boar sperm proteins induced by the capacitating agent bicarbonate. *Mol. Reprod. Dev*. **67:** 337-352.

Harrison RA, Ashworth PJ and Miller NG (1996) Bicarbonate/CO2, and effector of capacitation, induces a rapid and reversible change in the lipid architecture of boar sperm plasma membranes. *Mol. Reprod. Dev*. **45:** 378-391.

Harrison RA and Miller NG (2000) cAMP-dependent protein kinase control of plasma membrane lipid architecture in boar sperm. *Mol. Reprod. Dev*. **55:** 220-228.

Hanoune J and Defer N (2001) Regulation and role of adenylyl cyclase isoforms. *Annu. Rev. Pharmacol. Toxicol*. **41:** 145-174.

Haxton MJ and Black WP (1987) The eatiology of infertility in 1162 investigated couples. *Clin. Exp. Obstet.Gynecol.* **14:** 75-79.

Herrick SB, Schweissinger DL, Kim SQ, Bayan KR, Mann S and Cardullo RA (2005) The acrosomal vesicle of mouse sperm is a calcium store. *J. Cell Physiol.* **202:** 663-671.

Ho HC, Granish KA, Suarez SS (2002). Hyperactivated motility of bull sperm is triggered at axoneme by calcium not cAMP. *Dev Biol* **250:** 208-217

Ho H-C and Suarez SS (2001) An inositol 1,4,5-trisphosphate receptor-gated intracellular Ca^{2+} store is involved in regulating sperm hyperactivated motility. *Biol. Reprod.* **65:** 1606-1615.

Ho HC and Suarez SS (2001) Hyperactivation of mammalian spermatozoa: function and regulation. *Reproduction* **122:** 519-526.

Ho H-C and Suarez SS (2003) Characterization of the intracellular calcium store at the base of the sperm flagellum that regulates hyperactivated motility. *Biol. Reprod.* **68:** 1590-1596.

Ho K, Wolff CA and Suarez SS (2009) CatSper-null mutant spermatozoa are unable to ascend beyond the oviductal reservoir. *Reprod. Fertil. Dev*. **21:** 345-350.

Holt WV (2009) Is semen analysis useful to predict the odds that the sperm will meet the egg? *Reprod. Dom. Anim.* **44**(Suppl. 3): 31-38.

Holt WV and Fazeli A (2010) The oviduct as a complex mediator of mammalian sperm function and selection. *Mol. Reprod. Devol.* **77:** 934-943.

Holt WV and Harrison RAP (2002) Bicarbonate stimulation of boar sperm motility via a protein kinase A-dependent pathway: between-cell and between-ejaculate differences are not due to deficiencies in protein kinase A activation. *J. Androl.* **23:** 557-565.

Huitorel P, White D, Fouquet JP, Kann ML, Cosson J and Gagnon C (2002) Differential distribution of glutamylated tubulin isoforms along the sea urchin sperm. *Mol. Reprod. Dev*. **62:** 139-148.

Hull MG, Glazener CM, Kelly NJ, Conway DI, Foster PA, Hinton RA, Coulson C, Lambert PA, Watt EM and Desai KM (1985) Population study of causes, treatment, and outcome of infertility. *Br. Med. J.(Clin Res Ed)* **291:** 1693-1697.

Huszar G, Ozkavukcu S, Jakab A, Celik-Ozenci C, Sati GL and Cayli S (2003) Hyaluronic acid binding ability of human sperm reflects cellular maturity and fertilizing potential: selection of sperm for intracytoplasmic sperm injection. *Curr. Opin. Obstet. Gynecol.* **18:** 260-267.

Ignotz GG, Suarez SS (2005). Calcium/calmodulin and calmodulin kinase II stimulate hyperactivation in demembranated bovine sperm. *Biol Reprod* **73:** 519-526.

Inaba K (2003) Molecular architecture of the sperm flagella: molecules for motility and signaling. *Zool. Sci.* **20:** 1043-1056.

Inoue N, Satouh Y, Ikawa M, Okabe M and Yanagimachi R (2011) Acrosome-reacted mouse spermatozoa recovered from the perivitelline space can fertilize other eggs. *PNAS.* **108:** 20008-20011.

Irvine DS and Aitken RJ (1986) Measurement of intracellular calcium in human spermatozoa. *Gamete. Res.* **15:** 57-72.

Ishijima S (2013) Regulations of microtubule sliding by Ca^{2+} and cAMP and their roles in forming flagellar waveforms. *Cell Stuct. Funct.* **38:** 89-95.

Jain T and Gupta RS (2007) Trends in the use of ICSI in the USA. *N Engl J Med* **357:** 251-257.

Jakab A, Sakkas D, Delpiano E, Cayli S, Kovanci E, Ward D (2005) Intracytoplasmic sperm injection: a novel selection method for sperm with normal frequency of chromosomal aneuploidies. *Fertil. Steril.* **84:** 1665-1671.

Jaiswal BS and Conti M (2001) Identification and functional analysis of splice variants of the germ cell soluble adenylyl cyclase. *J. Biol. Chem* **276:** 31698-31708.

Jensen BM, Bjerrum PJ, Jessen TE, Nielsen JE, Joensen EN, Olesen IA, Petersen JH, Jull A, Dissing S and Jorgensen N (2011) Vitamin D is positively associated with sperm motility and increases intracellular calcium in human sperm. *Hum. Reprod.* **26:** 1307-1317.

Jensen BM, Nielasen JE, Jorgensen A, Rajpert-de ME, Kristensen DM, Jorgensen N, Skakkebaek NE, Juul A and Leffers H (2010) Vitamin D receptor and vitamin D metabolizing enzymes are expressed in the human male reproductive tract. *Hum. Reprod.* **25**: 1303-1311.

Jin JL, O'Doherty AM, Wang S, Zheng H, Sanders KM and Yan W (2005) Catsper 3 and catsper4 encode two cation channel-like proteins exclusively expressed in the testis. *Biol. Reprod.* **73:** 1235-1242.

Johnston RC, Mbizvo MT, Summerbell D, Kovacs GT and Baker HW (1994) Relationship between stimulated hyperactivated motility of human spermatozoa and pregnancy rate in donor insemination: a preliminary report. *Hum. Reprod.* **9:** 1684-1687.

Kalab P, Peknicova J, Geussova G and Moos J (1998) Regulation of protein tyrosine phosphorylation in boar sperm through a cAMP-dependent pathway. *Mol. Reprod. Dev.* **51:** 304-314.

Kamenetsky M, Middelhaute S, Bank EM, Levin LR, Buck J and Steegborn C (2006) Molecular details of cAMP generation in mammalian cells: a tale of two systems. *J. Mol. Biol.* **362:** 623-639.

Kawase O, Ueno S, Minakata H, Hoshi M and Matsumoto M (2004) Guanylyl cyclase cGMP-specific phosphodiesterase participate in the acrosome reaction of starfish sperm. *Zygote* **12:** 345-355.

Kervancioglu ME, Djahanbakch O and Aitken RJ (1994) Epithelial cell culture and the induction of sperm capacitation. *Fertil. Steril.* **61:** 1103-1108.

Kilic F, Kashikar ND, Schmidt R, Alvarez L, Dai L, Weyand I, Wiesner B, Goodwin N, Hagen V and Kaupp UB (2009) Caged progesterone: a new tool for studying rapid nongenomic actions of progesterone. *J. Am. Chem. Soc.* **131:** 4027-4030.

Kim E, Yamashita M, Kimura M, Honda A, Kashiwabara S and Baba T (2008) Sperm penetration through cumulus mass and zona pellucida. *Int. J. Dev. Biol.* **52:** 677-682.

Kirkman-Brown JC, Punt EL, Barratt CL and Publicover SJ (2002) Zona pellucida and progesterone-induced calcium signalling and acrosome reaction in human spermatozoa. *J. Androl.* **23:** 306-315.

Kobori H, Miyazaki S and Kuwabara Y (2000) Characterization of intracellular Ca^{2+} increase in response to progesterone and cyclic nucleotides in mouse spermatozoa. *Biol. Reprod.* **63:** 113-130.

Krausz C, Bonaccorsi L, Luconi M, Fuzzi B, Criscuoli, L Pellegrini S, Forti G and Baldi E (1995) Intracellular calcium increase and acrosome reaction in response to progesterone in human spermatozoa are correlated with in-vitro fertilization. *Hum. Reprod.* **10:** 120-124.

Krausz C, Bonaccorsi L, Maggio P, Luconi M, Criscuoli L, Fuzzi B, Pellegrini S, Forti G and Baldi E (1996) Two functional assays of sperm responsiveness to progesterone and their predictive values in in-vitro fertilization. *Hum. Reprod.* **11:** 1661-1667.

Kunz G, Beil D, Deininger H, Wildt L and Leyendecker G (1996) The dynamics of rapid sperm transport through the female genital tract: evidence from vaginal sonography of uterine peristalsis and hysterosalpingoscintigraphy. *Hum. Reprod.* **11:** 627-632.

Kurjak M, Fritsch R, Saur D, Schusdziarra V and Allescher HD (1999) NO releases bombesin-like immunoreactivity from enteric synaptosomes by cross-activation of protein kinase A. *Am. J. Phisiol.* **276:** G1521-G1530.

Kuzan FB, Fleming AD and Seidel GE (1984) Successful fertilization in vitro of fresh intact oocytes by perivitelline (acrosome-reacted) spermatozoa of the rabbit. *Fertil. Steril.* **41:** 766-770.

Lanzafame F, Chapman MG and Guglielmino A (1994) Pharmacological stimulation of sperm motility. *Hum. Reprod.* **9:** 192-199.

Leclerc P, de Lamirande E and Gagnon C (1998) Interaction between Ca^{2+}, cyclic 3',5' adenosinemonophosphate, the superoxide anion, and tyrosine phosphorylation pathways in the regulation of human sperm capacitation. *J. Androl.* **19:** 434-443.

Lee MA and Storey BT (1986) Bicarbonate is essential for fertilization of mouse eggs: mouse sperm require it to undergo acrosome reaction. *Biol. Reprod.* **34:** 349-356.

Lefievre L, Bedu-Addo K, Conner SJ, Machado-Oliveria GSM, Kirkman-Brown JC, Afnan MA, Publicover SJ, Ford C and Barratt CLR (2007) Counting sperm does not add up any more: time for a new equation? *Reproduction* **133**: 675-684.

Lefievre L, De Lamirande E and Gagnon C (2002) Presence of cyclic nucleotide phosphodiesterases PDE1A, existing as a stable complex with calmodulin, PDE3A in human spermatozoa. *Biol. Reprod.* **67:** 423-430.

Lefievre L, De Lamirande E and Gagnon C (2000) The cyclic GMP-specific phosphodiesterase inhibitor, sildenafil, stimulates human sperm motility and capacitation but not acrosome reaction. *J. Androl.* **21:** 929-937.

Lindemann CB and Lesich KA (2010) Flagellar and cliary beating: the proven and the possible. *J. Cell Sci.* **123:** 519-528.

Liu DY, Liu ML, Clarke GN, Baker HWG. (2007). Hyperactivation of capacitated human sperm correlates with the zona pellucida-induced acrosome reaction of zona pellucida-bound sperm. *Hum. Reprod.* **22:** 2632-2638

Liu J, Nagy Z, Joris H, Tournaye H, Smitz J, Camus M, Devroey P and Van Steirteghem A (1995) Analysis of 76 total fertilization failure cycles out of 2732 intracytoplasmic sperm injection cycles. *Hum. Reprod.* **10:** 2630-2636.

Liu J, Xia J, Cho KH, Clapham DE and Ren D (2007) CatSperbeta, a novel transmembrane protein in the CatSper channel complex. *J. Biol. Chem.* **282:** 18945-18952.

Lishko PV, Botchkina IL and Kirichok Y (2011) Progesterone activates the principal channel of human sperm. *Nature* **471:** 387-392.

Lobley A, Pierron V, Reynolds L, Allen L and Michalovich D (2003) Identification of human and mouse CatSper3 and CatSper4 genes: characterization of a common interaction domain and evidence for expression in testis. *Reprod. Biol. Endocrinol*. **1:** 53.

Luconi M, Krausz C, Forti G and Baldi E (1996) Extracellular calcium negatively modulates tyrosine phosphorylation and tyrosine kinase activity during capacitation of human spermatozoa. *Biol Reprod.* **55:** 207-216.

McGrady AV, Nelson L and Ireland M (1974) Ionic effects on the motility of bull and chimpanzee spermatozoa. *J. Reprod. Fertil.* **40:** 71-76.

MacRea TH (1997) Tubulin post-translational modifications – enzymes and their mechanisms of action. *Eur. J. Biochem.* **244:** 265-278.

Marquez B and Suarez SS (2004) Different signaling pathways in bovine sperm regulate capacitation and hyperactivation. *Biol. Reprod.* **70:** 1626-1633.

Marquez B and Suarez SS (2007) Bovine sperm hyperactivation is promoted by alkaline-stimulated Ca^{2+} influx. *Biol. Reprod.* **76:** 660-665.

Mehats C, Andersen CB, Filopanti M, Jin SL and Conti M (2002) Cyclic nucleotide phosphodiesterases and their role in endocrine signaling. *Trend. Endocrinol. Metab.* **13:** 29-35.

Morita Z and Chang MC (1970) The motility and aerobic metabolism of spermatozoa in laboratory animals with special reference to the effects of cold shock and the importance of calcium for the motility of hamster spermatozoa. *Biol. Reprod.* **3:** 169-179.

Mortimer D (1986) Elaboration of a new culture medium for physiological studies on human sperm motility and capacitation. *Hum Reprod* **1:** 247-250.

Mortimer ST (1997) A critical review of the physiological importance and analysis of sperm movement in mammals. *Hum. Reprod. Update* **3:** 403-439.

Mortimer ST and Mortimer D (1990) Kinematics of human spermatozoa incubated under capacitating conditions. *J. Androl.* **11:** 195-203.

Mortimer ST and Swan MA (1995) Kinematics of capacitating human spermatozoa analyzed at 60 Hz. *Hum. Reprod.* **10:** 873-879.

Mortimer ST, Swan MA, and Mortimer D (1998) Effect of seminal plasma on capacitation and hyperactivation in human spermatozoa. *Hum. Reprod.* **13:** 2139-2146.

Morton B, Harrigan-Lum J, Albagli L and Jooss T (1974) The activation of motility in quiescent hamster sperm from the epididymis and cyclic nucleotides. *Biochem. Biophys. Res. Commun.* **56:** 372-379.

Munire M, Shimizu Y, Sakata Y, Minaguchi R. and Aso T (2004) Impaired hyperactivation of human sperm in patients with infertility. *J. Med. Dent. Sci.* **51:** 99-104.

Murase M (1992) The dynamics of cellular motility. Chichester, UK: John Wiley.

Nassar A, Mahony M, Blackmore P, Morshedi M, Ozgur K and Oehninger S (1998) Increase of intracellular calcium is not a cause of pentoxifylline-induced hyperactivated motility or acrosome reaction in human sperm. *Fertil. Steril.* **69:** 748-754.

Negri P, Grechi E, Tomasi A, Fabbri E and Capuzzo A (1996) Effectiveness of pentoxifylline in semen preparation for intrauterine insemination. *Hum. Reprod.* **6:** 1236-1239.

Neil JM and Olds-Clarke P (1987) A computer-assisted assay for mouse sperm hyperactivation demonstrates that bicarbonate but not bovine serum albumin is required. *Gamete Res.* **18:** 121-140.

Neri-Vidaurri PC, Torres-Flores V and Gonzales-Martinez MT (2006) A remarkable increase in the sensitivity of voltage-dependent calcium channels occurs in human sperm incubated in capacitatig conditions. *BBRC* **343:** 105-109.

Nijs M, Creemers E, Cox A, Jannsen M, Vanheudsen E, Van der Elst J and Ombelet W (2010) Relationship between hyaluronic acid binding and outcome in ART: a pilot study. Andrologia **42**: 291-296.

Nolan JP, Magargee SF, Posner RG and Hammerstedt RH (1995) Flow cytometric analysis of transmembrane phospholipid movement in bull sperm. *Biochemistry* **34:** 3907-3915.

Ignotz GG and Suarez SS (2005) Calcium/calmodulin and calmodulin kinase II stimulate hyperactivation in demembranated bovine sperm. *Biol Reprod* **73:** 519-526.

Inaba K (2002) Dephosphorylation of Tctex2-related dynein light chain by type 2A protein phosphatase. *Biochem. Biophys. Res. Commun.* **297:** 800-805.

O'Connell M, McClure N, Powell LA, Steele EK and Lewis SE (2003) Differences in mitochondrial and nuclear DNA status of high-density and low-density sperm fractions after density centrifugation preparation. *Fertil. Steril.* **79** Suppl. 1: 754-762.

O'Donnell JM and Frith S (1999) Behavioral effects of family-selective inhibitors of cyclic nucleotide phosphodiesterases. *Phamacol. Biochem. Behav.* **63:** 185-192.

O'Rand MG and Widgren EE (2012) Loss of calcium in human spermatozoa via EPPIN, the semenogelin receptor. *Biol. Reprod.* **86:** 1-7.

Oehninger S (2011) Clinical management of male infertility in assisted reproduction: ICSI and beyond. *Int J Androl* **34:** 319-329.

Oehninger S and Kruger T (1995) The diagnosis of male infertility by semen quality. *Hum. Reprod.* **10:** 1037-1041.

Okamura N, Tajima Y, Soejima A, Masuda H and Sugita Y (1985) Sodium bicarbonate in seminal plasma stimulates the motility of mammalian spermatozoa through direct activation of adenylate cyclase. *J. Biol. Chem.* **260:** 9699-96705.

Oko RJ (1995) Developmental expression and possible role of perinuclear theca proteins in mammalian spermatozoa. *Reprod. Fertil.* Dev. **7:** 777-797.

Oko RJ and Clermont Y (1990) Mammalian spermatozoa: structure and assembly of the tail. In Controls of Sperm Motility: BBiological and Clinical Aspects, ed. C Gagnon. Boca Raton, FL:CRC Press, pp. 3-28.

Ombelet W, Vandeput H, Janssen M (1997) Treatment of male infertility due to sperm surface antibodies: IUI or IVF? *Hum. Reprod.* **12:** 1165-1170.

Oren-Benaroya R, Orvieto R, Gakamsky A, Pinchasov M and Eisenbach M (2008) The sperm chemoattractant ecreted from human cumulus cell is progesterone. *Hum. Reprod.* **23:** 2339-2345.

Pacey AA, Davies N, Warren MA, Barratt CL and Cooke D (1995) Hyperactivation may assist human spermatozoa to detach from intimate association with the endosalpinx. *Hum. Reprod.* **10:** 2603-2609.

Pacey AA, Hill CJ, Scudamore IW, Warren MA, Barratt CL and Cooke D (1995) The interaction in vitro of human spermatozoa with epithelial cells from the human uterine (fallopian) tube. *Hum. Reprod.* **10:** 360-366.

Pang SC, Chan PJ and Lu A (1993) Effects of pentoxifylline on sperm motility and hyperactivation in normozoospermic and normokinetic semen. *Fertil. Steril.* **60:** 336-343.

Parrish JJ, Susko-Parrish JL and First NL (1989) Capacitation of bocine sperm by heparin: inhibitory effect of glucose and role of intracellular pH. *Biol. Reprod*. **41:** 683-699.

Pomorski T, Herrman A, Zimmermann B, Zachowski A and Muller P (1995) An improved assay for measuring the transverse redistribution of fluorescent phospholipids in plasma membranes. *Chem. Phys. Lipids* **77:** 139-146.

Porter ME and Sale WS (2000) The 9+2 axoneme anchors multiple inner arm dyneins and a network of kinases and phosphatases that control motility. *J. Cell Biol*. **151:** F37-F42.

Publicover SJ and Barratt CL (2011) Sperm motility: things are moving in the lab! *Mol. Hum. Reprod.* **17:** 453-456.

Publicover S, Harper CV and Barratt C (2007) [Ca2+]i signalling in sperm--making the most of what you've got. *Nat Cell Biol* **9:** 235-42.

Puente MA, Tartaglione CM and Ritta MN (2011) Bull sperm acrosome reaction induced by gamma-aminobutyric acid (GABA) is mediated by GABAergic receptors type A. *Animal Reprod. Sci.* **127:** 33-37.

Quill TA, Ren D, Clapham DE and Garbers DL (2001) A voltage-gated ion channel expressed specifically in spermatozoa. *Proc. Natl. Acad. Sci.* **98:** 12527-12531.

Quill TA, Sugden SA, Rossi KL, Doolittle LK, Hammer RE and Garbers DL (2003) Hyperactivated motility driven by CatSper2 is required for fertilization. *Proc. Natl. Acad. Sci.* **100:** 14869-14874.

Ralt D, Goldenberg M and Fetterolf P (1991) Sperm attraction to a follicular factor(s) correlates with human egg fertilizability. *Proc. Natl. Acad. Sci.* **88:** 2840-2844.

Randall JM and Templeton AA (1991) Infertility: the experience a tertiary referral centre. *Health Bull (Edinb)* **49:** 48-53.

Razali NM and Wah YB (2011) Power comparisons of Shapito-Wilk, Kolmogorow-Smirnov, Lilliefors, and Anderson-Darling test. *J. Stats. Model. Anal.* **2:** 21-23.

Rees JM, Ford WCL and Hull MGR (1990) Effect of caffeine and of pentoxifylline on the motility and metabolism of human spermatozoa. *J. Reprod. Fertil.* **90:** 147-156.

Reid IA (1999) Role of phosphodiesterase isoenzymes in the control of renin secretion: effects of selective enzyme inhibitors. *Curr. Pharm. Des.* **5:** 725-735.

Ren D, Navarro B, Perez G, Jackson AC, Hsu S, Shi Q, Tilly JL and Clapham DE (2001) A sperm ion channel required for sperm motility and male fertility. *Nature* **413:** 603-609.

Robertson L, Wolf DP and Tash JS (1988) Temporal changes in motility parameters related to crosomal status: identification and characterization of populations of hyperactivated sperma. *Biol. Reprod.* **39:** 797-805.

Rosatto M, Ion Popa F, Ferigo M, Clari G and Foresta C (2005) Human sperm express cannabinoid receptor CB1, the activation of which inhibits motility, acrosome reaction, and mitochondrial function. *J. Clin. Endocrinol. Metab.* **90**: 984-991.

Rojas FJ, Bruzzone ME and Moretti-Rojas I (1992) Regulation of cyclic adenosine monophosphate synthesis in human ejaculated spermatozoa. II. The role of calcium and bicarbonate ins on the activation of adenylyl cylase. *Hum. Reprod.* **7:** 1131-1135.

Ryu HM, Lin WW, Lamb DJ, Chuang W, Lipshultz LI and Bischoff FZ (2001) Increased chromosome X, Y, and 18 nondisjunction in sperm from infertile patients that were identified as normal by strict morphology: implication for intracytoplasmic sperm injection. *Fertil. Steril.* **76:** 879-883.

Sakkas D (2013) Novel technologies for selecting the best sperm for in vitro fertilization and intracytoplasmic sperm injection. *Fertil. Steril.* **99:** 1023-1029.

Salicioni AM, Platt MD, Wertheimer EV, Arcelay E, Allaire A, Sosnik J and Visconti P (2007) Signaling pathways involved in sperm capacitation. *Spermatology* **65:** 245-260.

Sanchez V, Wistuba J and Mallidis C (2013) Semen analysis: update on clinical value, current needs and future prospectives. *Reproduction* **146:** R249-R258.

Schmidt L, Munster K and Helm P (1995) Infertility and the seeking of infertility treatment in a representative population. *Br. J. Obstet. Gynaecol.* **65:** 245-259.

Segare-Patil V, Galvankar M, Satiya M, Bhandari B, Gupta SK and Modi D (2012) Differential concentration and time dependent effects of progesterone on kinase activity, hyperactivation and acrosome reaction in human spermatozoa. *Int. J. Androl.* **35:** 633-644.

Setchell BP, Maddocks S and Brooks DE (1994) Anatomy, vasculature, innervation, and fluids of the male reproductive tract. In: The Physiology of Reproduction, Volume 1. Edited by Knobil E and Neill JD, Raven Press, New York, pp. 1063-1175.

Sharpe RM (2012) Sperm counts and fertility in men: a rocky road ahead. *EMBO Reports* **13:** 398-403.

Sharpe RM and Irvine DS (2004) How strong is the evidence of a link between envorinmental chemicals and adverse effects on human reproductive health. *Bmj* **328:** 447-451.

Shi QX and Roldan ER (1995) Bicarbonate/CO2 is not required for zona pellucida- or progesterone-induced acrosomal exocytosis of mouse spermatozoa but is essential for capacitation. *Biol. Reprod.* **52:** 540-546.

Si Y and Okuno M (1999) Regulation of microtubule sliding by a 36-kDA phosphoprotein in hamster sperm flagella. *Mol. Reprod. Dev.* **52:** 328-334.

Slama R, Hansen OK, Ducot B, Bohet A, Sorensen D, Giorgis AL, Eijkemans MJ, Rosetta L, Thalabard JC, Keiding N and Bouyer J (2012) Estimation of the frequency of involuntary infertility on a nation-wide basis. *Hum Reprod.* **27:** 1489-1498.

Smith JF, Syritsyna O, Fellous M, Serres C, Mannowetz N, Kirichok Y and Lishko PV (2013) Disruption of the principal, progesterone-activated sperm Ca^{2+} channel in a CatSper2-deficient infertile patient. *PNAS* **110:** 6823-6828.

Smith SJ, Cieslinski LB, Newton R, Donnelly LE, Fenwick PS, Nicholson AG, Barnes PJ, Barnette MS and Giembycz MA (2004) Discovery of BRL 50481 [3-(N,N-dimethylsulfonamido)-4-methyl-nitrobenzene], a selective inhibitor of phosphodiesterase 7: in vitro studies in human monocytes, lung macrophages, and CD8+ T-lymphocytes. *Mol. Pharmacol.* **66:** 1679-1689.

Spira A (1986) Epidemiology of human reproduction. *Hum. Reprod.* **1:** 111-115.

Stauss CR., Votta TJ and Suarez SS (1995) Sperm motility hyperactivation facilitates penetration of the hamster zona pellucida. *Biol. Reprod* **53**: 1280-1285.

Strunker T., Goodwin N., Brenker C., Kashikar ND., Weyand ID., Seifert R., Kaupp UB. (2011). The CatSper mediates progesterone-induced calcium influx in human sperm. *Nature* **471**: 382-387

Suarez SS (2008) Control of hyperactivation in sperm. *Hum. Reprod. Update* **14:** 647-657.

Suarez SS and Dai XB (1992) Hyperactivation enhances mouse sperm capacity for penetrating viscoelastic media. *Biol. Reprod.* **46:** 686-691.

Suarez SS, Katz DH, Owen DH, Andrew JB and Powell LR (1991) Evidence for the function of hyperactivated motility in sperm. *Biol. Reprod* **44:** 375-381.

Sukcharoen N, Keith J and Irvine DS (1995) Definition of the optimal criteria for identifying hyperactivated human spermatozoa at 25 Hz using in-vitro fertilization as a functional end-point. *Hum. Reprod.* **10:** 2928-2937.

Sun F, Bahat A, Gakamsky A, Girsh E, Katz N, Giojalas LC, Tur-Kaspa I and Eisenbach M (2005) Human sperm chemotaxis: both the oocyte and its surrounding cumulus cells secrete chemoattractants. *Hum. Reprod.* **20:** 761-767.

Takada S, Wilkerson CG, Wakabayashi K, Kamiya R and Witman GB (2002) The outer dynein arm-docking complex: characterization of a subunit (Oda1) necessary for outer arm assembly. *Mol. Biol. Cell* **13:** 1015-1029.

Talbot P, DiCarlantonio G, Zao P, Penkala J and Haimo LT (1985) Motile cells lacking hyaluronidase can penetrate the hamster oocyte cumulus complex. *Dev. Biol.* **108:** 387-398.

Taneto H, Krapf D, Hino T, Sanchez-Cardenas C, Darszon A, Yanagimachi R and Visconti PE (2013) Ca^{2+} ionophore A23187 can make mouse spermatozoa capable of fertilizing *in vitro* without cAMP-dependent phosphorylation pathways. *PNAS* **110:** 18543-18548.

Tararbit K, Lolong N, Thieulin AC, Houyel L, Bonnet D, Goffinet F and Khoshnood B (2013) The risk for four specific congenital heart defects associated with assisted reproductive technologies: a population-based evaluation. *Hum. Reprod.* **28:** 367-374.

Tash JS and Means AR (1982) Regulation of protein phosphorylation and motility of sperm by cyclic adenosine monophosphate and calcium. *Biol. Reprod.* **26:** 745-763.

Tash JS and Means AR (1983) Cyclic adenosine 3', 5' Monophosphate, calcium and protein phosphorylation in flagellar motility. *Biol Reprod* **28:** 75-104.

Terriou P, Hans E, Giorgetti C, Spach JL, Salzmann J, Urrutia V and Roulier R (2000) Pentoxifylline initiates motility in spontaneously immotile epididymal and testicular spermatozoa and allows normal fertilization, pregnancy, and birth after intracytoplasmic sperm injection. *J. Assist. Reprod. Genet.* **17:** 194-199.

Tesarik J, Mendoza C and Carreras A (1992) Effects of phosphodiesterase inhibitor caffeine and pentoxifylline on spontaneous and stimulus-induced acrosome reactions in human sperm. *Fertil. Steril.* **58:** 1185-1190.

Tesarik J, Thebault A and Testart J (1992a) Effect of pentoxifylline on sperm movement characteristics in normoozoospermic and asthenozoospermic specimens. *Hum. Reprod.* **7:** 1257-1263.

Thonneau P and Spira A (1991) Prevalence of infertility: international data and problems of measurement. *Eur. J. Obstet. Gynecol. Reprod. Biol.* **38:** 43-52.

Torres-Flores V, Hernandez-Rueda YL, Neri-Vidaurri PDC, Jimenez-Trejo F, Calderon-Salinas V, Molina-Guarneros JA and Gonzalez-Martinez MT (2008) Activation of protein kinase A stimulates the progesterone induced calcium influx in human sperm exposed to phosphodiesterase inhibitor papaverine. *J. Androl.* **29:** 549-557.

Tournaye H, Janssens R, Verheyen G, Devroey P and Van Streiteghem A (1994) Invitro fertilization in couples with previous fertilization failure using sperm incubated with pentoxifylline and 2-deoxyadenosine. *Fertil. Steril.***62:** 574-579.

Trisini AT, Singh NP, Duty SM and Hauser R (2004) Relationship between human sperm parameters and deoxyribonucleic acid damage assessed by the neutral comet assay. *Fertil. Steril.* **82:** 1623-1632.

Turner RM (2003) Tales from the tail, what do we really know about sperm motility? *J. Androl.* **24:** 790-803.

Turner RM (2006) Moving to the beat, a review of mammalian sperm motility regulation. *Reprod. Fertil. Dev.* **18:** 25-38.

Van der Steeg JW, Steures P, Eijkemans MJ, Habbema JD, Hompes PG, Kremer JA, Van Der Leeuw-Harmsen L, Bossuyt PM, Repping S, Silber SJ, Mol BW and Van Der Veen F (2011) Role of semen analysis in subfertile couples. *Fertil. Steril.* **95:** 1013-1019.

Van Waart J, Kruger TF, Lombard CJ and Ombelet W (2001) Predictive value of normal sperm morphology in intrauterine insemination (IUI): a structured literature review. *Hum. Reprod. Update* **7:** 495-500.

Varano G, Lombardi A, Cantini G, Forti G, Baldi E and Luconi M (2008) Src activation triggers capacitation and acrosome reaction but not motility in human spermatozoa. *Hum. Reprod.* **23:** 2652-2662.

Visconti PE, Bailey JL, Moore GD, Pan D, Olds-Clarke P and Kopf GS (1995) Capacitation of mouse spermatozoa. I. Correlation between the capactitation state protein tyrosine phosphorylation. *Development* **121:** 1129-1137.

Visconti PE, Krapf D, Vega-Baltran JLV, Acevedo JJ and Darszon A (2011) Ion channels, phosphorylation and mammalian sperm capacitation. *Asian J. Androl.* **13:** 395-405.

Wang C, Lee GS, Leung A, Surrey ES and Chan SYW (1993) Human sperm hyperactivation and acrosome reaction and their relationship to human *in vitro fertilization*. *Fertil. Steril.* **59:** 1221-1227.

Wang H, Liu J, Cho KH and Ren D (2009) A novel, single, transmembrane protein CATSPERG is associated with CATSPERI channel protein. *Biol. Reprod.* **81:** 539-544.

Wasco WM and Orr GA (1984) Function of calmodulin in mammalian sperm: presence of a calmodulin-dependent cyclic nucleotide phosphodiesterase associated with demembranated rat caudal epididymal sperm. *Biochem. Biophys. Res. Comm.* **118:** 636-642.

Welch JE, Brown PL, O'Brien DA, Magyar PL, Bunch DO, Mori C and Eddy EM (2000) Human glyceraldehyde 3-phosphate dehydrogenase-2 gene is expressed specifically in spermatogenic cells. *J. Androl.* **21:** 328-338.

Wennemuth G, Babcock DF and Hille B (2003) Calcium clearance mechanism of mouse sperm. *J. Gen. Physiol.* **122:** 115-128.

Wennemuth G, Carlson AE, Harper AJ and Babcock DF (2003) Bicarbonate actions on flagellar and Ca^{2+}-channel responses: initial events in sperm activation. *Development* **130:** 1317-1326.

Whan LB, West MCL, McClure N and Lewis SEM (2006) EEffects of delta-9-tetrahydrocannabinol, the primary psychoactive cannabinoid in marijuana, on human sperm function *in vitro*. *Fertil. Steril.* **85:** 653-660.

World Health Organization (2010) WHO Laboratory Manual for the Examination and Processing of Human Semen. 5th Edition. WHO Press. Geneva, Switzerland.

Witman GB (1990) Introduction to Cilia and Flagella, in Ciliary and Flagellar Membranes, ed. RA Bloodgood. New York: Plenum.

Yanagimachi R. (1970). The movement of golden hamster spermatozoa before and after capacitation. *J. Reprod. Fertil* **23:** 193-196

Young LG and Nelson L (1974) Calcium ions and control of the motility of sea urchin spermatozoa. *J. Reprod. Fertil.* **41:** 371-378.

Yovich JL (1993) Pentoxifylline- actions and applications in assisted reproduction. *Hum Reprod* **8:** 1786-1791.

Yovich JM, Edirisinghe WH, Cummins JM and Yovich JL (1988) Preliminary results using pentoxifylline in a pronuclear strage tubal transfer program for severe male factor infertility. *Fertil. Steril.* **50:** 179-181.

Yovich JM, Edirisinghe WR, Cummins JM and Yovich JL (1990) Influence of pentoxifylline in severe male factor infertility. *Fertil Steril.* **53:** 715-722.

Yudin AI, Hanson FW and Katz DF (1989) Human cervical mucus and its interaction with sperm: a fine-structural view. *Biol. Reprod.* **40:** 661-671.

Zeng Y, Oberdorf JA and Florman HM (1996) pH regulation in mouse sperm: identification of Na(+)-, Cl(-)-, and HCO3(-)-dependent and arylaminobenzoate-dependent regulatory mechanisms and characterization of their roles in sperm capacitation. *Dev. Biol.* **173:** 510-520.

Zhu JJ, Barratt CLR and Cooke ID (1994a) The sequential effects of human cervical mucus, oviductal fluid and follicular fluid on sperm function. *Fertil. Steril.* **61:** 1129-1135.

Zhu JJ, Pacey AA and Barratt CLR (1994b) Computer-assisted measurement of hyperactivation in human spermatozoa – differences between European and American versions of Hamilton-Thorn motility analyzers. *Hum. Reprod.* **9:** 456-462.

Zucchi A, Mearini E, Porena M, Carlini E, Saccardi C, Arienti G and Palmerini CA (2006) Cytosolic calcium levels in spermatozoa are modulated differently in healthy subjects and patients with varicocelle. *Fertil. Steril* **85:** 144-148.